NCHRP
REPORT 469

NATIONAL COOPERATIVE HIGHWAY RESEARCH PROGRAM

Fatigue-Resistant Design of Cantilevered Signal, Sign, and Light Supports

TRANSPORTATION RESEARCH BOARD

NATIONAL RESEARCH COUNCIL

NATIONAL COOPERATIVE HIGHWAY RESEARCH PROGRAM

NCHRP REPORT 469

Fatigue-Resistant Design of Cantilevered Signal, Sign, and Light Supports

R. J. DEXTER
M. J. RICKER
University of Minnesota
Minneapolis, MN

SUBJECT AREAS
Bridges, Other Structures, and Hydraulics and Hydrology • Materials and Construction

Research Sponsored by the American Association of State Highway and Transportation Officials
in Cooperation with the Federal Highway Administration

TRANSPORTATION RESEARCH BOARD — NATIONAL RESEARCH COUNCIL

NATIONAL ACADEMY PRESS
WASHINGTON, D.C. — 2002

NATIONAL COOPERATIVE HIGHWAY RESEARCH PROGRAM

Systematic, well-designed research provides the most effective approach to the solution of many problems facing highway administrators and engineers. Often, highway problems are of local interest and can best be studied by highway departments individually or in cooperation with their state universities and others. However, the accelerating growth of highway transportation develops increasingly complex problems of wide interest to highway authorities. These problems are best studied through a coordinated program of cooperative research.

In recognition of these needs, the highway administrators of the American Association of State Highway and Transportation Officials initiated in 1962 an objective national highway research program employing modern scientific techniques. This program is supported on a continuing basis by funds from participating member states of the Association and it receives the full cooperation and support of the Federal Highway Administration, United States Department of Transportation.

The Transportation Research Board of the National Research Council was requested by the Association to administer the research program because of the Board's recognized objectivity and understanding of modern research practices. The Board is uniquely suited for this purpose as it maintains an extensive committee structure from which authorities on any highway transportation subject may be drawn; it possesses avenues of communications and cooperation with federal, state and local governmental agencies, universities, and industry; its relationship to the National Research Council is an insurance of objectivity; it maintains a full-time research correlation staff of specialists in highway transportation matters to bring the findings of research directly to those who are in a position to use them.

The program is developed on the basis of research needs identified by chief administrators of the highway and transportation departments and by committees of AASHTO. Each year, specific areas of research needs to be included in the program are proposed to the National Research Council and the Board by the American Association of State Highway and Transportation Officials. Research projects to fulfill these needs are defined by the Board, and qualified research agencies are selected from those that have submitted proposals. Administration and surveillance of research contracts are the responsibilities of the National Research Council and the Transportation Research Board.

The needs for highway research are many, and the National Cooperative Highway Research Program can make significant contributions to the solution of highway transportation problems of mutual concern to many responsible groups. The program, however, is intended to complement rather than to substitute for or duplicate other highway research programs.

Note: The Transportation Research Board, the National Research Council, the Federal Highway Administration, the American Association of State Highway and Transportation Officials, and the individual states participating in the National Cooperative Highway Research Program do not endorse products or manufacturers. Trade or manufacturers' names appear herein solely because they are considered essential to the object of this report.

NCHRP REPORT 469

Project D10-38(2) FY'94

ISSN 0077-5614

ISBN 0-309-06724-3

Library of Congress Control Number 2002101490

Price $36.00

NOTICE

The project that is the subject of this report was a part of the National Cooperative Highway Research Program conducted by the Transportation Research Board with the approval of the Governing Board of the National Research Council. Such approval reflects the Governing Board's judgment that the program concerned is of national importance and appropriate with respect to both the purposes and resources of the National Research Council.

The members of the technical committee selected to monitor this project and to review this report were chosen for recognized scholarly competence and with due consideration for the balance of disciplines appropriate to the project. The opinions and conclusions expressed or implied are those of the research agency that performed the research, and, while they have been accepted as appropriate by the technical committee, they are not necessarily those of the Transportation Research Board, the National Research Council, the American Association of State Highway and Transportation Officials, or the Federal Highway Administration, U.S. Department of Transportation.

Each report is reviewed and accepted for publication by the technical committee according to procedures established and monitored by the Transportation Research Board Executive Committee and the Governing Board of the National Research Council.

Published reports of the

NATIONAL COOPERATIVE HIGHWAY RESEARCH PROGRAM

are available from:

Transportation Research Board
National Research Council
2101 Constitution Avenue, N.W.
Washington, D.C. 20418

and can be ordered through the Internet at:

http://www.trb.org/trb/bookstore

Printed in the United States of America

FOREWORD

By Staff
Transportation Research Board

This report contains the findings of a study on fatigue resistance of cantilevered signal, sign, and light supports. The report includes design examples illustrating the application of the fatigue provisions of the AASHTO *Standard Specifications for Structural Supports for Highway Signs, Luminaires, and Traffic Signals*; guidance on design, installation, inspection, and maintenance of these structures; and recommended specifications for anchor rods. The material in this report will be of immediate interest to bridge and structural engineers, traffic engineers, and manufacturers.

Research performed under NCHRP Project 10-38 was published as *NCHRP Report 412*. Recommended specifications developed in that project, along with recommendations from NCHRP Project 17-10, have been incorporated into the AASHTO 2001 *Standard Specifications for Structural Supports for Highway Signs, Luminaires, and Traffic Signals*.

The NCHRP Project 10-38 research also identified additional areas of study necessary to permit full implementation of the proposed revisions. NCHRP Project 10-38(2), "Fatigue-Resistant Design of Cantilevered Signal, Sign, and Light Supports," was initiated to address many of these areas. In particular, the research provides information on loads resulting from variable-message signs, methods for mitigating galloping effects, methods for tightening anchor bolts, methods for identifying structures and sign configurations susceptible to galloping, and characterization of importance factors. In addition, example designs were prepared to provide a comprehensive assessment of the effects of the design provisions developed in NCHRP Project 10-38. Finally, guidance on the design, installation, inspection, and maintenance of cantilevered supports was developed.

The research was performed at the University of Minnesota, in Minneapolis, Minnesota. The report fully documents the work performed. The recommended anchor rod specifications; seven design examples; and the guidance manual on design, installation, inspection, and maintenance are included as appendixes.

CONTENTS

AUTHOR ACKNOWLEDGMENTS

The research reported herein was performed under NCHRP Project 10-38(2) by the Departments of Civil Engineering at the University of Minnesota, Texas Tech University, and the University of Wyoming. The University of Minnesota was the contractor for this study. The work undertaken at Texas Tech University and the University of Wyoming was under subcontracts with the University of Minnesota.

Robert J. Dexter, Associate Professor of Civil Engineering, University of Minnesota, was the principal investigator. The other author of this report is Matthew J. Ricker, Research Assistant, University of Minnesota, now at BKBM Engineers in Minneapolis. The work was done under the general supervision of Professor Dexter. The work at Texas Tech was done under the supervision of Professors Partha Sarkar and James McDonald. The work at the University of Wyoming was done under the supervision of Professors H. R. (Trey) Hamilton, III, and Jay Puckett.

The authors are especially grateful to Professor Ronald Cook at the University of Florida and Research Assistant Dylan Richard, who shared the research they have performed for Florida DOT, allowed us to participate in field-testing of a signal support structure in Tampa, and tested one of our dampers in their laboratory. The authors are also grateful to departments of transportation and many individuals in many states for providing data to us and helping us with field inspections and instrumentation, especially Minnesota, Illinois, Wisconsin, Florida, Texas, California, Colorado, and Wyoming. Finally, we are indebted to the project panel for their careful review of this research and their helpful suggestions.

CHAPTER **1**

INTRODUCTION

1.1 PROBLEM STATEMENT

Cantilevered signal, sign, and light support structures have a single vertical column (referred to as an upright, post, or pole). The horizontal part of the structure is referred to as the mast arm (usually in reference to a monotube), the truss (for other than monotubes), or the cantilever. In the fourth edition of the *Standard Specifications for Structural Supports for Highway Signs, Luminaires, and Traffic Signals* (hereafter referred to as the 2001 Specifications [1]), structures supported on both sides of the roadway are referred to as bridge supports. Bridge supports are also called span-type structures, sign bridges, or overhead structures (although this latter term is sometimes used to describe both cantilever and bridge supports).

Cantilevered support structures can be an attractive option because the cost is typically less than 40 percent of the cost of bridge supports. Also, the single upright increases motorist safety by reducing the probability of vehicle collision.

However, cantilevered structures are much more flexible than bridge supports because of the single post. The flexibility of cantilevered structures has been increasing over the last few decades as the span of cantilevered support structures has been increasing. The span has increased because (1) the setback distance of the upright from the roadway has increased for safety reasons and (2) these structures are increasingly being used on roads with more lanes. Today, it is not unusual for the cantilever to span more than 12 m (40 ft). Florida has installed a signal support structure with a 27-m (90-ft) mast arm and several on the order of 24 m (80 ft). These mast arms appear like "weeping willows" under dead-load deflection.

The flexibility gives these structures low resonant frequencies of about 1 Hz, and the wind-gust velocity often fluctuates at frequencies in this range. The damping is extremely low, usually far less than 1 percent of critical damping. These conditions make cantilevered support structures particularly susceptible to large-amplitude vibration due to various wind-loading phenomena.

Not surprisingly, as the flexibility of these support structures has increased over the years, so have the number of problems with vibration and fatigue. A number of other factors have also contributed to the increase in the number of such problems. The relatively recent advent of backplates (used on signal fixtures to block the sun and enhance the visibility of the signal) has increased the susceptibility to galloping of the signal support structures [2]. The size and location of flat-panel signs has also increased over the years—larger signs are now placed asymmetrically with their center of gravity above the center of gravity of the horizontal mast arm or support truss, increasing the torsional motion of the mast arms. Finally, large variable-message signs (VMSs) are increasingly used, and these signs present a large horizontal surface that increases the effect of truck-induced gusts [3].

A survey of state departments of transportation conducted in 1990 [2] revealed that the occurrence of failures with cantilevered support structures in particular was increasing. Three years later, a survey was conducted as part of the first phase of this research project [4]. Among the 36 states that responded, approximately one-half had experienced problems with wind-induced vibration of cantilevered support structures. Several states reported occurrences of horizontal mast arm displacement ranges in excess of 1.2 m (48 in.) under steady-state winds with velocities in the range of 5 m/s to 15 m/s (10–35 mph). A recent survey conducted for this project indicates that the rate of occurrence of these problems is still increasing. A recent survey conducted as part of NCHRP Project 17-10 revealed similar results. Fifty-nine percent of the 40 responding states reported wind-damage failures [5].

Large-amplitude vibration is not necessarily a problem with regard to the integrity of the structure. However, a large number of motorist complaints occur when the displacement range exceeds 200 mm (8 in.) [4]. Motorists cannot clearly see the signals or signs and are concerned about driving under the vibrating structures.

More significant problems have also occurred as the high stress ranges associated with the vibration eventually causes fatigue cracking of various details (e.g., anchor bolts, column base details, and mast-arm-to-column connection details) [4]. A few collapses of these structures are typically reported each year. In some cases, vehicles have collided with the fallen structures, resulting in serious injuries and fatalities. There are also many cases of nuisance fatigue cracks that are discovered before the cracking leads to collapse. The economic cost of inspecting, repairing, or replacing nuisance cracks is substantial.

However, considering the sheer number of these structures, the actual probability of failure of the average support structure is small compared with accepted probabilities of

failure of bridges and buildings. The few collisions that occur between vehicles and collapsed cantilevered support structures are not at all significant when considered in terms of the total number of highway collisions. However, the perceived significance of these collisions between vehicles and collapsed cantilevered support structures is enhanced because the collisions are totally unexpected (i.e., the failures take place in weather that is not that unusual, and the public does not expect these support structures to be a hazard). For these reasons, the probability of failure of these sign, signal, and light support structures should be decreased to a more acceptable level.

Accordingly, the overall objective of the research described in this report is to prepare specifications and commentary for the design, installation, and maintenance of these support structures that will reduce the probability of excessive vibration and fatigue cracking.

1.2 PROJECT BACKGROUND

In response to the growing number of problems with excessive vibration and fatigue cracking, the National Cooperative Highway Research Program (NCHRP) initiated Project 10-38 to improve the vibration and fatigue design provisions for cantilevered sign, signal, and light support structures. In the United States, sign, signal, and light support structures are designed using the AASHTO *Standard Specifications for Structural Supports for Highway Signs, Luminaires, and Traffic Signals* [1, 6]. The 1994 version (and previous versions) of the specifications were vague and insufficient with respect to the design of support structures for vibration and fatigue. Furthermore, the commentary to the 1994 Specifications did not contain adequate guidance for their application.

The first phase of this research was conducted from 1993 to 1996 at Lehigh University. In the first phase, vortex shedding, galloping, natural wind gusts, and truck-induced wind gusts were identified as wind-loading phenomena that could lead to excessive vibration or fatigue. Equivalent static loads were determined to estimate the stress range resulting from each of these loading conditions using static structural analysis. The results of the first phase of the research and proposed new design specifications and commentary to increase resistance to vibration and fatigue were published as *NCHRP Report 412* [4].

During the course of the first phase of this research, another NCHRP research project, Project 17-10, began at the University of Alabama at Birmingham. NCHRP Project 17-10 was directed at revising all aspects of the 1994 Specifications other than vibration and fatigue. The proposed specifications and commentary from NCHRP Project 10-38 [4] were incorporated into the revised overall 2001 Specifications at the end of NCHRP Project 17-10. The results and proposed specifications that were developed during NCHRP Project 17-10 were published as *NCHRP Report 411* [7]. Based on these research projects, vibration and fatigue provisions have been included in the 2001 Specifications.

Because of the inadequacy of the 1994 Specifications, the proposed design provisions for vibration and fatigue of cantilevered support structures that were published in *NCHRP Report 412* have been used by a few agencies for designing cantilevered sign and signal structures [8]. A few agencies have also used draft copies of the 2001 Specifications, which are only slightly different than what was proposed in *NCHRP Report 412*. Because there are no comparable design guidelines for bridge supports (i.e., overhead sign structures), the proposed revisions have been applied in the fatigue design checks for these structures, as well.

In addition to showing the present lack of reliable design guidance in the industry, the preliminary acceptance of the proposed revisions shows that the proposed revisions are practical and useable. Preliminary indications are that the fatigue design provisions of the 2001 Specifications (1) are complex but clear, (2) force the designers to choose more fatigue-resistant design details, (3) in some cases require an increase in the section sizes of structural elements, and (4) result in costs that are less than 20 percent higher.

There is one exception to this acceptance, however, and that is a clause that was added to the 2001 Specifications that was not part of the specifications proposed in *NCHRP Report 412*. This clause (i.e., that connections welded to a tube shall be checked for punching shear stress range according to AWS D1.1 Category K_2) has caused a great deal of problems for the design of "box-type" connection of a single-pole mast arm to the upright. In fact, this clause has rendered this common type of connection for signal support structures all but impossible to successfully design. The authors believe this clause is excessively conservative, and recommendations are made in this report to remedy this problem.

There are many other areas of the design of these cantilevered sign, signal, and light support structures in which there is still considerable uncertainty. The first phase of NCHRP Project 10-38 could not completely cover all of the issues. For example, the research in the first phase of NCHRP Project 10–38 was originally planned to primarily investigate vortex shedding. At that time, vortex shedding was thought to be the primary source of the wind-induced vibration in the cantilevered sign, signal, and light support structures.

As NCHRP Project 10-38 progressed, however, it became clear that there are multiple sources of wind-induced vibration, depending on the type of support structure. The research was refocused on galloping as the primary source of problems for signal and sign structures. Many judgments had to be made in the course of determining the proposed design loads. For example, the forces in the structure resulting from galloping continue to increase as wind velocities increase. At conservatively high wind velocities, these forces would be so large as to render the design of cantilevered support structures unfeasible. Therefore, judgment was required to choose the appropriate level of galloping-induced forces.

The proposed galloping loads, in particular, have been criticized as being too conservative. However, measurements of stress ranges in galloping sign support structures in California [9] have indicated that the equivalent static loads were about twice the equivalent static loads proposed in *NCHRP Report 412*. Therefore, the equivalent static loads for galloping that were proposed in *NCHRP Report 412* might actually be unconservative. Measurements of strain on a galloping signal-support structure at Texas Tech (described later in this report) were consistent with the recommended galloping loads.

In the first phase of NCHRP Project 10-38, natural wind gusts were not thought to be the main source of fatigue damage. Therefore, natural wind-gust loading was only studied analytically using wind spectra and drag coefficients published in the literature. Contrary to expectations, analyses showed that natural wind-gust loading could also cause significant displacement and fatigue. Finally, VMS had just begun to be deployed on cantilevered structures during the course of the first phase of NCHRP Project 10-38.

Despite the uncertainty and the expanding number of issues, the development of the proposed revisions to the 1994 Specifications required some estimate of the loading from all of these possible wind-loading phenomena. Obviously, many judgments based upon inadequate data were made in order to produce a complete design specification. Therefore, further research was conducted in this second phase to further refine and to permit full implementation of the proposed revisions. In particular, the second-phase research aimed at evaluating potential mitigation devices to reduce the effect of vibration.

In addition to the research on design issues and mitigation devices, the second phase of the project also focussed on installation and maintenance of support structures. In particular, research on tightening of anchor rod nuts was conducted. A recommended specification for the design, installation, inspection, and repair of anchor rods was developed (see Appendix A). This recommended anchor rod specification is analogous to the Research Council on Structural Connections (RCSC) specification for high-strength bolts [10], which is included in the AASHTO Bridge Specifications [11]. Training materials in the form of a short-course presentation were developed for design, installation, inspection, and maintenance of these support structures.

This report outlines the findings of this additional research. The research was carried out simultaneously in seven parallel areas:

- VMS issues;
- Mitigation strategies;
- Characterization of at-risk structures;
- Quantification of importance factors;
- Anchor rod tightening research;
- Design examples; and
- Training materials and guidance on design, installation, inspection, and maintenance.

In addition to work performed by the authors, work was also performed at the Wind Engineering Research Center (WERC) at Texas Tech University. WERC has a cantilevered signal support structure mounted outdoors on a turntable that can be turned into the prevailing wind and made to gallop under appropriate wind conditions. WERC performed previous research on the mitigation of galloping of signal support structures for the Texas DOT using this facility. The work at Texas Tech was performed under the direction of Professors James R. McDonald and Partha Sarkar.

Another subcontract was to Professors H. R. (Trey) Hamilton, III, and Jay Puckett at the University of Wyoming. Prompted by several collapses of signal support structures, UW has been investigating the mitigation of vibration in signal support structures, the fatigue resistance of mast-arm-to-upright connections, and non-destructive evaluation (NDE) methods of inspection for several years in cooperation with Wyoming Department of Transportation (WYDOT).

Extensive vibration mitigation testing has also been performed at the University of Florida over the past few years. Although not a subcontractor on this project, Professor Ronald Cook and his research assistants shared their results with the authors and provided the authors with the opportunity to test their damping device and others in the field in Florida. Ronald Cook has also been instrumental in developing new American Concrete Institute (ACI) specifications and commentary for the strength of anchor rods. These specifications focus primarily on the strength of the concrete and are complementary to the proposed specifications for anchor rods in Appendix A, which refer to the ACI specifications for concrete strength.

1.3 ORGANIZATION OF THE REPORT

This report presents the results of field, analytical, and laboratory studies. Results of a literature review and survey of transportation agencies were previously reported and, therefore, are reviewed only briefly where relevant in this report. Changes to the 2001 Specifications are recommended where appropriate.

A detailed presentation of the research findings is presented in Chapter 2. Main sections of the chapter pertain to ongoing vibration and fatigue problems, as well as the seven research areas listed previously.

Chapter 3 reviews the vibration and fatigue recommendations made in *NCHRP Report 412* and adapted as part of the 2001 Specifications. It also interprets the results of the findings presented in Chapter 2 and recommends changes to the 2001 Specifications where they are necessary.

Chapter 4 summarizes the research presented throughout the report and makes several recommendations for further research.

CHAPTER 2

FINDINGS

2.1 SUMMARY OF ONGOING VIBRATION AND FATIGUE PROBLEMS

This chapter presents a summary of the significant findings from the second phase of NCHRP Project 10-38. The chapter reviews the results of the literature review and a survey of transportation officials, as well as domestic and foreign academic and professional contacts. Typical structure inventories were determined, vibration and fatigue problems were documented, and installation and maintenance issues were identified. The cost impact of the fatigue provisions of the 2001 Specifications [1] is discussed for the few agencies that have begun to use it. The 2001 Specifications were based on the results of the first phase of the project presented in *NCHRP Report 412*.

The research in *NCHRP Report 412* was prompted in part by increasing cases of excessive vibration and a few collapses of structures from fatigue cracking. The rate of occurrences of such problems has continued and may even have increased. This may be due in part to engineers' willingness to use cantilevered support structures for increasing spans, as much as 27 m (90 ft) recently.

An article in *Roads and Bridges* by Collins and Garlich [12] stated that inspections of sign, signal, and light support structures have revealed the following problems:

- Cracked anchor rods both above and within the concrete foundation;
- Loose nuts and missing connectors from both anchor rods and structural bolts;
- Cracked and broken welds;
- Fractured tubes;
- Clogged drain holes, debris accumulation, and corrosion;
- Internal corrosion of tubular members (resulting in a reduced section);
- Poor fit-up of flanged connections with cracking and missing bolts; and
- Installation of signs exceeding design square footage, causing structure overload.

Table 2-1 shows a list of states that have had significant problems with sign, signal, or light support structures.

The Wisconsin Department of Transportation has reported numerous recent problems with its sign, signal, and light support structures. Because of the DOT's proximity to the University of Minnesota, a number of sites have been visited for inspection.

Wisconsin and Minnesota make an interesting contrast that is convenient to study. Presumably, both of these states are exposed to similar wind and truck traffic. Yet Minnesota has had relatively few (if any) problems in comparison with Wisconsin. The primary reason for this difference is believed to be that Minnesota has standard design drawings that are quite conservative, whereas Wisconsin allows vendors to design the support structures themselves, presumably according to the 1994 Specifications.

Minnesota puts most signals on mast arms consisting of two-chord trusses, whereas most states use a monotube mast arm for signals. Most sign support structures in Minnesota are bridge supports (i.e., overhead support structures) where the sign bridge consists of four-chord trusses fabricated from welded angles rather than tubes, as in most other states. The trusses in the few cantilevered structures are also four-chord trusses composed of angles, rather than the two-chord tubular trusses that are more commonly used elsewhere. It is assumed that the additional torsional stiffness of the three-dimensional, four-chord truss relative to the planar two-cord truss makes these four-chord trusses inherently more resistant to galloping.

The connections between angles are also more fatigue-resistant than the typical tubular connections [4]. The number and size of anchor rods and other details used in Minnesota are also conservative compared with most other states. Because there have been essentially no failures or vibration problems in Minnesota, the new 2001 Specifications should not require these structures to be substantially redesigned. Calculations summarized in Section 2.4.1 of this report show that very few structures in the inventory of Minnesota Department of Transportation (Mn/DOT) sign support structures have to be modified at all to meet the 2001 Specifications. Therefore, those parts of the fatigue design provisions of the 2001 Specifications are not excessively conservative, or at least are not more conservative than some states' present practice.

In addition to corrosion problems, there are numerous reports of excessive vibration and fatigue cracking in light poles [13]. Aluminum light poles appear to be especially susceptible to vibration and fatigue because the modulus of elasticity and the fatigue resistance are three times less than those

TABLE 2-1 Documented excessive vibration and fatigue cracking of sign, signal, and light support structures

Location	Date	Failed Component(s)	Notes
AK	1994	Column base	High-mast luminaires
AR	?	Column base	Cracked fillet welds between baseplate and stiffener
		Truss connections	Cracked tube-to-tube welds
CA	1995	Column base	Failure of VMS after 18 months Loose/missing anchor rods Cracks around hand holes and baseplate detail
	1999	Column base	Failure from socket-weld cracking
CO	1994	Mast arm connection	Failures in 3 sign structures over 5 years old
CT	1996	Anchor bolt	Crack found during inspection
		Truss connection (Alum.)	Crack found during inspection
FL	1996	?	Excessive deflections on bridge support overhead VMS structure
	1997	Mast arm connections	15-m span signal support structure
GA	1994	Anchor bolt	Failed bridge support structure
ID	?	Truss connections (Alum.)	Tube-to-tube welds
IL	?	Mast arm connection	
KS	1997?	?	Failure of numerous signal structures
KY	?	Column base	Cracks found in fillet welds connecting stiffener
		Truss connections (Alum.)	50 cracked tube-to-tube welds
LA	?	Anchor rods	Found to be loose/missing
MD	?	High-mast luminaires	Weathering steel
MI	1990	Anchor rods	Failure of 2 sign structures with truss-type mast arms; others found loose/missing
	?	Mast arm connection	Cracks in pipe wall at weld termination
	?	Truss connections	Cracks in pipe wall near tube-to-tube weld
MN	1999	Handhole	Crack found near handhole
MO	1996	Mast arm connection	Failures of several signal support structures
NE	?	Monotube signs	
NV	1996	?	Failure of VMS structure
NH	1993?	Truss connections (Alum.)	Found many cracks during inspection (Fig 2-1)
NJ	1995	?	Excessive deflections on VMS
		Column base	Failures of light poles
NM	1992	Column base	Failure of VMS socket joint after only a few weeks
	?	Anchor rods	Found to be loose/missing
	?	Hand hole	Cracking discovered
NY	?	Anchor rods	Found to be loose
		Hand hole	Cracks discovered
NC	?	Anchor rods	Found to be loose/missing
ND	1998	?	Excessive vibration of 15-m span signal
OR	1993	Column base	Failure of 25% of 160 straight square light poles in 6 months
TX		?	Excessive vibration of signal poles
		Anchor rods	Found to be loose/missing
VA	1993	Column base, Anchor rods	Cantilevered variable message sign
	1996	?	Cantilevered variable message sign
	?	Truss connections	Cracked tube-to-tube welds
	?	Anchor rods	Found to be loose
WA	?	Anchor rods	Found loose or missing in cantilever sign structures
		Truss connections	Cracked welds at ends of diagonals
WV	?	Anchor rods	Found cracked/loose/missing during inspection
	?	Column base and mast arm connections	Cracks found at toe of groove weld, toe of fillet weld in socket joint, and fillet weld of stiffener, broken U-bolts
WI	1997	Numerous	See discussion in text
WY	1995	Mast arm connection	Cracks in 30% of signal structures inspected
		Anchor rods	Found to be loose/missing

of steel are. The driving force for these problems is believed to be vortex shedding, although there are also numerous problems with bridge-mounted light poles that may be excited by traffic-induced vibrations in the bridge.

In many cases where vibration of light poles (not on bridges) was observed, it was reported to be in double curvature or triple curvature (commonly referred to as the second or third mode, although the actual mode number is usually greater than two or three). This observation is consistent with the Strouhal relation, which would indicate that the diameter of most light poles is too small for first-mode vibration [4]. *NCHRP Report 412* [4] only considered first-mode vibration of light poles.

It is notable that many of the light poles experiencing fatigue cracking are tapered. *NCHRP Report 412* stated that tapered light poles should generally not be susceptible to vortex shedding and associated vibration or fatigue. This assertion was based on the *Ontario Highway Bridge Design Code* (OHBDC), which has extensive provisions for designing light poles against vortex shedding [14]. The OHBDC states that the vortex shedding should only take place on a tapered pole over a range in diameters from −10 percent to +10 percent of the critical diameter from the Strouhal relation. The research team's calculations showed that the resulting vortex shedding forces would not be significant; therefore, the research team decided it was best to just exempt tapered poles from the vortex-shedding requirements.

Researchers from University of Western Ontario, where the wind tunnel testing to support the OHBDC vortex-shedding provisions was performed, believe that the "plus-to-minus 10 percent of the diameter" rule, in conjunction with first-mode, vortex-shedding pressures, is no longer valid. The numerous field observations of vibration and fatigue would also seem to confirm that the rule is not valid. Changes to the 2001 Specifications are proposed in Chapter 3 to correct this problem.

Florida has installed thousands of new cantilever, monotube signal support structures since it lost nearly all the span-wire-mounted traffic signals in the path of Hurricane Andrew in 1992. Some of these structures have spans as long as 27 m (90 ft), and, perhaps not surprisingly, the structures are having problems with vibration of these long flexible mast arms. According to a recent article in *Civil Engineering* magazine [15], Florida DOT had two mast arms collapse in 1997.

Traffic signal structures in Wyoming have also experienced fatigue damage. Two structures collapsed as a result of fatigue cracking of the mast-arm-to-post box connection. Calculations performed on these failed structures show that the structures are underdesigned with respect to the 2001 Specification provisions. Subsequent inspections revealed that nearly one-third of the more than 800 poles inspected had visible fatigue cracks at the surface of the post near the base of the weld between the built-up box and the post. The cracking, which usually propagates from the corners of the box connection, was found on both the top and the bottom of the connection. Similar vibration and cracking of mast arm connections of signal support structures has also occurred in North Dakota and the City of Denver. In Denver, cracking of the baseplate connection also occurred.

California had been using a cantilevered bent-monotube support structure for some of its VMSs. One of these VMS support structures on Interstate 15 failed in 1995. Further inspections of the more than 200 statewide VMS structures revealed that many of the structures had fatigue cracks at the post-to-baseplate connection.

Four wind-loading phenomena were identified in *NCHRP Report 412* as possible sources of large-amplitude vibrations that could lead to fatigue failures (i.e., galloping, vortex shedding, natural wind gusts, and truck-induced wind gusts). As is indicated in Table 2-2, different structural types are affected by different wind-loading phenomena.

TABLE 2-2 Susceptibility of types of support structures to various wind-loading phenomena

Type of Structure	Galloping	Vortex Shedding	Natural Wind	Truck Gusts
Cantilevered Sign (one- or two-chord)	X		X	X
Cantilevered Sign (four- chord)			X	X
Bridge Support Sign or Signal		*	X	X
Cantilevered Signal	X		X	X
Luminaire		X	X	

Note: X indicates structure is susceptible to this type of loading
* Vortex shedding has occurred in a monotube bridge support (overhead sign) and can occur in cantilevered structures if the sign or signal attachment is not attached.

As stated in the note to Table 2-2, bridge supports fabricated as a monotube have been susceptible to vortex shedding. It is not clear if two-chord trusses in bridge supports are susceptible to vortex shedding (from the signs) or galloping, because two-chord bridge supports (i.e., overhead support structures) are not very common. However, because this susceptibility has never been reported, it seems clear that three-dimensional, three-chord or four-chord trusses are not susceptible to excessive vibration from vortex shedding or galloping. Presumably, the resistance of three-dimensional trusses to galloping arises from the additional torsional stiffness relative to monotube and planar two-chord trusses. (Galloping requires twisting of the mast arm, as well as vertical motion.) It should be sufficient to design these three-chord and four-chord bridge supports for natural wind and truck-induced wind gusts only.

Cantilevered sign support structures fabricated in three- or four-chord trusses have also never been reported to vibrate from vortex shedding or galloping. Therefore, it is concluded that even cantilevered four-chord trusses do not need to be designed for the galloping load. Three-chord trusses for cantilevered structures are not as common as they are for bridge supports, and, therefore, no statement can be made about their performance in cantilevered structures.

If the number of cycles before failure exceeds the number of cycles of the fatigue threshold or constant-amplitude fatigue limit (CAFL), then an infinite-life fatigue design approach may be used. For example, the number of cycles associated with the CAFL for Category E is about 10 million cycles. If the structure were to vibrate at 1.0 Hz, it would accumulate 3,600 cycles per hour. If the structure vibrated for 100 h every year (about 1 percent of the time), it would accumulate over 10 million cycles in 28 years. For better details such as Category C, the CAFL occurs at only about 3 million cycles, which would be reached in just over 8 years.

The infinite-life approach for fatigue design was developed in previous NCHRP research [16] and is used in the AASHTO LRFD Bridge Specifications [11]. One advantage of the infinite-life approach for structures with complex stress histories is that it is not necessary to accurately predict the entire future stress range distribution. The fatigue design procedure simply requires an estimate of the stress range with an exceedence level of 1:10,000, which is called the "fatigue-limit-state stress range." The infinite-life approach relies upon the CAFL as the parameter determining the fatigue resistance. The emphasis in fatigue testing of details should, therefore, be on defining the CAFL.

The fatigue-limit-state wind loads and the fatigue detail categorization from *NCHRP Report 412* were incorporated into the 2001 Specifications for the design of cantilevered signal, sign, and luminaire support structures. In a few cases, changes were made to the 2001 Specifications that made the specifications more stringent than those proposed in *NCHRP Report 412* were. In particular, a fatigue design requirement was added for circular tubular members that AWS D1.1 Category K_2 fatigue curve be satisfied for the punching shear stress range. This particular provision of the American Welding Society (AWS) is known to be overly conservative. This new provision has made it difficult if not impossible to design a typical box-type connection of a mast arm to a pole, often used in simple signal support structures. Wyoming has developed an alternative full-circle, ring-stiffened connection that will work. However, fabricators of this type of structure claim that the costs are unnecessarily increased because of the difficulty of complying with this provision.

Another contentious part of the 2001 Specifications is the importance factors, and these will be discussed in detail later in this chapter. The importance factors are used to allow different levels of reliability for structures in different environments.

The remainder of this chapter is arranged in the seven emphasis areas of the Phase II research:

- VMS issues;
- Mitigation strategies;
- Characterization of at-risk structures;
- Quantification of importance factors;
- Anchor rod tightening research;
- Design examples; and
- Training materials and guidance on design, installation, inspection, and maintenance.

2.2 VMS ISSUES

VMSs installed on cantilevered support structures are susceptible to galloping, natural wind gusts, and truck-induced wind gusts. VMSs mounted on bridge supports are not expected to be susceptible to galloping due to the torsional rigidity of the sign bridge. However, bridge supports are still expected to be susceptible to natural wind gusts and truck-induced wind gusts.

As shown in Table 2-1, there was a collapse of one cantilevered VMS and cracks found in several similar VMSs in California in 1995. Instrumentation and monitoring showed that these structures were galloping in steady winds. There was a collapse in 1993 of a VMS in Virginia that was believed to be due to truck-induced wind gusts. Truck-induced wind gusts are also believed to be the cause of excessive vibration of VMS structures in New Jersey and Florida. There have also been failures of VMSs in Nevada and New Mexico, although the cause of these failures hasn't been reported.

VMSs have sometimes been mounted on structures intended only to support ordinary flat-panel signs that weigh much less without making calculations of the effect of the additional load and area of the VMS. Explicit calculations must be performed for both the strength and the fatigue resistance for these VMS structures. Engineers often believe that the additional mass of these VMSs has contributed to the problems. However, the extra mass would primarily affect

the strength and dead-load deflection, whereas the problems have been fatigue cracking and dynamic live-load deflection (i.e., vibration).

As far as the dynamic behavior and the fatigue resistance are concerned, the mass would only tend to decrease the natural frequency of the structure. This effect is typically countered by an increase in stiffness to control the dead-load deflection. Therefore, the additional area of the VMS, rather than the mass, is believed to cause the problems. The soffit area on the underside of the sign is especially believed to cause the problems.

2.2.1 Truck-Gust Loading Recommended in *NCHRP Report 412*

The passage of trucks beneath cantilevered support structures tends to induce gust loads on the frontal area and the underside of the members and the attachments mounted on the mast arms of these structures. The magnitude of natural wind-gust pressures is much larger than the pressures on the frontal area from truck-induced loading in the horizontal direction. Therefore, for the purposes of fatigue design, truck-induced wind loads normal to the sign are not critical and are not considered in design. The vertical truck-induced pressure on the underside of the members and attachments is of primary concern.

The observed motion of the VMS structure that eventually failed in Virginia confirms that the vertical pressure is of primary concern. This structure and similar structures were observed to be vibrating in the vertical plane.

VMSs are particularly susceptible to truck-induced wind gusts because of their thickness (i.e., depth) in the direction parallel to traffic flow that is exposed to this vertical pressure. Many of the VMSs are designed for a person to walk in and are up to 1.2 m or 4 ft in depth. New flat-panel technology is becoming available that may eliminate this problem.

DeSantis and Haig [17] modeled the sign structure that failed in Virginia. They used a simple model for the truck-gust load. The model assumed that the velocity of the wind in the upward direction was equal to the truck velocity. The equivalent static truck-gust pressure was determined by using the static-wind-pressure formula where velocity V = 105 km/h (65 mph). To account for an increase in the relative truck speed due to head winds, the gust factor of 1.3 was also included. DeSantis and Haig showed that applying this wind load in a static analysis gave a displacement that was consistent with the observed amplitude of the vibration.

The fatigue loads provided in the 2001 Specifications are load ranges (i.e., double amplitudes) because they are supposed to be used to calculate stress ranges. Because the applied truck-gust pressure obtained from the assumptions described previously is calibrated to the amplitude of the vibration (i.e., maximum minus mean), the pressure is doubled to represent the range (i.e., maximum minus minimum), assuming that on the first cycle the downward and upward displacements are equal. Using these assumptions, an equivalent static vertical pressure range of 1,760 Pa (36.6 psf) can be obtained.

This pressure must be multiplied by the appropriate drag coefficient and the area projected onto a horizontal plane to determine the vertical truck-gust force range. This force range is applied in a static analysis without combining this load with any other loads. The value of the "stress" obtained from that analysis actually represents the stress range. The stress range should be compared with the CAFL of the details to ensure resistance to fatigue.

Drag coefficients are shown in Table 3-5 of the 2001 Specifications. A drag coefficient of 1.7 should be used for the drag coefficient of a VMS box, as is recommended in Note 7 of Table 3-5 of the 2001 Specifications. It is agreed that this drag coefficient is appropriate; however, at the time of *NCHRP Report 412*, a drag coefficient of 1.45 was typically assumed. Because DeSantis and Haig's analysis was calibrated to the observed displacement using a drag coefficient of 1.45 (resulting in a factored pressure of 2,550 Pa), a lower equivalent static pressure of 1,500 Pa should have been recommended to be used with the drag coefficient of 1.7 so that the result would be the same factored pressure (2,550 Pa).

2.2.2 Truck-Gust Pressure Measured on a Cantilever VMS Support Structure

In 1995, a cantilevered VMS support structure on Route 17 in northern New Jersey was observed to be vibrating significantly in the vertical plane. This VMS structure was taken down for fear it would develop fatigue cracks. In 1997, this same cantilevered VMS was erected at a different location on Interstate 80 in northern New Jersey. The structure was then instrumented and monitored for 3 months for the New Jersey Department of Transportation (NJDOT) [3, 18]. Details about this study are only summarized in the following.

Pressure transducers were mounted on the front face of the sign to measure vertical truck gusts at different heights above the bottom of the sign. These data exhibited a gradient with distance from the trucks, as did the truck-gust pressures measured in Florida by Cook et al. [19]. Linear extrapolation of the data from New Jersey indicates that the pressure would essentially go to zero at a height of 4.5 m (15 ft) above the bottom of the existing VMS box.

Measured stress ranges in the post from truck-induced wind gusts were as high as 14 MPa (2 ksi). The equivalent static pressure on the horizontal area of the sign and truss that would cause this stress range is 525 Pa (11 psf). This pressure is the worst-case equivalent static pressure that was deduced from the monitoring over a 3-month period.

The design truck-gust pressure recommended in *NCHRP Report 412* is about five times bigger than the maximum equivalent static pressure from strain gauge data in the New Jersey research. This would seem to suggest that design truck-gust pressure recommended in *NCHRP Report 412* was too

conservative. However, it is not believed that the design truck-gust pressure should be reduced to the level measured in New Jersey. The structure on Route 80 did not vibrate significantly the way it did previously on Route 17. Also, there were no significant natural winds during this period, and it is not known what synergistic effect this might have.

It is possible that the bottom of the VMS was farther from the tops of the trucks for this structure on Route 80 than for the structures that have vibrated significantly in Virginia and elsewhere. This structure on Route 80 was 5.4 m (17.8 ft) from the surface of the road. The gradient in the pressure is high, and this could explain the decreased effect for this structure.

Many engineers are concerned that the airfoils used on the cabs of the trucks cause a higher truck-induced pressure. Trucks with and without airfoils were run under the instrumented VMS on Route 80, and there was very little difference in the response, indicating that the airfoil does not cause greater pressure.

Conversations with researchers at Mack Trucks also indicated that airfoils should not cause increased pressure on the VMS. The purpose of the airfoils is to increase the fuel efficiency of the trucks. In order to do this, the airflow must be kept laminar as it passes over the trailer behind the cab. If the flow remains laminar, the upward gust will be lessened because the air flows along the trailer instead of going turbulently up into the bottom of the sign.

These researchers at Mack Trucks have done wind tunnel tests on trucks with and without airfoils. Their data confirm that the flow stays laminar along the trailer when airfoils are used. This information suggests that the presence of airfoils should not increase the dynamic pressure acting on the sign.

2.2.3 Testing of Monotube Cantilever VMS Support Structures in California

Field testing of cantilevered VMS structures has also been performed for Caltrans [9, 20]. Bent monotube cantilever VMS structures located on Interstate 15 (I-15) and California Highway 58 (R-58) were tested. The response (e.g., fundamental frequencies, damping ratios) of the I-15 structure, which was instrumented before erection, was observed under wind-induced loading. Conversely, the response of the R-58 structure was measured by means of free vibration test. A finite element analysis was also performed to determine the resonant frequencies of a typical Caltrans VMS structure. The three tests yielded similar results: fundamental frequencies slightly greater than 1 Hz (1.04–1.10 Hz) and damping ratios less than 1 percent of critical (0.4–0.7 percent).

Galloping occurred during the monitoring period, particularly when the hot, dry, steady Santa Anna winds blew down from the mountains. Stress ranges measured during galloping indicate that the static equivalent loads were as high as 2,000 Pa [9, 20]. This equivalent static load is twice the recommended value of 1,000 Pa from *NCHRP Report 412*. However, the high equivalent static pressure measured in California is not that unusual considering that the equivalent static pressures for galloping from the wind tunnel tests ranged up to 1,770 Pa (37 psf) and the equivalent static pressures from the field tests ranged up to 1,290 Pa (27 psf). It is known that the galloping load will continue to increase with increasing wind velocity.

It is felt that the steady-state winds at this location in California are possibly the worst in the country. Galloping requires torsional twisting motion; therefore, the bent monotube support structure may be particularly susceptible to galloping, especially when the sign is mounted eccentrically on the mast arm tube, as was done in this case. In view of these data, it is felt that the equivalent static design pressure range for galloping recommended in *NCHRP Report 412* is sufficiently conservative and represents a reasonable compromise between safety and practicality. At least these measurements show that the equivalent static design pressure range for galloping recommended in *NCHRP Report 412* is not overly conservative.

2.2.4 Finite Element Modal Analyses to Characterize Frequencies and Mode Shapes

Two commercially available computer programs, ABAQUS [21] and Visual Analysis [22] were used in the first two (of four total) finite element modal analyses of VMS structures. ABAQUS is a highly detailed program, while Visual Analysis is a user-friendly, straightforward program. Both programs were used to determine whether the time saved when using Visual Analysis was a worthwhile trade-off for any losses in accuracy and reliability that may result.

In ABAQUS, three-node, quadratic beam elements were used to model the cylindrical pipe members in each of the cantilevered VMS structures. Three-node, triangular plate elements were also used in the box-truss model to connect the truss to the post. Both VMS structures were modeled "full-scale" (i.e., exact member dimensions were used). Because only prismatic members were used, the finite element mesh size was not of great importance; however, all members were divided into sections approximately 0.3 m (1 ft) in length.

Visual Analysis used two-node beam elements and three- and four-node plate elements. Again, both structures were modeled full-scale. Analyses were run with two different mesh sizes. One mesh size was similar to the one used in the ABAQUS analyses. The other used the largest elements possible (i.e., nodes were only created at locations where members originating from different directions intersected).

For both programs, the VMS was modeled as a series of masses distributed over the area of the support structure covered by the sign. One lumped mass was applied to each node on the top and bottom chord located behind the sign. For the four-chord trusses, the masses were only applied to the chords adjacent to the sign. In order to distribute the sign mass uniformly, the quotient of the total mass and the number of nodes was applied to each node.

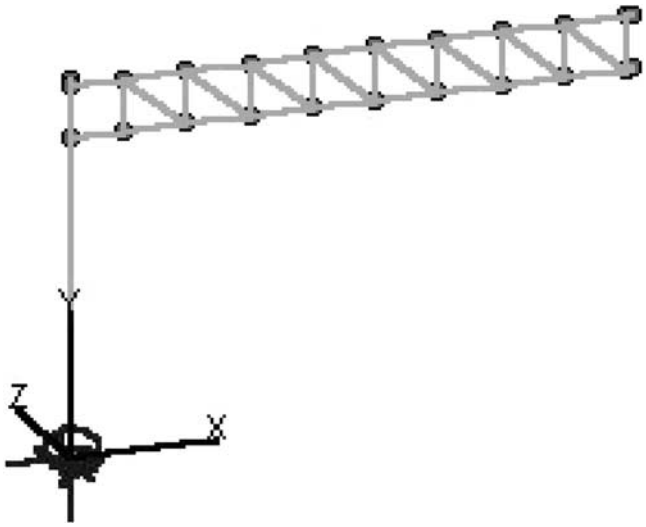

Figure 2-1. Finite element model of New Jersey VMS structure.

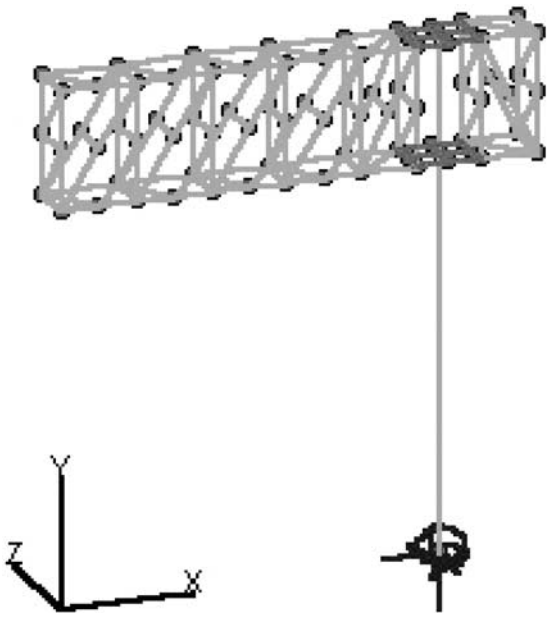

Figure 2-2. Finite element model of California VMS structure.

Anchor rods, foundations, and soil conditions were not considered in the analyses. Instead, the base of each structure was defined as the bottom of the post and was modeled as completely fixed (i.e., no displacement or rotation was allowed in any of the three principal directions). The interim report from the first phase of this project [23] showed that worst-case connection stress ranges result when the fixed-base assumption is employed. Thus, using a completely fixed base is a conservative estimation.

Dynamic modal analyses were conducted to determine the first six mode shapes and the corresponding modal frequencies for two cantilevered VMS structures: a two-chord truss used in New Jersey (see Figure 2-1) and a four-chord box truss used in California (see Figure 2-2). The two-chord New Jersey structure was chosen because experimental data collected by Johns and Dexter [18] could be used to verify the validity of the finite element model. The structure is 9.1 m (29.9 ft) tall, and the cantilevered truss is 13.3 m (43.5 ft) long and 1.3 m (4.2 ft) high. Cross-section properties of the round tubular members used in the steel structure can be found in Table 2-3.

The frequencies for all three finite element models (one ABAQUS and two Visual Analysis with varying mesh sizes) agreed quite well with the experimental values for the first two modes. Drawings of the first two mode shapes can be found in Figures 2-3 and 2-4. The first mode involves twisting the structure about the axis of the post (i.e., the y-axis in Figure 2-3), resulting in out-of-plane or horizontal truss motion. The experimentally determined frequency for this mode was 0.87 Hz. ABAQUS predicted a frequency of 0.851 Hz, and Visual Analysis estimated values of 0.840 Hz and 0.834 Hz for the small- and large-member (coarse mesh) models, respectively.

The second mode involves in-plane bending of the post (i.e., bending about the z-axis in Figure 2-4), resulting in vertical truss motion. For the second mode (i.e., in-plane, vertical truss motion), the experimental frequency was 1.22 Hz, while the analytical values were 1.228 Hz, 1.186 Hz, and 1.174 Hz. These three results are all considered sufficiently accurate.

Experimental values were not available for the four higher modes, but the analytical values were still determined. For the third mode, the ABAQUS and small-member Visual Analysis frequencies were nearly identical (4.170 Hz and 4.160 Hz, respectively), while the large-member Visual Analysis value differed by 8 percent (3.826 Hz). Although none of the values were very similar, the large-member Visual Analysis values were in better agreement with ABAQUS than the small-member values for the two highest modes were. A complete

TABLE 2-3 New Jersey two-chord truss VMS structure cross-section properties

Member	Outside Diameter		Thickness	
	(cm)	(in.)	(mm)	(in.)
Post	66.0	26.0	15.9	0.625
Top and Bottom Chords	38.1	15.0	12.7	0.500
Verticals	14.1	5.56	9.5	0.375
Diagonals	14.1	5.56	9.5	0.375

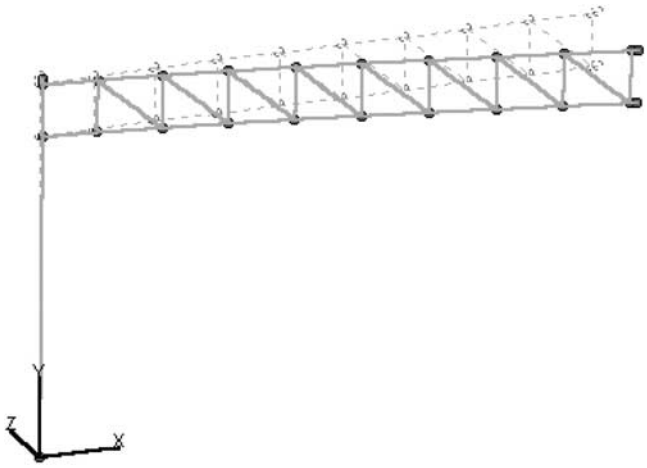

Figure 2-3. First-mode shape (out-of-plane) of NJDOT two-chord truss VMS structure.

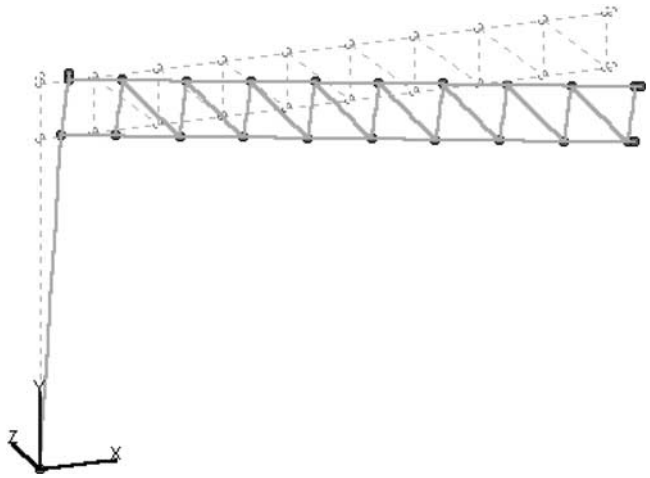

Figure 2-4. Second-mode shape (in-plane) of NJDOT two-chord truss VMS structure.

list of the modal frequencies for each of the first six modes and each of the finite element models is presented in Table 2-4.

The Caltrans structure was selected for modeling because its use is now widespread in California. It replaced the bent monotube structures (an example of this type of support is shown in Figure 2-5) similar to the one that collapsed from galloping in San Bernardino County in 1995 [20].

The steel Caltrans structure is 9.48 m (31.1 ft) tall. The truss is constructed exclusively of angles and is 8.69 m (28.5 ft) long, 2.18 m (7.2 ft) high, and 0.91 m (3.0 ft) deep. The length of the cantilevered portion of the truss is 7.09 m (23.2 ft). Cross-section properties of the members used in the structure can be found in Table 2-5.

In addition to the three types of analyses performed on the New Jersey structure (i.e., ABAQUS and two different member sizes in Visual Analysis), a fourth analysis was completed on the Caltrans structure. The additional analysis investigated the effectiveness of three-node, instead of four-node, plates in the connection of the truss to the post. The frequencies for all four finite element models were very similar. For the first mode (i.e., out-of-plane, horizontal truss motion), ABAQUS predicted a frequency of 1.630 Hz. Visual Analysis estimated values of 1.771 Hz, 1.857 Hz, and 1.764 Hz for the small-member four-node plate, small-member three-node plate, and large-member four-node plate models, respectively. For the second mode (i.e., in-plane, vertical truss motion), the analytical values were 1.948 Hz, 1.947 Hz, 1.922 Hz, and 1.910 Hz. Drawings of the first two mode shapes can be found in Figures 2-6 and 2-7.

Unlike the analyses of the New Jersey two-chord truss structures, the precision of the four different analysis types did not decrease greatly for the higher modes of the Caltrans structure. The greatest discrepancy between the two types of analysis is 16 percent for Modes 3–6. Assuming that the more detailed ABAQUS model is the most accurate of the four, the large-member (i.e., coarse mesh) model using the four-node plate elements is the most accurate of the three Visual Analysis models. A complete list of the modal frequencies for each of the first six modes for each of the finite element models is presented in Table 2-6.

Because the frequencies obtained using the large-member (i.e., coarse mesh), four-node plate model in Visual Analysis were not in great error relative to those determined with ABAQUS, Visual Analysis was deemed suitable for the modal analyses of the second pair of VMS structures. The only relatively large errors that existed when using Visual Analysis

TABLE 2-4 NJDOT two-chord truss VMS structure modal frequencies

Test Method	(Out-of-Plane) f_1 (Hz)	(In-Plane) f_2 (Hz)	f_3 (Hz)	f_4 (Hz)	f_5 (Hz)	f_6 (Hz)
Experimental	0.87	1.22	-	-	-	-
ABAQUS	0.851	1.228	4.170	5.411	7.532	10.251
V.A.-small	0.840	1.186	4.160	4.914	9.654	11.568
V.A.-large	0.834	1.174	3.826	4.843	8.903	11.046

Note:
V.A.-small represents small (i.e. 0.3 m) elements used in Visual Analysis
V.A.-large represents large elements used in Visual Analysis

Figure 2-5. At-risk bent monotube sign in foothills of Rocky Mountains.

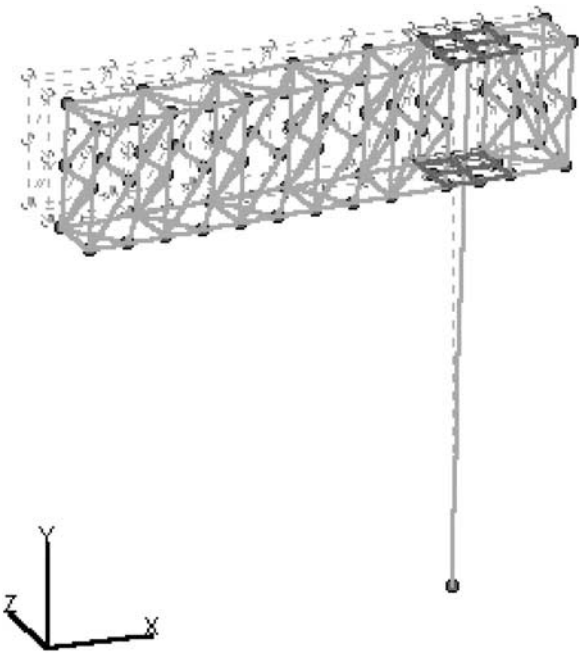

Figure 2-6. First-mode shape (out-of-plane) of Caltrans box-truss VMS structure.

occurred in the higher modes. However, probably all of the vibration and fatigue damage in sign and signal support structures occur as a result of vibration in the closely matched first or second modes. Therefore, the computation of the frequencies and mode shapes for the higher modes is not critical.

The third and fourth structures to be modeled were a pair of cantilevered Illinois Department of Transportation (IDOT) VMS structures. In one of the structures, the VMS is mounted on a single-plane Vierendeel structure (see Figure 2-8). The second VMS is mounted on a typical IDOT trussed flat-panel sign structure (see Figure 2-9).

The Vierendeel structure is constructed of steel structural tubes (with rectangular cross-section), the dimensions of which can be found in Table 2-7. The entire structure is 7.60 m (24.9 ft) tall, while the mast arm is 10.26 m (33.7 ft) long and 2.95 m (9.7 ft) tall. The weight of this VMS, as well as that of the box-truss-mounted VMS, was estimated by IDOT personnel to be 35.6 kN (8,000 lb). However, because the exact weight of the VMS was unknown, analyses were performed for various weights in 1-kip increments. When the estimated sign weight of 35.6 kN (8 kips) was used for the Vierendeel structure, the frequencies for the out-of-plane and in-plane mode shapes were calculated to be 1.283 Hz and 1.917 Hz, respectively. These first two mode shapes are shown in Figures 2-10 and 2-11. A complete list of the first six modal frequencies for the Vierendeel structure with sign weights varying from 0 kN to 53.4 kN (0–12 kips) is provided in Table 2-8.

The second IDOT structure uses a four-chord (i.e., box) aluminum truss supported by a steel post. The prismatic post is 7.16 m (23.5 ft) tall, 45.7 cm (18 in.) in diameter, and 14.3 mm (0.562 in.) thick. The truss is 9.45 m (31.0 ft) long, 1.68 m (5.5 ft) high, and 0.76 m (2.5 ft) deep and is constructed of

TABLE 2-5 California box-truss VMS structure cross-section properties

Member	Large Dimension[a]		Thickness	
	(mm)	(in.)	(mm)	(in.)
Post	610	24.0	12.7	0.50
Top and Bottom Chords	152	6.0	12.7	0.50
Verticals	76.2	3.0	6.4	0.25
Vertical Diagonals	76.2	3.0	6.4	0.25
Horizontals	44.5[b]	1.75[b]	6.4	0.25
Horizontal Diagonals	31.8[c]	1.25[c]	6.4	0.25
Interior Diagonals	44.5	1.75	6.4	0.25

[a] Large dimension refers to the outside diameter of the tubular post and the leg length of the symmetric angles used in the truss.
[b] Legs of horizontal members at the extreme tips of the truss and adjacent to the post are 50.8 mm (2.0 in.) long.
[c] Legs of horizontal diagonal members adjacent to the post are 50.8 mm (2.0 in.) long.

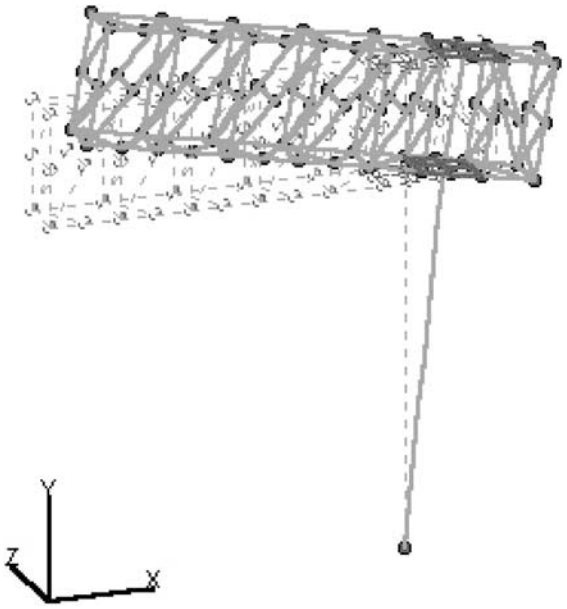

Figure 2-7. Second-mode shape (in-plane) of Caltrans box-truss VMS structure.

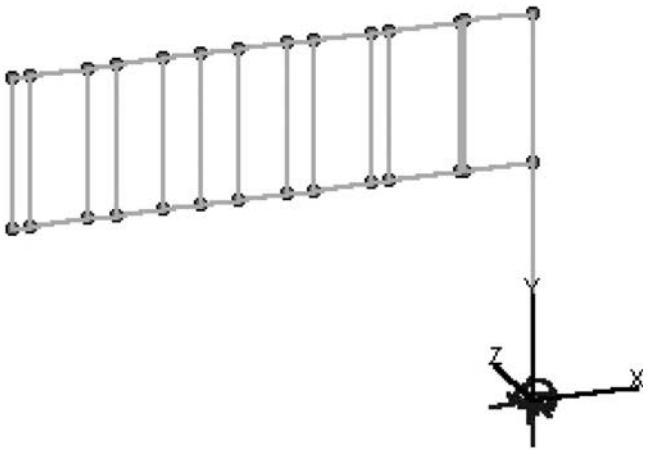

Figure 2-8. Finite element model of IDOT Vierendeel VMS structure.

round tubular members, the dimensions of which can be found in Table 2-9. The first two modal frequencies for the box-truss structure were calculated to be 1.021 Hz (out-of-plane) and 1.353 Hz (in-plane). Figures 2-12 and 2-13 depict the first two mode shapes for the box-truss structure. A complete list of the first six modal frequencies for the box-truss structure with sign weights varying from 0 kN to 53.4 kN (0–12 kips) is provided in Table 2-10.

2.2.5 VMS Pull-Down Testing in Illinois to Characterize Frequencies and Damping Ratios

To verify the accuracy of the finite element analyses, as well as to determine damping ratios, pull-down tests were performed on the two VMS structures in the Chicago area on August 7–8, 2000. Both structures were mounted in the center median of the I-90/I-94 (Kennedy) Expressway and were used to provide information regarding the availability of the center express lanes.

The Vierendeel structure faces the southeast-bound lanes at Mile Marker 84 near the Lawrence Avenue overpass (see Figures 2-14 and 2-15). Three strain gauges were bonded to the post approximately 40 cm (16 in.) above the baseplate. Two gauges were placed on the side of the post directly under the mast arm to measure mast arm motion in the vertical plane (i.e., in-plane motion). The third gauge was placed on the side of the post facing approaching traffic to capture horizontal mast arm motion (i.e., out-of-plane motion) (see Figures 2-16 and 2-17). Strain readings were recorded at a frequency of 50 Hz using a Campbell Scientific CR9000 datalogger.

Periodic loads were applied to the tip of the cantilever by hand to induce large-amplitude resonant oscillations. The rope used to apply the loads was then released, and the structure was allowed to vibrate freely for approximately 1 min. A sample in-plane strain trace covering both the loading and free vibration portions of the test is shown in Figure 2-18. In the figure, the load was released at a time of approximately 9 s or 10 s. As the figure shows, there are two distinct parts of the strain trace. The damping ratio changes from a very high value to a relatively low value after the first handful of cycles. For this particular example, the damping ratio was 1.80 percent for the first nine cycles and only 0.19 percent between the ninth and seventy-first cycles.

TABLE 2-6 Caltrans box-truss VMS structure modal frequencies

Test Method	(Out-of-Plane) f_1 (Hz)	(In-Plane) f_2 (Hz)	f_3 (Hz)	f_4 (Hz)	f_5 (Hz)	f_6 (Hz)
ABAQUS	1.630	1.948	3.700	7.045	11.333	26.544
V.A.-small-4[1]	1.771	1.947	4.047	6.926	11.171	22.929
V.A.-small-3[2]	1.857	1.922	4.182	6.924	11.334	23.229
V.A.-large-4[3]	1.764	1.910	3.804	6.911	11.084	22.889

[1]V.A.-small-4 represents small (i.e. 0.3 m) beam and 4-node plate elements used in Visual Analysis.
[2]V.A.-small-3 represents small (i.e. 0.3 m) beam and 3-node plate elements used in Visual Analysis.
[3]V.A.-large-4 represents large beam and 4-node plate elements used in Visual Analysis.

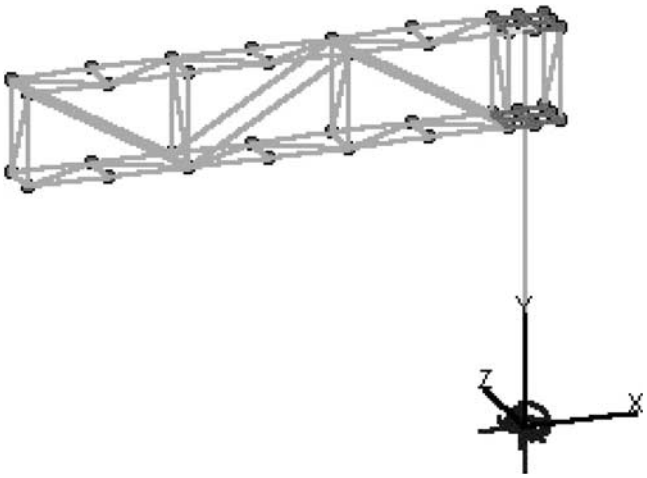

Figure 2-9. Finite element model of IDOT box-truss VMS structure.

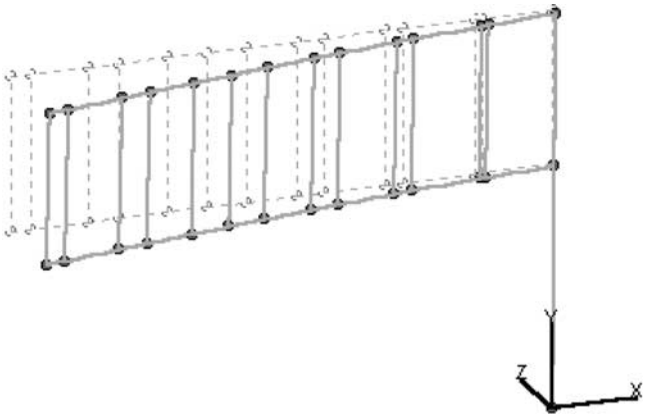

Figure 2-10. First-mode shape (out-of-plane) of IDOT Vierendeel VMS structure.

The change in damping ratio occurred during every in-plane test. Independent of the initial strain range and the cycle number, the change occurred whenever the strain range was reduced to approximately 20 or 30 microstrain. In terms of stress, this corresponds to about 4–7 MPa (0.6–1.0 ksi). For instance, when the initial strain range was 95 microstrain in Figure 2-18, the sharp change in damping ratio occurred after nine cycles (when the strain range was reduced to roughly 30 microstrain). However, when the initial strain range was only 48 microstrain in another test, the sharp change in damping ratio occurred after only four cycles (at which point the strain range was just below 30 microstrain).

The average measured in-plane frequency was 1.71 Hz, independent of the strain range. The high-amplitude damping ratio (i.e., before the sharp reduction) varied from 0.78 percent to 2.77 percent, depending on the gauge analyzed and the peak points that were chosen to calculate the damping ratio. On average, the high-amplitude damping ratio was 1.71 percent. The low-amplitude damping ratio (i.e., after the sharp reduction) varied from 0.09 percent to 0.31 percent and averaged 0.20 percent.

Although the extremely low damping ratios after the sharp change initially may seem to be a large fatigue-related problem, they are actually quite insignificant. As noted previously, the damping ratio decreased when the strain range was less than 30 microstrain, which equates to a stress range of 6.2 MPa (0.9 ksi). Even the worst fatigue details (Categories ET and K_2) have constant amplitude fatigue limits greater than 6.2 MPa (8 MPa [1.2 ksi] and 7 MPa [1.0 ksi], respectively). Thus, the stress cycles that occur when the damping ratio is small are not large enough to create fatigue damage, and, in turn, the long time it takes to completely dissipate the stress is not harmful to the structure.

Unlike the in-plane damping ratio, the out-of-plane damping ratio was independent of the strain range (see Figure 2-19). Because of time constraints, only two out-of-plane tests were run. Measured damping ratios were 0.56 percent and 0.73 percent (0.65 percent average). The out-of-plane natural frequency was 1.22 Hz.

The measured frequencies differ from the analytical values for a 35.6-kN (8-kip) VMS of 1.283 Hz and 1.917 Hz (for out-of-plane and in-plane, respectively) by only 5 percent and 12 percent. In addition to the uncertainty in the sign weight, another possible explanation for the small discrepancy between the experimental and finite element values may be that the base of the structure was modeled to be completely fixed. A structure with a partially fixed base would be more flexible and would subsequently have a lower frequency.

The box-truss structure faces the northwest-bound traffic on the south side of Hubbard's Cave near Mile Marker 50

TABLE 2-7 IDOT Vierendeel VMS structure dimensions

Member	Tube Dimension 1*		Tube Dimension 2		Thickness	
	(cm)	(in.)	(cm)	(in.)	(mm)	(in.)
Post	46.7	18.375	61.0	24	19.1	0.75
Top and Bottom Chords	45.7	18	15.2	6	12.7	0.5
Verticals	45.7	18	15.2	6	12.7	0.5

* Dimension 1 is dimension parallel to traffic flow

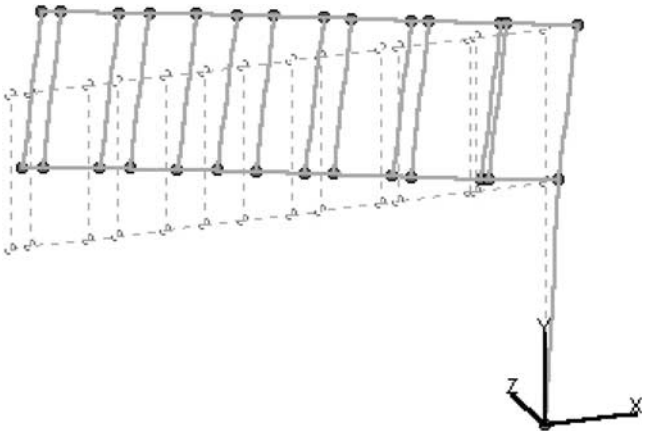

Figure 2-11. Second-mode shape (in-plane) of IDOT Vierendeel VMS structure.

(see Figures 2-20 and 2-21). Three strain gauges were also applied to this structure: two measuring in-plane motion and one measuring out-of-plane motion.

Because of an unfortunate loss of power to the data-logger when the tests were completed, the data files were lost. However, strain readings were displayed on a computer screen while the tests were being conducted, allowing an analysis to be made. From visual inspection of the signal, the damping ratio of the box-truss structure was noticeably smaller than that of the Vierendeel structure. Little reduction in displacement of the truss tip was observable after 30 s of free vibration. The strain range appeared to decrease by approximately one-fourth after 10 free vibration cycles, which corresponds to a damping ratio of just less than 0.5 percent.

Although no experimental frequencies compare with the analytical values, there is no reason to believe that the analytical frequencies for the box truss are in much greater error than the analytical values for the Vierendeel structure were. In addition, the in-plane frequency of the box-truss structure was definitely less than that of the Vierendeel structure (it took less frequent pulls of the rope to excite the box-truss structure), as the finite element analyses suggest.

2.2.6 Spectral Finite Element Analyses to Investigate Effects of Natural Wind-Gust Loading

Spectral analyses were also performed using ABAQUS and the finite element models of the New Jersey and California cantilevered VMS structures discussed in the previous section. The spectral analyses were performed to investigate

TABLE 2-8 IDOT Vierendeel VMS modal frequencies

Total Sign Weight (kips)	Sign Mass per Node ($k\text{-}s^2/ft$)	(Out-of-Plane) f_1 (Hz)	(In-Plane) f_2 (Hz)	f_3 (Hz)	f_4 (Hz)	f_5 (Hz)	f_6 (Hz)
0	0	1.742	2.571	5.258	7.533	8.805	16.766
1	0.002588	1.657	2.452	5.052	7.251	8.456	16.180
2	0.005176	1.583	2.347	4.867	7.002	8.146	15.665
3	0.007764	1.518	2.255	4.699	6.780	7.868	15.208
4	0.01035	1.461	2.173	4.546	6.581	7.618	14.796
5	0.01294	1.410	2.100	4.407	6.399	7.390	14.422
6	0.01553	1.363	2.033	4.279	6.233	7.181	14.079
7	0.01812	1.321	1.972	4.161	6.079	6.989	13.762
8	**0.02070**	**1.283**	**1.917**	**4.052**	**5.938**	**6.813**	**13.470**
9	0.02329	1.248	1.866	3.951	5.806	6.649	13.176
10	0.02588	1.215	1.818	3.857	5.682	6.496	12.836
11	0.02847	1.185	1.774	3.769	5.567	6.353	12.520
12	0.03106	1.157	1.734	3.687	5.458	6.219	12.227

TABLE 2-9 IDOT box-truss VMS structure dimensions

Member	Outside Diameter		Thickness	
	(cm)	(in.)	(mm)	(in.)
Post	45.7	18	14.3	0.562
Top and Bottom Chords	14.0	5.5	7.9	0.312
Verticals	4.45	1.75	4.8	0.188
Vertical Diagonals	6.35	2.5	4.8	0.188
Horizontals	4.45	1.75	4.8	0.188
Horizontal Diagonals	4.45	1.75	4.8	0.188
Interior Diagonals	4.45	1.75	4.8	0.188

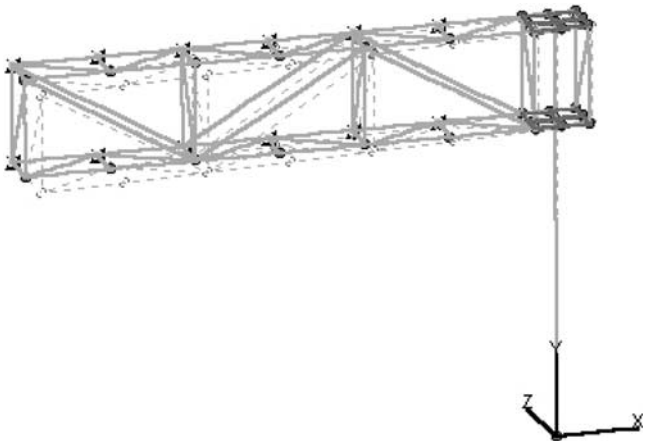

Figure 2-12. First-mode shape (out-of-plane) of IDOT box-truss VMS structure.

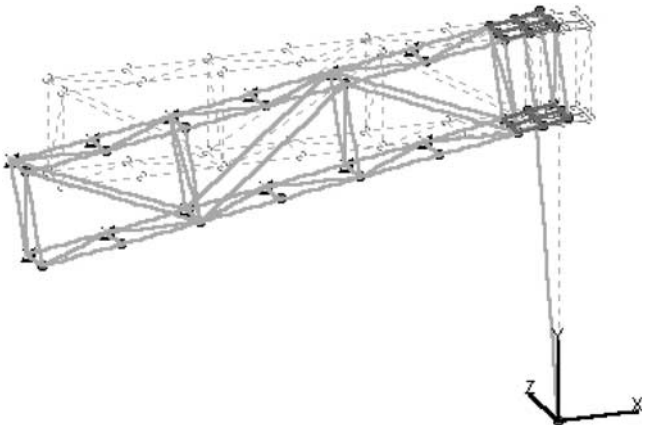

Figure 2-13. Second-mode shape (in-plane) of IDOT box-truss VMS structure.

TABLE 2-10 IDOT box-truss VMS modal frequencies

Total Sign Weight (kips)	Sign Mass per Node ($k\text{-}s^2/ft$)	(Out-of-Plane) f_1 (Hz)	(In-Plane) f_2 (Hz)	f_3 (Hz)	f_4 (Hz)	f_5 (Hz)	f_6 (Hz)
0	0	3.282	3.655	5.956	11.660	14.555	34.063
1	0.002588	2.237	2.748	5.488	8.711	10.472	22.478
2	0.005176	1.802	2.287	5.170	7.344	8.854	17.612
3	0.007764	1.550	1.999	4.893	6.509	7.868	14.941
4	0.01035	1.380	1.798	4.642	5.931	7.178	13.202
5	0.01294	1.257	1.647	4.415	5.500	6.656	11.954
6	0.01553	1.161	1.529	4.209	5.163	6.242	11.003
7	0.01812	1.084	1.433	4.023	4.889	5.903	10.248
8	**0.02070**	**1.021**	**1.353**	**3.855**	**4.660**	**5.619**	**9.632**
9	0.02329	0.968	1.285	3.703	4.464	5.374	9.113
10	0.02588	0.922	1.226	3.566	4.293	5.161	8.670
11	0.02847	0.882	1.175	3.441	4.141	4.974	8.285
12	0.03106	0.847	1.129	3.327	4.005	4.806	7.948

Figure 2-14. Approach side of IDOT Vierendeel VMS structure.

Figure 2-15. Leave side of IDOT Vierendeel VMS structure.

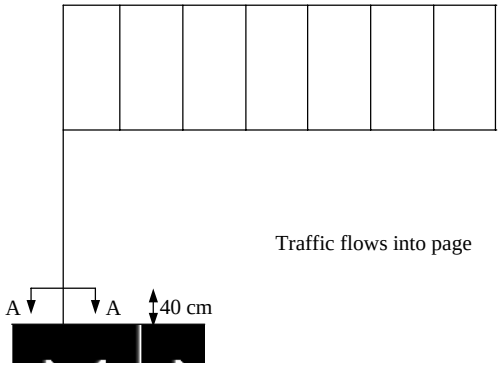

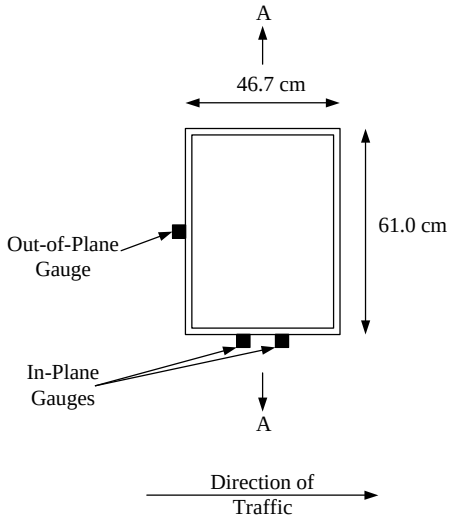

Figure 2-16. Gauge layout of IDOT Vierendeel VMS structure.

Figure 2-17. Instrumented IDOT Vierendeel VMS post.

the applicability of the natural wind-gust pressure equation recommended in *NCHRP Report 412* to VMS.

A time history of the wind velocity, the resulting pressure, or the structural response to the wind can be represented either as a function of time (i.e., in the time domain) or, by performing a Fourier Transform on the time history, as a function of frequency (i.e., in the frequency domain). In the spectral analysis, randomly occurring natural wind gusts and the associated drag forces are applied to a structure in the frequency domain (i.e., spectrally) instead of in the time domain. Strictly speaking, this type of analysis is only valid for linear systems. However, the relation of the drag force to the velocity is commonly linearized as an approximation. This type of spectral analysis is commonly used to estimate the statistics of the structural response to wind, ocean waves, earthquakes, and other random phenomena [24, 25].

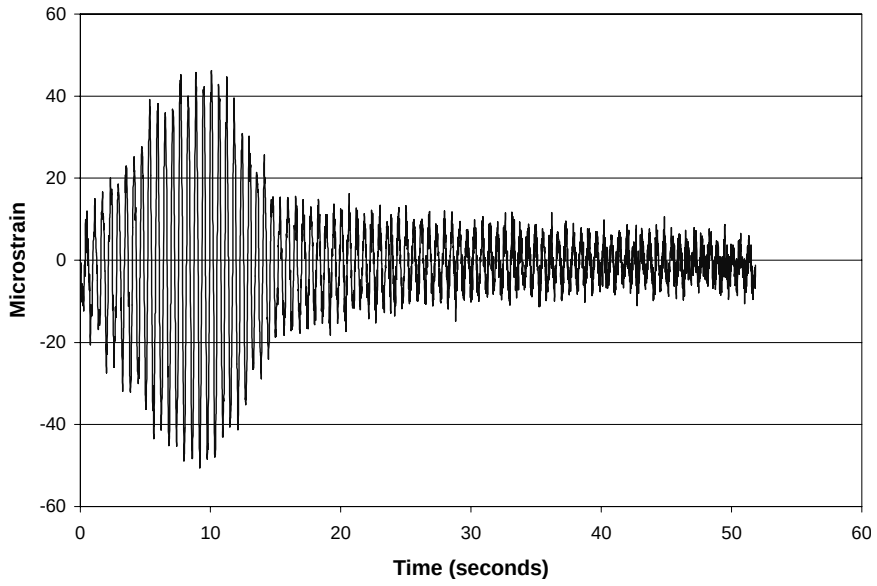

Figure 2-18. In-plane strain trace from IDOT Vierendeel VMS post.

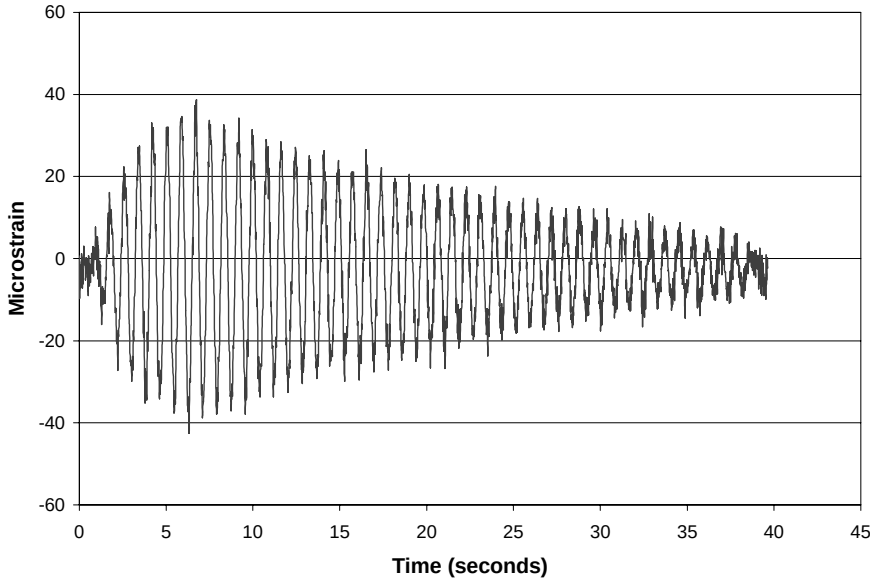

Figure 2-19. Out-of-plane strain trace from IDOT Vierendeel VMS post.

The velocity spectrum used in these analyses was developed by Davenport [26] and is depicted in Figure 2-22. As the spectrum shows, the magnitude of a particular wind gust is a function of the frequency of the gust. The most dominant gusts have frequencies near 0.01 Hz (i.e., one cycle every 100 s). The wind velocity spectrum is then transformed to create linearized force spectra. Drag force spectra are then applied to the structure of interest to obtain spectra of the dynamic stress at critical connection details. Equivalent static pressures causing similar connection stresses are then back-calculated.

The first step of the spectral analysis was to perform the finite element modal analysis on the structure to determine the first six natural frequencies, f_i. The results of the ABAQUS modal analyses for the NJDOT and Caltrans structures were presented in the previous section and summarized in Tables 2-4 and 2-6. The structure and its attachments were then divided up into a set of distinct vertical-plane surfaces exposed to the wind, to which the drag forces would be applied. Example vertical-plane surfaces include the frontal area of a sign and the horizontally projected area of a structural member. Distinct surfaces should not be divided into multiple smaller surfaces. The NJDOT structure was divided into 11 distinct surfaces, as shown in Figure 2-23. The surfaces are

- The VMS (one surface),
- The column (one surface),
- The exposed portions of the top and bottom chords (two surfaces),

Figure 2-20. Approach side of IDOT box-truss VMS structure.

Figure 2-21. Side view of IDOT box-truss VMS structure.

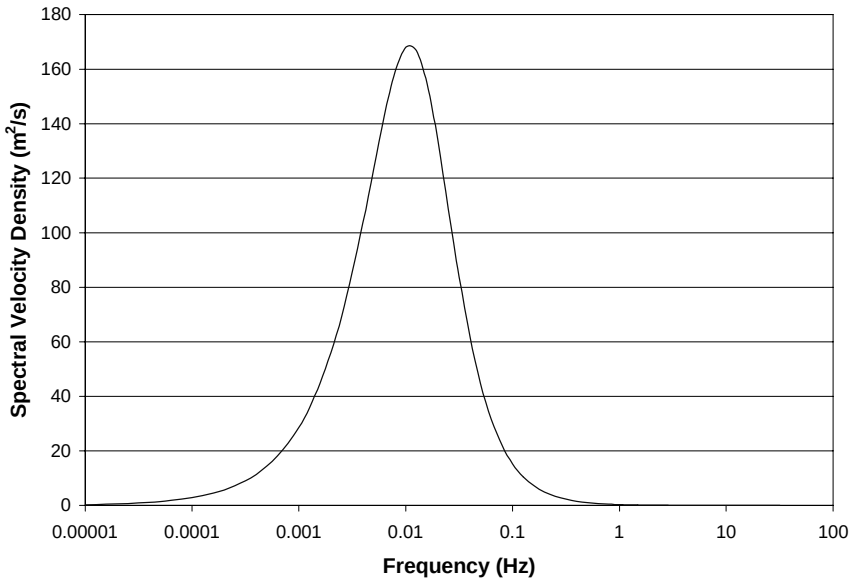

Figure 2-22. Velocity spectrum for $V_{10} = 17$ *m/s.*

- The exposed vertical struts (four surfaces), and
- The exposed diagonal struts (three surfaces).

After the individual surface areas and their centroids were determined, the drag coefficient (C_D) for each surface was identified. All values used in the analyses were taken from Table 3-5 of the 2001 Specifications. It should also be noted that a value of 1.7 was used for the drag coefficient of the sign, as is recommended in Note 7 of Table 3-5 of the 2001 Specifications.

The constant (C) was then calculated for each surface according to Morrison's Equation that relates the drag pressure (P) to the square of the velocity (V):

$$P = CV^2 \tag{2.1}$$

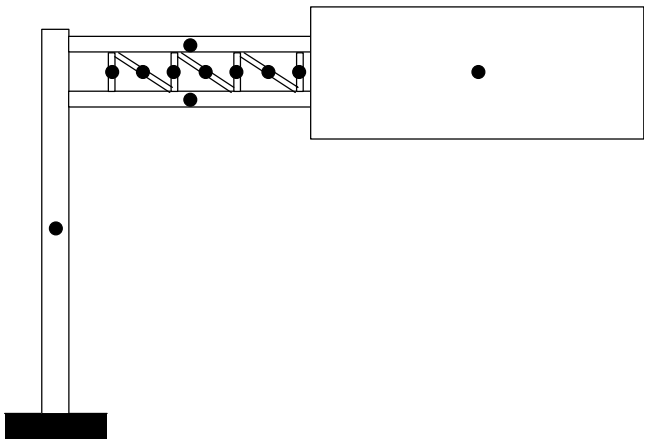

Figure 2-23. NJDOT VMS structure divided into distinct vertical-plane surfaces.

where

$$C = \frac{\rho C_D}{2}$$

and

ρ = the density of standard air (1.22 kg/m^3).

Each spectral analysis is for a stationary random process—that is, the mean wind velocity is assumed to be constant. Therefore, spectral analyses are carried out for a range of mean wind velocities. For fatigue analysis, it is not necessary to analyze the response to extreme wind speeds that have a mean recurrence interval greater than 1 year.

To cover this range in wind speeds, a set of five to ten 10-m (33-ft) wind speeds covering the range of 0–27 m/s (0–60 mph) is sufficient. Ten-meter (33-ft) wind speeds are typically used because most meteorological data are recorded at a standard height of 10 m (33 ft). One of the five to ten chosen wind speeds is used in each run of the analysis and is represented by the symbol V_{10}.

Wind speeds decrease exponentially as elevation decreases because of boundary layer effects. Therefore, 10-m wind speeds were reduced because of the elevation of the center of gravity of each surface, y, according to

$$V_y = V_{10}\left(\frac{y}{y_{10}}\right)^{1/7} \tag{2.2}$$

where

y_{10} = elevation of the center of gravity at 10-m elevation = 10 m (33 ft).

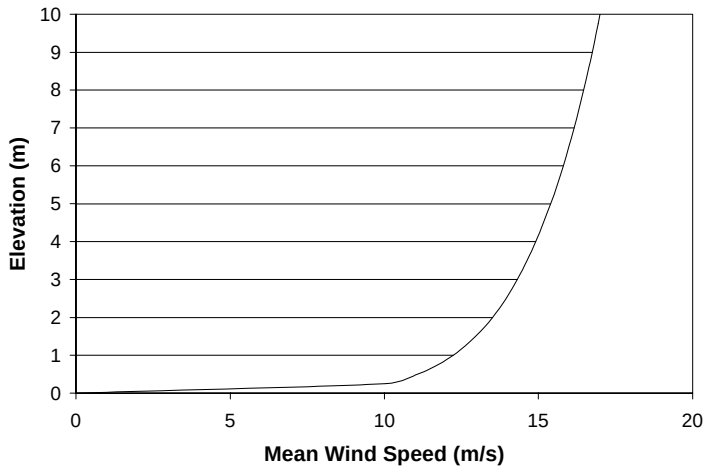

Figure 2-24. Mean wind velocity profile for $V_{10} = 17$ *m/s.*

Figure 2-24 shows the mean wind velocity profile for the case where the mean 10-m wind speed is 17 m/s (40 mph).

The fluctuating wind velocity results in fluctuating levels of drag forces. The velocity spectrum, which is outlined in detail below, can be converted to a force spectrum for each of the distinct surfaces. The following discussion shows how to calculate the conversion factor.

The drag force, *D*, acting on each surface can be defined as follows [27]:

$$D = \left(\frac{1}{2}\rho C_D\right) A V_y^2 = C A V_y^2 \tag{2.3}$$

where

A = the projected area of the body on a plane normal to the wind direction (m^2).

The turbulent wind velocity, V_y, can be divided into two components: the mean velocity, $\overline{V}_y$, and a fluctuating portion, V_y'. Hence,

$$V_y = \overline{V}_y + V_y' \tag{2.4}$$

$$\begin{aligned} D = C A V_y^2 &= C A\left(\overline{V}_y + V_y'\right)^2 \\ &= C A\left[\overline{V}_y^2 + 2\overline{V}_y V_y' + \left(V_y'\right)^2\right] \\ &\approx C A\left[\overline{V}_y^2 + 2\overline{V}_y V_y'\right] \end{aligned} \tag{2.5}$$

because the magnitude of the $(V_y')^2$ term is negligible relative to the other two terms. Similarly, the drag force, *D*, can be divided into mean and fluctuating components, $\overline{D}$, and D', respectively. Subsequently,

$$D = \overline{D} + D' \tag{2.6}$$

Similarly to Equation 2.3,

$$\overline{D} = C A \overline{V}_y^2 \tag{2.7}$$

From Equations 2.5, 2.6, and 2.7,

$$D = \overline{D} + D' = \overline{D} + 2CA\overline{V}_y V_y' \tag{2.8}$$

$$\therefore\ D' = 2CA\overline{V}_y V_y' \tag{2.9}$$

Multiplying both sides of Equation 2.9 by $\overline{V}_y$ yields:

$$D'\overline{V}_y = 2\left[CA\left(\overline{V}_y\right)^2\right]V_y' = 2\overline{D}V_y' \tag{2.10}$$

Therefore, the conversion factor, *H*, which is defined as the ratio of the fluctuating drag force to the fluctuating velocity, equals:

$$H = \frac{D'}{V_y'} = 2\left(\frac{\overline{D}}{\overline{V}_y}\right) = 2CA\overline{V}_y \tag{2.11}$$

Any random response, such as the gustiness of natural wind, can be represented as the summation of a series of periodic, sinusoidal waves. In turn, a series of periodic waves can be represented in the form of a spectral density curve. Figures 2-25, 2-26, and 2-27 illustrate this concept. Figure 2-25 shows the peak portion of a velocity spectrum divided into 10 equal-width bins. Each bin is represented by its average frequency ($\overline{\omega}_i$, where *i* varies from 1 to 10). The area of each bin is directly proportional to the amplitude of the corresponding wave. The 10 waves representing each of the bins are shown in Figure 2-26. Note that the three waves that dominated the velocity spectrum (e.g., $\overline{\omega}_1$ to $\overline{\omega}_3$) have the largest amplitudes. Figure 2-27 depicts the "random" velocity wave created by summing the 10 sine waves in Figure 26 using a random phase angle.

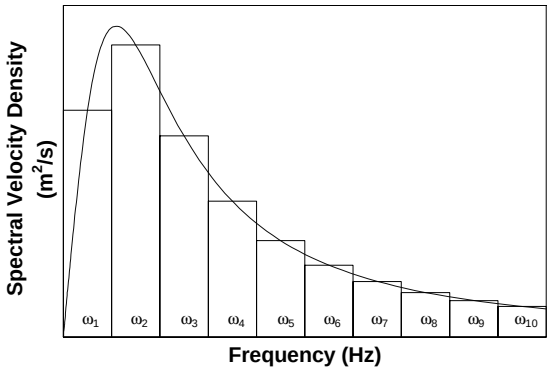

Figure 2-25. Wind velocity spectrum.

The velocity spectrum, $S_{v,i}(f_i)$, used in these analyses (and shown in Figure 2-22) was taken from the literature [26] and is defined by the following equation:

$$S_{v,i}(f_i) = \frac{4KV_{10}^2 x_i^2}{f_i(1+x_i^2)^{4/3}} \tag{2.12}$$

where the appropriate terrain coefficient, K, for open, grassy terrain (i.e., the worst case) is 0.005 and the dimensionless quantity x_i is defined as:

$$x_i = \frac{(1{,}200)f_i}{V_{10}} \tag{2.13}$$

(Note: 1,200 is in meters, and the velocity V_{10} must be in meters per second.) Only velocities (and forces) with frequencies similar to those of the structure will incite resonance. Thus, the response of the structure is "narrow-banded" (i.e., there is only a narrow range of frequencies in the response). Therefore, it was only necessary to calculate the magnitudes of x_i and $S_{v,i}(f_i)$ for the first six frequencies of the structure. The portion of the velocity spectrum covering the frequencies of interest for the Caltrans structure is presented in Figure 2-28.

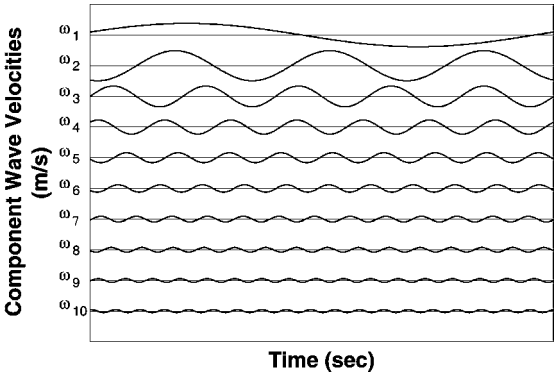

Figure 2-26. Component velocity waves from Figure 2-25.

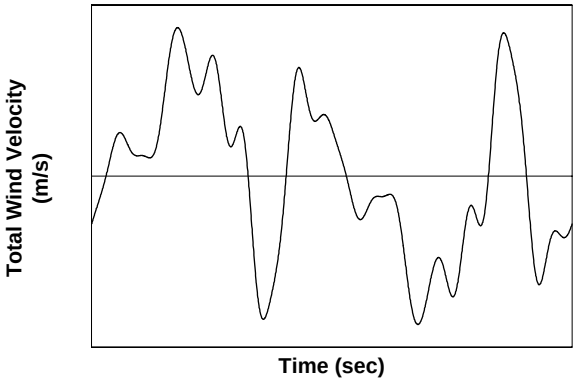

Figure 2-27. Sum of component velocity waves in Figure 2-26.

The magnitude of the force spectrum for each of the first six frequencies and for each surface, $S_{F,i}(f_i)$, was then calculated using the transform equation:

$$S_{F,i}(f_i) = H^2 S_{v,i}(f_i) \tag{2.14}$$

The calculated values of the force spectrum were then randomly applied to each surface and were completely correlated to each other through the use of a correlation function in ABAQUS. When two or more spectra are correlated, the resulting time histories are proportional and in phase such that peak loads occur simultaneously on all surfaces [24].

The primary results of interest from spectral analyses are the root-mean-squares (RMSs) of the stress response, σ_{rms}, at selected fatigue-critical connections. The RMS of the stress response, σ_{rms}, was converted to an effective stress range, S_r^{eff}, according to:

$$S_r^{eff} = 2.8\sigma_{rms} \tag{2.15}$$

Equation 2.15 is valid for a constant-amplitude wave where the amplitude of the wave is equal to 1.4 times the RMS. However, it can also be used as an approximation for random, narrow-banded time histories, like the one presented previously [24].

The next step is to back-calculate an equivalent static pressure range that, when applied in a static analysis, would give stress ranges equal to the S_r^{eff} calculated from the dynamic spectral analyses. In a linear analysis such as this, the stresses are all proportional. Therefore, the S_r^{eff} at any location from the spectral analysis can be used to back-calculate an equivalent static pressure range. In most cases, the largest stress ranges are at the column base (e.g., the Caltrans structure, as shown in Figure 2-29), so the S_r^{eff} at the column base was chosen for this calculation. (Note that Figure 2-30 shows that the peak dynamic stress ranges in the NJDOT structure were actually in the chords rather than the column base, although this location doesn't matter.)

The equivalent static pressure range is then "normalized" by dividing by the drag coefficient. The normalized equivalent

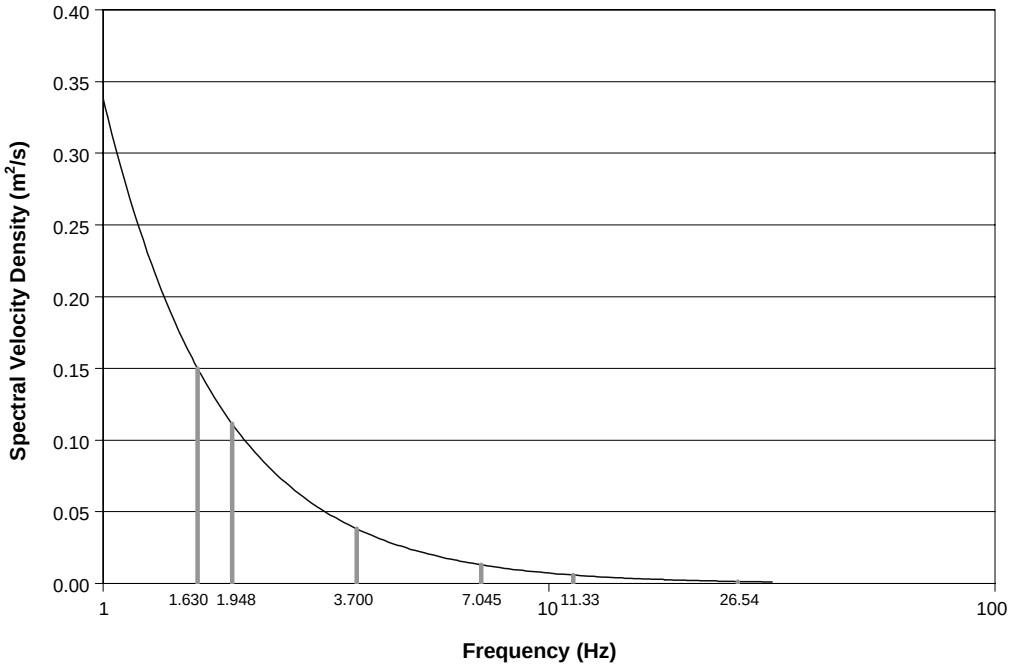

Figure 2-28. Velocity spectrum for V_{10} = 17 m/s emphasizing frequencies of interest.

static pressure range can then be applied to a variety of different surfaces by multiplying by the appropriate drag coefficient. Figures 2-31 and 2-32 show equivalent normalized static pressure ranges versus mean wind speeds for both structures.

At this point, only the equivalent static pressure range for the chosen mean (10-m) velocity had been determined. To broaden the analysis, the velocity-dependent portions of the analysis (all steps after the selection of a 10-m wind speed) were then rerun for the remaining 5 to 10 chosen mean wind speeds.

After separate analyses had been run for the complete set of wind speeds, two separate graphs were created for each structure. The first plotted effective connection stress ranges versus mean wind speeds. The second plotted the equivalent normalized static pressure ranges versus mean wind speeds.

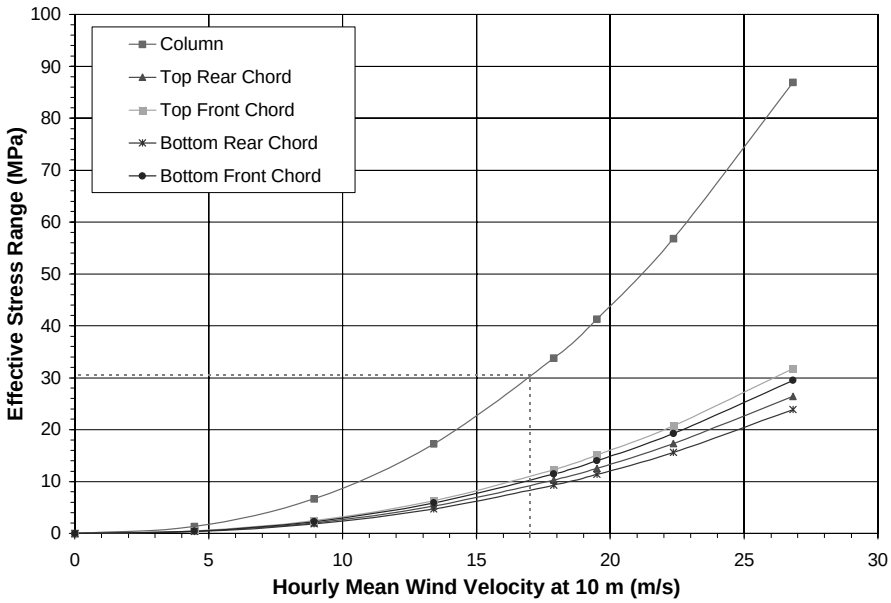

Figure 2-29. Dynamic response of Caltrans cantilevered VMS structure (box truss) to natural wind gusts.

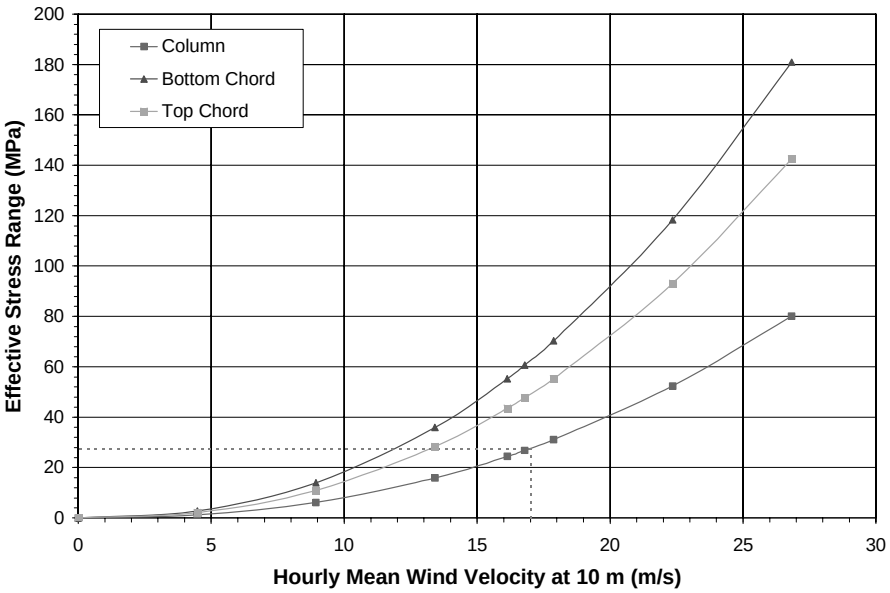

Figure 2-30. Dynamic response of NJDOT cantilevered VMS structure to natural wind gusts.

To use Figure 2-31 or 2-32 in design, the yearly mean wind velocity, V_m, for the geographic location of the structure should first be determined from meteorological records. The fatigue-limit-state wind velocity, v, can then be calculated using the following probability equation for a Rayleigh distribution [25]:

$$P_E(v) = e^{\frac{-\pi v^2}{4V_m^2}} \qquad (2.16)$$

where

$P_E(v)$ = the probability that velocity v will be exceeded and
e = the base of the natural logarithm (2.718).

As explained in *NCHRP Report 412*, there are so many cycles of wind loading over the life of a support structure that the "infinite-life" fatigue design approach is used. In the infinite-life approach, a fatigue-limit-state wind velocity is defined as the velocity that is exceeded 1:10,000 occur-

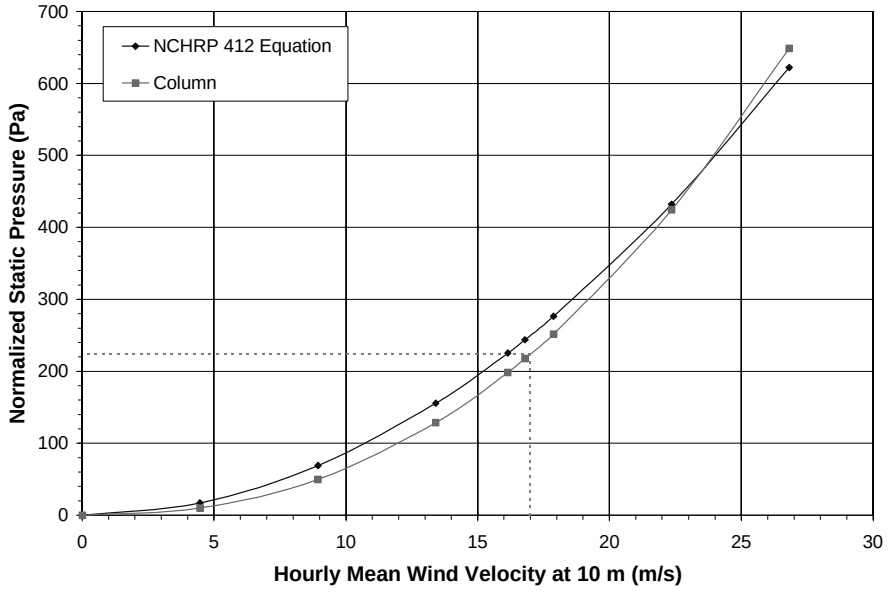

Figure 2-31. Normalized natural wind-gust static pressures (NJDOT VMS).

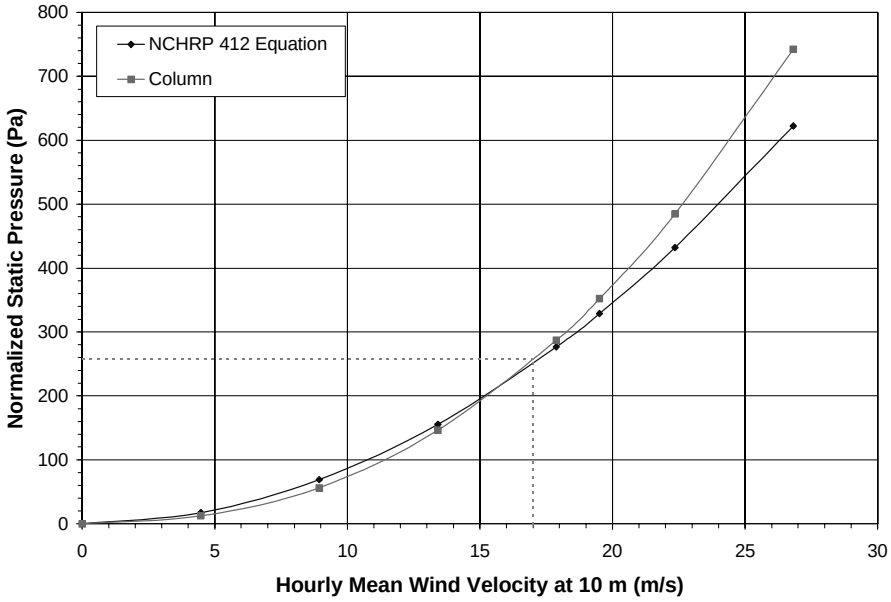

Figure 2-32. Normalized natural wind-gust static pressures (Caltrans VMS).

rences—that is, $P_E(v) = 0.0001$. The fatigue-limit-state velocity is used to calculate the equivalent static fatigue-limit-state pressure range. The connection details should be designed so that the fatigue-limit-state stress range resulting from the fatigue-limit-state pressure range is below the CAFL for the detail, so that essentially infinite life will result. It is shown below that $v = 3.4V_m$.

$$P_E(v) = e^{\frac{-\pi v^2}{4V_m^2}} = 0.0001 \tag{2.16a}$$

$$\frac{-\pi v^2}{4V_m^2} = \ln(0.0001) \tag{2.16b}$$

$$\frac{v^2}{V_m^2} = \frac{-4}{\pi}\ln(0.0001) \tag{2.16c}$$

$$\frac{v}{V_m} = \sqrt{\frac{-4}{\pi}\ln(0.0001)} = 3.4 \tag{2.16d}$$

The equivalent normalized static pressure range can then be determined by first entering Figure 2-31 or 2-32 at the abscissa of the fatigue-limit-state velocity, *v.* Move vertically until the best-fit line is intersected. The ordinate of that point is the equivalent normalized static pressure range for natural wind gusts for the particular geographic location and structure.

In *NCHRP Report 412*, 81 percent of the 59 U.S. cities studied had yearly mean wind velocities (at 10-m heights) of less than 5 m/s, and 98 percent were less than 5.8 m/s. A recent and more thorough study covering 285 U.S. cities found that 87 percent of the cities had yearly mean velocities of less than 5 m/s, and 98 percent were less than 5.8 m/s [28].

Thus, it was decided to use 5 m/s as the baseline yearly mean wind speed (corresponding to a fatigue-limit-state wind velocity of 17 m/s) in the recommended equivalent natural wind-gust pressure range equation below (Equation 11-5 in the 2001 Specifications):

$$P_{NW} = 250 C_D I_F \tag{2.17}$$

where

P_{NW} = the equivalent static pressure due to natural wind gust (Pa) and
I_F = the importance factor.

Equation 2.17 is to be used in locations where detailed wind records are not available. For locations with detailed records (particularly sites with yearly mean wind speeds higher than 5 m/s), the following equation is also provided in the commentary (Equation C 11-5 in the 2001 Specifications):

$$P_{NW} = 250 C_D I_F \left(\frac{V_m^2}{25}\right) \tag{2.18}$$

The curve defined by Equation 2.18 closely resembles the curves produced from the spectral analyses, particularly in the region containing the "limit-state" winds for the majority of the United States (V_m = 5–5.8 m/s, and v = 17–19.7 m/s) (see Figures 2-31 and 2-32). Therefore, the accuracy of the natural wind-gust pressure range design equations recommended in *NCHRP Report 412* and adopted in the 2001 Specifications has been verified.

In a recent study for an independent company [28], the fatigue-limit-state velocity was determined from available

wind velocity data for more than 285 sites in the United States, as well as 66 sites in the United Kingdom and 74 sites in Australia. These wind velocities are measured at a standard height of 10 m. A Rayleigh distribution was fit to the data for each site to estimate the exceedence probabilities.

Eighty percent of the 285 locations in the United States for which wind data were available have a fatigue-limit-state wind velocity less than 18 m/s. An additional 15 percent of the locations have a fatigue-limit-state wind velocity greater than 18 m/s but less than 21 m/s. The fatigue-limit-state wind velocity is less than 23 m/s (50 mph) for everywhere in the United States except four sites:

- Tatoosh Island, Washington: 28 m/s (62 mph),
- Clayton, New Mexico: 24 m/s (53 mph),
- Point Judith, Rhode Island: 24 m/s (53 mph), and
- Cheyenne, Wyoming: 24 m/s (53 mph).

In the United Kingdom, nearly one-third of the sites looked at had a fatigue-limit-state wind velocity that exceeded 23 m/s (50 mph). None of the locations in Australia had a fatigue-limit-state wind velocity that exceeded 23 m/s (50 mph).

It is noteworthy that Cheyenne is one of the four worst locations in the United States because there was a significant signal support structure cracking problem in Wyoming. Note that the fatigue-limit-state velocity is always going to be far lower that the wind speed used to design for the strength limit state (typically 32–46 m/s [70–100 mph]).

2.3 MITIGATION STRATEGIES

Vibration and fatigue in cantilevered structures can be mitigated in one of three ways:

- The simplest, and most expensive, method is to increase the stiffness of the structure by increasing member sizes or changing structural configuration (e.g., trusses instead of monotubes).
- Adding damping plates and louvered backplates, among other techniques, can alter the aerodynamic characteristics of the structure and preclude the possibility of galloping.
- Finally, motion can be damped using mechanical devices.

The first two methods prevent the onset of galloping, while the third reduces the intensity of the oscillations.

Examples of the first method include the use of bridge supports rather than cantilevered structures and the use of box trusses for mast arms (the latter use is common in Minnesota and other states). These configurations are believed to be too stiff to allow galloping to occur. Although the first method can be effective, it is sometimes perceived as too expensive.

The second method has a mixed track record. Damping plates were shown to be effective for signal poles with horizontal signal heads in research performed at Texas Tech University in 1995 [29]. These damping plates are widely used in Texas, although many of them are not properly installed. Louvered backplates have also been used, but signal poles outfitted with louvered backplates were still observed to gallop in Colorado.

Mitigation efforts in this research focused on the improvement of mechanical damping. Existing mechanical damping devices are not readily adaptable to cantilevered sign and signal support structures for three primary reasons: First, the simplistic design of signal structures (relative to redundant building structures) precludes the application of many devices created to dampen building motion. Second, galloping can cause millions of stress cycles, whereas many mitigation devices are only designed to resist a handful of loading cycles. Third, galloping vibrations occur in the vertical plane, while most dampers developed to date have been designed to mitigate horizontal motion.

Numerous mitigation devices are discussed in Soong and Dargush's *Passive Energy Dissipation Systems in Structural Engineering* [30] and summarized below. By definition, passive mitigation devices do not require an external energy source to function. They are installed to absorb some of the input energy (i.e., wind load) applied to the structure. Subsequently, less energy remains to be consumed by the structural members and their connections, and the degree of damage to the structure is reduced.

As is described by Soong and Dargush, metallic dampers use the plastic deformation (i.e., yielding) of metal components to dissipate energy. Obviously, the application of such a device is impractical when attempting to mitigate galloping because of the large number of stress cycles. In practicality, metallic dampers are only useful for the mitigation of infrequent (e.g., seismic) motions.

Friction dampers rely upon the friction created by the relative motion between two or more solids. As was the case with metallic dampers, friction dampers are not applicable for the mitigation of frequently occurring vibrations. The most common friction damper uses a limited-slip bolted joint. In such connections, bolts are not tightened to the slip-critical condition. Instead, they are left loose enough to allow motion between the bolted plies when problematic vibrations occur. Although such a connection could successfully dampen galloping vibrations, it could also lead to other problems such as fretting, bolt fatigue, and reduced serviceability.

As with friction dampers, the feasibility of viscoelastic dampers is limited. The shear deformation of viscoelastic materials is used to dissipate energy. Viscoelastic pads have been tested on traffic signal structures in the past, when they were placed between the baseplate and the foundation, between the flange plate and the built-up box, or both [31, 32]. For both of these applications, the viscoelastic pad is deformed in compression, not shear, which limits the pad's effectiveness. In addition, the inclusion of the compressible material between the bolted surfaces subjects the anchor

rods, the flange plate bolts, or both to excessive stress ranges and fatigue.

Whereas metallic, friction, and viscoelastic dampers use the inelastic deformation of solids to dissipate energy, the deformation of viscous fluids can also be used to consume kinetic energy in a structure. The most widely known example of a viscous fluid damper is a vehicle shock absorber. As is described in Section 2.3.3, researchers at the University of Wyoming have shown how effective shock absorbers can be on signal structures.

Tuned liquid dampers use inertial effects and viscous action to dissipate energy. Liquid is placed in a container that is rigidly mounted to the mast arm of the vibrating structure. As the structure moves, the liquid's inertia causes the liquid to move relative to the structure. Viscous effects in the boundary layer (i.e., near the container's walls) consume energy and dampen motion. By adjusting the shape of the container and the volume of the liquid, the frequency of the liquid's motion can be matched to that of the structure to increase the effectiveness of the damper.

Tests performed at the University of Florida found that several tuned liquid dampers unsuccessfully mitigated signal structure motion [32]. The most likely reason that the devices were unsuccessful is that they are really only effective in damping horizontal motion. In order for tuned liquid dampers to successfully mitigate vertical motion, structure accelerations greater than the acceleration of gravity (a condition that rarely, if ever, occurs during galloping) would be required. Without accelerations greater than 9.81 m/s (32.3 ft/s), the liquid will not move vertically relative to the mast arm and motion will not be damped.

Unlike tuned liquid dampers, large vertical structure accelerations are not required for tuned mass dampers to be effective. A spring mechanism (e.g., a coiled spring or cantilevered arm) connects a solid mass to the oscillating structure. Energy is dissipated by shifting the kinetic energy in the structure to the mass. The damper can be tuned to the structure's frequency by altering the magnitude of the mass and the stiffness of the spring.

Although tuned mass dampers are clearly the most plausible types of dampers for signal structures, difficulties still arise in their design. Because of the low frequencies at which signal structures vibrate (0.74 Hz for the Texas Tech structure described in Section 2.3.5), large static displacements in the springs are necessary. In the static state, the force provided by the spring balances the gravitational force. Therefore,

$$mg = k\Delta$$
$$\Delta = \frac{mg}{k} \tag{2.19}$$

where

m = the mass supported by the spring (kg),
g = the acceleration due to gravity (m/s^2),
k = the stiffness of the spring (N/m), and
Δ = the static displacement of the mass (m).

The damper is tuned to the frequency of the structure according to the following relationship:

$$(2\pi f)^2 = \omega^2 = \frac{k}{m} \tag{2.20}$$

where

f = the frequency of the structure (Hz) and
ω = the angular frequency of the structure (radians per second).

Substituting Equation 2.20 into Equation 2.19 yields

$$\Delta = \frac{g}{(2\pi f)^2} \tag{2.21}$$

Therefore, the only "variable" in the static displacement is the frequency to which the damper is tuned. However, the damper must be tuned to a frequency near that of the structure. Thus, the static displacement becomes a fixed quantity for each structure. For the Texas Tech frequency of 0.74 Hz, a static displacement of 0.45 m (18 in.) is necessary. In addition to these large static displacements, space must also be provided for the dynamic displacements that occur when the device is mitigating vibration. Thus, it becomes difficult to design tuned mass dampers that are not so large that they become aesthetically unpleasant.

The tuned mass dampers developed by researchers at the Universities of Wyoming and Florida that are discussed in Sections 2.3.2 and 2.3.3 also function as impact dampers. When large displacements are applied to the structure, the damper mass also vibrates significantly. In turn, the mass collides with its housing, which is rigidly mounted to the structure. The collision provides an impulse to the structure that opposes and dampens its motion. When the magnitude of the oscillations decreases and collisions no longer occur, the spring and mass function as a simple tuned mass damper.

It has been shown that combination impact-tuned mass dampers are most effective when they are tuned to a frequency slightly higher than that of the structure. The collisions prevent the motion from being completely harmonic and cause a slight phase shift between the motion of the structure and the damper. The higher damper frequency allows the damper to continually correct itself so that it continually impacts its housing near the point of maximum deflection in the structure (i.e., the summation of the shorter damper period and the time lost in the phase shift equals the longer structure period).

The following subsections outline the findings of a series of mitigation tests that have been performed in recent years. In addition to a summary of some of the devices used by luminaire manufacturers to mitigate vortex-shedding vibrations,

testing performed at the University of Florida, the University of Wyoming, and Texas Tech University is summarized.

2.3.1 Mitigation Strategies Currently Employed by Luminaire Manufacturers

Luminaire supports are susceptible to vortex shedding, which can result in very large force ranges. Luminaire manufacturers have a great deal of experience with damping devices to mitigate vibration. Ball-and-chain dampers (in which a metal ball is attached to a long chain hanging inside the pole and the ball swings around and collides with the wall of the tube) are effective. Dogbone dampers (also called Stockbridge dampers) consisting of two weights on the ends of a flexible shaft are also used successfully. These dampers usually have a frequency near the natural frequency of the pole, usually the mode that results in double curvature, typically called the second mode. (Actually, there are two orthogonal modes that are in single curvature, so this mode resulting in double curvature is actually the third or fourth mode, although it is commonly referred to as the second mode.) These dogbone dampers may be mounted on the interior or on the exterior, which makes them useful for retrofitting structures in the field.

The manufacturers may install the damper at the fabrication shop. This is the case for aluminum poles, which often have dampers installed. For steel poles, the strategy is often to try the structure without the dampers; then, if the structure is reported to vibrate, a damper is installed in the field. Such a strategy was used for light poles along the relatively new Interstate 78 in New Jersey, where about 1 in 10 structures has a dogbone damper mounted on the exterior.

A manufacturer of aluminum luminaire supports was visited to determine what types of mitigation devices are currently used in its field. Two types of dampers are currently used, and both have been found effective.

The factory-installed damper costs approximately $10 to fabricate, and the field-installed damper also appeared to be quite inexpensive. The factory-installed device consisted of an aluminum rod, free to impact the inside of the pole, mounted at two-thirds of the pole height. The mounting location was chosen because it is near the point of maximum deflection for double-curvature vibration (i.e., when the pole top remains relatively stationary). A Teflon ring was placed around the rod to reduce impact noise.

The field-installed damper used two aluminum 9-mm (0.375-in.) cables; each composed of seven smaller 3-mm (0.125-in.) strands. The two larger cables were then placed inside a 32-mm (1.25-in.), inside-diameter plastic tube. The semirigid tube and the cables inside it were then cut to approximately 80 percent of the total pole height. The damper was installed by sliding the tube inside the post through the handhole, and then letting it rest freely against the base and the inside of the post. When vortex-shedding forces initiate motion in the post, the tube and cables impact the insides of the post, damping out the motion.

New Jersey experienced cracking of numerous tapered aluminum light poles, some of which had dogbone dampers installed in them [13]. Dampers typically must have a frequency that is close to the vibration frequency in order to be effective. The dampers in these light poles were designed to work only when the pole is vibrating in double curvature, and the manufacturer's calculations indicate that the damping in this mode should increase from 0.18 percent of critical damping without the damper to 0.83 percent of critical damping with the damper.

Pull tests were performed on these light poles, but only the first mode could be excited in the pull tests. The pull tests indicate that the damping in the first mode is 0.40 percent of critical without the dampers, and only increases to 0.41 percent of critical with the dampers. These pull test results show that the dampers are totally ineffective in the first mode, as expected. It is possible that the vibration that caused the cracking took place in a mode that resulted in triple curvature, for which the dampers are probably also ineffective.

Although, in a few cases, the damping devices used for light poles have not been effective, the devices are usually effective. Therefore, this research is aimed primarily at finding effective damping devices for cantilevered sign and signal support structures. Unfortunately, very little from the experience of mitigation in light poles can be extrapolated to cantilever sign and signal support structures. Dampers placed inside the pole will be ineffective because most of the vibration is in the mast arms of these structures. Dampers are not effective when placed in a mast arm because they tend to lie on the bottom and not move around and bang into the sides as they do when they are suspended inside a pole. Finally, the dampers must be tuned to a frequency close to the natural frequency of vibration, which is much lower for the cantilevered sign and signal support structures, which always vibrate in the first mode only. The dampers developed for light poles have natural frequencies on the order of 6 Hz or greater, which are not useful for sign and signal supports, which vibrate at 1 Hz.

2.3.2 Summary of Mitigation Testing at the University of Florida

Over the past few years, numerous traffic signal vibration mitigation tests have been conducted at the University of Florida. Each subsequent study has built upon on the findings of the preceding studies. The most recent study [33] involved an extensive investigation of the most promising damping device, a modified version of the semituned tapered impact damper tested in Tampa and described in Section 2.3.4. The final damper design consists of a 3-ft-long, 152-mm (6-in.) inside diameter steel pipe housing, with a taper at the bottom. A 67-N (15-lb) weight with a diameter of 102 mm (4 in.) is suspended inside the housing by a spring with a stiffness of 121 N/m (0.69 lb/in.). The weight was intentionally made smaller than the housing in order to allow for out-of-

plane (i.e., horizontal) movement and impact of the mass. This damper will be referred to as the "Florida" damper.

Free vibration tests were first performed on the Florida damper. These tests were performed on a cantilevered signal support structure mounted to the floor in the structures laboratory. When no damper was on the structure, the vertical and horizontal damping ratios were 0.17 percent and 0.19 percent, respectively. After the damper was installed, these ratios increased to 7.27 percent and 3.02 percent, which are 43 times and 16 times the original damping ratios.

Free vibration tests do not accurately represent the natural condition when displacement ranges gradually increase from zero. Therefore, an eccentric mass and motor were used to apply a continual sinusoidal loading to the signal structure. For the unmitigated structure, horizontal displacement ranges at the tip of the mast arm exceeding 51 mm (2 in.) were recorded. Vertical displacements at the tip of the mast arm increased with each subsequent cycle to more than 356 mm (14 in.) until the motor was turned off because of fear that the structure may have been damaged. When the damper was installed, horizontal and vertical displacement ranges were limited to 24 mm and 36 mm (0.96 in. and 1.40 in.), respectively.

Similar free vibration tests were performed on three other structures in the field. Although the results of those tests were not as good as the results of the laboratory tests, the damper still performed extremely well. Vertical damping ratios from free vibration tests were always increased by at least a factor of 9.5. Horizontal damping ratios were increased by factors as low as 1.23, but the lowest recorded mitigated horizontal damping ratio was 1.35 percent. The eccentric mass was only applied to two of the three additional structures. As with the lab structure, vertical displacement ranges for both structures never reached a maximum value before the device was turned off. After the damper was installed, neither structure experienced displacement ranges greater than 58 mm (2.28 in.) in either direction.

The impact damper was also tested under natural conditions on the same signal near Tampa where free vibration testing was conducted (see Section 2.3.4). Data were only collected over a short period (approximately twenty 2-min data collection periods were presented). Without the damper installed, vertical displacement ranges continually increased as wind speeds increased (when winds primarily approached the structure from the rear of the signals, which has been shown to be the worst-case galloping condition). At wind speeds of 4.5 m/s (10 mph), vertical displacement ranges reached 41 mm (1.6 in.). However, when the damper was installed, changes in wind speed had no effect on vertical displacements. At speeds of 4 m/s (9 mph), displacement ranges only reached 8 mm (0.3 in.). The damper also performed well in the horizontal direction, eliminating the effects of wind speed and reducing maximum displacement ranges from 25 mm (1 in.) to 14 mm (0.55 in.).

One day, when testing was conducted with the damper installed, strong winds approached the structure from the front. Gusts as high as 11 m/s (25 mph) and average speeds reaching 8 m/s (17 mph) were recorded. The other three signal structures at the intersection were all observed to be moving considerably. Vertical and horizontal displacement ranges of 100–150 mm (4–6 in.) and 50–100 mm (2–4 in.), respectively, were estimated. However, maximum vertical and horizontal displacement ranges for the mitigated structure only reached 13 mm (0.5 in.) and 30 mm (1.2 in.), respectively.

Table 2-11 summarizes the performance of all the damping devices that were at least partially effective for cantilevered sign and signal support structures. The table shows the increases in damping ratios for the free vibration tests and the decreases in displacement ranges for the forced vibration tests and the natural wind tests. The Florida impact damper was effective for all three types of test, successfully damping out oscillations during the free vibration tests and preventing the onset of large-amplitude motion during the sinusoidal loading and natural wind tests.

2.3.3 Summary of Mitigation Testing at the University of Wyoming

A series of vibration mitigation tests have also been conducted by the University of Wyoming on a signal structure located in a Wyoming Department of Transportation (WYDOT) district yard (see Figures 2-33 and 2-34). As was the case with the testing at the University of Florida, each series of tests at the University of Wyoming improved upon the findings of previous studies. In the most recent research, five different mitigation devices were tested [34]. By altering the arrangement of the devices and by installing more than one damper at a time, 15 different test configurations were developed. Among the devices tested were struts, a shot-put impact damper, a prototype of the Florida impact damper, and the Wyoming strand impact damper.

Structures were excited using an eccentric mass oscillator similar to the one used at the University of Florida. The frequency of the oscillator was altered incrementally over a range of frequencies within ±10 percent of the structure's frequency. Maximum responses (i.e., mast-arm-tip acceleration and moment at the mast-arm-to-post connection) for each frequency were then plotted to create response spectra. The half-power method was used to calculate damping ratios based on the response spectra.

The in-plane strut consisted of a long (7.32-m, or 24-ft) tube connected to a typical automobile shock absorber. The device attaches to the mast arm and the luminaire extension of the post (see Figure 2-35). Applying the device increased the in-plane damping by nearly nine times and reduced the maximum moment at the mast-arm-to-post connection to one-ninth its original magnitude. (Because the increase in damping factor and decrease in moment factor are always the inverse of one another, only the decrease in moment will be referenced from this point on.) No decrease in the out-of-

TABLE 2-11 Summary of performance of various damping devices in various tests

Damping Device	Test Type	Response Reduction Factor*		Comments
		Vertical	Horiz.	
Fla impact	Lab free vibration	43**	16**	Tests performed by Univ. of Florida
Fla impact	Field free vibration	>9.5**	>1.2**	
Fla impact	Lab forced vibration	10	2	Device is effective, especially in vertical plane, but noisy
Fla impact	Field forced vib.	7	NA	
Fla impact	Wind gusts, front	5	2	
Fla impact	Wind gusts, rear	10	2	
Strut	Field forced vib.	9	1	Req. luminaire extension
Dual strut	Field forced vib.	6	2	Also req. cantilever
Shot-put	Field forced vib.	1.2	3	Very noisy
Fla impact	Field forced vib.	4	1.2	Wyoming structure
Strand	Field forced vib.	3	2.4	Effective vertical & horiz.
Fla impact	Field free vibration	6**	1**	Clearwater structure
Strand	Field free vibration	4.2**	2**	Clearwater structure
Strand	Field free vib.	3**	NA	Texas Tech structure
Strand	Galloping from rear	1.1 to 2.2	NA	Texas Tech structure

*Factor of decrease in response (displacement, acceleration, or strain) or factor increase in damping
** Wyoming tests showed that these factors were equivalent, as expected from vibration theory
NA = no data available

plane response was observed. A shortcoming of the in-plane strut is that it can only be installed on structures with luminaire extensions.

Another version of the strut damper involved adding a 1.2-m (4-ft) cantilever beam in the out-of-plane direction on the luminaire extension. The strut was then attached to the cantilever (instead of directly to the luminaire extension) to initiate out-of-plane damping (see Figure 2-36). Because of the relatively short length of the cantilever, decreases in the out-of-plane response were again negligible. Furthermore, the in-plane effectiveness of the device was reduced.

Both struts were also installed in conjunction with one another to form a dual-strut system (see Figure 2-37). In-plane moments were reduced by a factor of six (slightly less effective than the in-plane strut alone), and out-of-plane moments were nearly halved. However, a large amount of field welding was required to install the cantilevered strut, and the cantilevered strut was not that aesthetically pleasing. Therefore, the feasibility of the cantilevered- and dual-strut systems is limited.

The shot-put damper used the impacts of an 89-N (20-lb) shot-put rolling within a steel tube (see Figure 2-38). The

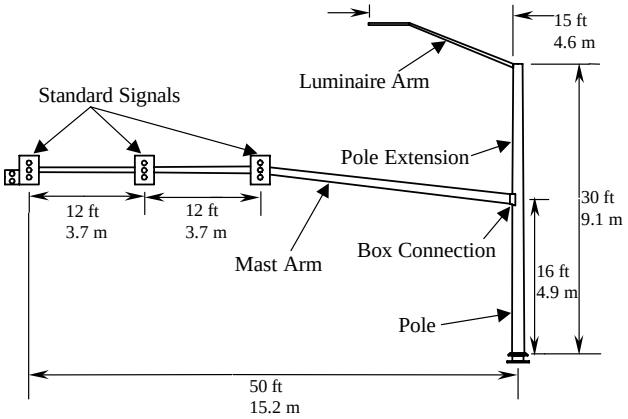

Figure 2-33. University of Wyoming traffic signal structure dimensions.

Figure 2-34. University of Wyoming traffic signal structure.

Figure 2-35. University of Wyoming in-plane strut damper.

tube was mounted in the horizontal plane, parallel to traffic (i.e., orthogonal to the mast arm) to dampen out-of-plane motion. Previous testing revealed that such an orientation was most beneficial. Steel plates at both ends of the tube could be adjusted to alter the distance that the shot-put rolled before impact. The damper was most efficient when the shot-put was allowed to roll 76 mm or 127 mm (3 in. or 5 in.). In-

Figure 2-36. University of Wyoming cantilevered strut damper.

Figure 2-37. University of Wyoming dual-strut damper.

plane moments were, on average, reduced by 20 percent, while out-of-plane moments were decreased by more than a factor of three. Drawbacks of the device include its large weight (more than 445 N, or 100 lb) and the serviceability problem created by the large impact noise. Reducing the noise by adding different impact materials would likely decrease the effectiveness of the device.

The early prototype of the Florida semituned-mass impact damper (102- to 51-mm [4- to 2-in.] taper) was also tested at the University of Wyoming (see Figure 2-39). This damper was the same damper that was tested in the field on the structure near Tampa, Florida (see Section 2.3.4). Again, the device performed fairly well. The in-plane moment was decreased to nearly one-fourth of its original magnitude. The maximum out-of-plane moment was only decreased by a fac-

Figure 2-38. University of Wyoming shot-put impact damper.

Figure 2-39. University of Florida semituned mass impact damper installed in Wyoming.

tor of 1.2. Like the shot-put damper, impact noises appear to be the biggest disadvantage of the Florida damper.

The strand impact damper developed at the University of Wyoming and tested in Tampa (see Section 2.3.4) and at Texas Tech (see Section 2.3.5) performed reasonably well (see Figure 2-40). The device consists of a 1,070-mm (42-in.)

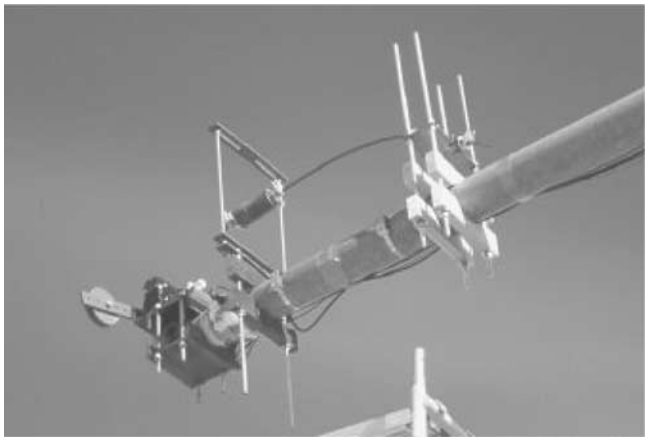

Figure 2-40. University of Wyoming strand impact damper.

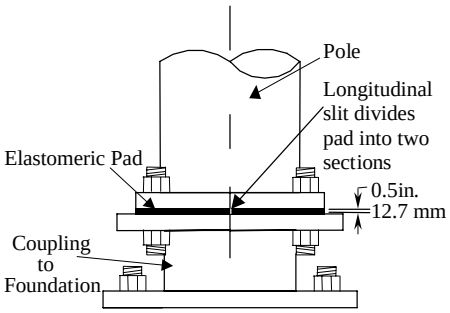

Figure 2-41. University of Wyoming elastomeric pad specifications.

long cantilevered 13-mm (0.5-in.) diameter prestressed concrete strand supporting a 4.5-kg (10-lb) mass at the free end. As the mast arm oscillates, the mass impacts steel plates mounted above and below the free tip of the strand. In its most efficient configuration, in-plane and out-of-plane moments were decreased by factors of 3.0 and 2.4, respectively. The greatest advantage of the strand damper is its effectiveness in both directions, making it a viable option in locations where out-of-plane motion is of great concern (like in Wyoming, where the structures are primarily affected by natural wind gusts rather than galloping). Impact noises are also a problem for the strand damper. Because this was the most promising damper tested in Wyoming, this damper will be referred to as the "Wyoming" damper.

The next set of tests studied the placement of an elastomeric pad under the baseplate (see Figures 2-41 and 2-42). In-plane and out-of-plane moments were decreased by factors of 1.2 and 1.5, respectively. A major flaw with this system is that it allows motion of the baseplate relative to the anchor rods, which will likely lead to anchor rod fatigue failure. In addition, the device is difficult to install on existing structures because it requires that the post be lifted off the anchor rods.

To test the effectiveness of two devices that were successful in orthogonal directions, the in-plane strut and elastomeric

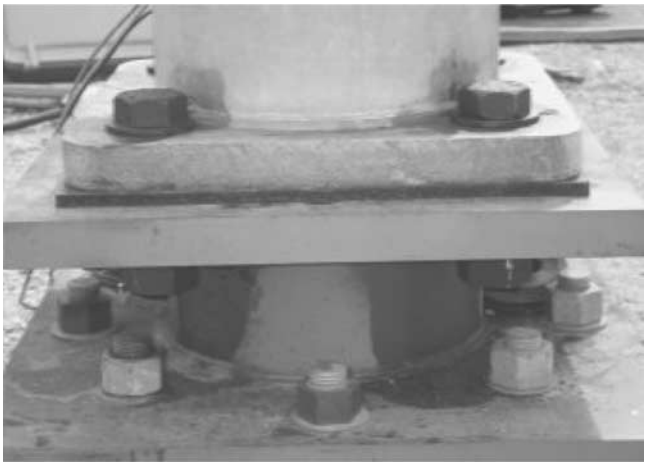

Figure 2-42. University of Wyoming elastomeric pad.

Figure 2-43. Tampa test cantilevered signal structure.

Figure 2-45. Built-up box connection of Tampa structure.

pad were combined for the final test. In spite of the addition of the other damper, both devices still performed well in their respective planes. The strut reduced in-plane moments by a factor of 8.2, and the pad lowered out-of-plane moments by a factor of 1.7. However, the anchor rod fatigue problem associated with the pad still existed.

The performance of these damping devices tested at the University of Wyoming is also summarized in Table 2-11.

2.3.4 Clearwater, Florida, Free Vibration Traffic Signal Pull-Down Tests to Investigate the Efficacy of Several Damping Devices

On July 8, 1999, a monotube cantilevered traffic signal structure located at the intersection of Ulmerton Road and Egret Boulevard in Clearwater, Florida (just outside of Tampa), was instrumented with strain gauges and monitored (see Figures 2-43 and 2-44). The 20.1-m (66-ft) mast arm was attached to the post with a standard built-up box connection (see Figure 2-45). This structure had been reported to exhibit excessive vibration, and it was hoped that the structure (and the dampers that were to be applied to it) could be tested in natural wind conditions. However, winds on the test day rarely exceeded 2 m/s (4.5 mph), which made it necessary to perform pull-down tests in order to examine the effectiveness of the proposed dampers. When a pull-down test is conducted, a rope is first attached to the structure near the tip of the mast arm. Tension is then applied by hand to the rope in harmony with the natural frequency of the structure until the structure is sufficiently excited (see Figure 2-46). The rope is then released, and the structure is allowed to vibrate freely while its response is measured.

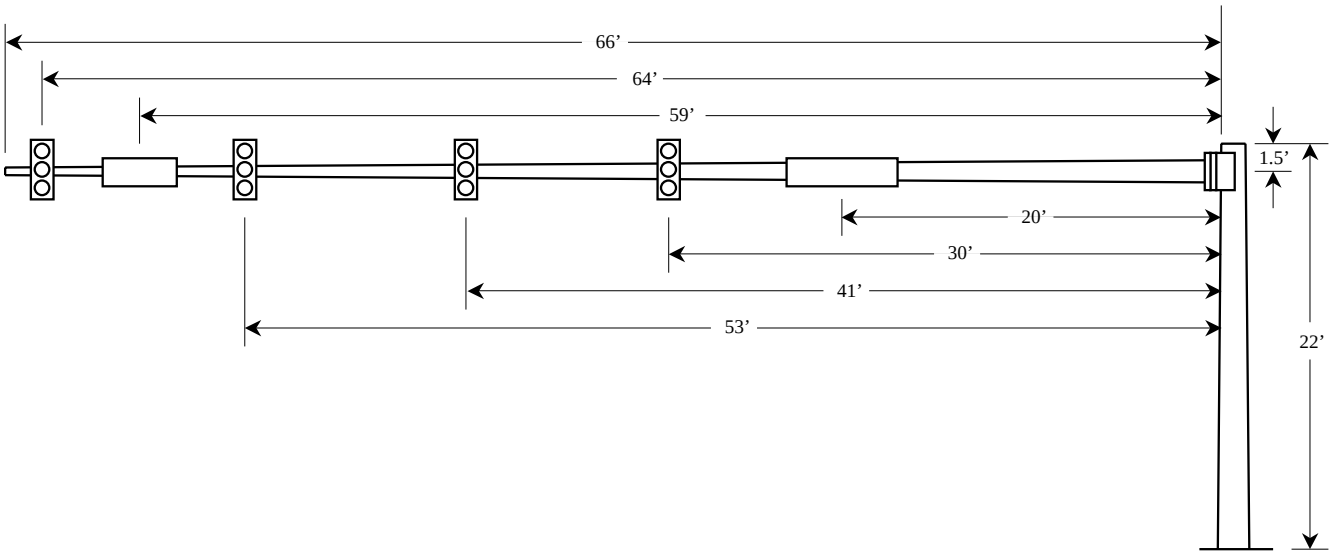

Figure 2-44. Tampa test structure dimensions.

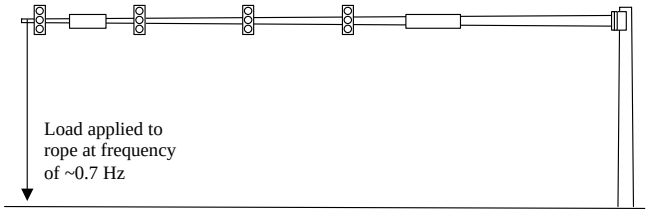

Figure 2-46. Structure excitation for pull-down test.

University of Minnesota researchers (Matthew Ricker and Robert Dexter) installed eight strain gauges on the structure: four each on the column and the mast arm. All gauges were placed in the longitudinal direction and spaced at 90° intervals around the circumference of the poles (see Figure 2-47). Strain readings, as well as wind speed and direction, were collected at a frequency of 50 Hz using a Campbell Scientific CR9000 datalogger. University of Florida researchers (Ronald Cook, David Bloomquist, and Dylan Richard) also instrumented the structure by installing vertical and horizontal accelerometers near the mast arm tip. All damping ratios and natural frequencies provided below are based on the strain readings recorded with the datalogger.

Over the course of the day, nine different unmitigated vibration tests were conducted. The results of these tests are summarized with the other test results in Table 2-11. For three of the tests, small initial vertical displacements (approximately 5–8 cm [2–3 in.]) were applied to the structure to investigate in-plane motion. Four more tests studied large vertical displacements (approximately 20 cm [8 in.]). For the final two tests, an angular initial displacement was applied to the structure in order to include out-of-plane effects (i.e., horizontal motion of the mast arm). For all of the tests (including those with mitigation devices installed), the magnitude and direction of the initial displacement had little, if any, effect on the calculated damping ratios. The average measured natural frequency and damping ratio of the unmitigated structure were 0.668 Hz and 0.13 percent, respectively, for in-plane motion (see Figure 2-48). In the out-of-plane direction, the average natural frequency was 0.615 Hz, while the average damping ratio was 0.57 percent. Tables 2-12 and 2-13 summarize the measured frequencies and damping ratios for both the unmitigated and mitigated structure.

The early prototype of the spring-mass damper developed at the University of Florida was tested eight times. The device consisted of a 102-mm (4-in.) diameter steel cylinder that housed a 6.8-kg (15-lb) mass hanging from a spring (see Figure 2-49). The cylinder has a taper at the bottom from 102 mm to 51 mm (4–2 in.) so that the impact of the mass with the bottom is gradual and creates friction. The cylinder was rigidly mounted near the tip of the mast arm, and the inertia of the mass caused the mass to impact the inside of the cylinder as the arm oscillated. As the amplitude of vibration was dampened (after 3–5 cycles), the mass no longer struck the bottom of the cylinder, but the device continued to be effective, functioning as a semituned mass damper. The in-plane damping ratio increased by a factor of 6 (see Figure 2-50), but the out-of-plane damping ratio decreased by a factor of 0.93.

The second damper tested was based on dampers used successfully on electric transmission towers. A 10.1-cm (4-in.) diameter polyvinyl chloride (PVC) tube was partially filled with sand and rigidly attached near the tip of the mast arm (see Figure 2-51). Because of the ineffectiveness of the device, only four tests were run. The presence of this device had no effect on in-plane motion (see Figure 2-52) and increased the out-of-plane damping ratio by a factor of 1.2. Most likely, the device was ineffective because the magnitude of the mast arm acceleration was not large enough to cause the sand to move relative to the PVC tube.

The strand damper developed at the University of Wyoming was tested only three times because of time constraints (see Figure 2-53). As the mast arm oscillated, the mass impacted steel plates mounted above and below the free tip

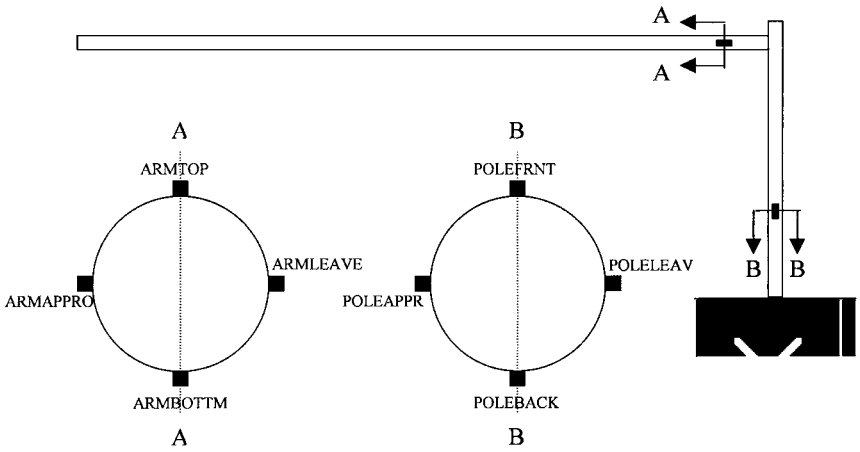

Figure 2-47. Tampa signal strain gauge layout.

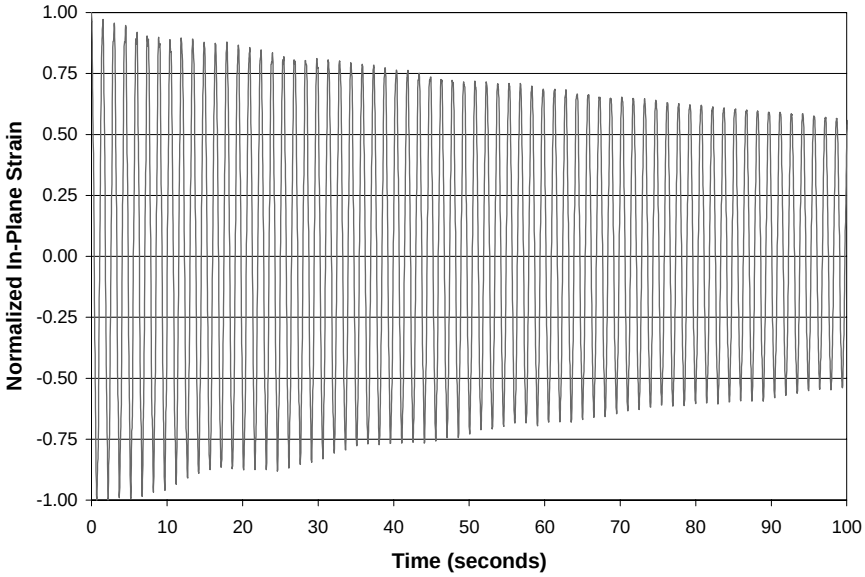

Figure 2-48. Free vibration of Tampa signal without mitigation devices installed.

of the strand. As was the case with the Florida impact damper, the behavior of the strand damper changed from functioning as an impact damper to functioning as a semi-tuned mass damper after the first few cycles. In-plane damping ratios were increased by a factor of 4.2 from 0.13 percent to 0.54 percent (see Figure 2-54), and out-of-plane ratios were increased by a factor of 2 from 0.57 percent to 1.14 percent.

As was the case with the Florida damper, the Wyoming strand damper tested in Tampa was also an early prototype. A recent report from the University of Wyoming stated that modifications ranging from the creation of a weatherproof housing to finding a way to reduce the impact noise are needed to meet serviceability requirements [34].

Because of time constraints, a fourth damper that was scheduled for the Tampa testing was instead tested at the University of Florida. The "snubber" damper consisted of a 5-mm (3/16-in.) steel cable spanning the corner of the column-to-mast-arm connection (see Figure 2-55). John Panak, a consultant from Austin, Texas, and a member of the NCHRP project panel for Project 10-38, suggested this snubber damper. The cable was approximately 1.5 m (5 ft) long and was attached to the column and mast arm using hook eyes and hose clamps. A turnbuckle was also included to tighten the cable. Unfortunately, the device performed unsuccessfully when subjected to the large initial displacements used in pull-down tests. However, it is still possible that such a damper may be successful in mitigating motion in natural wind conditions when unmitigated displacement ranges gradually increase from zero. The large force induced on the damper by the large initial displacement during the pull-down tests would never actually occur if the damper were

TABLE 2-12 Tampa in-plane frequencies and damping ratios

Mitigation Device Installed	Average In-Plane Frequency (Hz)	Average In-Plane Damping Ratio
None	0.668	0.13%
Florida Impact Damper	0.619	0.76%
PVC-Sand Damper	0.658	0.13%
Wyoming Strand Damper	0.630	0.54%

TABLE 2-13 Tampa out-of-plane frequencies and damping ratios

Mitigation Device Installed	Average Out-of-Plane Frequency (Hz)	Average Out-of-Plane Damping Ratio
None	0.615	0.57%
Florida Impact Damper	0.581	0.54%
PVC-Sand Damper	0.608	0.66%
Wyoming Strand Damper	0.585	1.14%

Figure 2-49. University of Florida spring-mass damper.

Figure 2-51. PVC-sand damper.

capable of successfully limiting vibrations in the early stages of galloping.

2.3.5 Testing at Texas Tech University

Galloping mitigation testing sponsored by the Texas Department of Transportation was conducted at Texas Tech University in 1995 [29]. A traffic signal structure mounted on a rotatable base was constructed. The rotatable base allows the structure to be aligned so that prevailing winds approach from directly behind the mast arm, a condition that increases the likelihood that galloping will occur. At that time, researchers at Texas Tech gathered some rare measurements of the response to galloping that were used in the first phase of this project to calibrate the galloping load.

The research at that time also showed the effectiveness of a large sign blank as a mitigation device for galloping. A 41-cm by 168-cm, flat-panel sign blank was mounted horizontally directly above the signal head closest to the mast arm tip. The sign blank was raised, so that a gap of 133 mm (5.25 in.) existed between the sign and the mast arm. Applying the sign blank reduced peak column strains by approximately a factor of seven during ideal galloping conditions. Subsequently, attempts have been made in Texas to mitigate galloping by installing the sign blanks on a high percentage of signal structures. However, the size and location of the sign blanks do not conform to the recommendations made in the Texas Tech study, rendering the devices potentially less effective (see Section 2.4.6). The research at that time also showed the ineffectiveness of several types of dampers,

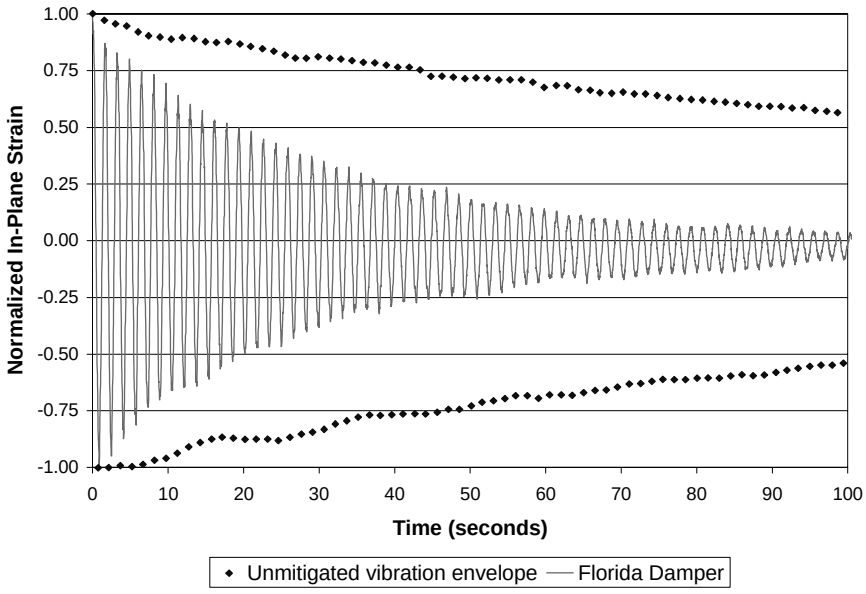

Figure 2-50. Free vibration of Tampa signal with Florida damper installed.

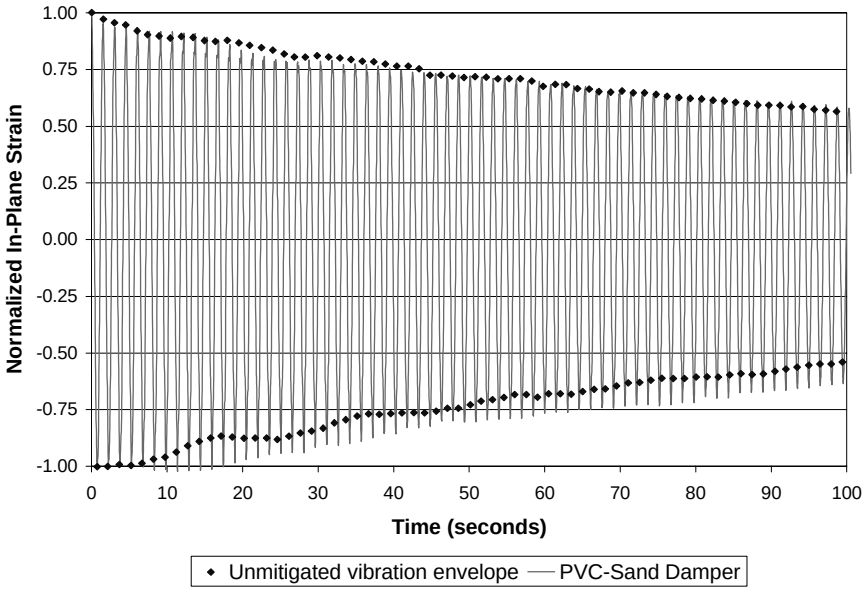

Figure 2-52. Free vibration of Tampa signal with PVC-sand damper installed.

including a liquid slosh damper that actually made the galloping response worse.

2.3.5.1 Unmitigated Galloping Data

For this project, the structure was refurbished (i.e., new instrumentation was installed) and used for further testing. Four strain gauges, oriented parallel to the axis of the post, were installed on the post 915 mm (3 ft) above the baseplate. Before mitigation testing at Texas Tech University's Wind Engineering Research Center (WERC) began, researchers again had the opportunity to collect stress data while the cantilevered monotube traffic signal structure at their facility was galloping. The structure uses a standard built-up box connection to attach a 14.6-m (48-ft) mast arm to a 5.8-m (19-ft) post (see Figures 2-56 and 2-57). No mitigation devices were installed at the time of this testing. Two signal attachments were mounted horizontally to the mast arm. A five-light signal head was mounted near the mast arm tip, while a three-light signal head was mounted 3.7 m (12 ft) from the tip. Backplates were attached to the signal heads, and wind flow was predominantly from the rear of the signal heads. Both of these conditions coincide with previous tow tank and field experiments conducted at Texas Tech, which showed that signal heads configured with backplates and subjected to flow from the rear were most susceptible to galloping [29].

Figure 2-53. University of Wyoming strand damper.

Data were collected during various 2-min intervals occurring between 5:15 and 6:00 p.m. Central Standard Time on November 30, 1999. Wind speeds perpendicular to the mast arm varied from 1.8 m/s to 7.2 m/s (4–16 mph) and averaged 4.5 m/s (10 mph). Measured stress ranges in the column due to in-plane vibrations varied from less than 10 MPa (1.5 ksi) to greater than 47 MPa (6.8 ksi) (see Figure 2-58). As is shown in Figure 2-59, the stress history during the testing was characteristic of large-amplitude galloping (i.e., large-amplitude, across-wind vibrations occurring at the natural frequency of the structure).

As is discussed in Section 3.1.1.2, *NCHRP Report 412* recommended applying an equivalent static shear pressure vertically to the surface area of all sign panels, signal heads, or both rigidly mounted to the horizontal mast arm, as seen in the normal elevation. The recommended magnitude of the vertical shear pressure range was $1{,}000I_F$ Pa ($21.0I_F$ psf). Using the maximum measured dynamic stress range in the column while the structure was galloping (47 MPa, or 6.8 ksi),

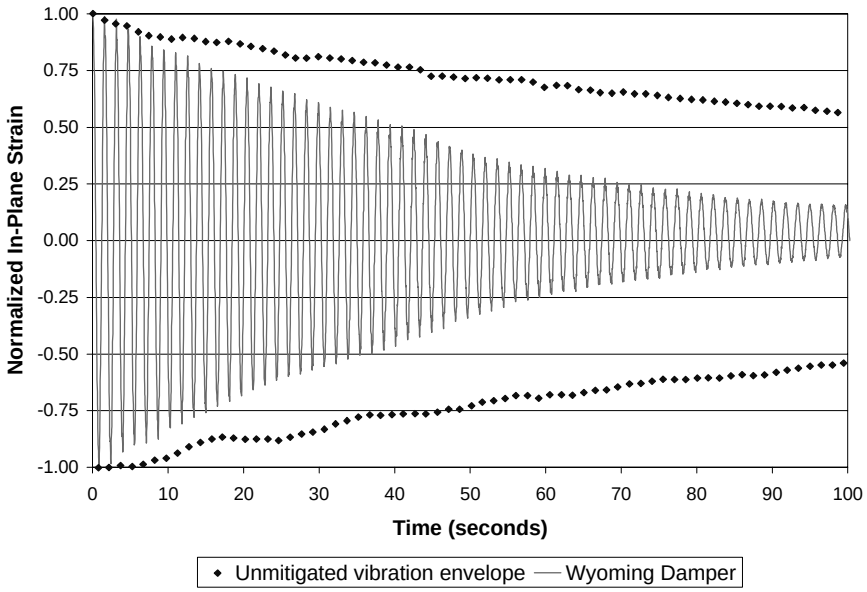

Figure 2-54. Free vibration of Tampa signal with Wyoming strand damper installed.

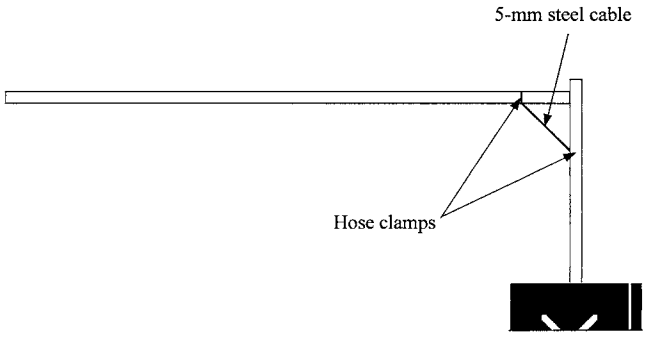

Figure 2-55. Snubber damper.

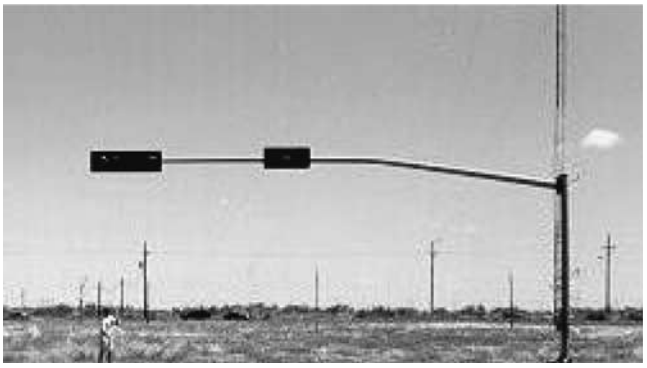

Figure 2-56. Texas Tech signal support structure.

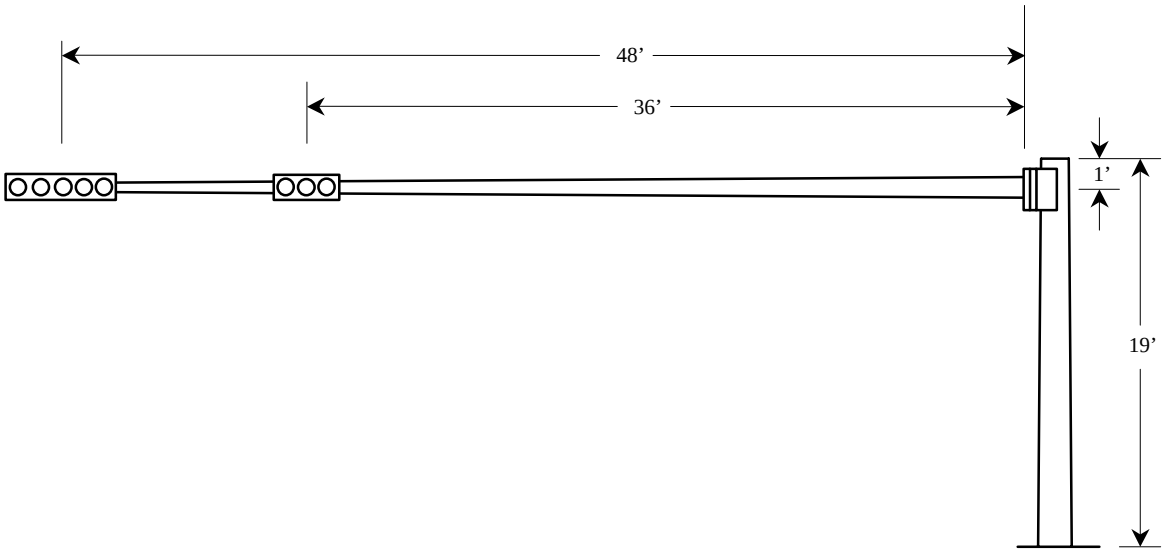

Figure 2-57. Dimensions of Texas Tech signal support structure.

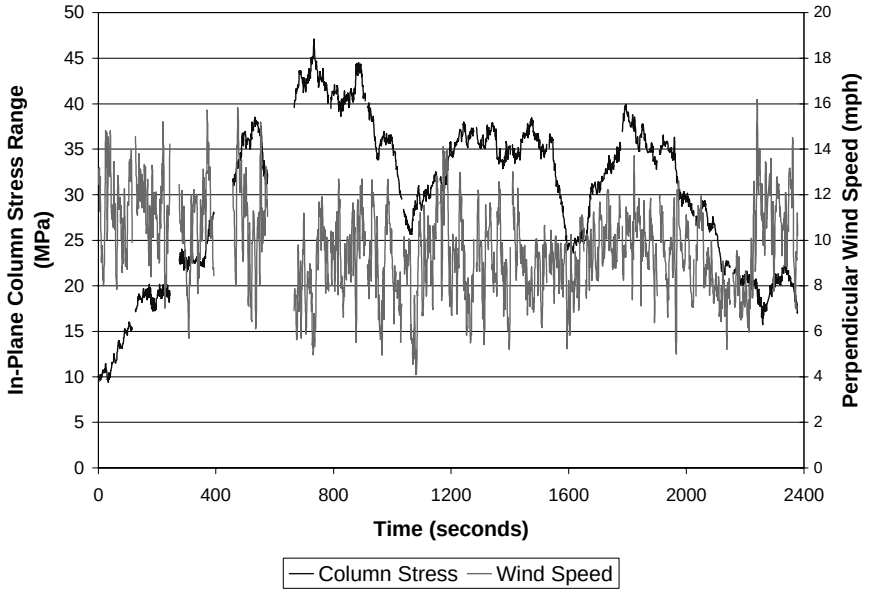

Figure 2-58. Time history of stress and wind speed during unmitigated galloping.

the equivalent static shear pressure acting on the two signal heads was back-calculated to be 952 Pa (19.9 psf). This value agrees very well with the recommended value of 1,000 Pa (21.0 psf). Thus, it is shown that the *NCHRP Report 412* galloping load is reasonable and not overly conservative. The measured stress ranges during galloping of a Caltrans bent monotube structure with a VMS (similar to the one that failed) also showed that the galloping load recommended in *NCHRP Report 412* was not excessively conservative. In fact, these stress ranges measured on the California VMS structure were about twice what would be predicted using the galloping load, as discussed previously in Section 2.2.3.

2.3.5.2 Mitigation Testing

The work plan for this project called for the testing of five mitigation strategies on five separate days at WERC. However, because of numerous problems, the structure was not ready for testing until the fall of 1999. The types of steady-state winds from the south that cause galloping usually occur

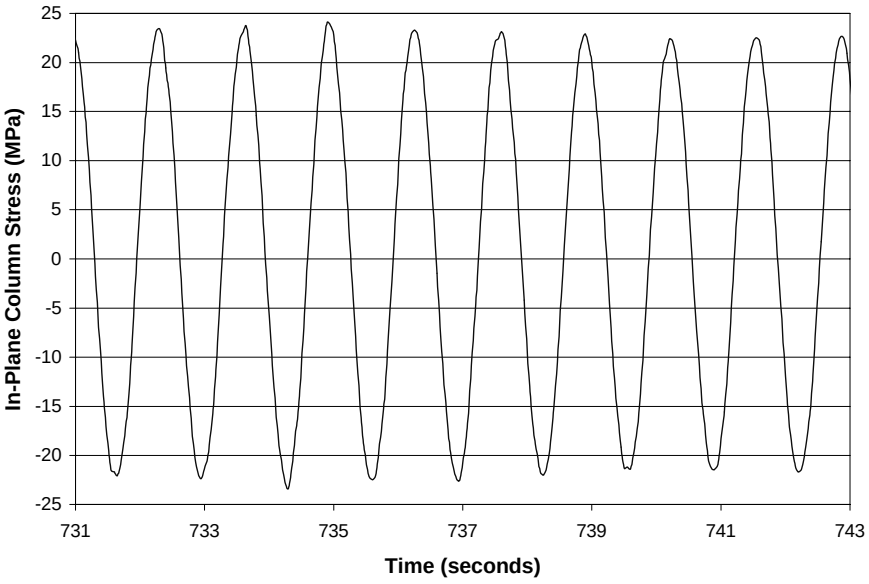

Figure 2-59. Unmitigated galloping stress during peak response.

in the spring and early summer. Unfortunately, because of unfavorable wind conditions for galloping, there were not many opportunities for testing in the spring and early summer of 2000. Consequently, only one mitigation device was tested in natural galloping wind conditions. In addition to the unmitigated galloping data collected on November 30, 1999 (see Section 2.3.5.1), data were also collected in March and May 2000 while the Wyoming strand damper was installed. Pull-down tests to measure the mechanical damping ratio, as well as natural wind vibration (i.e., galloping) tests, were also performed.

2.3.5.3 Pull-Down Testing to Determine Mechanical Damping Ratios

The version of the strand damper tested at Texas Tech was the same as that tested in Tampa in July 1999 (see Section 2.3.4). In order to determine if the mechanical damping ratio of the strand damper was highly dependent on the structure to which it was applied, pull-down tests similar to those in Tampa were performed. Two theoretical "zero" readings showed that wind effects on the structure were minimal at the time of testing. For one of the zero readings, the damper was "unrestrained," meaning that the cantilevered strand supporting the mass was free to vibrate. The damper was "restrained" for the other reading, meaning that the free end of the strand was tied down to prevent motion of the strand. The restrained case was meant to simulate an unmitigated state.

The zero readings with the damper restrained occurred before the pull-down tests and covered a period of 20 min. During this time, stress ranges in the column due to in-plane mast arm movement were minimal, rarely surpassing 1 MPa. The period during which the greatest stresses occurred is shown in Figure 2-60. The zero readings with the damper unrestrained were recorded after the pull-down tests and lasted 4 min. Stress ranges rarely reached 0.8 MPa, indicating that the wind conditions had not changed significantly during the pull-down testing (see Figure 2-61). (In fact, the magnitudes of both the restrained and unrestrained readings are so small that the dominant signal being recorded could simply be noise in the data acquisition system.) Thus, wind loading on the structure was negligible at the time of the free vibration testing.

Separate tests were performed to measure the in-plane frequencies and damping ratios for the restrained and unrestrained cases. Initial column base stress ranges of approximately 60 MPa were induced, and then the structure was allowed to vibrate freely for at least 50 cycles. With the damper restrained, the measured frequency was 0.721 Hz, and the damping ratio was 0.21 percent (see Figure 2-62). When the damper was allowed to oscillate unrestrained, the frequency was reduced slightly to 0.710 Hz, and the damping ratio was more than tripled to a value of 0.71 percent (see Figure 2-63).

Unlike the in-plane direction, the structure was highly damped out-of-plane. Nearly all oscillations were damped out within three cycles. Because large errors may exist from calculating damping ratios over a period of only three cycles, multiple tests were performed for both the restrained and unrestrained cases in the out-of-plane direction. Initial stress ranges of approximately 30 MPa at the mast arm base were generated before the structure was released. The frequency and

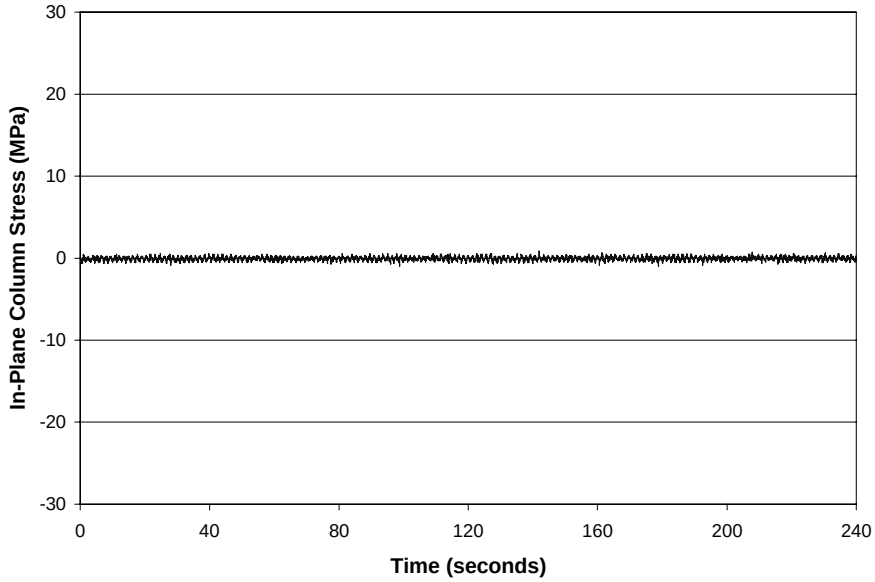

Figure 2-60. In-plane zero reading of Texas Tech signal structure with Wyoming strand damper restrained.

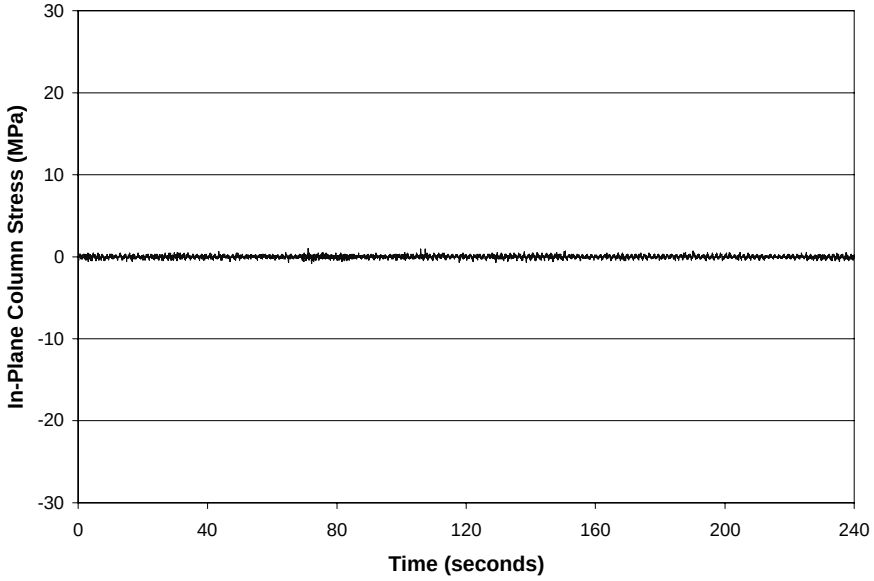

Figure 2-61. In-plane zero reading of Texas Tech signal structure with Wyoming strand damper unrestrained.

damping ratio averaged 0.339 Hz and 10.07 percent, respectively, with the damper restrained (see Figure 2-64). With the damper unrestrained, the frequency rose to 0.348 Hz, while the damping ratio actually decreased to 7.90 percent (see Figure 2-65). Although a decrease in damping may at first seem to be a problem, there is no cause for concern because the damping ratio is extremely large.

As was stated previously, in-plane damping ratios increased by factors of 3.0, 4.2, and 3.4 for the Wyoming, Tampa, and Texas Tech signal structures, respectively. The out-of-plane damping ratio increased by factors of 2.4 and 2.0 for the Wyoming and Tampa structures (which initially had low damping ratios), whereas it decreased by a factor of 0.8 for the Texas Tech structure (which had a very large initial damping ratio). Thus, independent of the structure, it is safe to assume that applying the strand damper will significantly increase the in-plane damping ratio. In addition, if the unmitigated structure has a low out-of-plane damping ratio, that

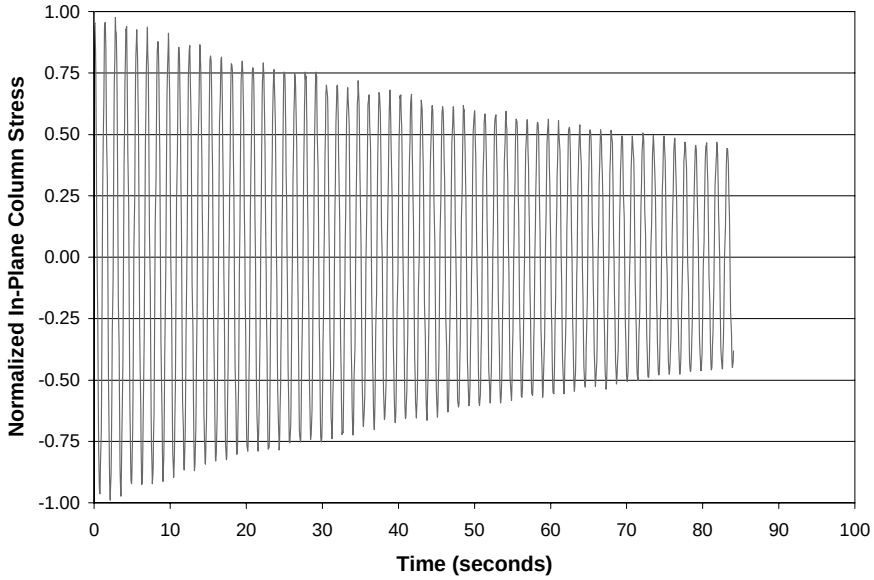

Figure 2-62. In-plane free vibration of Texas Tech signal with Wyoming strand damper restrained (manually excited).

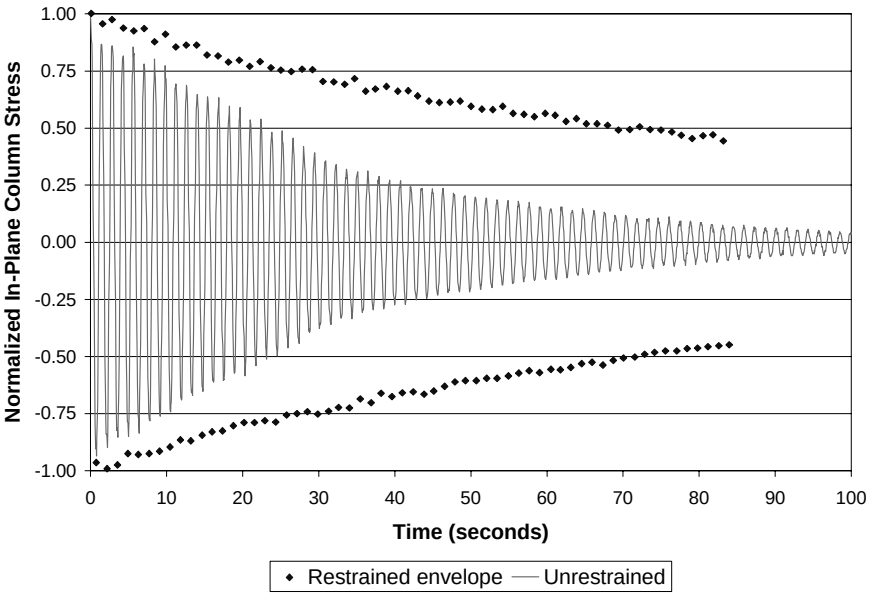

Figure 2-63. In-plane free vibration of Texas Tech signal with Wyoming strand damper unrestrained (manually excited).

ratio, too, will be improved with the installation of the strand damper.

2.3.5.4 Galloping Mitigation Tests

Twenty-four separate tests were performed on the Wyoming strand damper under conditions causing galloping. The first 16 of those tests lasted 5 min, while the duration of the final 8 tests was extended to 20 min. The tests were divided evenly between the restrained and unrestrained damper settings. Comparisons were then made between the two cases to quantify the effectiveness of the damper.

Galloping mitigation testing was conducted on 5 separate days. Because wind conditions are continuously changing, comparisons between restrained and unrestrained tests

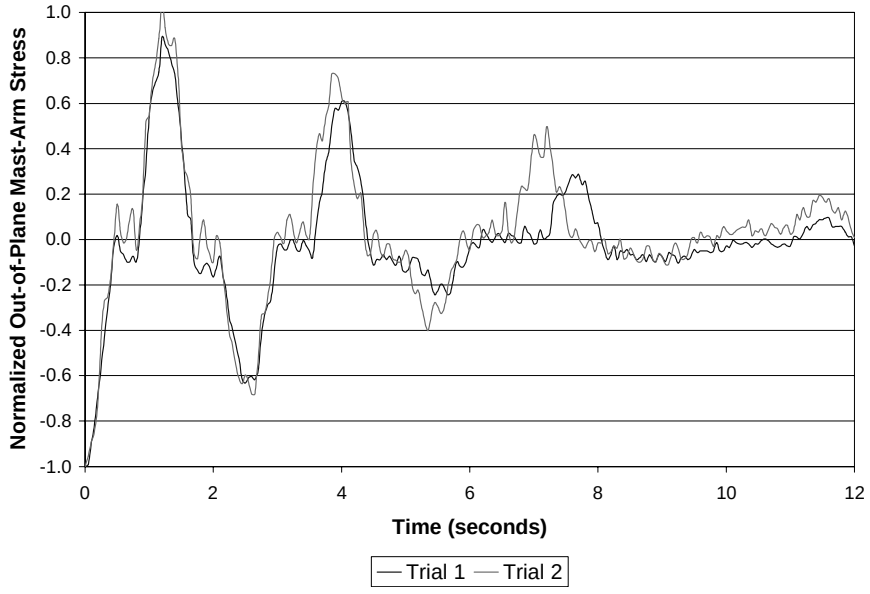

Figure 2-64. Out-of-plane free vibration of Texas Tech signal with Wyoming strand damper restrained (manually excited).

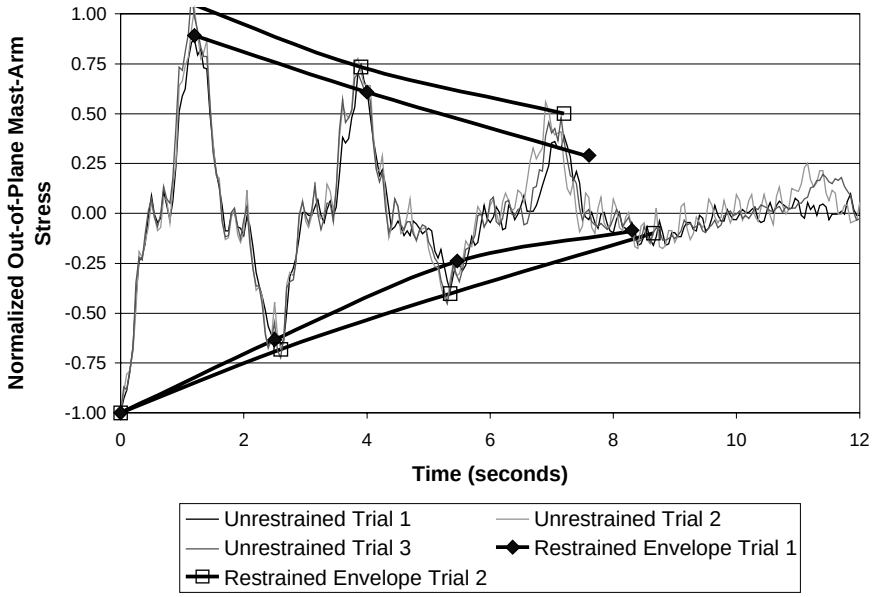

Figure 2-65. Out-of-plane free vibration of Texas Tech signal with Wyoming strand damper unrestrained (manually excited).

should be limited to those occurring under similar conditions (i.e., within minutes of each other). Because no unrestrained data were collected on one of the days, only the data from the other 4 days (i.e., when both restrained and unrestrained data were collected) are presented.

The first set of tests was performed on March 28, 2000. Four restrained and three unrestrained tests were recorded. While data were being recorded, wind speeds perpendicular to the mast arm approaching from the rear averaged 7.1 m/s (15.9 mph) and reached a peak value of 15.0 m/s (33.5 mph). There was little variation in the average wind speed for each test. Figure 2-66 shows the maximum stress range and the wind speed for the various time periods. The maximum in-plane stress ranges with the damper unrestrained are lower than those for the restrained damper. Thus, the unrestrained damper lessened the severity of the galloping

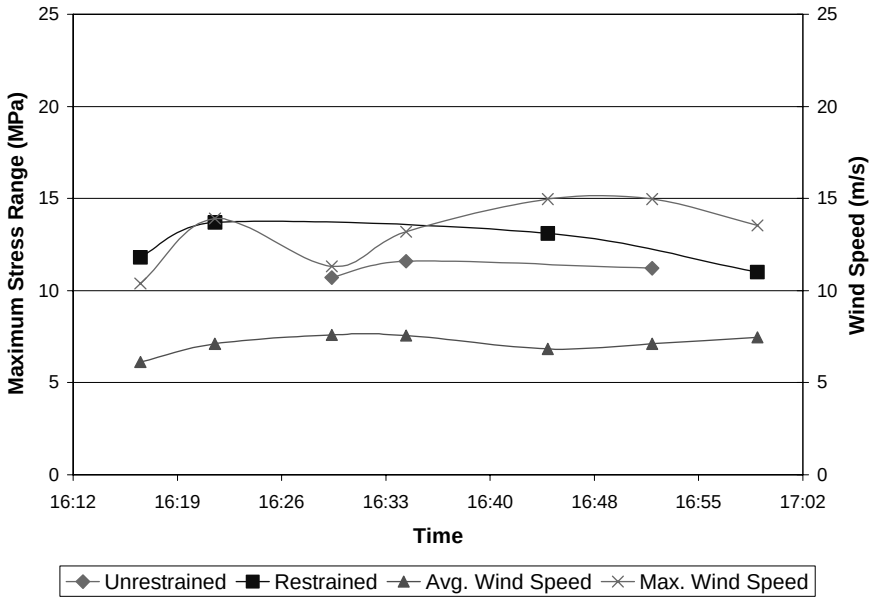

Figure 2-66. Maximum galloping stress ranges with Wyoming damper installed (March 28, 2000).

TABLE 2-14 Summary of Wyoming strand damper galloping mitigation at Texas Tech

Date	Average Wind Speed (m/s)	Peak Wind Speed (m/s)	Average Maximum Stress Range (MPa)		
			Restrained	Unrestrained	Reduction
3/28/00	7.1	15.0	12.4	11.2	10%
5/10/00	4.7	11.5	9.9	6.5	34%
5/16/00	6.6	14.5	16.0	7.4	54%
5/17/00	9.7	21.1	23.8	18.5	23%

stresses near the column base. Maximum restrained (i.e., unmitigated) stress ranges averaged 12.4 MPa (1.8 ksi). Maximum unrestrained (i.e., mitigated) stress ranges averaged 11.2 MPa (1.6 ksi), a decrease of only 10 percent (a factor of 1.1). Table 2-14 outlines the results of the strand damper testing at Texas Tech.

As shown in Figure 2-67, the strand damper was much more effective on May 10, 2000, the second day of tests, when wind speeds averaged 4.7 m/s (10.5 mph) and peaked at 11.5 m/s (25.7 mph). Other than the dip at time 14:26, the average wind speed was relatively steady. Visual comparison of the restrained and unrestrained curves clearly shows that the damper reduced the column stress ranges. Maximum restrained and unrestrained stress ranges averaged 9.9 MPa (1.4 ksi) and 6.5 MPa (0.9 ksi), respectively, a decrease of 34 percent or, to put this result in the same terms as previous test results, the response decreased by a factor of 1.5.

Although only three tests were available for comparison on May 16, the damper was again relatively effective (see Figure 2-68). Winds were very steady, averaging 6.6 m/s (14.7 mph) and reaching a maximum speed of 14.5 m/s (32.5 mph) while data were recorded. The maximum stress range recorded during the restrained test was 16.0 MPa (2.3 ksi). The average of the two maximum unrestrained stress ranges was 7.4 MPa (1.1 ksi), a difference of 54 percent (a factor of 2.2).

The strand damper again effectively reduced stress ranges on May 17, when wind speeds were the highest of the 4 test days. Wind speeds were steady, averaged 9.7 m/s (21.8 mph), and peaked at 21.1 m/s (47.3 mph) (see Figure 2-69). The two restrained maximum stress ranges averaged 23.8 MPa (3.5 ksi). Unrestrained maximum stress ranges averaged 18.5 MPa (2.7 ksi). Thus, the damper reduced the stress by 23 percent, or a factor of 1.3. (Two additional restrained tests were conducted on May 17, but were not included in this analysis because the tests occurred 80 min after the other five tests, by which time wind conditions had significantly changed.)

As Figures 2-66 through 2-69 show, maximum stress ranges, whether restrained or unrestrained, are clearly related to the average perpendicular wind speed. On average, every meter per second in average wind speed caused a 2-MPa column stress range in the unmitigated (i.e., damper restrained) structure due

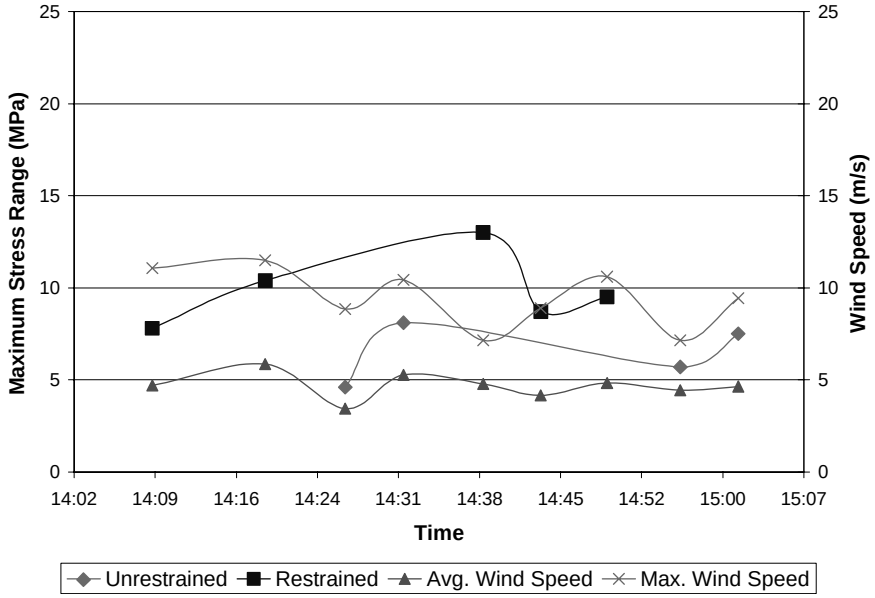

Figure 2-67. Maximum galloping stress ranges with Wyoming damper installed (May 10, 2000).

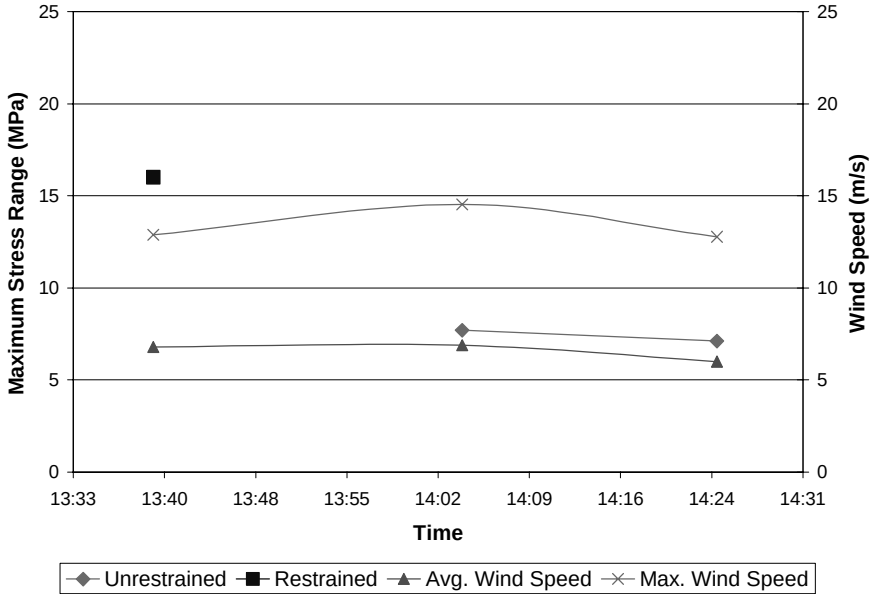

Figure 2-68. Maximum galloping stress ranges with Wyoming damper installed (May 16, 2000).

to galloping. The maximum recorded wind speed during each test also appears to be approximately twice the magnitude of the average wind speed.

Over the 4 days of testing, allowing the damper to oscillate decreased column stress ranges by an average of 30 percent. However, because of the long delay between the first and second test days, there is reason to believe that the manner in which the damper was installed for the first test may have differed from that for the other three tests. In addition, because of the low stress reduction that resulted on the first day (relative to the other 3 days), it is possible that the initial installation of the damper did not maximize its efficiency. If this assumption is correct, only the data recorded in May (when the damper was properly installed) should be analyzed, when the average stress reduction increased to a value of 37 percent.

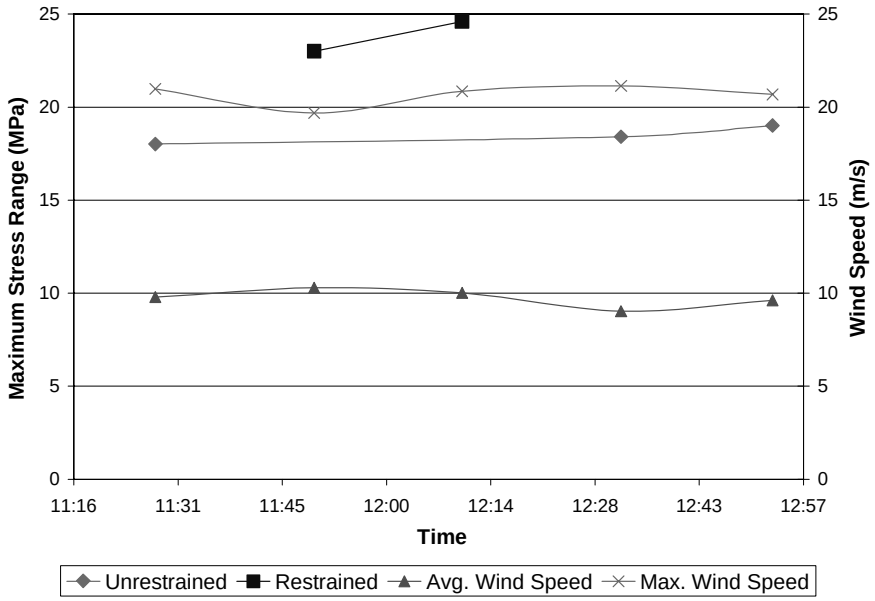

Figure 2-69. Maximum galloping stress ranges with Wyoming damper installed (May 17, 2000).

2.3.6 Summary of Mitigation Studies

Each of the three feasible mitigation devices (based on testing at the University of Florida, at the University of Wyoming, in the field in Tampa, and at Texas Tech) has one or more disadvantages. Therefore, it is difficult to make a firm recommendation for one mitigation configuration. For locations where out-of-plane vibrations are not a major concern, the in-plane strut and Florida damper appear to be the most viable options. If the owner finds the aesthetics of the strut acceptable and if the structure contains a luminaire extension, the in-plane strut is definitely the best option. However, if no extension exists, the Florida damper becomes the device of choice. If the owner deems impact noise a problem, a soundproofing medium could be placed between the impact surfaces. The degree to which the device is effective would likely decrease, but the device would still be quite effective. For locations where vibrations in both directions are a concern, the strand damper appears to be the best option. In addition to the noise problem, a housing will need to be constructed for the device before it can be installed. Wyoming researchers suggest the use of a large tube, which could also be used as the impact surface for the mass.

2.4 CHARACTERIZATION OF AT-RISK STRUCTURES

As mentioned in the introduction to this report, the actual probability of failure for cantilevered sign, signal, and light support structures due to wind-induced vibration is very small. In this case, failure is defined as fatigue cracking causing collapse or a loss of serviceability of the structure. Even the rate at which these structures are affected by large-amplitude vibrations (without necessarily leading to failure) is quite small. Therefore, it seems wasteful to some to increase the design requirements for vibration and fatigue when the vast majority of these structures are performing well.

One of the puzzling aspects of wind-induced vibration of these structures is that one structure may have a problem while essentially identical structures have performed well for decades. An objective of this project was to identify factors that put a structure at risk for wind-induced vibration and fatigue.

Because of variability in the response of structures to environmental loads, it is probably not possible to identify individual structures that will exhibit problems. In comparison, in a hurricane or earthquake, it is still not possible to identify which particular structures, among groups of similar structures at a given location, will be damaged. It is only possible to identify which classes of structures are more susceptible. It is often still the case that even while a majority of these susceptible structures survive an earthquake or hurricane with minimal damage, some of them are heavily damaged.

Identification of particular structures that will exhibit fatigue is especially difficult because fatigue is a process with an unusually large amount of inherent variability. Fatigue design is based on the lower-bound fatigue life: it is expected that if the stress ranges in service are exactly equal to the fatigue-design stress range, there will be a 2.5-percent probability of failure and a 97.5-percent probability of survival for a particular detail over the design life. In fact, it is generally observed that the mean life (with a 50-percent probability of failure) is a factor of two greater than the lower-bound life (with a 2.5-percent probability of failure).

When this inherent variability is combined with the substantial uncertainty in loads and load distribution in a structure, the total variability in fatigue life is extremely large, an order of magnitude or more. Therefore, even for structures like bridge girders that have been studied extensively with well-characterized fatigue details such as transverse stiffeners, it is impossible to identify which particular details will exhibit cracks within their design lives with a confidence any better than 1 percent. This represents the upper-bound confidence with which researchers can expect to identify structures at risk for fatigue due to wind-induced vibration.

Given this level of confidence as a standard, identifying structures that will be susceptible to natural wind gusts, truck-induced wind gusts, and vortex shedding is relatively easier than identifying structures that will be susceptible to galloping. As shown in this section, structures that have had problems with natural wind gusts, truck-induced wind gusts, and vortex shedding generally do not meet the fatigue-design requirements of the 2001 Specifications (after the 2001 Specifications were modified slightly per the recommendations in this report). However, it is still true that most of these structures that do not meet the 2001 Specifications may perform adequately throughout their design life with no problems.

However, as shown in the following section, structures that do meet the requirements generally perform well. Therefore, the fatigue design requirements for natural wind gusts, truck-induced wind gusts, and vortex shedding are well calibrated and can be used to identify structures that are at risk for fatigue.

Unfortunately, it appears to be much more difficult to identify structures that are susceptible to galloping. For example, in many cases of galloping signal supports, there will be a series of identical structures along a street, oriented the same way with respect to the prevailing wind, and only one of them is galloping while others are not. Because galloping is, in fact, a very rare occurrence, it is believed that numerous factors must combine their effects in order for galloping to occur.

The following section examines sign structures in Minnesota that are known to be resistant to vibration and fatigue. Subsequent sections examine structures that have had problems. Cost-effective ways to redesign these structures so that they would not be susceptible to fatigue are then discussed, so that researchers can quantify the significance of the impact of the fatigue design provisions of the 2001 Specifications.

Finally, specific site visits and local factors are discussed. Field visits to the sites of structures that have experienced problems typically reveal one or two factors that probably made these structures more susceptible. However, specific structures that do not meet the 2001 Specifications may be unaffected by fatigue and, therefore, need not be designed for fatigue or equipped with mitigation devices.

2.4.1 Fatigue Analyses of Cantilevered Sign Structures in Minnesota

In order to assess the conservatism of the truck-induced gust load ranges and natural wind load ranges recommended in *NCHRP Report 412*, an analysis of the cantilevered flat-panel sign structures used by Mn/DOT was performed. Because Mn/DOT sign structures almost never experience wind-induced fatigue damage, most, if not all, of the structures should follow the *NCHRP Report 412* design recommendations. A large number of failing Mn/DOT sign structures would indicate that the fatigue design recommendations were overly conservative.

Most Mn/DOT sign structures use four-chord, horizontal trusses fabricated from angles and supported by a single, round, tubular post. Because of the inherent stiffness of four-chord trusses, galloping is not possible [1]; therefore, this analysis did not include galloping. Vortex-shedding loads also do not need to be applied to these structures.

Various baseplate details, post diameters, post thicknesses, post heights, cantilever lengths, and sign areas were considered, resulting in 2,666 possible structures. Post diameters and thicknesses range from 457 mm to 508 mm (18–20 in.) and 6.35 mm to 23.8 mm (0.250–0.938 in.), respectively. Cantilever lengths up to 13.4 m (44 ft) and sign areas up to 32.5 m^2 (350 ft^2) are included in Mn/DOT's standard drawings for sign support structures. Stress ranges were calculated at all critical details using the sign width and cantilever length. The details at the column base are generally the most critical details for these structures (i.e., the details with the highest ratio of calculated stress range to CAFL). (The anchor rods had a much lower ratio of the calculated stress range to the CAFL.) The column base details, shown in Figure 2-70, and their CAFLs include the following:

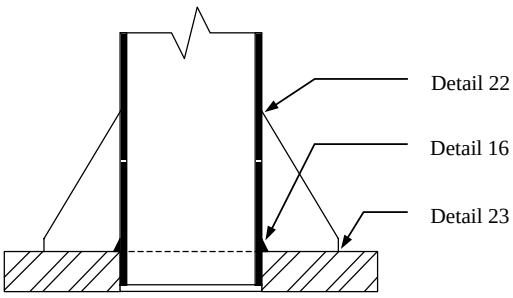

Figure 2-70. Baseplate connection details.

- The post is attached to the baseplate with a typical fillet-welded socket connection (Detail 16 in the 2001 Specifications). This Category E′ detail has a CAFL of 18 MPa (2.6 ksi).
- The stiffener-to-post connection is classified as Detail 22, because the stiffener intersects the post at an angle less than 60°. Ordinarily, this detail would be a Category C detail; however, it is a Category D detail because of the large stiffener thickness according to note (d) in Table 11-2 of the 2001 Specifications. Therefore, the CAFL for this detail is 48 MPa (7 ksi).
- The stiffener-to-baseplate connection is a transverse load-bearing, fillet-welded attachment with a thickness greater than 13 mm (0.5 in.) (Detail 23). The CAFL for this Category E detail is 30 MPa (4.5 ksi) for the stiffener-to-baseplate detail.

The stress ranges in all possible structures were calculated for natural wind-gust loads and truck-induced gust loads. The magnitude of the truck gusts applied in these analyses is the same as that recommended in *NCHRP Report 412* (i.e., $1{,}760C_DI_F$ Pa, or $36.6C_DI_F$ psf), not the revised value recommended in this report (i.e., $900C_DI_F$ Pa, or $18.8C_DI_F$ psf). The truck gusts were applied over the full width of any sign panels, unless the panels were longer than 7.3 m (24 ft). This procedure is in agreement with the *NCHRP Report 412* recommendations except for the maximum load application length of 7.3 m.

The possibility of signs longer than 7.3 m (24 ft) was overlooked in the development of the fatigue design provisions of the 2001 Specifications, and a recommendation has been made to change the 2001 Specifications to limit the length over which the load is applied. Applying the load over a length greater than 7.3 m assumes that three trucks will simultaneously pass beneath the structure. The likelihood that this will occur is extremely small, and the assumption is not appropriate for an infinite-life design check. In fact, it is believed that the probability of even two trucks with the worst-case configuration arriving simultaneously under the sign is also too small. Therefore, a recommendation is made in Section 3.2.1.5 of this report to limit the length over which truck gusts should be applied to 3.7 m (12 ft) to represent only one truck under the sign at a time.

The number of structures that "failed" (i.e., had the calculated stress range exceed the CAFL), was then determined. As Table 2-15 shows, none of the sections failed at the post-to-baseplate or stiffener-to-baseplate connections (Details 16 and 23). As well, only 1.2 percent of the structures failed at the stiffener-to-post connection (Detail 22), and none of the structures was overstressed by more than 15 percent.

The analysis was then run again using the recommendation made in this report (Section 3.2.1.5) to limit the length over which truck gusts should be applied to 3.6 m (12 ft) to represent only one truck under the sign at a time. In this case, only 0.1 percent of the structures failed (see Table 2-16). If

TABLE 2-15 Summary of Mn/DOT sign structure fatigue analysis check

Post		Base	Detail	Total	Failed	Percent	Max.
Diameter (in)	Thickness (in)	Type	Number	Structures	Structures	Failure	Stress (ksi)
18	0.25	A	16	320	0	0.0%	1.65
18	0.3125	A	16	265	0	0.0%	1.87
18	0.375	A	16	265	0	0.0%	1.80
18	0.4375	A	16	178	0	0.0%	1.85
18	0.5	A	16	320	0	0.0%	1.79
18	0.5625	A	16	178	0	0.0%	1.72
18	0.5625	B	16	307	0	0.0%	1.83
18	0.75	B	16	307	0	0.0%	1.71
18	0.9375	B	16	307	0	0.0%	1.61
20	0.375	B	16	1	0	0.0%	1.52
20	0.5	B	16	1	0	0.0%	1.43
20	0.5938	B	16	106	0	0.0%	1.82
20	0.8125	B	16	111	0	0.0%	1.67
18	0.25	A	22	320	20	6.3%	8.02
18	0.3125	A	22	265	5	1.9%	7.70
18	0.375	A	22	265	0	0.0%	6.49
18	0.4375	A	22	178	0	0.0%	5.84
18	0.5	A	22	320	0	0.0%	5.16
18	0.5625	A	22	178	0	0.0%	4.64
18	0.5625	B	22	307	5	1.6%	7.33
18	0.75	B	22	307	0	0.0%	5.67
18	0.9375	B	22	307	0	0.0%	4.68
20	0.375	B	22	1	1	100.0%	7.14
20	0.5	B	22	1	0	0.0%	5.46
20	0.5938	B	22	106	0	0.0%	6.21
20	0.8125	B	22	111	0	0.0%	4.69
18	0.25	A	23	320	0	0.0%	2.54
18	0.3125	A	23	265	0	0.0%	2.88
18	0.375	A	23	265	0	0.0%	2.77
18	0.4375	A	23	178	0	0.0%	2.85
18	0.5	A	23	320	0	0.0%	2.75
18	0.5625	A	23	178	0	0.0%	2.66
18	0.5625	B	23	307	0	0.0%	3.05
18	0.75	B	23	307	0	0.0%	2.85
18	0.9375	B	23	307	0	0.0%	2.68
20	0.375	B	23	1	0	0.0%	2.44
20	0.5	B	23	1	0	0.0%	2.29
20	0.5938	B	23	106	0	0.0%	2.92
20	0.8125	B	23	111	0	0.0%	2.67

TABLE 2-16 Summary of Mn/DOT sign structure fatigue analysis check with reduced truck-gust length (3.6 m)

Post		Base	Detail	Total	Failed	Percent	Max.
Diameter (in)	Thickness (in)	Type	Number	Structures	Structures	Failure	Stress (ksi)
18	0.25	A	22	320	3	0.9%	7.10
18	0.3125	A	22	265	0	0.0%	6.80
18	0.375	A	22	265	0	0.0%	5.76
18	0.4375	A	22	178	0	0.0%	5.84
18	0.5	A	22	320	0	0.0%	5.16
18	0.5625	A	22	178	0	0.0%	4.64
18	0.5625	B	22	307	0	0.0%	6.72
18	0.75	B	22	307	0	0.0%	5.21
18	0.9375	B	22	307	0	0.0%	4.30
20	0.375	B	22	1	0	0.0%	3.65
20	0.5	B	22	1	0	0.0%	2.79
20	0.5938	B	22	106	0	0.0%	5.34
20	0.8125	B	22	111	0	0.0%	4.13

the recommendation made in this report to reduce the magnitude of the truck-induced gust load were accepted, none of these structures would need to be redesigned.

This analysis shows that the truck gust and natural wind loads are not excessively conservative, or at least are not more conservative than Minnesota's present practice. The fact that Minnesota has not experienced vibration or fatigue problems shows that the 2001 Specifications can be used with confidence to identify structures that are not at risk.

2.4.2 Analysis of the Effects of Vortex Shedding on Tapered Luminaire Support Structures

In accordance with the preliminary findings of *NCHRP Report 412*, the 2001 Specifications recommend that vortex-shedding loads only be applied to symmetrical members that are tapered less than 0.0117 m/m (0.14 in./ft). This recommendation was based on the belief that the dimensions of most tapered members, when inserted into the Strouhal equation, yield critical wind velocities below 5 m/s (11 mph). When wind speeds are below this threshold velocity, an insufficient amount of energy is provided to excite the structure. In addition, a given wind velocity can only create a "lock-in" condition over a small range of member dimensions. Thus, vortex-shedding loads are only applied over a small portion of a tapered structure (i.e., where the dimensions are in the "lock-in" range) and cause what were thought to be insignificant connection stress ranges.

A videotape provided by a manufacturer showed a tapered luminaire support vibrating vigorously because of vortex shedding. The structure was oscillating in double curvature (i.e., peak displacements occurring near midheight and the pole top essentially remaining stationary). Displacement ranges were on the order of the section diameter. Double-curvature vibrations create much larger vortex-shedding pressures than first-mode vibrations because the critical wind speed is greater because of the higher resonant frequency. As a result, loading a short length of a tapered member with a large pressure can create forces large enough to lead to fatigue problems. The fourth design example completely outlines the loading of this tapered luminaire support (see Appendix B, Design Example 4). A brief explanation is also included below.

From the Strouhal equation, the critical wind velocity at which lock-in will occur is directly proportional to the natural frequency of the structure. For the videotaped structure, a finite element analysis determined that the first and second natural frequencies were 0.618 Hz and 6.952 Hz, respectively. Therefore, the critical wind velocity for double-curvature vibration is over 11 times greater than that for first-mode vibration. The equivalent static pressure range for vortex-shedding induced loads is proportional to the square of critical wind velocity. Therefore, the double-curvature pressure range is more than 126 times that for single curvature.

The *Ontario Highway Bridge Design Code* [14] recommends that vortex-shedding pressures be applied over the length of a tapered member for which the cross-sectional member dimension is within 10 percent of the critical dimension. Although this criterion drastically reduces the length over which vortex-shedding loads are applied, the magnitude of the double-curvature pressures (relative to single-curvature pressures) is so great that problematic fatigue stresses can still exist. As the design example shows, column-to-baseplate stresses nearly three times the CAFL can occur.

As these calculations and, most importantly, the videotape evidence show, vortex shedding can indeed create fatigue-related problems in tapered structures. Furthermore, the statement in the 2001 Specifications that tapered structures do not appear to be susceptible to vortex shedding has been disproved. The 2001 Specifications should be modified to require that tapered poles be checked for vortex shedding and that the higher modes should also be checked. If these changes are made to the 2001 Specifications, then the revised specifications will identify these at-risk structures adequately.

2.4.3 Fatigue Analysis of Failed Wyoming Signal Structure

This section describes details of the cracking in many signal support structures in Wyoming and the collapse of two structures. In fact, about 236 structures exhibited cracking, approximately 27 percent of all traffic signal structures that were inspected. The cracks were primarily located along the sides of the built-up box, mast-arm-to-post detail. The cities of Denver and Kansas City (Kansas) also experienced cracking of signal support structures with similar box details for the mast-arm-to-pole connections. This connection is known to have a relatively poor fatigue resistance.

On September 4, 1995, a cantilevered monotube traffic signal structure in Rock Springs, Wyoming, failed because of fatigue [35]. Investigation of the fallen structure revealed that the cracks had propagated through the pole wall at the toe of the weld connecting the built-up box. The 15.2-m (50-ft) tapered mast arm supported two three-light signal heads, one five-light signal head, and one flat-panel sign (762 by 610 mm, 30 by 24 in.). At the mast arm connection, the column diameter and thickness were 310 mm and 6.4 mm (12.2 in. and 0.25 in.), respectively. The built-up box was 310 mm (12.2 in.) wide, 467 mm (18.375 in.) tall, and 6.4 mm (0.25 in.) thick.

When galloping and natural wind loads were applied to the structure in accordance with *NCHRP Report 412*, the box-to-column connection was overstressed by factors of 3.62 and 2.43 in the in-plane and out-of-plane directions, respectively. In addition, the column section just below the box connection was overstressed by a factor of 2.68.

Calculations on a similar structure in Casper, Wyoming, in which a 480-mm (19-in.) pole crack was discovered, revealed comparable results. When the galloping and natural wind loads recommended in *NCHRP Report 412* were applied, the

box-to-column connection was overstressed by factors of 4.08 in the in-plane direction and 2.41 in the out-of-plane direction. Furthermore, the column section was overstressed by a factor of 1.98.

These calculations show that these at-risk structures are clearly identified by the 2001 Specifications. It is believed that these structures were affected by natural wind gusts and not by galloping. Wyoming is well known for the constant windy conditions. As noted previously in Section 2.2.6, Cheyenne, Wyoming, is among the four locations in the United States with the highest fatigue-limit-state wind velocity.

To a certain extent, the risk of failure from natural wind gusts can be correlated to the gustiness of the wind. The areas that have constant winds and pose the greatest risks for fatigue are not the same as those locations that have the highest design wind speed for strength calculations. The locations with the highest strength-design wind speeds are typically located near the coasts because the maximum winds are associated with gales or hurricanes. However, these winds may happen on average for 3 s every 50 years [36]. For fatigue design by the infinite-life approach, the fatigue-limit-state wind velocity, which is exceeded for an hour or two each year, is important. As discussed previously in Section 2.2.6, the fatigue-limit-state velocity was determined from available wind velocity data for over 285 sites in the United States, as well as 66 sites in the United Kingdom and 74 sites in Australia. A contour map was generated from these 285 sites in the United States [28]. This map could be used to identify sites where support structures would be particularly susceptible to fatigue from natural wind gusts.

Recently, Jay Puckett at the University of Wyoming has been examining the correlation between the failure rate of signal support structures in Wyoming and the wind power class, which is also available on maps of the United States and is proportional to the fluctuation in the wind. It is possible that such maps could also be used to identify structures that are at risk for natural wind-gust fatigue.

Significant in-plane motion occurs during buffeting by natural wind gusts, as well as the predominantly horizontal motion, and the 2001 Specifications do not explicitly take this occurrence into account. When the 2001 Specifications were written, it was anticipated that checking for fatigue under the galloping loads would always be necessary. The 2001 Specifications intended that the effect of galloping would be much larger than the in-plane effect of natural wind gusts. However, the authors overlooked the possibility that galloping loads would be ignored in some cases—for example, if mitigation devices were used. In this case, and if truck-induced loads are also ignored as allowed by the 2001 Specifications for signal support structures, there are no in-plane fatigue design loads.

Wyoming Department of Transportation (WYDOT) personnel justifiably believed that galloping did not relate to the failure. Therefore, they elected to rerun the analysis without galloping loads. Consequently, only out-of-plane stresses were checked in subsequent redesigns. Even without the galloping loads, however, these calculations still correctly showed that these structures would be at risk for fatigue.

Checking only the out-of-plane natural wind-gust load, the WYDOT calculations showed that increasing the thickness of the built-up box to 16 mm (0.625 in.) would result in an adequate design. However, because the cracking occurred in the post wall (not the built-up box), WYDOT personnel did not believe that increasing the box thickness would actually eliminate the cracking in the post. Therefore, they deemed the *NCHRP Report 412* provisions insufficient. However, if galloping loads had been included, the pole wall thickness would also have had to be increased, and this increase would have resulted in a satisfactory design.

The solution to this problem with the 2001 Specifications is to ensure that there is always some in-plane fatigue design load. The mitigation testing described in the previous section of this report showed that the galloping load is only reduced by a factor of 1.5 and not completely eliminated by the use of mitigation devices. Therefore, it seems appropriate that all structures should be designed for at least some galloping load. Section 3.2.1.4 recommends that the use of the mitigation device be used to alter the importance category from Category I to Category II. Thus, the change in importance category will cause a reduction in the galloping load (to 72 percent of Category I levels) rather than an elimination of it, which is consistent with the findings from the Texas Tech tests.

In lieu of this recommendation, it could be required that structures be designed for a vertical component to the natural wind-gust load. The effect would be approximately the same. Calculations showed that the truck-induced gust load, if it is reduced as recommended in this report, would not be sufficient to cause redesign of the pole wall thickness for these structures.

WYDOT personnel took a different approach to solving the problem of not having a required increase in the pole wall thickness when in-plane loads were not included in the analysis. A special clause was added to the 2001 Specifications that was not part of the specifications proposed in *NCHRP Report 412*: that connections welded to a tube shall be checked for punching-shear stress range according to AWS D1.1 Category K_2. This clause has caused problems for the design of a "box-type" connection of a single pole mast arm to the upright; in fact, this clause has rendered this common type of connection for signal support structures all but impossible to successfully design. Although this detail is certainly susceptible to fatigue, the research team believes that this clause is excessively conservative and that the previous recommendation that some fraction of the galloping loads always be included in the design of all sign and signal support structures should remedy this problem. The rationale for believing that punching shear stress is excessively conservative is discussed in Section 3.2.2.

2.4.4 Fatigue Analysis of Failed Caltrans Signal Structure

On December 12, 1999, a cantilevered monotube traffic signal structure near Rancho Cucamongo, California, failed because of fatigue [37]. The tapered mast arm (165-mm [6.5-in.] outside diameter at pole connection) supported one three-light signal head and two signs. One sign was a very large (1.83 m by 0.56 m [72 in. by 22 in.]) street sign mounted near the midpoint of the arm, and the other was a small "No U Turn" sign (approximate area of 0.4 m^2 [4 ft^2]) located between the other sign and the arm tip. The fatigue failure occurred at the pole-to-baseplate connection, at the toe of the socket connection's fillet weld. Cracks appeared to propagate from both sides of the post (i.e., beneath the mast arm and on the side opposite the mast arm). The outside diameter and thickness of the pole at the base were 238 mm (9.375 in.) and 4.55 mm (0.179 in.), respectively.

When John Dusel and R. Aguilar of Caltrans visited the site on December 28, 1999, vertical mast arm vibrations were observed on a nearby structure similar to the one that failed. The mast arm was reported to be galloping under steady winds of 7–11 m/s (15–25 mph). Winds were also powerful enough to rotate the large street sign into a near-horizontal plane. The location of the failed structure is approximately 6 m (20 ft) above the surrounding flat terrain. In addition, it is suspected that winds are channeled by mountains near the failure site, creating high-speed, steady winds (i.e., the ideal conditions for galloping).

Unfortunately, the signal head and signs were removed from the failed structure before Dusel and Aguilar had a chance to inspect them. Consequently, the exact placement of the signs and the size of the "No U Turn" sign could not be determined. According to Caltrans standard plans, the center of the street sign is to be located no farther than 3.2 m (10.5 ft) from the pole. District engineers, without designer approval, improperly added the "No U Turn" sign. Thus, the exact size or location of the sign is not included in the standard plans. In addition, because the large street sign did not appear to be rigidly mounted to the mast arm, the appropriateness of applying galloping loads to the sign was questioned. To deal with these uncertainties, four sets of calculations were performed to check the adequacy of the structure.

For the first set of calculations, the signal and both signs were subjected to galloping loads. For the "No U Turn" sign, the estimated area was used, and it was assumed to be located midway between the street sign and the arm tip. The street sign was assumed to be located as far from the pole as the plans allowed. This location resulted in a galloping stress range at the pole-to-baseplate connection of 53 MPa (7.7 ksi), which far exceeds the CAFL of a socket connection (18 MPa, or 2.6 ksi). When galloping loads were removed from the street sign, the stress range was reduced to 36 MPa (5.21 ksi), which is still much higher than the CAFL. A stress range of 44 MPa (6.38 ksi) occurred when galloping loads were only applied to the signal and the street sign. Again, this value exceeds the CAFL. Finally, galloping loads were only applied to the signal head and resulted in a stress range of 27 MPa (3.89 ksi). Even for this case, when the loading is clearly unconservative, stresses surpass the CAFL. Clearly, this structure was not properly designed to resist the galloping loads included in the 2001 Specifications. This finding reconfirms that the 2001 Specifications can identify the at-risk structures.

2.4.5 Cost-Effective Traffic Signal Structure Redesign Methods

A study was performed to investigate the most cost-effective ways to redesign a traffic signal structure to meet the fatigue design loads recommended in *NCHRP Report 412* and adopted in the 2001 Specifications. Simply increasing member sizes to reduce nominal gross-section stresses is rarely, if ever, a cost-effective redesign method. In lieu of eliminating particular fatigue loads by mitigating vibration, improving connection details is usually the most economical way to redesign a structure. The reasons for this are twofold:

- Connections are by far the most fatigue-prone portions of cantilevered signal, and for that matter all, structures. Increasing the fatigue resistance of the connection by raising the CAFL requires modifications at the connection only, whereas increasing the fatigue resistance by raising the section modulus requires that the entire member be modified. Thus, improving details is cost-effective because unnecessary changes are not made to the portions of the structure that are already adequately designed.
- Increasing member sizes enlarges the planar (i.e., wind-loaded) area of the structure. As a result, the magnitude of natural wind and truck-induced gust loads also increases.

The analyzed structure was taken from the first design example in *NCHRP Report 412*. It is a standard monotube signal structure supporting three signal heads. The dimensions of the structure can be found in Figure 2-71. Originally, the structure was designed to meet the requirements of the 1985 Specifications. The structure was redesigned 14 different ways to meet the requirements of the 2001 Specifications. Redesign methods varied from simply increasing section sizes to improving the connection details at one or more connections.

The weight of steel in the column and mast arm of the original structure was 6.90 kN (1.55 kips). Both the column and mast arm in the original structure are tapered. The column-to-baseplate and built-up-box-to-mast-arm connections use fillet-welded, tube-to-transverse plate (i.e., socket) connections (Detail 16, Fatigue Category E′). As well, a typical built-up-box-to-column connection (Detail 19, Fatigue Category K_2) is used.

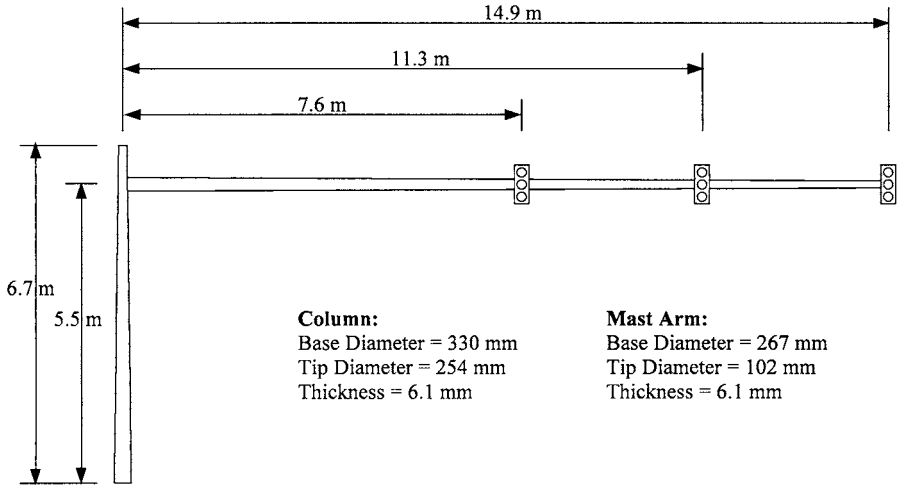

Figure 2-71. Redesigned traffic signal structure dimensions.

NCHRP Report 412 recommends a maximum vertical deflection range at the mast arm tip of 8 in. However, the 2001 Specifications do not include the 8-in. limit (the limit is only mentioned in the commentary). To account for this discrepancy, the structure was redesigned two different ways. To meet the *NCHRP Report 412* guidelines, both stress ranges and deflections were checked, whereas only stress ranges were checked for the 2001 Specifications. One other difference between *NCHRP Report 412* and the 2001 Specifications is the inclusion of Fatigue Category K_2. The design in *NCHRP Report 412* was redone to include the Category K_2 requirements. Therefore, the only difference between the two sets of analyses is whether the 8-in. deflection limit was checked.

2.4.5.1 Redesigns Meeting Both Stress Range and Deflection Criteria

For the stress-deflection analysis (see *NCHRP Report 412*), simply increasing the dimensions of the column and mast arm to resist the fatigue loads raised the total weight to 24.23 kN (5.45 kips), an increase of 251 percent. Obviously, the original structure was severely underdesigned to resist wind-induced fatigue loads (i.e., galloping, natural wind gusts, and truck-induced gusts). A summary of the "stress-deflection" analysis is included in Table 2-17.

The first connection redesign involved improving the fatigue categorization of the mast-arm-to-flange-plate connection from Category E′ (CAFL = 18 MPa) to Category E (CAFL = 31 MPa). This improvement can be achieved in the following ways:

- The weld itself can be improved first by replacing the fillet weld with a full-penetration groove weld, and then by either (a) attaching the backing ring to the plate with a full-penetration weld (Detail 11) or (b) attaching the backing ring (the thickness of which shall be limited to $\frac{3}{8}$ in.) to the plate with a continuous fillet weld (Detail E as recommended in Section 3.2.2 of this report).
- Properly sized stiffeners (i.e., gussets) can also be added to reduce the stress range at the fillet weld below the CAFL of 18 MPa (the detail at the stiffener tips will then control the design of the connection [Category E, Details 20–22]).

Improving the mast-arm-to-flange-plate connection to Category E reduced the weight of the column and mast arm to 18.83 kN (4.23 kips). This value is still 173 percent greater than the original structure, but it is also 22 percent less than the first redesign.

One design assumption made (for aesthetic reasons) was that the base diameter of the mast arm could be no larger than the diameter of the column at the height where the mast arm was attached. Thus, in order to increase the size of the mast arm, the entire column would also have to be enlarged. To avoid this costly result, the column taper was removed for the next design, which eliminated the unnecessary diameter increase at the column base. This slight design modification (along with the mast-arm-to-flange-plate connection improvement) reduced the structure weight to 15.96 kN (3.59 kips), a decrease of 34 percent from the first redesign.

For the fourth redesign, the column taper was restored and the attachment of the built-up-box-to-column connection was improved. Instead of simply fillet welding the top and bottom plates of the box to the column, as is shown in Detail 19, the plates were enlarged to completely surround the column (see Figure 2-72). The use of this ring-stiffener connection, which is currently employed by WYDOT, eliminates the problematic Category K_2 punching shear fatigue detail. Making this change lowered the structure

TABLE 2-17 Traffic signal redesigns (stress ranges and deflections checked)

	Sections Increased?	No	**Yes**	**Yes**	**Yes**	**Yes**	**Yes**	**Yes**	**Yes**
	Mastarm-to-Flange Plate Category	E'	E'	**E**	**E**	**E**	**E**	**D**	**D**
	Column-to-Baseplate Category	E'	E'	E'	E'	E'	**E**	**E**	**E**
	Column Tapered?	Yes	Yes	Yes	**No**	Yes	Yes	Yes	**No**
	Built-up Box Ring Stiffeners?	No	No	No	No	**Yes**	**Yes**	**Yes**	**Yes**
Column	diameter at base (mm)	330	**572**	**508**	**445**	**394**	**394**	**394**	330
	thickness (mm)	6.1	**11.1**	**11.1**	**11.1**	**9.5**	**7.9**	**7.9**	**7.9**
Mast-Arm	diameter at base (mm)	266	**507**	**444**	**445**	**330**	**330**	**318**	**330**
	thickness (mm)	6.1	**9.5**	**7.9**	6.1	**7.9**	**7.9**	6.1	6.1
Anchor Rods	diameter (mm)	38	38	38	38	38	38	38	38
	thread series	6	6	6	6	6	6	6	6
	number	4	4	4	4	4	4	4	4
	circle diameter (mm)	483	**724**	**660**	**597**	**546**	**546**	**546**	483
Flange Plate Bolts	diameter (mm)	32	**35**	**35**	**35**	32	32	32	32
	thread series	7	7	7	7	7	7	7	7
	number	4	4	4	4	4	4	4	4
	circle diameter (mm)	508	**660**	**596**	**597**	508	508	508	508
Built-Up Box	height (mm)	483	**634**	**571**	**572**	483	483	483	483
	width (mm)	266	**507**	**444**	**445**	**330**	**330**	**330**	**330**
	thickness (mm)	6.4	**9.5**	**9.5**	**9.5**	6.4	6.4	6.4	6.4
Fatigue Categories	Column-to-baseplate connection CAFL (MPa)	18	18	18	18	18	**31**	**31**	**31**
	Mastarm-to-flange plate connection CAFL (MPa)	18	18	**31**	**31**	**31**	**31**	**48**	**48**
	Column punching shear fatigue category	K_2	K_2	K_2	K_2	**N/A**	**N/A**	**N/A**	**N/A**
	Total Overstress (MPa)	113	**0**	**0**	**0**	**0**	**0**	**0**	**0**
	Unacceptable Deflection (mm)	190	**0**	**0**	**0**	**0**	**0**	**0**	**0**
	Weight of Steel (kN)	6.90	**24.23**	**18.83**	**15.96**	**12.57**	**11.66**	**9.73**	**9.69**
	Weight Increase from Original Structure	0%	**251%**	**173%**	**131%**	**82%**	**69%**	**41%**	**40%**
	Weight Decrease from First Redesign	N/A	**0%**	**22%**	**34%**	**48%**	**52%**	**60%**	**60%**

Note: Bold value indicates property is different from original structure.

weight by 48 percent to 12.57 kN (2.83 kips). Although the results of their work were not included in this analysis, Hamilton et al. also showed that using the complete ring-stiffener detail decreased in-plane and out-of-plane column stresses by 5–20 percent and 50 percent, respectively [38].

The column-to-baseplate connection was then improved from Category E′ to E, which can be accomplished just as the mast-arm-to-flange-plate improvements described previously. The combined column and mast arm weight was reduced to 11.66 kN (2.62 kips), 52 percent less than the original redesign when only section sizes were increased.

Next, the mast-arm-to-flange-plate connection was improved to Fatigue Category D. This improvement can be accomplished by first adding properly sized stiffeners (i.e., gussets) to reduce the stress range at the fillet weld connecting the mast arm to the flange plate below the socket connection CAFL of 18 MPa. To make the detail at the stiffener tip Category D, the weld termination must be ground smooth and meet the column face with either a transition radius greater than 51 mm (2 in.) or a taper less than 60° (Details 21 and 22). Either a full- or partial-penetration groove weld or a fillet weld can be used to attach the stiffener to the column. Making one of these changes can reduce the structure weight to 9.73 kN (2.19 kips), which is 60 percent less than the first redesign and only 41 percent greater than the original, greatly underdesigned structure.

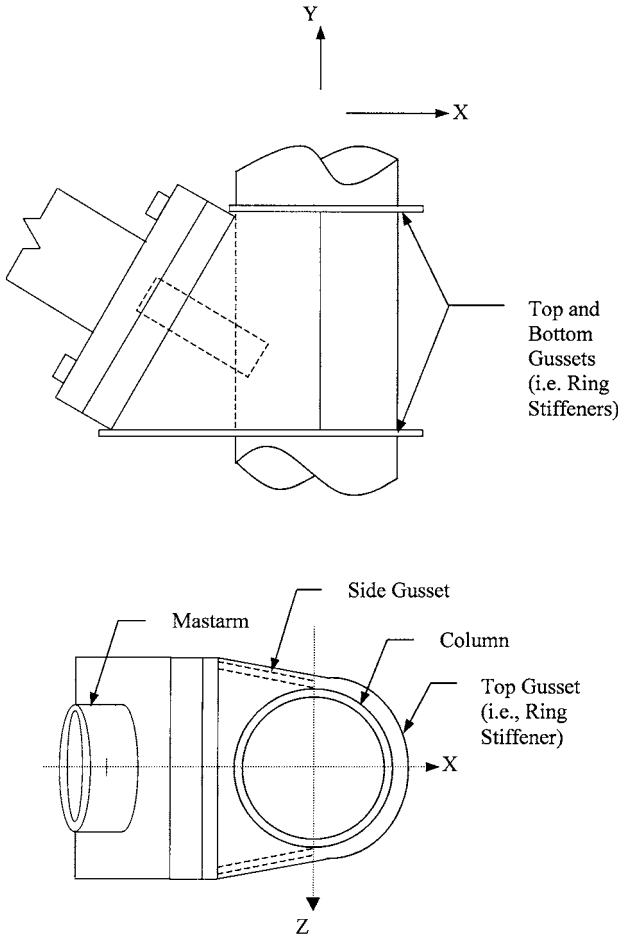

Figure 2-72. Built-up box using ring stiffeners.

For the final redesign, the column taper was again removed. This resulted in only a slight improvement over the previous redesign. A structure weight of 9.69 kN (2.18 kips), which is 40 percent greater than the original structure, would be sufficient.

2.4.5.2 Redesigns Meeting Only Stress Range Criterion

Because deflection rarely controls the fatigue design of structures with poor fatigue details (i.e., Categories E′ and E), the first five redesigns when only stress (and not deflection) was checked are exactly the same as those described previously. However, when more fatigue-resistant connections are used (i.e., Categories C and D), smaller section sizes can be used, and, consequently, deflections increase. Thus, because deflections were not an issue for the second set of redesigns, the smaller sections were adequate, and structure weights decreased. A summary of the "stress-only" analysis is available in Table 2-18.

The only difference between the original structure and the first redesign of the stress-only analysis (that wasn't also changed in the first set of redesigns) was that the mast-arm-to-flange-plate connection was improved to Category C. Properly sized stiffeners must be attached to the column with full-penetration groove welds. The weld termination must be ground smooth and intersect that column at a radius greater than 152 mm (6 in.) or a taper less than 15° (Detail 21). Doing so reduced the structure weight to 9.97 kN (2.24 kips), which is 59 percent less than redesigning by simply increasing member sizes.

In addition to the change above, the column-to-baseplate connection was improved to Category E and the column taper was removed for the next redesign. This decreased the weight to 9.33 kN (2.10 kips), which is 61 percent less than the first redesign and only 35 percent greater than the original structure.

For the following redesign, three changes were made:

- The mast-arm-to-flange-plate connection was downgraded to Category D (by detailing the stiffeners as described for the stress and deflection analysis);
- The column taper was restored; and
- The ring-stiffened, built-up box was used.

Making these changes allowed the structure weight to be reduced to 9.17 kN (2.06 kips), which is only 33 percent greater than the original structure. The column taper was then removed, which lowered the weight to 8.86 kN (1.99 kips), 28 percent greater than the original structure.

The mast-arm-to-flange-plate connection was then upgraded to Category C (as stated previously, this can be done by using properly sized stiffeners attached to the column with full-penetration groove welds) and the column taper was again restored. These changes reduced the structure weight to 8.60 kN (1.93 kips), a value that is only 25 percent larger than the original structure. Removing the column taper lowered the weight to 8.29 kN (1.86 kips). This final design is 66 percent smaller than the redesign achieved by simply increasing member sizes. In addition, it is only 20 percent larger than the original structure that was massively underdesigned for fatigue.

Improving connection details obviously has its costs. However, the increase in fabrication costs is far outweighed by the savings in material costs. As the last redesign showed, material costs could be reduced by a factor of three. Other studies have shown that increases in fabrication costs can be as low as 5–10 percent [18].

2.4.6 Field Visits of At-Risk Structures

Cantilevered structures that have already experienced vibration or fatigue problems were also visited in order to characterize at-risk structures. Structures from seven

TABLE 2-18 Traffic signal redesigns (only stress ranges checked)

	Sections Increased?	No	**Yes**	**Yes**	**Yes**	**Yes**	**Yes**	**Yes**	**Yes**	**Yes**	**Yes**	**Yes**	**Yes**
	Mastarm-to-Flange Plate Category	E'	E'	**E**	**E**	**E**	**E**	**C**	**C**	**D**	**D**	**C**	**C**
	Column-to-Baseplate Category	E'	E'	E'	E'	E'	**E**	E'	**E**	**E**	**E**	**E**	**E**
	Column Tapered?	Yes	Yes	Yes	**No**	Yes	Yes	Yes	**No**	Yes	**No**	Yes	**No**
	Built-up Box Ring Stiffeners?	No	No	No	No	**Yes**	**Yes**	No	No	**Yes**	**Yes**	**Yes**	**Yes**
Column	diameter at base (mm)	330	**572**	**508**	**445**	**394**	**394**	**368**	**343**	**394**	330	**394**	330
	thickness (mm)	6.1	**11.1**	**11.1**	**11.1**	**9.5**	**7.9**	**11.1**	**9.5**	**7.9**	**7.9**	**7.9**	**7.9**
Mast-Arm	diameter at base (mm)	266	**507**	**444**	**445**	**330**	**330**	266	266	**292**	**292**	266	266
	thickness (mm)	6.1	**9.5**	**7.9**	6.1	**7.9**	**7.9**	6.1	6.1	6.1	6.1	6.1	6.1
Anchor Rods	diameter (mm)	38	38	38	38	38	38	38	38	38	38	38	38
	thread series	6	6	6	6	6	6	6	6	6	6	6	6
	number	4	4	4	4	4	4	4	4	4	4	4	4
	circle diameter (mm)	483	**724**	**660**	**597**	**546**	**546**	**521**	**495**	**546**	483	**546**	483
Flange Plate Bolts	diameter (mm)	32	**35**	**35**	**35**	32	32	32	32	32	32	32	32
	thread series	7	7	7	7	7	7	7	7	7	7	7	7
	number	4	4	4	4	4	4	4	4	4	4	4	4
	circle diameter (mm)	508	**660**	**596**	**597**	508	508	508	508	508	508	508	508
Built-Up Box	height (mm)	483	**634**	**571**	**572**	483	483	**660**	**660**	483	483	483	483
	width (mm)	266	**507**	**444**	**445**	**330**	**330**	**304**	**343**	**330**	**330**	**330**	**330**
	thickness (mm)	6.4	**9.5**	**9.5**	**9.5**	6.4	6.4	**9.5**	**6.4**	6.4	6.4	6.4	6.4
Fatigue Categories	Column-to-baseplate connection CAFL (MPa)	18	18	18	18	18	**31**	18	**31**	**31**	**31**	**31**	**31**
	Mastarm-to-flange plate connection CAFL (MPa)	18	18	**31**	**31**	**31**	**31**	**69**	**69**	**48**	**48**	**69**	**69**
	Column punching shear fatigue category	K_2	K_2	K_2	K_2	**N/A**	**N/A**	K_2	K_2	**N/A**	**N/A**	**N/A**	**N/A**
	Total Overstress (MPa)	113	**0**	**0**	**0**	**0**	**0**	**0**	**0**	**0**	**0**	**0**	**0**
	Weight of Steel (kN)	6.90	**24.23**	**18.83**	**15.96**	**12.57**	**11.66**	**9.97**	**9.33**	**9.17**	**8.86**	**8.60**	**8.29**
	Weight Increase from Original Structure	0%	**251%**	**173%**	**131%**	**82%**	**69%**	**44%**	**35%**	**33%**	**28%**	**25%**	**20%**
	Weight Decrease from First Redesign	N/A	**0%**	**22%**	**34%**	**48%**	**52%**	**59%**	**61%**	**62%**	**63%**	**65%**	**66%**

Note: Bold value indicates property is different from original structure.

different locations throughout the country (six described in this section and one in the next section) were investigated. For each type of structure that was visited, there was at least one circumstance that was the likely source of the problem.

Numerous monotube traffic signal structures in the Lubbock, Texas, area were visited in November of 1999. Many of the structures were experiencing small-amplitude galloping (i.e., approximately 30-cm, mast-arm-tip vertical displacement ranges). Among the likely causes of vibration were high-speed, steady winds. The mast arms of structures experiencing the greatest displacements were oriented perpendicular to prevailing winds. In addition, the structures were located on streets lined with two- and three-story buildings. The buildings appeared to create a tunnel effect, channeling the winds down the street towards the signal structures. Attempts had been made to mitigate the galloping by applying damping plates similar to the ones tested at Texas Tech in 1995 [29]. However, the plates were severely undersized (approximately 15 cm by 30 cm instead of the 41-cm-by-168-cm size that was recommended) and located incorrectly (midway between two signal heads instead of directly above the signal head).

Three monotube signal structures that had experienced large-amplitude vibrations were visited in Tampa, Florida. Overloading (as many as four signal heads) of extremely long mast arms (as long as 23 m [75 ft]) appeared to be the primary cause of the problems. One of the structures located near the University of Tampa is shown in Figure 2-73. As the figure shows, the 22-m long cantilevered mast arm spans four lanes of traffic and an adjacent sidewalk. Attempts were made to mitigate vibrations by installing a damping plate, but the damping plate does not work with vertical signal heads. Also, it was improperly attached between the signal heads instead of above them (see Figure 2-74).

Another of the Tampa signal structures was located near the airport (see Figure 2-75). It was very similar to the University of Tampa structure, except that it featured two mast arms instead of one. The primary mast arm was approximately the same length as the university one (spanning three lanes and a large shoulder), and the secondary mast arm was about half that length. Not only was the primary mast arm

Figure 2-73. At-risk signal structure near University of Tampa.

Figure 2-75. At-risk signal structure near Tampa airport.

very long and heavily loaded (three signals and one illuminated sign), but it was also supported by a very poorly designed built-up box connection (see Figure 2-76). Large portions of the side gusset plates of the built-up box were cut out to provide access to the flange plate nuts. If either cap screws and a threaded built-up box flange plate or a wider flange plate had been used, the cutouts would not have been necessary.

The third signal that was visited in the Tampa area was the structure that mitigation testing was performed on (see Figure 2-43). As with the other two structures, a long, heavily loaded (four signal heads and two signs) mast arm appeared to be the source of the wind-induced vibrations.

Similar signal structures were visited in the Dallas area. None of these were specifically known to experience vibration problems. However, all of them had damper plates installed (see Figure 2-77), many of which were broken or installed incorrectly (see Figure 2-78).

A pair of cantilevered sign structures near Denver that had been reported to experience vibration problems was investigated. One structure was a two-chord truss (see Figure 2-79), while the other was a bent monotube (see Figure 2-5). Both structures are located in the foothills of the Rocky Mountains (see Figure 2-80). Winds seemed to intensify as they were channeled down the mountains near the structures.

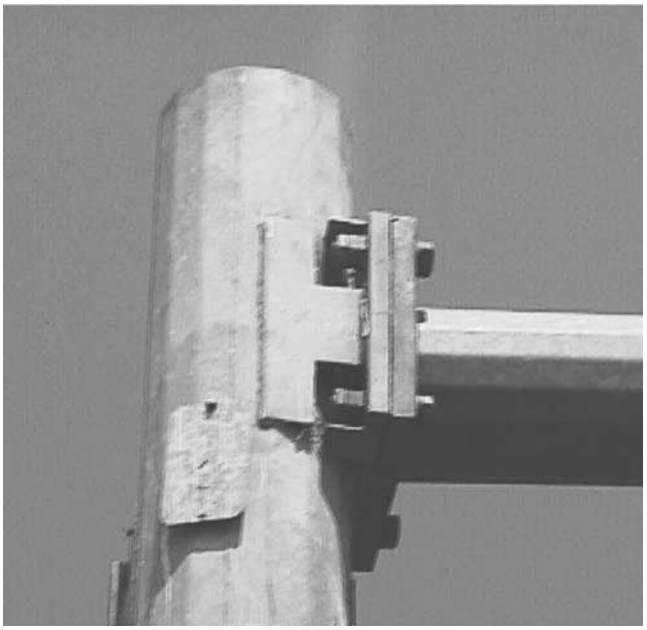

Figure 2-76. Poor built-up box connection on Tampa airport structure.

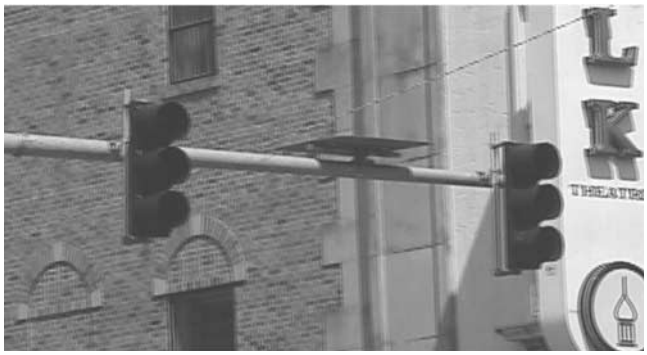

Figure 2-74. Improperly installed damping plate on University of Tampa structure.

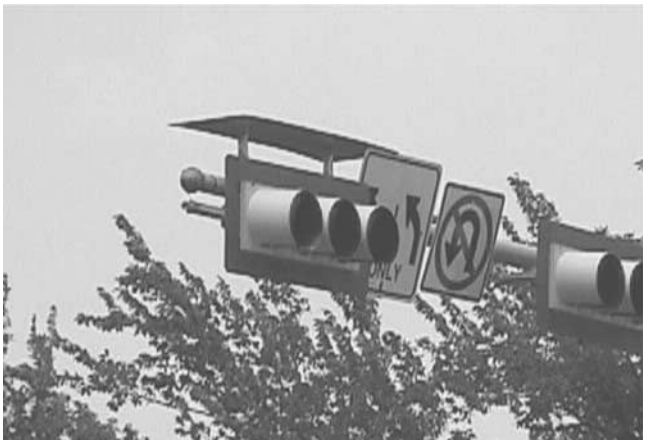

Figure 2-77. Damping plate properly installed on Dallas signal structure.

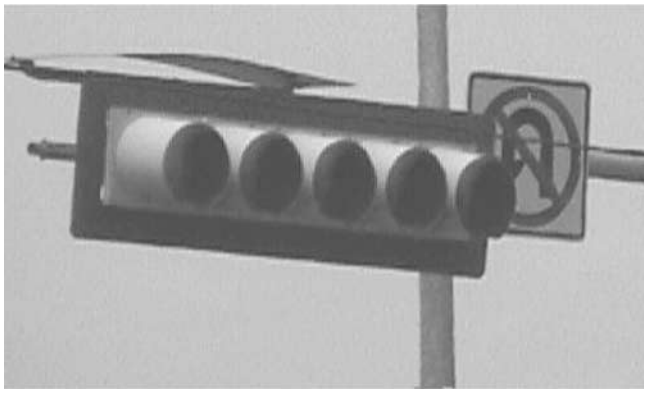

Figure 2-78. Broken damping plate improperly installed on Dallas signal structure.

Figure 2-80. Rocky Mountains near sign structures.

Also, most of these structures were bent-monotube structures, which are known to be more susceptible to galloping than multiple-chord trusses are.

Numerous fatigue failures of box-section luminaire supports in the St. Louis, Missouri, area have been reported. Subsequently, the fatigue-prone, column-to-baseplate connection was retrofitted, as is shown in Figure 2-81. The poorly designed original column-to-baseplate detail is likely the primary explanation for the failures. Welding of square and multisided tubes is also known to be more susceptible to welding defects.

Four-chord truss sign bridges in the Tampa, Florida, area that had been reported to vibrate greatly were also investigated. As Figure 2-82 shows, only the bottom two chords of the horizontal truss are attached to the upright trusses. Consequently, the box truss is essentially simply supported, as little rotational constraint is provided at its ends. If all four chords had been attached to the uprights, rotation at the connection and the effects of fluctuating wind loads on the structure would be limited.

2.4.7 Field Testing of At-Risk Signal Structure in Wyoming

In addition to the field investigations of at-risk structures performed by University of Minnesota researchers described previously, University of Wyoming researchers performed an extensive field study on a signal structure in Laramie, Wyoming [38]. The signal post supports a 15-m (50-ft) mast arm. Large-amplitude, wind-induced mast arm vibrations had been observed prior to the commencement of testing.

The primary objective of the testing was to determine actual in-plane and out-of-plane global (i.e., nominal) stresses

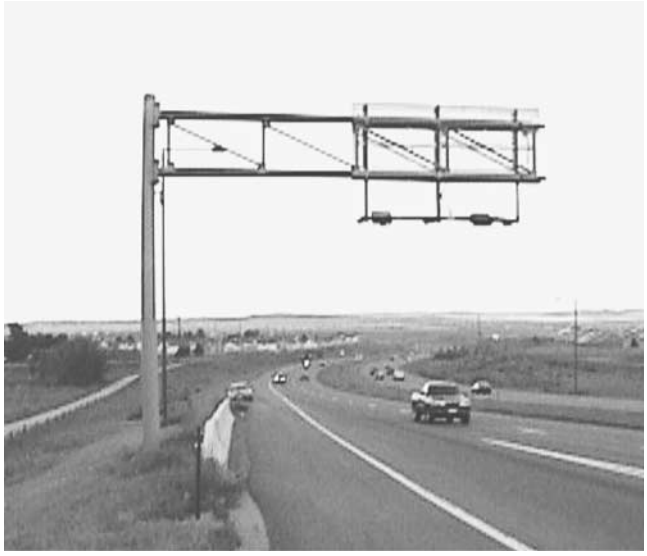

Figure 2-79. At-risk two-chord truss in foothills of Rocky Mountains.

Figure 2-81. Retrofitted luminaire base detail in St. Louis.

Figure 2-82. Four-chord truss sign bridge in Tampa.

in the built-up box connection and to quantify their interaction with each other. Wind speeds, wind direction, and stresses were recorded for a 13-month period. Stresses were only recorded when the wind speed was greater than 4.5 m/s (10 mph) for the first 9 months, whereas they were recorded continuously over the final 4 months.

As could easily be expected of a structure experiencing large vibrations, a relatively high percentage of the measured stress cycles in the built-up box exceeded the CAFL. For an infinite-life fatigue design, only 1 in 10,000 stress cycles are permitted to be larger than the CAFL (i.e., 0.01 percent of all cycles). According to the 2001 Specifications, the CAFL for the built-up box is 8 MPa (1.2 ksi) for both the in-plane and out-of-plane directions (Fatigue Category ET). However, during the 4-month period when stresses were continually recorded, more than 1.5 percent of the in-plane cycles and 0.1 percent of the out-of-plane cycles exceeded 9 MPa (1.3 ksi). Similarly, 1.9 percent of the in-plane and 0.3 percent of the out-of-plane cycles were greater than 7 MPa (1.0 ksi). The exact percentage of stress cycles that exceeded 8 MPa was not available because of the manner in which bins were partitioned in the stress range histogram.

Two in-plane and out-of-plane stress combination methods were evaluated. The square root of the sum of the squares (SRSS) method uses the following equation:

$$\sigma = \sqrt{(\sigma_{in})^2 + (\sigma_{out})^2} \tag{2.22}$$

where

σ = combined stress (MPa),
σ_{in} = in-plane stress (MPa), and
σ_{out} = out-of-plane stress (MPa).

The complete quadratic combination (CQC) method is a more complicated method that incorporates the rotational frequency and damping ratio in each direction as follows:

$$\sigma = \sqrt{\sum_{i=1}^{2}\sum_{j=1}^{2}\sigma_i \rho_{ij} \sigma_j} \tag{2.23}$$

where

σ_i = stress in mode i (MPa),
σ_j = stress in mode j (MPa),

The cross-modal coefficient ρ_{ij} is

$$\rho_{ij} = \frac{8(\xi_i \xi_j)^{1/2}(\xi_i + r\xi_j)r^{3/2}}{(1-r^2)^2 + 4\xi_i\xi_j r(1+r^2) + 4(\xi_i^2 + \xi_j^2)r^2} \tag{2.24}$$

where

$$r = \frac{\omega_j}{\omega_i},$$

ω_i = the angular frequency for mode i (radians per second),
ω_j = the angular frequency for mode j (radians per second),
ξ_i = the damping ratio for mode i, and
ξ_j = the damping ratio for mode j.

Both methods yielded similar results. Therefore, the SRSS method was determined to be the preferred method because of its relative simplicity.

Other important findings of the Wyoming field study were that high-speed winds appeared to cause greater out-of-plane displacements (and stresses) than in-plane displacements. In addition, McDonald et al.'s [29] finding that the installation of backplates and signs increases mast arm motion was verified.

2.4.8 Summary of the Characterization of At-Risk Structures

As has been shown previously, the provisions of *NCHRP Report 412* that were adopted in the 2001 Specifications have performed as expected for various structures that clearly either were or were not at risk. For the conservatively designed Minnesota four-chord sign structures that are clearly not at risk, the 2001 Specifications predict that the structures are adequately designed for fatigue. For the failed signal structures in Wyoming and California (which obviously were at risk), use of the 2001 Specifications would have predicted the failures.

The susceptibility of tapered members to vortex-shedding-induced fatigue problems has been witnessed and verified with calculations. As well, the cost-effectiveness of improving connection details instead of increasing member sizes was shown when structures must be redesigned to meet the fatigue provisions of the 2001 Specifications. Experience has shown that vortex shedding can lock in on any of at least the first three modes of vibration; therefore, changing the stiffness to alter the natural frequencies of light poles cannot prevent vortex shedding. Of course, the stiffer the pole, the lower the resulting stress ranges will be, so stiffness is always a positive factor.

Obviously, the more flexible any structure is, the more susceptible it is to wind-induced vibration. Almost all sign and signal support structures that have been tested in the field have natural frequencies in the range 0.5 Hz to 2 Hz. This is

probably due to the design for dead-load deflection because the frequency is proportional to the square root of the ratio of the stiffness divided by the mass. Increases in mass are accompanied by almost proportional increases in stiffness, keeping the ratio of these approximately constant.

Because most cantilevered sign and signal support structures have similar frequencies, it is not known if a change in this frequency would make the structure less susceptible to galloping and other forms of wind-induced vibration. Because the mass would be relatively unchanged, changing the frequency would be accomplished primarily by changing the stiffness. It is suspected that lowering the stiffness and frequency would make the vibration susceptibility worse and that increasing the stiffness and frequency would make it better. It is known that increasing the stiffness would decrease the stress and displacement amplitudes, and vice versa. This is probably not the most cost-effective way to solve the problem, however, because it would take a factor of four increase in the stiffness to cause a factor of two increase in the frequency. Designing structures to reduce the stress ranges for fatigue according to the 2001 Specifications should lead to stiffer structures in general, which should be beneficial.

Monotube structures are typically more susceptible to vibration than trusses are, although two-chord truss sign structures have been reported to gallop. There has never been a reported problem with vibration or fatigue of cantilevered four-chord trusses, so it is suggested in the 2001 Specifications that these trusses do not need to be designed for galloping.

Experience with signal support structures that have been reported to have problems indicates that both horizontally and vertically mounted signal heads are susceptible. Signal heads mounted eccentrically, as well as those essentially centered on the mast arm, have been reported to vibrate. The further the signal head or sign is out on the mast arm, the more susceptible the structure is to vibration because of the longer moment arm. Various shapes of signal heads are also susceptible, including those with and without backplates and those with louvered backplates. Previous research at Texas Tech University [29] also examined the lift and drag characteristics of various shapes of signal heads and found that many different types were potentially susceptible. At this time, it is not possible to rule out the susceptibility of any type. One exception is articulated signal heads—that is, signal heads not rigidly mounted on the support structure. Articulated signal heads or signs are not susceptible to galloping or other types of wind-induced vibration. Also, span-wire supports are typically not susceptible to galloping. However, traffic engineers typically do not want to have articulated signal heads.

Field visits of at-risk structures performed by researchers at the Universities of Minnesota and Wyoming have shown that some circumstances explaining the vibration or fatigue problem usually exist. Among these circumstances are

- High-speed, steady winds channeled toward the structure;
- Overloading of extremely long cantilevered arms;
- Poor connection details; and
- Improperly installed mitigation devices.

Although the identification of these problems appears quite obvious after the fact, it is difficult to know in advance if such conditions will actually lead to vibration and fatigue problems. Therefore, it is possible to identify structures that are clearly not at risk using the 2001 Specifications. However, of the structures that are identified by the 2001 Specifications as at risk, a large number may still function properly with no fatigue or vibration problems. It is not really possible to identify which of these at-risk support structures will not be affected by fatigue and which, therefore, do not have to be designed for fatigue or provided with a mitigation device.

2.5 QUANTIFICATION OF IMPORTANCE FACTORS

Importance factors are used in specifications to reflect different levels of importance of structures and different consequences of failure. For example, ASCE 7-98 [36] defines the importance factor for buildings and other structures for wind loads as "a factor that accounts for the degree of hazard to human life and damage to property." The design wind loads are multiplied by the importance factors, which indirectly change the level of structural reliability or probability of failure of these structures.

ASCE 7-98 defines four categories of buildings and other structures:

- Category I factors ". . . represent a low hazard to human life in the event of failure"; examples include agricultural and minor storage facilities.
- Category II factors include "all . . . except those listed in Categories I, III, and IV."
- Category III factors ". . . represent a substantial hazard to human life in the event of failure"; examples include schools and buildings where more than 300 people congregate in one area.
- Category IV factors include ". . . essential facilities"; examples include hospitals, fire stations, rescue stations, and police stations.

For wind loads, an importance factor of 1.0 is used for Category II buildings, which would include typical occupancies such as offices and residences. These structures are designed for the full strength of the design loads—for example, for wind, the design loads are selected to represent gusts with a 0.02-percent probability of occurrence per year (or equivalently a 50-year mean return period).

With the load factors and resistance factors used in recent specifications, the resulting probability of failure for buildings and bridges during their lifetime is theoretically on the order of 0.3 percent, although this probability is only a theo-

retical target for the specifications and does not have any credibility as an actual failure probability. It is widely accepted that the actual failure rate is much smaller than this probability. For example, there are approximately 600,000 bridges in the United States, and the failure rate is only about one or two per year, excluding the occurrence of illegal trucks on posted historical bridges with low ratings. This rate would correspond to a probability of failure over a 75-year life of 0.025 percent.

A higher importance factor of 1.15 is used for the critical Category III and IV structures. This 15-percent increase in the design load will decrease the probability of failure to less than 0.1 percent in this case. It is relatively expensive to achieve this level of reliability, but it is deemed worthwhile for these critical structures.

An importance factor of 0.87 is used to reflect the lower consequences of failure of Category I buildings. These structures are not likely to be occupied when there is severe weather and can be designed more economically to a lower level of reliability and not represent a greater hazard to the public.

Similarly, cantilevered support structures can be separated into at least three categories of importance. At one extreme are cantilevered support structures in rural areas where there is low traffic and the consequences of a failure are relatively minimal. A majority of cantilevered support structures may fit in this category. The present level of reliability achieved with the 1994 Specifications is deemed by most agencies to be satisfactory for these structures. At the other extreme are structures on high-speed, high-traffic highways for which a collapse will almost certainly lead to a collision. Most agencies would like a higher level of reliability for at least this category of structures, even if this increase meant a higher economic cost. There are also probably a large number of structures that do not clearly fit in either of these categories and are in an "in between" category.

Therefore, importance factors were proposed in *NCHRP Report 412* and were adopted in the 2001 Specifications to adjust the level of structural reliability of cantilevered support structures for different conditions. Table 2-19 lists the importance factors that were recommended in *NCHRP Report 412* for Category I, II, and III structure types. (The order of the categories is opposite the order in ASCE 7-98, with Category I being most important.) The table is further subdivided to provide importance factors for the design of cantilevered signal, sign, and luminaire structures when considering galloping, vortex shedding, natural wind, and truck-induced wind gusts. These importance factors should be applied to the fatigue-limit-state wind load ranges prior to determining the fatigue resistance, maximum mast arm displacement of cantilevered support structures, or both.

Definitions of the three importance categories are as follows:

- Category I—critical cantilevered support structures installed on major highways,
- Category II—other cantilevered support structures installed on major highways and all cantilevered support structures installed on secondary highways, and
- Category III—cantilevered support structures installed at low-risk locations.

The reliability of Category III structures was calibrated to be approximately the same as the present level of reliability for cantilevered support structures designed by the 1994 Specifications. Most of these cantilevered support structures have performed satisfactorily over the years. In fact, as noted in the introduction to this report, the probability of failure of the average cantilevered support structure designed by the 1994 Specifications is actually low in comparison with buildings or bridges. Certainly, the risk of colliding with a collapsed support structure is negligible in comparison with the other risks involved in driving a motor vehicle.

To attempt to quantify the reliability of cantilevered support structures, the failure probability per year can be estimated by dividing the number of failures of these structures per year by the total number of support structures of any specific type. Unfortunately, there are not very good data available for computing these failure probabilities.

TABLE 2-19 Importance factors for vibration and fatigue design

Category		Importance Factor			
		Galloping	Vortex Shedding	Natural Wind	Truck Gusts
I	Sign	1.0	x	1.0	1.0
	Signal	1.0	x	1.0	1.0
	Luminaire	x	1.0	1.0	x
II	Sign	0.72	x	0.85	0.90
	Signal	0.64	x	0.77	0.84
	Luminaire	x	0.66	0.74	x
III	Sign	0.43	x	0.69	0.79
	Signal	0.28	x	0.53	0.67
	Luminaire	x	0.31	0.48	x

Note: x - Structure is not susceptible to this type of loading.

The failures or occurrences of excessive vibration that have been reported were summarized in Table 2-1. Sometimes there was an unusually large failure rate. For example about 236 signal support structures (about 27.3 percent of all those inspected) were cracked in Wyoming. These failures were due to a poor mast arm connection detail (i.e., built-up box detail) and to particularly high constant wind speeds, among the worst in the United States. Also, 1–2 percent of all the sign support structures in Wisconsin were found to be cracked in recent inspections. This was due to the use of poor fatigue details and aluminum, which has inherently lower fatigue strength than steel for comparable details.

Excluding these unusual circumstances leading to local rashes of failures, there have been about 100 cases of excessive vibration or fatigue that have occurred over a 7-year period. Considering that there are even more incidents than researchers know about, there is an estimated failure rate of at least 20 per year for cantilevered support structures.

Based on survey data, it is estimated that there are approximately 3 million publicly owned cantilevered sign, signal, and light support structures in the United States. Therefore, the annual failure rate is probably within the range from 0.0001 percent to 0.001 percent. If the cantilevered support structures have a design life of about 30 years, this annual failure rate represents a probability of failure over the lifetime within a range of 0.003 percent to 0.03 percent.

So the present probability of failure for cantilevered support structures is probably less than, but comparable to, the theoretical lifetime probability of failure for buildings and bridges (on the order of 0.025 percent). However, the present failure rate for cantilevered support structures is greater than can be tolerated by the agencies and the public. The difference between support structures and bridges is that the smaller number of bridges at the same probability of failure will result in rare occurrences of bridge failures. The period between major failures leading to loss of life on a national level will be several years, and this is long enough for the public to tolerate.

With the much larger number of support structures at approximately the same probability of failure, however, there will be frequent sign and signal support structure failures, much as there are presently. It seems that a different standard of reliability or acceptable probability of failure applies at least for the most critical support structures (i.e., those structures that, if collapsed, would likely result in fatalities due to collision with a motor vehicle on the roadway).

The importance factors adjust the anticipated failure rate for the three categories of cantilevered support structures. For example, the importance factor for Category I, the most important cantilevered support structures, is 1.0, so these structures are designed for the full strength of the fatigue-limit-state, design-load ranges. The fatigue-limit-state, design-load ranges represent rarely occurring, wind-loading phenomena. The failure rate for structures designed for Category I under the 2001 Specifications can only be estimated.

Most of the at-risk structures that were discussed in the previous section would have to have been redesigned if they were checked by the rules for Category I in the 2001 Specifications. Therefore, it is reasonable to assume that if they had been designed for Category I, they would not have failed. One exception to this assertion is the bent monotube VMS support structures that failed from galloping in California. When one of these structures was instrumented, it was found that stress ranges were greater than what would be predicted from the fatigue-limit-state design load range for galloping. Therefore, if this structure had been redesigned for the 2001 Specification, it may still have experienced stress ranges greater than the CAFL and, therefore, may still have cracked.

On the basis of these findings, it is reasonable to assume that most of the present 20 or more failures per year would be eliminated if all structures were designed for Category I under the 2001 Specification. So, if there were a failure rate of 1 per year rather than 20, the probability of failure over the lifetime would be 20 times less than for Category III, or somewhere within a range of 0.00015 percent to 0.0015 percent. These probabilities of failure are very uncertain and are provided here for the sake of comparison only.

The proposed rules to determine what category to use for what type of structures are as follows. The criteria for Category I are clearly defined. Structures not meeting these criteria for Category I should be examined to see if they meet the criteria for Category III. If the structure meets neither of these sets of criteria, then it is in Category II.

Structures classified as Category I present a high hazard in the event of failure. It is recommended that all structures without proven mitigation devices on roadways with a speed limit in excess of 60 km/h (35 mph) and average daily traffic (ADT) exceeding 10,000 in one direction (regardless of the number of lanes) or average daily truck traffic (ADTT) exceeding 1,000 in one direction (also regardless of the number of lanes) be classified as Category I structures.

At the 10,000 ADT rate, there is a vehicle under the structure at an average of every 8.6 seconds. This means that a structure's collapse is very likely to result in a collision, and the consequences of that collision will be severe because of the high speed limit. The limit on ADTT is based on the possibility of truck-induced gust loads. If there are 1,000 trucks per day, then there could be more than 10 million truck-gust cycles applied to the structure over a 28-year lifetime, which is enough to initiate fatigue cracking if the stress ranges are just above the CAFL.

Structures on state highways or U.S. highways with lower speed limits or lower ADT or ADTT than discussed previously should also be included in Category I if any of the following conditions apply:

- They are cantilevered structures with a span in excess of 17 m (55 ft) or high mast towers in excess of 30 m (100 ft).

- They are located in an area that is known to have wind conditions that are conducive to vibration. (This would include any areas with a mean annual wind speed in excess of 5 m/s [11 mph].)
- They are located near the foothills of mountain ranges.

The last two criteria reflect the greater susceptibility of these specific types of structures, as discussed in the previous section. This would include most structures on such highways in Wyoming, for example, because of the exceptionally gusty winds in that state. Structures should be classified as Category III if they are located on secondary roads (i.e., roads other than state highways and U.S. highways) with speed limits of 60 km/h (35 mph) or less. Structures on secondary streets in residential areas are in Category III.

All structures not explicitly meeting the criteria for either Category I or Category III should be classified as Category II. This would include any structures with mitigation devices that would otherwise meet the Category I criteria. As discussed previously, the testing at Texas Tech showed that the mitigation devices significantly reduce the amplitude of the vibration, but they do not totally eliminate the effect of the galloping load. Being in Category II will enhance the level of reliability from what is presently accepted, but should not cause significant redesign costs.

The Category III importance factors shown in Table 2-19 were calibrated so that structures using these importance factors will have, on average, the same reliability as the present inventory of structures designed by the 1994 Specifications. Twenty-five typical cantilevered sign, signal, and luminaire support structures were analyzed for this calibration. Eighteen representative support structures (i.e., six of each type) were analyzed during the first phase of this project using the limit-state wind loads proposed in *NCHRP Report 412*. Seven additional structures (those included in the design examples in this report) were analyzed during this phase of the project. The dimensions and details of these 25 structures were taken from drawings supplied by departments of transportation in a variety of states. Although the structures in the design examples were redesigned, the dimensions and details of these structures before they were redesigned were used for the calibration because the researchers wanted the calibration to represent present structures.

For each of the four fatigue-limit-state load ranges that are applicable to a particular type of support structure, a ratio of the CAFL at the most critical detail to the calculated stress range at that detail is calculated. The calculated stress range is determined from a static analysis with the applied load equal to the fatigue-limit-state load range. All of the details are examined for each load case, and the most critical detail is identified that has the lowest ratio of the CAFL to the calculated stress range. The critical detail is often the mast-arm-to-pole connection (where the mast-arm moment is greatest), the column base details, or the anchor rods, depending on the relative proportions and details. The example design problems in Appendix B may be examined to see which details were the most critical in those particular structures.

The importance factors for Category III are the average of the most critical ratio for each structure. The ratios that were obtained were consistent for similar wind loads and varied by no more than ±50 percent of the mean value.

Because seven additional structures have been analyzed since *NCHRP Report 412* was written, the values in Table 2-19 differ slightly from those in *NCHRP Report 412*. Most of the new Category III importance factors are within 10 percent of those recommended in *NCHRP Report 412*, indicating that the calibration was adequate. The new importance factors are larger in all cases, and only the galloping and natural wind importance factors for sign structures were increased by more than 10 percent.

Finally, importance factors for Category II were defined as the average of Category I and III importance factors. Assuming the relationship between the fatigue-design load and the probability of failure is linear, the probability of failure for these Category II structures should be the average of the probability of failure for Category I and Category III. So, the probability of failure over the lifetime for Category II would be between 0.0015 percent and 0.015 percent.

The probability of experiencing the full-fatigue-design wind loads in the 2001 Specifications is not any less for the Category II and III structures. Therefore, if these Category II and III structures do experience the full-fatigue-design wind loads, they are only designed for a fraction of these loads, and, therefore, fatigue cracking or excessive deflection would eventually be expected. The rationale is that for Category II and III structures, the consequences of a failure are not as serious.

Because the probability of cracking is greater for these Category II and Category III structures, the inspection interval should actually be shorter. However, it also makes sense to inspect the critical Category I structures frequently. It is recommended that all the structures be inspected visually from the ground with binoculars every 2 years. Anchor rods should be struck with a hammer to see if they have a consistent ringing sound. It is not felt that ultrasonic testing or other NDE is necessary or productive. There is only a short time window between the development of a crack detectable with these methods and the growth of these cracks to a large enough size to cause collapse.

Any structures experiencing fatigue cracking should be taken down immediately. Other similar structures should be inspected as soon as possible. In this case, the use of ultrasonic testing or other NDE methods may be helpful. If the other structures are not damaged, then, at a minimum, mitigation devices should be installed on these structures.

Any structures that are reported to be undergoing excessive vibration should be retrofitted within 1 month with an acceptable mitigation device.

2.6 ANCHOR ROD TIGHTENING RESEARCH

As shown in Table 2-1, many of the fatigue problems with support structures have manifested in the anchor rods (often erroneously called anchor bolts). In *NCHRP Report 412*, extensive fatigue testing was performed on anchor rods, and these data were assimilated with the data of Frank [39] and Stoker et al. [40]. For anchor rods with misalignment less than or equal to 1:40, it was shown that the fatigue resistance in the region of finite life was found to be AASHTO Category E′ for snug-tight anchor rods.

If the anchor rods are properly tensioned, the fatigue resistance may be taken as AASHTO Category E. Proper pretension was defined as one-third of a turn beyond snug. The fatigue-test data indicate that proper tightening between the double nuts changes the failure mode from the first thread that engages the top nut to some location below the bottom nut. This change occurs because proper tensioning reduces the actual stress range between the nuts (in a manner analogous to properly tightened tension connections) and also probably because some bending and stress concentration is eliminated. Tightening of one-third turn past snug tight is more than enough to induce this change.

The testing described in *NCHRP Report 412* shows that the CAFL for anchor rods with misalignment up to 1:40 is 48 MPa (7 ksi) for both snug and fully tightened anchor rods. Note that this is not the usual CAFL for Category E or E′. Thus, the detail is characterized by a different category in the infinite-life region than in the finite-life region. The effect of proper pretension on the CAFL was relatively small and less than one full category. Therefore, there is essentially no difference between the design of snug and fully tightened anchor rods.

Of course, whenever practical, anchor rods should be installed in the fully tightened condition (i.e., tightened to one-third of a turn beyond snug for most anchor rod sizes). Although no benefit is recommended when designing fully tightened anchor rods for infinite life, it should be noted that the fully tightened condition precludes the possibility of anchor rod nuts becoming loose under service-load conditions. As a result, the fully tightened condition is inherently better with respect to the fatigue performance of anchor rods.

Large-diameter rods will require the use of a hydraulic wrench with external lubrication of the threaded and bearing surfaces in order to achieve a fully tightened condition. Tightening anchor rods greater than 51 mm (2 in.) in diameter with coarse pitch threads to one-third of a turn beyond snug will most likely yield the anchor rod material, especially for lower-strength anchor rod material. The proper tensioning of 75-mm diameter anchor rods was addressed in research performed by Johns and Dexter for the State of New Jersey [18].

The anchor rods that were used by NJDOT for the VMS structures were A36 steel. The minimum amount of tensile stress that should be in a high-strength bolt is 70 percent of the ultimate strength; however, these anchor rods are not high-strength bolts. Using 70 percent of the ultimate strength for mild steel would still be above the yield point; therefore, a minimum tensile stress of 60 percent of ultimate shall be used on the anchor rod.

Torque is a notoriously poor way to ensure pretension, but it is the only way to check the tension after tightening.

The tightening pattern of high-strength bolts in flanged connections should be in a star pattern the same as the anchor rods. This could be facilitated by using two bucket trucks, one on each side of the truss. Each person should take a turn tightening the appropriate bolt. These bolts should also be incrementally tightened when going through the star pattern.

A group of researchers at Texas A&M University led by Ray James completed a study titled, *Tightening Procedures for Large-Diameter Anchor Bolts* [41]. Tightening methods used in the field were documented. Analyses were performed to identify which factors affect the stress in the anchor rods. Tightening methods were tested in the laboratory using an upright and foundation assembly from a typical cantilever sign-support structure and from a typical high-mast luminaire.

It was found that anchor rods tightened to one-sixth turn (60°) beyond the snug-tight condition did not loosen. The only method that worked consistently was a slug wrench and a 7-kg (16-lb) sledgehammer. Tightening, loosening, and then retightening anchor rods resulted in higher preloads.

A wrench with a 3,000-mm (10-ft) long cheater pipe could not reliably produce enough torque. Torque was not a reliable indicator of bolt pretension. The same slug wrench is recommended for periodic inspection of the tightness. Striking the nut with a hammer and ultrasonic testing were not found to be reliable inspection methods.

When these tests were concluded, the assemblies were fatigue tested. The findings of the two fatigue tests were consistent with the recommendations of fatigue categories in *NCHRP Report 412* for the anchor rods and the upright-to-baseplate (i.e., socket joint) detail. The anchor rods were not critical; rather, the upright-to-baseplate connection cracked. (Examples in *NCHRP Report 412* show that the baseplate connection is typically more critical than the anchor rods.) The Texas A&M University report indicates that anchor rod alignment is more important than anchor rod preload concerning the fatigue life of large-diameter anchor rods.

The results of these and other studies were assimilated into a recommended specification for anchor rods and commentary, which are included in Appendix A of this report. The recommended specification includes materials, design, installation, inspection, repair, and maintenance. The recommended specification parallels the current Research Council on Structural Connections (RCSC) *Specification for Structural Joints Using ASTM A325 or A490 Bolts* [10], which is invoked by the AASHTO bridge specifications [11]. These results are also included in the guidelines for installation, inspection, maintenance, and repair in Appendix C.

2.7 DESIGN EXAMPLES

Seven examples outlining the complete fatigue design procedure for various cantilevered structures are included in the appendixes. The first four structures were designed according to the fatigue provisions of the 2001 Specifications. The design of the final three structures includes the recommended changes to the specifications made in this report. The seven structures are

- A monotube traffic signal structure with five signal heads and two signs;
- A bent monotube VMS structure;
- A four-chord (i.e., box) truss VMS structure;
- A tapered luminaire support structure;
- A two-chord truss VMS structure;
- A two-chord truss, flat-panel sign structure; and
- A monotube traffic signal structure with luminaire extension and ring-stiffened, built-up box connection.

2.8 TRAINING MATERIALS AND GUIDANCE ON INSTALLATION, INSPECTION, MAINTENANCE, AND REPAIR

Appendix C provides training materials that provide a brief overview of materials, fatigue, and design issues. One section (Section C.3) is a brief overview of the wind-induced vibration problem with cantilevered support structures. Various wind-loading phenomena affecting support structures are described, including conditions that make structures more or less susceptible to these wind-loading phenomena. Mitigation devices appropriate to different types of wind-loading are discussed.

Because the anchor rods and field-installed bolts play an important role in proper installation and performance, a section on selecting and installing anchor rods in the foundation (Section C.4) is provided. Selection of high-strength structural bolts for other field connections is also discussed. However, other aspects of fabrication are not covered in this guide. AASHTO and American Welding Society documents, particularly AWS D1.1, "Structural Welding Code—Steel," may be referred to for fabrication requirements and guidance.

The next section of this guide (Section C.5) focuses on installation practices. Preinstallation inspection is discussed. The primary issues in installation are the sequence of assembly and the bolt-tightening procedures. Only those aspects of installation that are relevant to vibration and fatigue are discussed.

In-service inspection of cantilevered support structures is covered in the following section (Section C.6). A detailed discussion is provided of adequate inspection intervals for various cantilevered support structure types. A brief overview of the fatigue classification of details is presented, including a discussion of some of the most fatigue-prone details and where the cracks typically appear. The relative merits of various NDE methods are discussed, but the emphasis is on visual inspection. Periodic checking of anchor rod nuts and other bolted joints to see if they remain tight is also discussed.

Techniques for periodic maintenance are discussed, including touch-up of galvanizing or repainting and periodic retightening of anchor rods and other bolts. Repair techniques for anchor rods that are also useful for correcting construction errors are discussed (Section C.7). Repair of small fatigue cracks in structural members is discussed. Criteria for when fatigue cracks may be repaired or when the structure should be replaced are provided.

The guide in Appendix C is intended to go along with the PowerPoint presentation. (Note: The PowerPoint presentation is not published in this report. Copies may be obtained from the NCHRP upon request.) These design guidelines should be used in combination with the 2001 Specifications.

CHAPTER 3

INTERPRETATION, APPRAISAL, AND APPLICATIONS

3.1 REVIEW OF EXISTING SPECIFICATION

The 2001 *Standard Specifications for Structural Supports for Highway Signs, Luminaires, and Traffic Signals* [1] provides guidelines for the design of cantilevered sign, signal, and light support structures in the United States. The 1994 Specifications [6] included very limited vibration and fatigue design guidelines (i.e., only vortex shedding was included). Recommendations made as a result of the first phase of this project (*NCHRP Report 412*) led to the inclusion of an entire fatigue design chapter (Section 11) in the 2001 Specifications [1].

A few discrepancies exist between the *NCHRP Report 412* recommendations and 2001 Specifications. Most notably, punching shear equations and Fatigue Category K_2 were added to Detail 19 (fillet-welded tube-, angle-, and plate-to-tube connections). Not only does the inclusion of Category K_2 greatly reduce the CAFL of such connections, but the punching shear equations also amplify the out-of-plane bending stress ranges. As a result, economical designs become much more difficult to achieve. This controversial change is discussed in detail in Section 2.4.3.

Another significant difference between *NCHRP Report 412* and the 2001 Specifications is the exclusion of a specific vertical deflection limit. *NCHRP Report 412* recommends that the vertical deflection range of monotube mast arm tips be limited to 200 mm (8 in.) under the application of either galloping or truck-induced, gust-equivalent static pressure ranges. However, the 2001 Specifications only require that such deflections "should not be excessive so as to result in a serviceability problem, because motorists cannot clearly see the arm's attachments or are concerned about passing under the structures" [1].

A brief overview of "Section 11—Fatigue Design" from the 2001 Specifications is included below. This is followed by discussion of the affirmation of, and recommended changes to, these provisions. It is envisioned that recommended changes will be considered for future editions of the specifications.

3.1.1 Wind-Induced, Limit-State Fatigue Loads

The application of complex dynamic fatigue loads induced by galloping, vortex shedding, natural wind gusts, and truck-induced gusts is simplified in the 2001 Specifications through the use of equivalent static loads. Maximum stress ranges induced by dynamic loads are estimated with static loads that will create similar stress responses. Consequently, it is not necessary for designers to conduct dynamic analyses. Instead, simple static analyses are sufficient.

3.1.1.1 Importance Factors

The magnitude of the fatigue pressures can be adjusted through the application of importance factors. Structures are first classified into one of three importance categories:

- Category I—critical cantilevered support structures installed on major highways,
- Category II—other cantilevered support structures installed on major highways and all cantilevered support structures installed on secondary highways, and
- Category III—cantilevered support structures installed at all other locations.

Although some subjective criteria are given, the assignment of structures into categories is left largely to engineering judgment.

Category I structures are designed to resist the least frequently occurring wind-induced fatigue loads because the failure of such a structure would create a large hazard. Therefore, importance factors of 1.0 are always used for Category I structures (i.e., fatigue loads are not reduced).

The least critical structures, Category III, use importance factors less than 1.0. The ramifications of a Category III structure failure would be much less than those of a Category I structure. Therefore, taking greater risk in the design of Category III structures (by applying reduced loads) can be justified. The Category III importance factors were determined using an analysis performed in Phase I of this project. The design of a Category III structure is intended to be similar to one designed using the 1994 Specifications (i.e., before fatigue provisions were included). Category II importance factors were determined by simply averaging the Category I and III factors for a given structure type, which obviously results in values less than 1.0.

These importance factors should be applied to the limit-state wind loads prior to determining the cantilevered support structures' fatigue resistance, maximum mast arm displacement, or both.

3.1.1.2 Galloping

The first of the four fatigue loads, galloping, is to be applied to sign and traffic signal structures. The equivalent static load is defined in terms of a vertical shear pressure (i.e., across wind) that is to be applied to the projected area on a vertical plane of all mast arm attachments (e.g., signs, signal heads, and signal head backplates). The magnitude of the pressure, P_G, is defined as follows:

$$P_G = 1,000 I_F \text{ (in Pa)} \tag{3.1}$$

$$P_G = 21 I_F \text{ (in psf)} \tag{3.1a}$$

Presently, the 2001 Specifications allow the designer to ignore the galloping loads if an approved vibration mitigation device is used. The device can be applied either at the time of erection or at a later date after a galloping problem has been observed. The 2001 Specifications also allow for the exclusion of galloping loads in the design of box-truss (i.e., four-chord) structures. Such structures have never been observed to gallop, presumably because of their inherently high degree of three-dimensional stiffness.

3.1.1.3 Vortex Shedding

Nontapered luminaire support structures are to be designed to resist vortex-shedding fatigue loads. The critical wind velocity for a prismatic member, V_C, is calculated according to the following equations:

$$V_C = \frac{f_n d}{S_n} \text{ (for circular sections)} \tag{3.2}$$

$$V_C = \frac{f_n b}{S_n} \text{ (for multisided sections)} \tag{3.2a}$$

where

f_n = the first natural frequency of the structure (Hz),
d = the member diameter (m),
b = the flat-to-flat width of the member (m), and
S_n = the Strouhal number.

The Strouhal number is 0.18 for circular sections, 0.15 for multisided sections, and 0.11 for rectangular sections. The equivalent static pressure range, P_{VS}, is applied in the direction perpendicular to the wind to the horizontally projected area (i.e., the area projected on the vertical plane) of all members according to the following equations:

$$P_{VS} = \frac{0.613 V_C^2 C_D I_F}{2\beta} \text{ (in Pa)} \tag{3.3}$$

$$P_{VS} = \frac{0.00118 V_C^2 C_D I_F}{2\beta} \text{ (in psf)} \tag{3.3a}$$

where

C_D = the drag coefficient for the section of interest, as specified in Table 3-5 of the 2001 Specifications, and
β = the damping ratio, which is "conservatively" estimated as 0.005.

Although no testing was conducted on light poles during this project, there is reason to believe that a damping ratio of 0.5 percent actually may not be conservative. Field testing of the cantilevered signal structure near Tampa showed that its unmitigated damping ratio was 0.13 percent, one-fourth of the value recommended for light supports in the vortex-shedding section of the 2001 Specifications.

As was the case with galloping, vortex-shedding pressures can be excluded if approved vibration mitigation devices are installed. The commentary on vortex shedding recommends using average section properties when designing structures tapered less than 0.0117 m/m (0.14 in./ft).

3.1.1.4 Natural Wind Gusts

Natural wind gusts are to be applied to all three types of cantilevered structures (sign, signal, and light supports). They are applied in the along-wind direction to the horizontally projected (i.e., exposed) areas of all members, signs, signals, and so forth according to the following equations:

$$P_{NW} = 250 C_D I_F \text{ (in Pa)} \tag{3.4}$$

$$P_{NW} = 5.2 C_D I_F \text{ (in psf)} \tag{3.4a}$$

The equations above are based on 5 m/s (11.2 mph) yearly mean wind speeds because 81 percent of cities evaluated in Phase I had mean wind speeds below 5 m/s. For locations with more detailed meteorological data, a more precise equation is also provided in the commentary:

$$P_{NW} = 250 C_D \left(\frac{V_m^2}{25}\right) I_F \text{ (in Pa)} \tag{3.5}$$

$$P_{NW} = 5.2 C_D \left(\frac{V_m^2}{125}\right) I_F \text{ (in psf)} \tag{3.5a}$$

where

V_m = the yearly mean wind velocity (in meters per second in the Pascal equation and in miles per hour in the pounds-per-square-foot equation).

Even though the 2001 Specifications do not explicitly require it, Equations 3.5 and 3.5a should always be used in locations where it is known that the yearly mean wind speed is greater than 5 m/s because not doing so would lead to an unconservative design.

3.1.1.5 Truck-Induced Gusts

Truck-induced gust equivalent static pressure ranges are applied to the areas on the undersides (i.e., projected area on a horizontal plane) of members, signs, signals, attachments, walkways, and lighting fixtures. At a minimum, the pressure is to be applied to the outer 3.7 m (12 ft) of the mast arm, which is equal to the width of one traffic lane. If sign panels or enclosures longer than 3.7 m are present, the truck-gust load is to be applied over their full length, regardless of how large they are. The truck-gust pressure, P_{TG}, which is based on 30 m/s (65 mph) traffic speeds, is defined as follows:

$$P_{TG} = 1760 C_D I_F \text{ (in Pa)} \tag{3.6}$$

$$P_{TG} = 36.6 C_D I_F \text{ (in psf)} \tag{3.6a}$$

Alternative equations are provided for structures erected at locations with truck speeds less than 30 m/s:

$$P_{TG} = 1760 C_D \left(\frac{V}{30}\right)^2 I_F \text{ (in Pa)} \tag{3.7}$$

$$P_{TG} = 36.6 C_D \left(\frac{V}{65}\right)^2 I_F \text{ (in psf)} \tag{3.7a}$$

where

V = the velocity (in meters per second in the Pascal equation and in miles per hour in the pounds-per-square-foot equation).

The 2001 Specifications also allow for the exclusion of truck-induced gust loads on signal structures at the discretion of the owner.

3.1.2 Allowable Deflection Limits

The recommendation in *NCHRP Report 412* that vertical displacement ranges at the tips of cantilevered structures be limited to 200 mm (8 in.) is not required in the 2001 Specifications. Instead, the specifications only state that mast arm tip deflections should not be so excessive that the serviceability of the structure is limited. Excessive vertical oscillations not only make motorists uneasy, but also can render the structure useless if the signs supported by the structure cannot be read quickly and easily.

3.1.3 Fatigue Resistance of Connection Details

Table 11-2 in the 2001 Specifications lists 24 typical cantilevered support structure details. The details in Table 11-2 were taken from standard plans provided by various states during the first phase of this project. Some states did not respond to the survey in which the request for plans was made. In addition, all states that did respond did not include standard plans with their response. Thus, Table 11-2 likely does not include every type of connection detail used in the United States. The use of new connection details, such as Wyoming's ring-stiffened, built-up box, has also arisen since *NCHRP Report 412* was written.

In addition to descriptions and examples of the details (including figures), the stress category of each detail is included. Using the stress category, material type (steel or aluminum), and Table 11-3 (of the 2001 Specifications), the constant-amplitude fatigue limit of the connection can be determined.

3.2 DEVELOPMENT OF THE PROPOSED SPECIFICATION CHANGES

3.2.1 Wind-Induced, Limit-State Fatigue Loads

In addition to the importance factor discussion in Section 2.5, galloping, vortex shedding, natural wind gust, and truck-induced wind gust fatigue loadings were also investigated during the course of this research project. The magnitudes of galloping, natural wind gust, and truck-induced wind gust equivalent static pressures were examined. The applicability of the vortex-shedding pressure equation to tapered members and the effects of double-curvature vibrations were examined.

3.2.1.1 Importance Factors

Revisions to the section on importance factors were discussed in Section 2.5. Table 2-19 lists the revised importance factors that are now recommended for the Specifications.

Definitions of the three importance categories should be revised to read as follows:

- Category I—critical cantilevered support structures installed on major highways,
- Category II—cantilevered support structures installed on other highways, and
- Category III—cantilevered support structures installed at low-risk locations.

The procedure to determine which category to use for design will be as follows. The criteria for Category I will be clearly defined. Structures not meeting these criteria for Category I will be examined to see if they meet the criteria for Category III. If the structure meets neither of these sets of criteria, then it is in Category II.

Structures classified as Category I present a high hazard in the event of failure and will be designed to resist rarely occurring wind loading and vibration phenomena described previously. It is recommended that all structures without proven

mitigation devices on roadways with a speed limit in excess of 60 km/h (35 mph) and average daily traffic (ADT) exceeding 10,000 in one direction (regardless of the number of lanes) or average daily truck traffic (ADTT) exceeding 1,000 in one direction (also regardless of the number of lanes) be classified as Category I structures.

Structures without mitigation devices on state highways or U.S. highways should also be included in Category I if any of the following conditions apply:

- They are cantilevered structures with a span in excess of 17 m (55 ft) or high-mast towers in excess of 30 m (100 ft).
- They are located in an area that is known to have wind conditions that are conducive to vibration. This would include any areas with a mean annual wind speed in excess of 5 m/s (11 mph).
- They are located near the foothills of mountain ranges.

Structures should be classified as Category III if they are located on secondary roads (i.e., roads other than state highways and U.S. highways) with speed limits of 60 km/h (35 mph) or less. All structures not explicitly meeting the criteria for either Category I or Category III should be classified as Category II. This would include any structures with mitigation devices that would otherwise meet the Category I criteria.

The testing at Texas Tech (see Section 2.3.5) showed that the mitigation devices significantly reduce the amplitude of the vibration, but do not totally eliminate the effect of the galloping load. Being in Category II will enhance the level of reliability from what is presently accepted, but should not cause significant redesign costs.

Structures classified as Category III will be designed to the same level of reliability, on average, as those structures designed to meet the 1994 Specifications. A slightly revised set of importance factors is proposed in Table 2-19. The revisions of the Category III importance factors are the result of additional design calibrations conducted on several typical cantilevered sign, signal, and luminaire support structures. The importance factors for Category II were defined as the average of Category I and III importance factors, as was done previously to achieve a level of reliability halfway between the status quo and the Category I design loads.

It is recommended that all the structures be inspected visually close-up every 4 years, examining the connection of the mast arm or truss to the post from a bucket truck or ladder. Anchor rods should be struck with a hammer to see if they have a consistent ringing sound. Structures that are known to be inadequately designed or are similar to those that have exhibited fatigue should be inspected more frequently.

It is recommended that structures experiencing fatigue cracking be taken down immediately. Procedures are provided in Appendix C for repair of small fatigue cracks if a judgment is made that it will be safe to attempt to repair. Other similar structures should be inspected as soon as possible. In this case, the use of ultrasonic testing or other NDE methods may be helpful. If the other structures are not damaged, then, at a minimum, mitigation devices should be installed on these structures.

Any structures that are reported to be undergoing excessive vibration should be retrofitted as soon as possible with an acceptable mitigation device or taken down.

3.2.1.2 Galloping

Galloping loads were verified at Texas Tech's Wind Engineering Research Center (WERC) (see Section 2.3.5.1). Stresses resulting from unmitigated galloping of a traffic signal were measured, and equivalent static shear pressures were back-calculated. A maximum galloping shear pressure of 952 Pa (19.9 psf) was determined. This value agrees very well with the galloping pressure in the 2001 Specifications of 1,000 Pa (21 psf). Thus, present galloping loads appear to be appropriate and should remain unchanged.

The measurements on galloping VMS structures in California indicate that even larger galloping pressures can be experienced. Therefore, these loads are certainly not excessively conservative.

3.2.1.3 Natural Wind Gusts

Spectral finite element analyses were performed to verify the natural wind-gust pressure equation in the 2001 Specifications (see Section 2.2.6). An appropriate velocity spectrum was first transformed into a force spectrum. The forces within the spectrum were then randomly applied to two VMS structures as part of a dynamic analysis simulating natural wind-gust loading. Equivalent static pressures that would yield the same column-base stresses that were recorded in the dynamic analysis were then determined. At a yearly mean wind speed of 5 m/s (11.2 mph), the two analyses resulted in equivalent static pressures of $224C_D$ Pa and $258C_D$ Pa. Both of these values agree very well with the current natural wind-gust pressure equation of $250C_D$ Pa.

In addition to the spectral finite element analyses, the design of a large inventory of Mn/DOT sign structures was examined. Mn/DOT structures are generally considered to be designed very conservatively, so the predicted failure of many structures due to the application of the recommended natural wind-gust and truck-induced gust equation would be unexpected and would provide evidence that the equation is grossly overconservative. However, failure was only predicted for 1.5 percent of the 2,666 structures studied. (The exact percentage of failures due to natural wind-gust loading is unknown.) Thus, present natural wind-gust loads appear to be appropriate and should remain unchanged.

Natural wind-gust pressures were also measured on light poles in Australia [28]. The relation of the wind pressures to

the velocity was consistent with the spectral finite element analyses, and the typical maximum pressure values seen in a year correspond well with the recommended design load. Therefore, there is no reason to revise the natural wind-gust loads presently in the 2001 Specifications.

3.2.1.4 Galloping/Natural Wind-Gust Interaction

The failures in Wyoming were most likely due to natural wind gusts rather than galloping. Research described in Section 2.2.6 shows that the fatigue design wind load (i.e., the wind-gust loads that occur for a few hours each year) are particularly severe in Wyoming, the greatest in the United States, in fact. These gust loads are not correlated to the maximum design loads, which are most severe near the coasts because of gales and hurricanes.

In *NCHRP Report 412,* it was assumed the interaction between galloping and natural wind gusts would implicitly be designed for when both galloping and natural wind are considered separately, but the implications of galloping being suppressed by a mitigation device were not considered during Phase I. The research team has observed signal support motion on very windy days, and there is considerable vertical motion, as well as horizontal motion. It is unlikely that a horizontal sign blank would eliminate small-amplitude vertical deflections due to natural wind gusts. Nonetheless, *NCHRP Report 412* allows for the exclusion of galloping loads whenever a sign blank or other proven mitigation device is installed. Thus, interactions between vertical and horizontal motion in natural wind may not be accounted for in this case.

It is recommended that mitigation devices not be used to eliminate a design load entirely, as is presently allowed in the 2001 Specifications. Rather, it is recommended that the mitigation device be used to alter the importance category from Category I to Category II. Thus, the change in importance category will cause a reduction in the galloping load (to 72 percent of Category I levels) rather than an elimination of it, which is consistent with the findings from the Texas Tech tests.

The truck-gust loading on the horizontal projected area of the mast arm and signal may also be sufficient to account for this interaction effect. In four-chord trusses, which are exempt from galloping loads because of their high torsional stiffness, it is essential that some minimum truck-gust loading be used.

3.2.1.5 Truck-Induced Wind Gusts

Although the magnitude of truck-induced gust loads was not measured or analyzed as part of this project like galloping and natural wind loads were, separate research projects have studied the issue. In *NCHRP Report 412,* an equivalent static pressure range of $1760C_D$ Pa was recommended for truck-gust loading. According to the 1994 Specifications, the drag coefficient for the underside of a VMS was 1.45, so the total pressure range on a VMS was intended to be 1.45 by 1760 Pa, or 2,550 Pa. Note that this design pressure range represents both the upward and downward part of the loading cycle.

Because truck-gust loading was a phenomenon that was not recognized at the beginning of the first phase of the project, this recommendation was based on just a few observations of the vibration amplitude of VMS structures and, therefore, was very conservative. Subsequently, NJDOT sponsored the instrumentation and monitoring of a VMS to determine the appropriate truck-gust loading [18]. The maximum measured stress ranges during the 3-month monitoring period (including the drag coefficient) were consistent with an equivalent static pressure range of 530 Pa, less than 21 percent of the originally intended design pressure recommended in *NCHRP Report 412* (2,550 Pa). Therefore, it would appear that the recommendation in *NCHRP Report 412* was too conservative. However, it is not known how much the response would vary if the conditions were different (i.e., if there were more natural wind at the same time or different lane positions relative to the sign location). The displacement amplitudes at the I-80 location where the truck-gust loads were measured were never near the displacement amplitudes that were reported when the structure was originally erected at a different location. Therefore, the appropriate design pressure is still not certain.

The 2001 Specifications recommend a drag coefficient for the underside of a VMS of 1.7, thus making the design pressure much larger than originally intended (now it is 1.7 by 1,760 Pa, or 2,990 Pa). This is obviously way too conservative. Furthermore, there have not been as many reports of problems with VMS structures as there were 4 years ago. Therefore, it seems that a reduction in the design truck-gust pressure is appropriate. It is proposed that the recommended design pressure be reduced to 900 Pa (18.8 psf) before the drag coefficient. With the new drag coefficient of 1.7 for VMS, this will make the design pressure equal to 1,500 Pa. This is less than the originally intended design pressure of 2,550 Pa, but is still almost three times greater than what was measured in New Jersey. It is recognized that the optimum design criterion is somewhere in between 530 Pa and this recommended value of 1,500 Pa.

For locations with truck speeds less than 30 m/s, the following pressure equations can be used:

$$P_{TG} = 900C_D\left(\frac{V}{30}\right)^2 I_F \text{ (in Pa)} \tag{3.8}$$

$$P_{TG} = 18.8C_D\left(\frac{V}{65}\right)^2 I_F \text{ (in psf)} \tag{3.8a}$$

where

V = the velocity (in meters per second in the Pascal equation and in miles per hour in the pounds-per-square-foot equation).

It is also recommended that the length over which the truck-gust load is applied to the sign and structural components be reduced. Originally, *NCHRP Report 412* proposed that the truck-gust load be applied over the length of the sign or 3.7 m (12 ft, or one lane width), whichever was greater. For some very long signs, this is obviously too conservative because it implies the simultaneous arrival under the sign of two or more "worst-case" trucks. Therefore, it is recommended that truck-gust loads be applied only over a 3.7-m length. The location of this length will depend on the structure. The load should be applied over the 3.7-m length that creates the worst-case stress ranges. For most cases, this will be the outermost 3.7 m of the structure (i.e., at the tip of the arm), because most attachments are located near the tip (resulting in both a large pressure-application area and a long moment arm). It is also recommended that a clause be added stating that it is unnecessary to load any portion of the structure not located directly above a traffic lane (i.e., above the shoulder) because 30-m/s truck traffic will not be loading those portions of the structure.

Another recommended modification from the New Jersey design criteria is a gradient for the truck-induced gust design pressure. Measurements indicated that truck-gust loads are full strength for elevations of 6 m (19.7 ft) or less and decrease linearly to zero at a height of 10 m (32.8 ft).

The following statement in the commentary of the 2001 Specifications should also be removed: "To improve fuel economy, many trucks are outfitted with deflectors to divert the wind flow upward and minimize drag created by the trailer" [1]. The installation of such devices actually decreases the upward truck-induced wind gust by creating an aerodynamic transition between the cab and the trailer.

3.2.1.6 Vortex Shedding

As was discussed in Section 2.4.2, a tapered luminaire support structure was captured on videotape vibrating in double curvature. Furthermore, calculations performed on the structure verified that double-curvature, vortex-shedding vibrations can lead to fatigue-related problems (i.e., stresses greater than the CAFL can result). For the calculations, the vortex-shedding pressure was applied over the length of the pole in which the diameter was within ±10 percent of the critical diameter.

Designing all luminaire structures for double-curvature, vortex-shedding pressures would usually lead to unnecessarily conservative designs. Therefore, it is recommended that a statement be added to the vortex-shedding section, similar to the one in the galloping section of the 2001 Specifications, allowing for mitigation after a problem has been exhibited. That way, proven damping devices like those used by manufacturers as discussed in Section 2.3.1 will only need to be installed if a double-curvature vibration problem exists. In addition, designing structures to resist double-curvature stress ranges will not be necessary.

It is also recommended that all tapered structures, regardless of the magnitude of the taper, be checked for vortex shedding. Pressures should be applied over the length of the pole in which the diameter is within ±10 percent of the critical diameter. Various critical diameters should be checked in order to ensure designing for the worst-case moment. Usually, three or four diameters should be checked.

3.2.2 Fatigue Resistance of Connection Details

Although no fatigue testing was performed during this project, questions involving the ambiguity of some of the details in Table 11-2 of the 2001 Specifications arose during the life of the project. Consequently, it is recommended that the following changes be made to the 2001 Specifications.

Detail 11 ("Full-penetration groove-welded tube-to-transverse plate connections with the backing ring attached to the plate with a full-penetration weld.") should be modified to also include the case where the backing ring is attached to the plate with a continuous fillet weld. The reasoning behind originally requiring that the backing ring be attached with a full-penetration weld was to eliminate the notch effect that can form between the backing ring and the plate when tack welds are used to attach the ring. However, if a continuous fillet weld is used and the thickness of the backing ring is limited to 10 mm ($^3/_8$″), the notch will be relatively small and will be buried (which decreases its detrimental effect by a factor of two).

Detail 14 ("Members with axial and bending loads with fillet-welded end connections without notches perpendicular to the applied stress. Welds distributed around the axis of the member so as to balance weld stresses.") should be modified to include guidance on the size of coped holes for slotted tube-to-gusset connections. It is recommended that the diameter of the coped hole be the greatest of the following:

- 25 mm (1 in.),
- Twice the gusset plate thickness, and
- Twice the tube thickness.

Detail 18 ("Fillet-welded mast-arm-to-column pass-through connections.") should include a note that the main member (i.e., column) should also be designed for Stress Category E using the section modulus of the main member and moment just below the connection of the branching member (i.e., mast arm). This clause is similar to the last part of Note (b) for Detail 19 ("Fillet-welded T-, Y-, and K-tube-to-tube, angle-to-tube, or plate-to-tube connections.").

For Detail 22 ("Non-load bearing longitudinal attachments with L > 102 mm [4 in.] and fillet or partial-penetration groove welds. The main member is subjected to longitudinal loading, and the weld termination embodies a transition radius or taper with the weld termination ground smooth."), the Stress Category D condition should also include the case when $\alpha \leq 15°$. This change is appropriate because a connection with $\alpha \leq 15°$ is at least as fatigue resistant as one with

$15° < \alpha \leq 60°$. Therefore, the complete Category D condition should read "$R > 51$ mm (2 in.) or $\alpha < 60°$."

The Category ET CAFL reduction included in Note (a) should also be included (or referenced) in Note (b).

A twenty-fifth detail, the ring-stiffened WYDOT built-up box, should be added to Table 11-2. A drawing of this detail was shown in Figure 2-72. The stress in the branching member (i.e., the built-up box) should be checked for Stress Category ET. The CAFL for Category ET should also be reduced according to Note (a) where appropriate. The stress in the main member (i.e., the column) should be checked for Fatigue Category E. The complete ring stiffeners eliminate punching shear; therefore, it is not necessary to check the Category K_2 clauses included in Note (b).

As discussed previously, the 2001 Specifications included the addition of the check of punching shear for branch-to-tube connections versus the Category K_2 CAFL. This additional check was deemed necessary at the time because these structures were not being designed for truck-gust loading, galloping, or any in-plane loading at all. The problem was that the design process without in-plane loads was not causing the designer to have to increase the thickness of the pole, even though the cracking manifested in the pole. The only check was the Category ET check for the branching member (i.e., the mast arm), which, at the interface to the pole, was the box connection plates.

This was an oversight at the time of *NCHRP Report 412*. It was thought that the stress range in the pole would be controlled by the in-plane loads. The box connection is a Category E detail with respect to the stress range in the pole. If the stress range were too high, the tube would have to be made thicker or greater in diameter, or both.

It was envisioned that these in-plane loads would be checked in some cases. For example, it was recognized at the time that the vibration due to natural wind gusts has a significant in-plane component, but it was felt that if the out-of-plane natural wind-gust load and the in-plane galloping and truck-gust load were all checked separately, the connection would be well designed.

The punching-shear concept comes from AWS D1.1, *Structural Welding Code—Steel* [42]. AWS D1.1 indicates that the stress range in the branch member should be less than the Category ET S-N curve. AWS D1.1 also indicates that the chord member, in this case the top of the post, should be checked for punching-shear stress range. The punching-shear stress range should be less than the Category K_2 curve.

This punching-shear approach was developed decades ago for offshore structures, but has been applied to a wide variety of tubular structures [43, 44]. Better approaches, based on the "hot-spot" stress, have subsequently been developed by the American Petroleum Institute and other groups and are now used for offshore structures in lieu of the punching-shear approach [43–46]. The AWS D1.1 punching-shear approach is outdated and known to be inaccurate in many cases [43–45].

Full-scale fatigue tests were performed for a commercial company. Several connection details were tested that are similar to box connection details, except the wall thickness of the pole was very thin (3 mm). Therefore, it could be designed using the tubular joint provisions in AWS D1.1, including the punching-shear concept.

The circumferential stress ranges at the toe of the weld are difficult to predict. Strain-gauge measurements indicate that these secondary stresses are highly variable.

The definition of the nominal stress range for the box detail is the nominal bending stress (i.e., combined vertical and horizontal bending) in the sidewall or the top or bottom plates.

AWS D1.1 indicates that the stress range in the branching member should be less than the Category ET curve. The CAFL for Category ET is 1.2 ksi. AWS D1.1 also indicates that the chord member, in this case the pole top, should be checked for punching-shear stress range. The punching-shear stress range should be less than the Category K_2 curve. Note 3 in Table 2.6 of AWS D1.1 indicates that the fatigue strength given by the K_2 S-N curve should be further reduced if the ratio of the radius of the tube to its thickness is greater than 24. For the R/t ratio of 33 for the tested pole tops, this reduction factor is 0.80. The CAFL for Category K_2 is 1 ksi without the reduction.

AWS D1.1 also requires that the shear stress in the throat of the weld be checked against Category FT S-N curve. The leg length of the welds is usually the same or greater than the thickness of the tubes; therefore, these shear stresses are about 40 percent greater than the bending stress. However, the Category FT curve is about four times higher in fatigue strength; therefore, the Category FT curve will not govern in these connections unless the weld becomes much less than half the wall thickness. The welds are typically on the same order as the wall thicknesses; therefore, the Category FT will not be discussed further.

The anticipated life can be calculated from the Category ET check or for the reduced K_2 S-N curve using the punching-shear stress range. Both checks predict a lower life than what was observed experimentally, but the equation based on punching shear is excessively conservative. Using the punching-shear S-N curve, the calculated life is an average of 11 percent of the actual life.

Therefore, the punching-shear concept clearly is no good for these connection details. Note 2 of Table 2.6 in AWS D1.1 states that the ET and K_2 curves are based on typical geometries and may not be generally applicable and that the hot-spot approach is preferable. There is no doubt that "punching" action makes this detail so poor. Yet, despite the appeal of the punching-shear concept, the test data show that this approach is excessively conservative when applied to similar connections.

The nominal stress approach is more accurate and easier to use than the punching-shear stress approach and is, therefore, preferred. Therefore, it is recommended that the punching-shear check be deleted from the 2001 Specifications.

The best solution to the original problem is to require some minimum level of in-plane loading for all cases. Therefore, it is proposed that galloping load not be disregarded except for four-chord truss supports and bridge supports (i.e., overhead signs). Even if mitigation devices are used, full-scale tests in galloping conditions at Texas Tech show that the effect of the galloping in terms of strain range in the pole is equivalent to about 65 percent of the unmitigated galloping load. Therefore, it is proposed that a mitigation device only be used to get from Importance Category I to Importance Category II. At Importance Category II, the structure will still have to be designed for about 72 percent of the galloping load. Four-chord trusses must be designed for truck-gust loading at a minimum, even if the clearance is such that the truck-gust load goes to zero. In this way, all structures will have to be designed for some minimum level of in-plane loading, which will serve to control the stress range in the pole. Using example design calculations that the research team has performed on the failed Wyoming signal support structure (see Section 2.4.3) and on discussions with the manufacturer of these signal support structures about their calculations, it is clear that the ET category, combined with the galloping load and natural wind-gust load, would have required substantial redesign of the box connections that have failed in the past. Thus, this approach is calibrated to require redesign where necessary, but also to not be too conservative. The research team is certain that the K_2 category is too conservative.

The issue will not be fully resolved until a statistically significant set of full-scale fatigue tests is performed. The cost of acquiring sufficient data would be between $50,000 and $100,000.

The research team's thinking about how increasing the thickness of the box connection plates should reduce the stress concentration is based on the assumption that the fillet welds would be sized to develop the attachment plate, which is typical detailing practice. Thus, the fillet welds will increase with the increased plate thickness. The increased weld leg length contacting the pole would result in a proportional decrease in the concentrated stress in the pole wall. If a guarantee that the filet welds will increase is desired, consider requiring that fillet welds be sized to develop the attachment plates for this connection.

Another alternative would be to invoke Category F for the shear stress range in the welds, which is in the allowable strength design/load factor design (ASD/LFD) specification for bridges, American Welding Society (AWS), and American Institute of Steel Construction (AISC). However, this Category F is also very suspect and is based on flimsy data. The test data are very old, and it is not clear what the test conditions were. The authors have never seen a failure due to these shear stress ranges in practice, and the calculations are very tedious and confusing to designers. Therefore, this check seems unnecessary, perhaps because fillet weld size usually increases proportionally with attachment plate thickness, so invoking Category F doesn't "govern" the design. Consequently, Category F was eliminated (or essentially replaced with Category E) in the load and resistance factor design (LRFD) specification for bridges. This is why Category F was not included in the proposed specifications in *NCHRP Report 412*.

It is definitely true, and supported by test data, that connections the same diameter as the post are significantly better than connections narrower than the post, regardless of whether there are gaps at the top and bottom plate. The research team believes that a continuous closed box (i.e., with no gaps in the corners) is the best alternative, and this detail is now used in galvanized light poles.

3.2.3 Recommended Mitigation Devices

As was described in Section 2.3.5.4, only one galloping mitigation device was tested under natural conditions at Texas Tech. However, recent studies performed at the Universities of Florida and Wyoming have closely simulated natural vibration conditions by using an eccentric mass and motor loading device.

When the Wyoming strand damper was tested under natural conditions at Texas Tech, galloping stress ranges were always lowered, but were never eliminated. It appears that when the device is properly tuned to the natural frequency of the structure upon which it is installed, in-plane galloping stresses are reduced by approximately 35–40 percent.

Testing at both Florida and Wyoming showed that the Florida semituned mass impact damper successfully prevents the onset of large in-plane stresses when a sinusoidal loading is applied. Wyoming testing also showed that the in-plane strut is an effective in-plane mitigation device and that the strand damper is the most efficient two-dimensional mitigation device.

With the exception of the strand damper testing at Texas Tech, none of these devices have been subjected to extensive natural wind loadings. Therefore, it is too early to recommend that galloping pressures be completely eliminated when any one of the devices is installed. Until more extensive testing is performed, it is recommended that galloping loads be reduced by allowing Importance Category II to be used rather than Importance Category I. This will effect a reduction in the galloping forces to 72 percent of their Category I values. This is consistent with the Texas Tech tests on the Wyoming strand damper. This appears to be a conservative estimate because both the Florida damper and the Wyoming in-plane strut performed better than the strand damper during the sinusoidal loading tests.

CHAPTER **4**

CONCLUSIONS AND SUGGESTED RESEARCH

4.1 CONCLUSIONS

Research was performed on wind loading, dynamic response, and fatigue of cantilevered sign, signal, and luminaire support structures. The analytical and experimental research was conducted to improve upon the fatigue design recommendations adopted in the *2001 AASHTO Standard Specifications for Structural Supports for Highway Signs, Luminaires, and Traffic Signals* [1]. Following are the primary conclusions from this research:

- Data from a Texas Tech University full-scale signal support structure that was galloping in the wind verified the accuracy of the galloping equivalent static pressure equation included in the 2001 Specifications.
- Vibration mitigation testing has identified three devices that will likely decrease galloping-induced stresses by at least 35 percent. Based on these results, it is recommended that, if mitigation devices are provided, the designer not be allowed to totally ignore the galloping load, but rather be able to use Importance Category II rather than Importance Category I, which will reduce the magnitude of the loads.
- Spectral finite element analyses of the response of two VMS supports verified the accuracy of the natural wind-gust equivalent static pressure equation included in the 2001 Specifications.
- Based on measurements made on an instrumented VMS support in New Jersey, truck-induced gust pressures are maximum at the bottom of the sign (i.e., 6 m [19.7 ft] from the roadway) and decrease linearly to zero at 10 m (32.8 ft).
- Because the simultaneous arrival under a sign of two or more trucks in multiple lanes is a relatively rare event, truck-induced gust pressures should be applied only over a 3.7-m (12-ft) length, regardless of the size of any signs. This change makes the 2001 Specifications consistent with the bridge design specifications, where design for fatigue is always based on the presence of a single truck.
- The magnitude of the truck-induced gust equivalent static pressure equation should be reduced to $900C_d$ Pa ($18.8C_d$ psf) for the following reasons:
  - The original equation ($1{,}760C_D$ Pa) was based on limited data;
  - Fewer problems have been reported with VMS (the most susceptible structures to truck gusts) over the last 4 years, even though these were not designed according to the 2001 Specifications;
  - Truck-induced gust pressures measured on an instrumented cantilevered VMS support in New Jersey were much lower than those recommended in the 2001 Specifications; and
  - The original equation ($1{,}760C_D$ Pa) was calibrated to be used with an incorrect drag coefficient (C_D) of 1.45 (the drag coefficient should be 1.7, as is presently in the 2001 Specifications).
- A review of the 2,666 Mn/DOT cantilevered four-chord sign structures indicated that four-chord cantilevered supports are not susceptible to galloping. These structures did not need to be redesigned for the natural wind-gust or the (previously proposed) truck-induced gust equivalent static pressure equations in the 2001 Specifications, indicating that these equations are not overly conservative.
- An assessment of numerous at-risk structures that have exhibited excessive vibration or fatigue problems indicates that there is generally some factor, usually an unusual wind environment, that makes the location or type of structure particularly susceptible to vibration. Knowledge of these factors was used to more specifically define which structures should be considered in Importance Category I (i.e., those structures designed for the full effect of the fatigue design loads). However, it is difficult to rule out the possibility of excessive vibration or fatigue in the vast majority of structures.
- The double-curvature mode vibration of tapered luminaire support structures will necessitate either larger design pressures or immediate vibration mitigation.
- Modifications to five connection details included in Table 11-2 of the 2001 Specifications are recommended. The inclusion of an additional connection detail in Table 11-2 is also recommended.
- The removal of the punching-shear criteria and Fatigue Category K_2 from Table 11-2 is recommended.

4.2 SUGGESTED RESEARCH

Based on the findings and limitations of this research program, further research on the following is recommended:

- **Fatigue testing.** The largest remaining area of uncertainty is the fatigue resistance of the diverse details used for these support structures. Therefore, it is strongly recommended that full-scale fatigue tests be conducted on several of the most common fatigue-critical connection details in Table 11-2 of the 2001 Specifications. In particular, the controversial built-up-box-to-column connection (Detail 19) and the full-penetration, tube-to-transverse plate connection with various backing ring details (Detail 11) should be tested. Such testing would provide data on which proper CAFL could be based.
- **Continuation of mitigation testing.** The galloping mitigation research that unfortunately could not be completed as part of this project should be continued. Researchers at the Universities of Wyoming and Florida have developed promising mitigation devices that have been proven successful in situations closely simulating natural conditions. However, other than the testing of the strand damper at Texas Tech during this project, extensive testing on any of these devices under natural conditions has yet to be performed. The data that have been obtained from the outdoor testing at Texas Tech have been the most useful and unchallengeable data that have been used so far in Phase I and in this Phase II research. For example, on the basis of pull-down tests and artificial laboratory tests with shakers, it was widely assumed that these mitigation devices would eliminate galloping. Only the tests at Texas Tech could verify the effectiveness of these devices, and these tests showed that galloping forces were only reduced, not eliminated. However, outdoor testing depends on the occurrence of favorable winds, which are seasonal and rare, even when the season is right. Combined with the fact that the winds must occur when researchers are available to conduct tests, it is understandable that these tests may take a great deal of time and patience.
- **Wind load testing.** Although little uncertainty exists about the magnitudes of the vortex-shedding and galloping equivalent static pressure ranges, long-term field testing to verify the natural wind-gust and, particularly, truck-induced gust pressures is still needed. Testing should base equivalent static pressures on stresses induced in support members, rather than on actual pressure measurements. Pinpoint pressure readings, on the one hand, only cover small areas and poorly describe the effects of an entire gust on a structure. Support member stresses, on the other hand, average the effects of the entire air mass applied to the structure. Equivalent static pressure ranges can then be back-calculated from the measured stresses.

REFERENCES

1. American Association of State Highway and Transportation Officials, *Standard Specifications for Structural Supports for Highway Signs, Luminaires, and Traffic Signals,* Washington, D.C., 2001.
2. Federal Highway Administration, *FHWA Electronic Information System Survey on Sign Structure Failures,* U.S. Department of Transportation, Washington, D.C., spring 1990.
3. Dexter, R. J., K. Johns, and R. DiBartolo, "Smart Sign Support," *Civil Engineering,* American Society of Civil Engineers, Reston, Virginia, September 2000.
4. Kaczinski, M. R., R. J. Dexter, and J. P. Van Dien, *NCHRP Report 412: Fatigue-Resistant Design of Cantilevered Signal, Sign, and Light Supports,* Transportation Research Board, National Research Council, Washington, D.C., 1998.
5. Fouad, F. H., N. Delatte, J. Davidson, and E. A. Calvert, *Standard Specifications for Structural Supports for Highway Signs, Luminaires, and Traffic Signals,* Interim Report (unpublished), NCHRP Project 17-10(2), Transportation Research Board, National Research Council, Washington, D.C., September 1999. (The information in this interim report will be published as an NCHRP report.)
6. American Association of State Highway and Transportation Officials, *Standard Specifications for Structural Supports for Highway Signs, Luminaires, and Traffic Signals,* Washington, D.C., 1994.
7. Fouad, F. H., E. A. Calvert, and E. Nunez, *NCHRP Report 411: Structural Supports for Highway Signs, Luminaires, and Traffic Signals,* Transportation Research Board, National Research Council, Washington, D.C., 1998.
8. Dexter, R. J., R. G. Janacek, and T. N. Schickel, "Fatigue Design for Sign Support Structures," *Proceedings of the International Bridge Conference,* Pittsburgh, June 1997.
9. Gilani, A., and A. Whitaker, "Fatigue-Life Evaluation of Steel Post Structures. I: Background and Analysis," *Journal of Structural Engineering,* March 2000.
10. Research Council on Structural Connections, *Specification for Structural Joints Using ASTM A325 or A490 Bolts,* c/o American Institute of Steel Construction, Chicago, Illinois, 1996.
11. American Association of State Highway and Transportation Officials, *Standard Specifications for Highway Bridges—LRFD,* first edition, Washington, D.C., 1994.
12. Collins, T. J., and M. J. Garlich, "Sign Structures Under Watch," *Roads and Bridges,* July 1997.
13. Johns, K. W., and R. J. Dexter, *Fatigue Testing and Failure Analysis of Aluminum Luminaire Support Structures,* Lehigh University, ATLSS Report No. 98-06, May 1998.
14. Ontario Ministry of Transportation, *Ontario Highway Bridge Design Code,* third edition, Ontario, Canada, 1992.
15. American Society of Civil Engineers, "Metal Fatigue Slides to a Stop," *Civil Engineering,* Vol. 68, No. 10, Reston, Virginia, October 1998.
16. Fisher, J. W., A. Nussbaumer, P. B. Keating, and B. T. Yen, *NCHRP Report 354: Resistance of Welded Details Under Variable Amplitude Long-Life Fatigue Loading,* Transportation Research Board, National Research Council, Washington, D.C., 1993.
17. DeSantis, P. V., and P. Haig, "Unanticipated Loading Causes Highway Sign Failure," *Proceedings of ANSYS Convention,* 1996.
18. Johns, K. W., and R. J. Dexter, *Fatigue Related Wind Loads on Highway Support Structures,* Final Report to New Jersey Department of Transportation, ATLSS Report No. 98-03, Lehigh University, April 1998.
19. Cook, R. A., D. Bloomquist, A. M. Agosta, and K. F. Taylor, *Wind Load Data for Variable Message Signs,* Structures and Materials Research Report 96-1, Engineering and Industrial Experiment Station, University of Florida, Gainesville, Florida, April 1996.
20. Gilani, A. S., J. W. Chavez, and A. S. Whittaker, *Fatigue Life Evaluation of Changeable Message Sign Structures, Volume 1: As-Built Specimens,* Earthquake Engineering Research Center, University of California at Berkeley, November 1997.
21. *ABAQUS,* Version 5.3, Hibbitt, Karlsson & Sorenson, Inc., Pawtucket, Rhode Island, 1993.
22. *Visual Analysis,* Version 3.12.EDU, Integrated Engineering Software, Bozeman, Montana, 1998.
23. Kaczinski, M. R., R. J. Dexter, and J. P. Van Dien, *Fatigue-Resistant Design of Cantilevered Signal, Sign, and Light Supports,* Interim Report (unpublished), NCHRP Project 10-38, Transportation Research Board, National Research Council, Washington, D.C., 1994.
24. Simiu, E., and R. H. Scanlon, *Wind Effects on Structures: An Introduction to Wind Engineering,* John Wiley and Sons, New York, New York, 1996.
25. Liu, H., *Wind Engineering—A Handbook for Structural Engineers,* Prentice Hall, Englewood Cliffs, New Jersey, 1991.
26. Davenport, A. G., "The Spectrum of Horizontal Gustiness Near the Ground in High Winds," *Quarterly Journal,* Vol. 87, Royal Meteorological Society, London, England, 1961.
27. Lundquist, R. C., K. D. Johnson, and M. C. Bamptom, *Aerodynamically Induced Stresses in Traffic Signals and Luminaire Supports,* Mechanics Research Report MRI-TR-2430-1, Bridge Department, California Division of Highways, 1972.
28. Musco Lighting, *Engineering Report for MUSCO Lighting Crossarm to Pole Connections,* Oskaloosa, Iowa, March 2000.
29. McDonald, J. R., K. C. Mehta, W. W. Oler, and N. Pulipaka, *Wind Load Effects on Signals, Luminaires, and Traffic Signal Structures,* Report 1303-1F, Wind Engineering Research Center, Texas Tech University, Lubbock, Texas, 1995.
30. Soong, T. T., and G. F. Dargush, *Passive Energy Dissipation Systems in Structural Engineering,* John Wiley and Sons, Chichester, England, 1999.
31. Riggs, G. S., H. R. Hamilton, and J. A. Puckett, *Increased Damping in Cantilevered Traffic Signal Structures,* University of Wyoming, Laramie, Wyoming, October 1998.
32. Cook, R. A., D. Bloomquist, M. A. Kalajian, V. A. Cannon, and D. Arnold, *Mechanical Damping Systems for Traffic Signal Mast Arms,* University of Florida, Gainesville, Florida, October 1998.
33. Cook, R. A., D. Bloomquist, D. S. Richard, M. A. Kalajian, V. A. Cannon, and D. P. Arnold, *Design, Testing, and Specification of a Mechanical Damping Device for Mast Arm Traffic Signal Structures,* University of Florida, Gainesville, Florida, January 2000.

34. McManus, P. S., *Evaluation of Damping in Cantilevered Traffic Signal Structures Under Forced Vibrations*, MS Thesis, University of Wyoming, Laramie, Wyoming, December 2000.
35. Huck, P., Fax transmittal to Robert Dexter regarding failure of Wyoming Traffic Signal Structures, 2000.
36. American Society of Civil Engineers, "Minimum Design Loads for Buildings and Other Structures," *ASCE 7-98*, Reston, Virginia, 1998.
37. Dusel, J. P., *Summary Report of Fatigue Failure of Type 16-2-80 Signal Support Structure*, California Department of Transportation, January 2000.
38. Hamilton, H. R., J. A. Puckett, B. Gray, and P. Wang, *Traffic Signal Pole Research*, Interim Report to Wyoming Department of Transportation, University of Wyoming, Laramie, Wyoming, January 2000.
39. Frank, K. H., "Fatigue Strength of Anchor Bolts," *Journal of the Structural Division*, Vol. 106, No. ST6, American Society of Civil Engineers, Reston, Virginia, 1980.
40. Stoker, J. R., J. P. Dusel, and R. Travis, *Determination of Fatigue Characteristics of Hot-Dipped Galvanized A307 and A449 Anchor Bars and A325 Cap Screws*, State of California, Department of Transportation, Division of Engineering Services, Sacramento, California, 1984.
41. James, R. W., P. B. Keating, R. W. Bolton, F. C. Benson, D. E. Bray, R. C. Abraham, and J. B. Hodge, *Tightening Procedures for Large-Diameter Anchor Bolts*, Texas Transportation Institute, Texas A&M University, June 1997.
42. ANSI/AWS D1.1, *Structural Welding Code—Steel*, American Welding Society, Miami, 1998.
43. Marshall, P. W., *Design of Welded Tubular Connections*, Elsevier, New York, New York, 1992.
44. Radaj, D., *Design and Analysis of Fatigue Resistant Welded Structures*, Halsted Press, New York, New York,1990.
45. Gurney, T. R., *Fatigue of Thin Walled Joints under Complex Loading*, Abington Publishing, Cambridge, United Kingdom, 1997.
46. Van Wingerde, A. M., J. A. Packer, and J. Wardenier, "Criteria for the Fatigue Assessment of Hollow Structural Section Connections," *Journal of Constructional Steel Research*, Vol. 35, 1995.

GLOSSARY OF VARIABLES

A = projected area of the body on a plane normal to the wind direction, m^2

b = flat-to-flat width of the member, m

C = constant, Ns^2/m^4

C_D = drag coefficient

d = member diameter, m

D = drag force, kg/m^3

$\overline{D}$ = mean drag force, N

D' = fluctuating drag force, N

e = base of the natural logarithm

f = frequency of the structure, Hz

f_i = natural frequencies, Hz

f_n = first natural frequency of the structure, Hz

g = acceleration due to gravity, m/s^2

I_F = importance factor

H = ratio of the fluctuating drag force to the fluctuating velocity, Ns/m

k = stiffness of the spring, N/m

K = terrain coefficient

m = mass supported by the spring, kg

P = drag pressure, Pa

$P_E(v)$ = probability that velocity v will be exceeded

P_G = equivalent static pressure due to galloping, Pa

P_{NW} = equivalent static pressure due to natural wind gust, Pa

P_{TG} = equivalent static pressure due to truck gust, Pa

P_{VS} = equivalent static pressure due to vortex shedding, Pa

r = ratio of frequency for mode j to frequency for mode i

$S_{F,i}(f_i)$ = magnitude of the force spectrum, N^2s

S_n = Strouhal number

S_r^{eff} = effective stress range, MPa

$S_{v,i}(f_i)$ = magnitude of the velocity spectrum, m^2/s

v = fatigue-limit-state wind velocity, m/s

V = velocity, m/s

V_C = critical wind velocity for vortex shedding, m/s

V_m = yearly mean wind velocity, m/s

V_y = turbulent wind velocity, m/s

$\overline{V}$ = mean velocity of wind, m/s

V_y' = fluctuating portion of wind velocity, m/s

V_{10} = wind velocity at 10-m elevation, m/s

ω = angular frequency of the structure, radians per second

ω_i = angular frequency for mode i, radians per second

$\overline{\omega}_i$ = average frequency of a bin where i varies from 1 to 10, radians per second

ω_j = angular frequency for mode j, radians per second

x_i = dimensionless quantity

y = elevation of the center of gravity of each surface, m

Δ = static displacement of the mass, m

β = damping ratio

ρ = density of standard air, $1.22\ kg/m^3$

ρ_{ij} = cross-modal coefficient

σ = combined stress, MPa

σ_i = stress in mode i, MPa

σ_{in} = in-plane stress, MPa

σ_j = stress in mode *j*, MPa

σ_{out} = out-of-plane stress, MPa

σ_{rms} = root-mean-square of the stress response, MPa

ξ_i = damping ratio for mode *i*

ξ_j = damping ratio for mode *j*

APPENDIX A

RECOMMENDED ANCHOR ROD SPECIFICATION AND COMMENTARY

PART 1

RECOMMENDED SPECIFICATION FOR STEEL-TO-CONCRETE JOINTS USING ASTM F1554 GRADES 36, 55, AND 105 SMOOTH ANCHOR RODS; AND ASTM A615 AND A706 GRADE 60 DEFORMED BARS

1 GENERAL REQUIREMENTS

1.1 Scope

This Specification covers the design, installation, inspection, and repair of cast-in-place anchor rods and associated components (Section 2) of steel to concrete joints. This Specification does not cover welded headed studs or post-installed anchor rods, although these may be allowed as alternative design anchors. This Specification is intended to be invoked in a structural design code or specification. This Specification relates only to those aspects of the connected materials that bear upon the performance of the anchor rods. For the design strength of the concrete, this Specification refers to current American Concrete Institute criteria. The resistance factors (f factors) specified by the American Concrete Institute shall correspond with the load factors and combinations given in Section 1.2. This Specification does not cover the design strength of the baseplate and other steel connected material, which is covered in the invoking specification. For the dimensional, material, and testing requirements, this Specification refers to current American Society for Testing and Materials specifications.

1.2 Loads, Load Factors and Load Combinations

The design and construction of the structure shall conform to the invoking structural design specification, which should be a load and resistance factor design specification. Although loads, load factors and load combinations are not explicitly specified in this Specification, the resistance factors herein are based upon loads, load factors and load combinations as specified in ASCE 7. When the design is governed by other load criteria, the resistance factors specified herein shall be adjusted as appropriate.

1.3 Referenced Standards and Specifications

The following standards and specifications are referenced. All referenced standards and specifications shall be the most current issue unless otherwise specified. If applicable, the equivalent standards and specifications from the American Association of State Highway and Transportation Officials (AASHTO) or other governing agency shall be used.

- **American Concrete Institute**
  - ACI 318 Building Code Requirements for Structural Concrete
- **American Institute of Steel Construction**
  - Load and Resistance Factor Design Specification for Structural Steel Buildings
  - Code of Standard Practice for Steel Buildings and Bridges
- **American National Standards Institute**
  - ANSI/ASME B1.1 Unified Screw Threads
  - ANSI/ASME B18.2.2 Square and Hex Nuts
- **American Society for Testing and Materials**
  - ASTM F1554 Standard Specification for Anchor Bolts, Steel, 36, 55, and 105-ksi Yield Strength
  - ASTM A615 Standard Specification for Deformed and Plain Billet-Steel Bars for Concrete Reinforcement
  - ASTM A706 Standard Specification for Low-Alloy Steel Deformed and Plain Bars for Concrete Reinforcement
  - ASTM A153 Standard Specification for Zinc Coating (Hot-Dip) on Iron and Steel Hardware
  - ASTM B695 Standard Specification for Coatings of Zinc Mechanically Deposited on Iron and Steel
  - ASTM A780 Standard Practice for Repair of Damaged and Uncoated Areas of Hot-Dip Galvanized Coatings
  - ASTM A563 Standard Specification for Carbon and Alloy Steel Nuts
  - ASTM F436 Standard Specification for Hardened Steel Washers
  - ASTM F959 Standard Specification for Compressible-Washer-Type Direct Tension Indicators for Use with Structural Fasteners
- **American Society of Civil Engineers**
  - ASCE 7 Minimum Design Loads for Buildings and Other Structures
- **American Welding Society**
  - AWS D1.1 Structural Welding Code–Steel

1.4 Drawing Information

The Engineer of Record shall specify the following information in the contract documents:

- The joint type and whether the anchor rods will be pretensioned (Section 3);
- The shape and dimensions of the anchor rods:
  - Smooth Bent Rods
  - Smooth Headed Rods
  - Deformed Bars
  - Alternative Anchor Rods (as permitted in Section 2.7);
- The thread type and class of thread tolerances (Section 2.3.2) and length of threaded portion;
- The grade and any supplementary requirements (including galvanizing or other coating) of anchor rod (Section 2.3.1);
- The style, grade, finish, and number of nuts per anchor rod (Section 2.4);
- The grade and shape of any plates, templates, and washers to be used in the anchor rod joint assembly (Sections 2.5 and 2.6);
- The arrangement of joint components including baseplate, templates, nuts, and washers (Sections 2.5.3, 2.6 and 3); and
- The installation method for vibrating-machinery joints (Section 5) or alternative design anchors.

2 JOINT COMPONENTS

2.1 Manufacturer Certification of Components

Manufacturer certifications documenting conformance as required below for anchor rods, nuts, and washers shall be available to the Engineer of Record and Inspector prior to installation of anchor rods.

2.2 Shipping and Storage of Components

Galvanized anchor rods, nuts, and washers shall be shipped pre-assembled. Anchor rods, nuts, and washers shall be protected from dirt and moisture at the site of installation.

2.3 Anchor Rods

2.3.1 Specifications

Smooth anchor rods shall meet the requirements of ASTM F1554. Deformed bars shall conform to ASTM A615 or A706. ASTM A615 deformed bars shall not be used if there is seismic loading or if the anchor rods must be designed for the fatigue limit state. Additionally, galvanized deformed bars shall conform to ASTM A767.

2.3.2 Thread Dimensions and Tolerances

Threads dimension shall meet the requirements of ANSI/ASME B1.1 and shall have Class 2A or 1A tolerances. The rod length used shall be such that the end of the bolt is flush with or projecting beyond the face of the nut when installation is complete.

2.4 Nuts

Nuts shall meet the requirements of ASTM A563. The grade, surface finish and style of such nuts shall be as given in Table 2.1. Hex and heavy-hex nut dimensions shall meet the requirements of ANSI/ASME B18.2.2.

2.5 Baseplates, Anchor Rod Holes, and Anchor Rod Group Assemblies

2.5.1 Baseplates

Plates shall be structural grade steel and may be galvanized or have other coatings. Uncoated steel shall not be used where it may remain in contact with moisture or vegetation. Edges may be thermally cut. The design of the baseplate shall conform to the invoking specification. For double-nut moment joints and vibrating-machinery joints, the thickness of the baseplate shall be equal to or greater than the nominal diameter of the anchor rod.

2.5.2 Anchor Rod Holes

The nominal dimensions of shear and normal holes for anchor rods shall be equal to or less than the dimensions shown in Table 2.2. Holes may be punched, drilled, or thermally cut. For statically loaded joints, thermally cut holes need not be ground. For seismically loaded joints or joints that are required to be designed for the fatigue limit state according to Section 4.6, the roughness of the inside surface of holes shall not exceed 1000 microinches. The clear distance between the edge of the hole and the edge of the adjacent hole or the edge of the baseplate shall be equal to or greater than the nominal anchor rod diameter.

2.5.2.1 Shear Holes. If anchor rods are required by Section 4.3 to contribute to the shear strength of the joint, shear holes shall be used in the baseplate.

2.5.2.2 Normal Holes. When anchor rods are not required by Section 4.3 to contribute to the shear strength of the joint, the holes may be as large as normal holes.

2.5.3 Anchor Rod Group Assemblies

A minimum of four anchor rods is required in any anchor rod joint. Provision shall be made to maintain the spacing and alignment of anchor rods within tolerances during placing and curing of the concrete. For anchor rod joints designed for seismic or fatigue limit states, plates or rings at least ¼ inch thick, with nuts on both sides, placed at two locations along the length of the anchor rods are recommended to maintain the spacing and alignment of the anchor rods. One of the plates or

TABLE 2.1 Acceptable ASTM A563 nut, grade, finish, and style and ASTM F436 washer type and finish for threaded anchor rods

Anchor Rod	Anchor Rod Size (in.)	Finish	ASTM A563 nut style, grade and finish	ASTM F436 washer type and finish
F1554 Grade 36 A615 Grade 40	¼ - 1 ½	Plain (uncoated)	Hex: A, B, D, DH; plain Heavy Hex: A, B, C, C3, D, DH, DH3; plain	1; plain
		Galvanized	Hex: A[a], B, D, DH; galvanized and lubricated Heavy Hex: A, B, C, C3, D, DH, DH3; galvanized and lubricated	1; galvanized
	Over 1 ½ - 4	Plain (uncoated)	Heavy Hex: A, B, C, C3, D, DH, DH3; plain	1; plain
		Galvanized	Heavy Hex: A, B, C, C3, D, DH, DH3; galvanized and lubricated	1; galvanized
F1554 Grade 55 A615 Grade 60 A706 Grade 60	¼ - 1 ½	Plain (uncoated)	Hex: A, B, D, DH; plain Heavy Hex: A, B, C, C3, D, DH, DH3; plain	1; plain
		Galvanized	Heavy Hex: A[b], B[b], C, C3, D, DH, DH3; galvanized and lubricated	1; galvanized
	Over 1 ½ - 4	Plain (uncoated)	Heavy Hex: A, B, C, C3, D, DH, DH3; plain	1; plain
		Galvanized	Heavy Hex: A[b], B[b], C, C3, D, DH, DH3; galvanized and lubricated	1; galvanized
F1554 Grade 105	¼ - 1 ½	Plain (uncoated)	Hex: D, DH; plain Heavy Hex: C, C3, D, DH, DH3; plain	1; plain
		Galvanized	Heavy Hex: DH, DH3; galvanized and lubricated	1; galvanized
	Over 1 ½ - 4	Plain (uncoated)	Heavy Hex: DH, DH3; plain	1; plain
		Galvanized	Heavy Hex: DH, DH3; galvanized and lubricated	1; galvanized

[a] Applicable only to F1554 grade 36 anchor rods
[b] Applicable only to F1554 grade 55 anchor rods
[c] Applicable only if washer is required

TABLE 2.2 Maximum nominal anchor rod hole dimensions

Anchor Rod Diameter d_b, in.	Maximum Permitted Nominal Anchor Rod Hole Dimensions[a,b], in.	
	Shear Holes (diameter)	Normal Holes (diameter)
½	$^{5}/_{8}$	$1^{1}/_{16}$
$^{5}/_{8}$	$^{13}/_{16}$	$1^{3}/_{16}$
¾	$^{15}/_{16}$	$1^{5}/_{16}$
$^{7}/_{8}$	$1^{1}/_{16}$	$1^{9}/_{16}$
1	$1^{1}/_{4}$	$1^{13}/_{16}$
$1^{1}/_{4}$	$1^{9}/_{16}$	$2^{1}/_{16}$
$1^{1}/_{2}$	$1^{13}/_{16}$	$2^{5}/_{16}$
$1^{3}/_{4}$	$2^{1}/_{16}$	$2^{3}/_{4}$
≥ 2	$d_b + {}^{5}/_{16}$	$d_b + 1^{1}/_{4}$

[a] The upper tolerance on the tabulated nominal dimensions shall not exceed $^{1}/_{16}$-in.
[b] The slightly conical hole that naturally results from punching operations with properly matched punches and dies is acceptable.

rings may be above the top of concrete so that it can be reused as a template. The assemblies shall be protected from damage following installation.

2.6 Washers

2.6.1 Standard Washers

Standard flat circular washers and standard square or rectangular beveled washers shall meet the requirements of ASTM F436. The type and finish of such washers shall be as given in Table 2.1.

2.6.2 Plate Washers

Plate washers shall be of structural grade steel and may be galvanized or have other coating. Uncoated steel shall not be used where it may remain in contact with moisture or vegetation. Plate washers shall be large enough to completely cover the holes. The thickness of baseplate washers shall have sufficient strength and stiffness to resist dishing into the holes and shall be a minimum of $\frac{3}{8}$-in.

2.6.3 Use of Washers

Washers shall be used as required in Sections 2.6.4.1 and 2.6.4.2.

2.6.3.1 Threaded-Shear-and-Uplift Joints (as defined in Section 3.1). Washers are not required in threaded-shear-and-uplift joints, except as required in Section 2.6.3.1.1 and 2.6.3.1.2.

2.6.3.1.1 Sloping Surfaces. When the outer face of the baseplate has a slope that is greater than 1:20 with respect to a plane that is normal to the anchor axis, an ASTM F436 beveled washer shall be used to compensate for the lack of parallelism.

2.6.3.1.2 Normal Hole. When a normal hole is used in the baseplate, a plate washer shall be used to cover the hole.

2.6.3.2 Double-Nut-Moment and Vibrating-Machinery Joints (as defined in Sections 3.2 and 3.3). Washers are required between both nuts and the baseplate in double-nut-moment joints and under the nut in vibrating-machinery joints.

2.7 Alternative-Design Anchors or Washers

When approved by the Engineer of Record, the use of alternative-design anchors is permitted, including post-installed anchors, welded headed studs, washer-type indicating devices, or other alternatives. Detailed installation and inspection instructions shall be prepared in a supplemental specification that is approved by the Engineer of Record.

3 JOINT TYPE

For anchor rod joints, the Engineer of Record shall specify the joint type in the contract documents as threaded-shear-and-uplift, double-nut-moment, or vibrating-machinery.

3.1 Threaded-Shear-and-Uplift Joints

Anchor rods in threaded-shear-and-uplift joints shall be designed in accordance with the applicable provisions of Sections 4.1 and 4.3 through 4.6, installed in accordance with Section 5.1 and inspected in accordance with Section 7.

3.2 Double-Nut-Moment Joints

Anchor rods in double-nut-moment joints shall be designed in accordance with the applicable provisions of Sections 4.1 through 4.6, installed in accordance with Section 5.2, and inspected in accordance with Section 7. Grout need not be placed under the baseplate in double-nut moment joints. Electrical wires exposed between the baseplate and the concrete shall be protected from damage by animals with a wire mesh or other suitable protection.

3.3 Vibrating-Machinery Joints

Anchor rods in vibrating-machinery joints shall be designed in accordance with the applicable provisions of Sections 4.1 and Sections 4.3 through 4.6, installed in accordance with Section 5.3, and inspected in accordance with Section 7.

4 LIMIT STATES IN ANCHOR ROD JOINTS

The design strength of an anchor rod joint shall be equal to or greater than the effect of the factored loads on the joint. The design strength of an anchor rod joint shall be calculated from equilibrium and deformation compatibility at the limit state. The axial and shear force contributions of each anchor rod in the joint and any compression or friction forces from contact between steel baseplate and concrete shall be considered. The capacity of the foundation, the strength of the baseplate, or the strength of the steel or concrete connected parts, as determined in accordance with the applicable specifications, may also limit the design strength.

For threaded-shear-and-uplift joints and vibrating-machinery joints, the contributions to the joint strength from bearing and shear friction of the baseplate on the concrete or grout shall be calculated in accordance with current American Concrete Institute criteria. Shear friction strength should be calculated using the factored load combination that gives minimum possible compression from dead load along with the maximum uplift that is consistent with the lateral load that is

being evaluated. The effect of live load should not be included when calculating the shear friction strength unless the live load causes the lateral load or uplift.

All types of anchor rod joints shall have design strength greater than the factored loads during erection, including a minimum lateral load equal to 5.0 percent of the axial load from dead load during erection. For threaded-shear-and-uplift joints, if the bearing strength and shear friction strength of the baseplate on the concrete are greater than the factored design loads in service, then the anchor rods need not be designed for strength or fatigue from service loads.

The axial force in anchor rods that are subject to tension, or combined shear and tension, shall be calculated with consideration of the effects of the externally applied tensile force and any additional tension resulting from prying action produced by deformation of the baseplate.

For anchor rod joints in tension or flexure, the design tensile strength of contributing anchor rods shall be determined in accordance with Section 4.1.

For threaded-shear-and-uplift joints, the bearing strength of the baseplate on the concrete shall be greater than the total compression effects, including axial load and flexure.

For double-nut-moment joints, the anchor rods shall be designed for the total compression effects, including axial load and flexure, neglecting bearing of the baseplate on concrete or grout. For double-nut-moment joints, the design compressive strength of contributing anchor rods shall be determined in accordance with Section 4.2.

For threaded-shear-and-uplift and vibrating-machinery joints, shear strength or torsional strength may be taken as the larger of:

- the friction strength between the baseplate and the concrete surface; or,
- the smaller of the sum of the steel shear strengths of the contributing individual anchor rods or the concrete shear strength of the anchor group.

It is not permitted to combine the friction strength and the shear strength of the anchor rods.

In double-nut-moment joints, shear strength or torsional strength shall be taken as the smaller of the sum of the steel shear strengths of the contributing individual anchor rods or the concrete shear strength of the anchor group. If the clear distance between the bottom of the bottom leveling nut and the top of concrete is less than the nominal anchor rod diameter, bending of the anchor rod from shear forces or torsion may be ignored.

If anchor rods are required to contribute to the shear strength of the anchor rod joint:

- the hole in the baseplate must be a shear hole as defined in Section 2.5.2,
- the design shear strength of contributing anchor rods shall be determined in accordance with Section 4.3,
- the interaction of combined shear and tension on individual anchor rods shall be limited in accordance with Section 4.4, and
- if a shear hole is used, the design bearing strength of the baseplate at anchor rod holes due to a shear force acting on the anchor rod shall be determined in accordance with Section 4.5.

When anchor rods are subject to more than 20,000 repeated applications of significant axial tension or tension from flexure, the fatigue limit state shall be checked in accordance with Section 4.6.

4.1 Design Tensile Strength

The design tensile strength of the joint shall be taken as the smallest of the sum of the steel tensile strengths of the contributing individual anchor rods or the concrete tensile strength of the anchor group. Concrete tensile strength and the development length of deformed bars shall be calculated in accordance with current American Concrete Institute criteria.

The design steel tensile strength for an anchor rod is the fracture strength in the threaded section. The design steel tensile strength of a threaded anchor rod is independent of the installed anchor rod pretension.

The design strength for fracture in the threaded section is $\phi\,(R_t)_f$, where $\phi = 0.75$ and:

$$(R_t)_f = F_u A_{ts} \tag{4.1}$$

where

$(R_t)_f$ = nominal fracture strength of an anchor rod, kips
F_u = specified minimum tensile strength from Table 4.1, ksi
A_{ts} = tensile stress area from Table 4.2, in.^{2}

4.2 Design Compressive Strength

For threaded-shear-and-uplift and vibrating-machinery joints, the design compressive bearing strength of the baseplate over the compressed concrete shall be calculated according to current American Concrete Institute criteria.

TABLE 4.1 Tensile properties for anchor rods

Tensile Property	ASTM F1554 Rod Grade 36	ASTM F1554 Rod Grade 55	ASTM F1554 Rod Grade 105	ASTM A615 and A706 Bars Grade 60
Minimum Yield Strength F_y, ksi	36	55	105	60
Minimum Tensile Strength F_u, ksi	58	75	125	80

TABLE 4.2 Tensile stress areas for threaded anchor rods

Unified coarse Thread series (UNC)		
Nominal Size (in.)	Gross Area ($in.^2$)	Stress Area ($in.^2$)
½	0.20	0.14
5/8	0.31	0.23
¾	0.44	0.33
7/8	0.60	0.46
1	0.79	0.61
1 1/8	0.99	0.76
1 ¼	1.23	0.97
1 ½	1.77	1.41
1 ¾	2.41	1.90
2	3.14	2.50
2 ¼	3.98	3.25
2 ½	4.91	4.00
2 ¾	5.94	4.93
3	7.07	5.97
3 ¼	8.30	7.10
3 ½	9.62	8.33
3 ¾	11.04	9.66
4	12.57	11.08
8 Thread Series (8 UN)		
Nominal Size (in.)	Gross Area ($in.^2$)	Stress Area ($in.^2$)
1 1/8	0.99	0.79
1 ¼	1.23	1.00
1 ½	1.77	1.49
1 ¾	2.41	2.08
2	3.14	2.77
2 ¼	3.98	3.56
2 ½	4.91	4.44
2 ¾	5.94	5.43
3	7.07	6.51
3 ¼	8.30	7.69
3 ½	9.62	8.96
3 ¾	11.04	10.34
4	12.57	11.81

The precompression of the concrete in vibrating-machinery joints due to pretensioning the anchor rods need not be added to the applied compression. It shall be assumed that the anchor rods do not contribute to compressive strength for threaded-shear-and-uplift and vibrating-machinery joints.

For double-nut-moment joints, the design compressive strength (for axial load and compression due to flexure) shall be taken as the smaller of:

a) the sum of the steel compressive strengths of the contributing anchor rods; or,
b) the concrete compressive strength of the contributing anchor rod group.

The design steel compressive strength for an anchor rod in a double-nut-moment joint with a clear distance between the bottom of the bottom leveling nut and the top of concrete equal or less than four anchor rod diameters is ϕR_c, where $\phi = 0.9$ and:

$$R_c = F_y A_g \tag{4.2}$$

where

R_c = nominal steel compressive strength of an anchor rod, kips
F_y = specified minimum yield stress from Table 4.1, ksi
A_g = gross area based on the nominal diameter of the anchor rod, $in.^2$

If the clear distance is greater than four diameters, buckling of the anchor rod shall be considered using the column design criteria of the invoking specification, but the design steel compressive strength shall not exceed that given by Equation 4.2.

The design compressive bearing strength of anchor rod heads and bends and the compressive development length of deformed bars for double-nut-moment joints shall be calculated in accordance with current American Concrete Institute criteria.

4.3 Design Shear Strength

If the anchor rods are required for shear or torsional strength in an anchor rod joint, the design strength shall be the smaller of the concrete strength for the anchor rod group in shear or torsion, calculated in accordance with current American Concrete Institute criteria, and the sum of the shear strengths of the contributing anchor rods. The design shear strength for an anchor rod fastened with one or two nuts to a baseplate with shear holes, which is independent of the installed anchor rod pretension, is $\phi (R_v)_s$, where $\phi = 0.75$ and:

$$(R_v)_s = 0.6 F_u A_{ts} \tag{4.3}$$

where

$(R_v)_s$ = nominal steel shear strength of an anchor rod, kips
F_u = specified minimum tensile strength from Table 4.1, ksi
A_{ts} = tensile stress area of the anchor rod from Table 4.2, $in.^2$

4.4 Combined Shear and Tension

When anchor rods transmit combined shear and tension forces, the ultimate limit-state interaction shall be limited as:

$$\left(\frac{P_u}{\phi R_t}\right)^{5/3} + \left(\frac{V_u}{\phi R_v}\right)^{5/3} \leq 1.0 \tag{4.4}$$

where

P_u = required tensile strength (factored tensile force) of contributing anchors, kips
V_u = required shear strength (factored shear force) of contributing anchors, kips

ϕR_t = design tensile strength of anchors determined in accordance with Section 4.1, kips
ϕR_v = design shear strength of anchors determined in accordance with Section 4.3, kips

4.5 Design Bearing Strength at Anchor Rod Shear Holes

The design bearing strength at anchor rod shear holes shall be taken as the sum of the strengths of the individual anchor rod shear holes in the baseplate.

The design bearing strength of the baseplate at an anchor rod shear hole is ϕR_n, where $\phi = 0.75$ and:

$$R_n = 2.0 d_b t F_u \tag{4.5}$$

where

R_n = nominal bearing strength of the baseplate, kips
F_u = specified minimum tensile strength of the baseplate, ksi
d_b = nominal anchor rod diameter, in.
t = thickness of the baseplate, in.

4.6 Tensile Fatigue

Anchor rods subject to more than 20,000 repeated applications of significant axial tension or tension from flexure shall be checked for the fatigue limit state. Baseplates, nuts, and other components need not be checked, unless required by the invoking specification.

For fatigue, the force ranges in the anchor rods should be calculated from the unfactored, repeated live loads using elastic analysis. Axial forces in the anchor rods from tension, compression, and from flexure shall be considered. For all types of joints, the entire force range shall be assumed to be applied to the anchor rods, even if they are pretensioned. Bending of the anchor rods need not be considered, with the exception of double-nut moment joints when the clear distance between the bottom of the leveling nut and the concrete exceeds the diameter of the anchor rods. Shear forces may be ignored for purposes of calculating the fatigue effect, even if they act in combination with the axial forces.

Stress range is defined as the magnitude of the change in nominal stress due to the application or removal of the unfactored live load. The entire range in stress shall be included, even if during part of the cycle the stress is in compression. In the case of a load reversal, the stress range in an individual anchor rod shall be computed as the algebraic difference between the peak stress due to the live load applied in one direction and the peak stress due to the live load applied in the other direction. If the baseplate thickness is less than the diameter of the anchor rods, the applied stress ranges shall include any additional tension resulting from prying action produced by the unfactored live load.

The applied stress range is computed by dividing the axial force ranges by the tensile stress area in Table 4.2. If bending of the anchor rods is included in the analysis, the bending stress range shall be added to the stress range from the axial forces. The stress range shall not be amplified by stress concentration factors.

No further evaluation of fatigue resistance is required if the stress in the anchor rod remains in compression during the entire cycle (including the minimum dead load) or if the stress range is less than the threshold stress range, F_{TH}. The maximum applied stress range shall not exceed the allowable stress range computed as follows:

$$F_{SR} = \left(\frac{C_f}{N}\right)^{0.333} \geq F_{TH} \tag{4.6}$$

where

F_{SR} = allowable stress range, ksi
C_f = constant equal to 3.9×10^8
N = number of stress range cycles during the life of the structure
F_{TH} = threshold stress range equal to 7 ksi

5 INSTALLATION AND CONSTRUCTION INSPECTION

Proper installation is the responsibility of the contractor, and inspection and testing is to be performed by the contractor. Records shall be kept of the dates and results of testing and inspection, and these records shall be available for the Engineer of Record or their designated representative for review. The Engineer of Record may require that their representative witness the inspection and testing.

The anchor rods shall be assembled into an anchor rod group and provision shall be made to maintain the spacing and alignment of anchor rods within tolerances during placing and curing of the concrete, as specified in Section 2.5.3. The threads must be protected from damage during installation.

If the embedded head of an ASTM F1554 anchor rod is a nut, or is fastened with nuts, the head-nut or the nuts fastening the head shall be prevented from rotating while the anchor rod is tightened with a jam nut or other locking device.

Vibrating the concrete in the vicinity of the anchor rod group shall ensure adequate consolidation of the concrete.

The anchor rods shall not be subjected to erection or service loads until the concrete has reached 75 percent of the design strength or as approved by the Engineer of Record.

Joints other than threaded-shear-and-uplift joints require pretensioning. There may be only one structural element attached to the baseplate (usually a column or post) during the tightening, and it shall be plumbed and supported by a crane during tightening. Cantilevered beams or arms with span in excess of 10 feet shall not be attached to the element during the tightening of the anchor rods.

5.1 Threaded-Shear-and-Uplift Joints

Installation sequence:

1. Anchor rods shall be secured against relative movement and misalignment.
2. If a template is used, the hole pattern shall be verified by comparing the top template to the baseplate to be erected. Any deviation between the hole positions outside of the tolerances must be reported to the Engineer of Record and the correction must conform to the requirements of Section 6.
3. The template set (or other device) with anchor rods shall be secured in its correct position in accordance with the drawings.
4. The concrete shall be placed and cured.
5. If a top template is above the concrete surface, it may be removed 24 hours after placing the concrete.
6. The exposed part of the anchor rods shall be cleaned with a wire brush or equivalent.
7. After installation, the anchor rods shall be inspected visually to verify that there is no visible damage to the threads and that their position, elevation, and projected length from the concrete are within the tolerances specified on the drawings. In the absence of required tolerances, the position, elevation, and projected length from the concrete shall be within the tolerances specified in the American Institute of Steel Construction (AISC) Code of Standard Practice for Steel Buildings and Bridges.
8. If necessary, the baseplate may be leveled with any properly designed leveling plate or grout pad, in accordance with the drawings or approved by the Engineer of Record.
9. If washers are required in accordance with Section 2.6.3, they shall be placed.
10. Nuts shall be cleaned and tightened with the full effort of the installer following a star pattern. Any thread damage requiring unusually large effort to turn the nut shall be reported to the Engineer of Record.
11. Any correction because the anchor rods are damaged or out of tolerance must conform to the requirements of Section 6.
12. If the joint may be seismically loaded or if it was designed for fatigue, nuts shall be turned in increments following a star pattern using at least two full tightening cycles to the nut rotation specified in Table 5.1. Before turning, the reference position of the nut in the snug-tight condition shall be marked with a suitable marking on the corner at the intersection of two flats with a corresponding reference mark on the baseplate at each bolt. After tightening, the nut rotation shall be verified, and the nut shall be prevented from loosening using a jam nut or other suitable locking device.

5.2 Double-Nut-Moment Joints

Installation sequence:

1. The torque wrench used for tightening the nuts or final torque verification should have a torque indicator that is calibrated annually. A certification of such calibration shall be available to the Engineer of Record. A torque multiplier may be used.
2. The verification torque is computed using Equation 5.1.

$$T_v = 0.12 d_b T_m \tag{5.1}$$

where

T_v = the verification torque (inch-kips)
d_b = the nominal body diameter of the anchor rod (inches)
T_m = the minimum installation pretension (kips) given in Table 5.2.

3. Prior to placing the anchor rods in the concrete, an Anchor Rod Rotation Capacity test shall be run with at least one anchor rod from every lot. This test may be run using the baseplate or a plate of equivalent grade, thickness, and finish. The plate must be restrained against movement from the torque that will be applied. The test consists of steps 10 through 18 below, with the exception of step 12 (since there is only one anchor rod). The nut shall be rotated to at least the required

TABLE 5.1 Nut rotation for turn-of-nut pretensioning of UNC threads

Anchor Rod Diameter, in.	Nut Rotation [a,b,c]	
	F1554 Grade 36	F1554 Grades 55 and 105 A615 and A706 Grade 60
≤ 1 ½	1/6 turn	1/3 turn
> 1 ½	1/12 turn	1/6 turn

[a] Nut rotation is relative to anchor rod. The tolerance is plus 20 degrees.
[b] Applicable only to UNC threads.
[c] Beveled washer shall be used if: a) the nut is not into firm contact with the baseplate; or b) the outer face of the baseplate is sloped more than 1:40.

TABLE 5.2 Minimum anchor rod pretension for double-nut-moment joints

Anchor Rod Diameter, in.	Minimum Anchor Rod Pretension T_m, kips			
	ASTM F1554 Rod Grade 36[a]	ASTM F1554 Rod Grade 55[b]	ASTM F1554 Rod Grade 105[b]	ASTM A615 and A706 Bars Grade 60[b]
1/ 2	4	6	11	7
5/ 8	7	10	17	11
3/ 4	10	15	25	16
7/ 8	13	21	35	22
1	18	27	45	29
1 1/8	22	34	57	37
1 1/4	28	44	73	47
1 1/2	41	63	105	67
1 3/4	55	86	143	91
2	73	113	188	--
2 1/4	94	146	244	156
2 1/2	116	180	300	--
2 3/4	143	222	370	--
3	173	269	448	--
3 1/4	206	320	533	--
3 1/2	242	375	625	--
3 3/4	280	435	725	--
4	321	499	831	--

[a] Equal to 50 percent of the specified minimum tensile strength of rods, rounded to the nearest kip.
[b] Equal to 60 percent of the specified minimum tensile strength of rods, rounded to the nearest kip.

rotation given in Table 5.1. After the test, the nuts shall be removed and inspected for damage to their threads. Then the anchor rod is removed from the test plate and restrained while the nuts shall be turned onto the bolts at least one rod diameter past the location of the leveling nut and top nut in the test, then backed off by one worker using an ordinary wrench (without a cheater bar). The threads are considered damaged if an unusual effort is required to turn the nut. If there is no damage to the anchor rod or nut during this test, they may be used in the joint. If there is damage to the threads or an inability to attain at least the verification torque, the lot of anchor rods shall be rejected.

4. Anchor rods shall be secured against relative movement and misalignment. (Note: A template is required for leveling the leveling nuts. The hole pattern shall be verified by comparing the template to the baseplate to be erected. Any deviation between the hole positions outside of the tolerances must be reported to the Engineer of Record, and the correction must conform to the requirements of Section 6.)
5. The template set (or other device) with anchor rods shall be secured in its correct position in accordance with the drawings.
6. The concrete shall be placed and cured.
7. If a top template is above the concrete surface, it may be removed 24 hours after placing the concrete.
8. The exposed part of the anchor rods shall be cleaned with a wire brush or equivalent and lubricated.
9. The anchor rods shall be inspected visually to verify that there is no visible damage to the threads and that their position, elevation, and projected length from the concrete are within the tolerances specified on the drawings. In the absence of required tolerances, the position, elevation, and projected length from the concrete shall be according to the AISC Code of Standard Practice for Steel Buildings and Bridges. If the joint is required to be designed for fatigue in accordance with Section 4.6, the misalignment from vertical shall be no more than 1:40. The nuts shall be turned onto the bolts well past the elevation of the bottom of the leveling nut and backed off by one worker using an ordinary wrench without a cheater bar. Thread damage requiring unusually large effort shall be reported to the Engineer of Record. Any correction to the anchor rods joint because they are out of tolerance or the threads are damaged must conform to the requirements of Section 6.
10. If threads of anchor rods were lubricated more than 24 hours before placing the leveling nut or have been wet since they were lubricated, the exposed threads of the anchor rod shall be relubricated. Leveling nuts shall be cleaned, threads and bearing surfaces lubricated, and placed on the anchor rods.
11. Leveling nut washers shall be placed on the anchor rods. Beveled washers shall be used if the nut cannot be brought into firm contact with the baseplate.
12. The template shall be placed on top of the leveling nuts to check the level of the nuts. In some cases, if indicated on the drawings, it is permitted to set the baseplate at some angle other than level. If this angle exceeds 1:40, beveled washers shall be used. Verify

that the distance between the bottom of the bottom leveling nut and the top of concrete is not more than one anchor rod diameter (unless specified otherwise on the drawings).
13. The baseplate and structural element to which it is attached shall be placed.
14. Top nut washers shall be placed. Beveled washers shall be used if the nut cannot be brought into firm contact with the baseplate.
15. Threads and bearing surfaces of the top nuts shall be lubricated, placed and tightened to between 20 and 30 percent of the verification torque following a star pattern.
16. Leveling nuts shall be tightened to between 20 and 30 percent of the verification torque following a star pattern.
17. Before further turning the nuts, the reference position of the top nut in the snug-tight condition shall be marked on an intersection between flats with a corresponding reference mark on the baseplate at each bolt. Top nuts shall be turned in increments following a star pattern (using at least two full tightening cycles) to the nut rotation specified in Table 5.1 if UNC threads are used. (If 8UN threads are used, the appropriate nut rotation shall be shown on the drawings or specified by the Engineer of Record.) After tightening, the nut rotation shall be verified.
18. A torque wrench shall be used to verify that a torque at least equal to the verification torque is required to additionally tighten the leveling nuts and the top nuts. An inability to achieve this torque shall be interpreted to indicate that the threads have stripped and this must be reported to the Engineer of Record.
19. After at least 48 hours, the toque wrench shall again be used to verify that a torque at least equal to 110 percent of the verification torque is required to additionally tighten the leveling nuts and the top nuts. For cantilever or other non-redundant structures, this verification is required at least 48 hours after erection of the remainder of the structure and any heavy attachments to the structure.
20. If the joint will be seismically loaded or was designed for fatigue, the nut shall be prevented from loosening unless a maintenance plan is in place to verify at least every four years, in accordance to Section 7, that a torque equal to at least 110 percent of the verification torque is required to additionally tighten the leveling nuts and the top nuts.

5.3 Vibrating-Machinery Joints

Installation sequence:

1. The assembly of sleeve and anchor rod shall be secured in its correct position in accordance with the drawings.
2. If a template is used, the hole pattern shall be verified by comparing the top template to the baseplate to be erected, and any deviation between the hole positions outside of the tolerances must be reported to the Engineer of Record. The correction must conform to the requirements of Section 6.
3. The concrete shall be placed and cured.
4. If a top template is above the concrete surface, it may be removed no sooner than 24 hours after placing the concrete.
5. The exposed part of the anchor rods shall be cleaned with a wire brush or equivalent and lubricated.
6. The opening of the sleeve shall be cleaned of debris and sealed off.
7. After removal of the template, if any, the anchor rods shall be inspected visually to verify that there is no visible damage to the threads and that their position, elevation, and projected length from the concrete are within the tolerances specified on the drawings. In the absence of required tolerances, the position, elevation, and projected length from the concrete shall be within the tolerances specified in the AISC Code of Standard Practice for Steel Buildings and Bridges. The nuts shall be turned onto the bolts at least one rod diameter past the elevation of the bottom of the baseplate and backed off by one worker using an ordinary wrench without a cheater bar. Any damage resulting in unusual effort to turn the nut shall be reported to the Engineer of Record and any correction must conform to Section 6.
8. The baseplate and one structural element or piece of equipment or machinery shall be placed.
9. Washers shall be placed.
10. If threads of anchor rods were lubricated more than 24 hours before placing the nut or have been wet since they were lubricated, the exposed threads of the anchor rod shall be relubricated. Nuts shall be cleaned and the threads and bearing surfaces lubricated.
11. The pretension and pretensioning method shall be as specified on the drawings, along with the procedures and requirements for an installation verification test, if necessary.

6 REPAIR AND MODIFICATION

Any correction, repair, or modification in anchor rod joints shall meet the Design Limit States in Section 4 and applicable guidelines of this section. The Engineer of Record shall approve any correction, repair, or modification before further work on the anchor rod joint can proceed. The repair methods below may be used at the discretion of the Engineer of Record.

It is not permitted to run a die over the threads to remove excessive zinc.

For anchor rods that do not have to be designed for seismic loading or fatigue and are out of alignment tolerance but can still fit in the holes, the misalignment may be corrected

using beveled washers. If the anchor rods cannot fit in the holes, there are two alternatives:

a) For threaded-shear-and-uplift joints with normal holes (as defined in Section 2.5.2), the hole may be enlarged by thermal cutting. Plate washers must be redesigned to cover and prevent dishing into the enlarged hole. The minimum clear distance at least equal to the nominal diameter of the anchor rod must be maintained from the edge of the hole to the edge of the baseplate or the edge of an adjacent hole.
b) The anchor rods may be straightened using the procedures below until they can fit in the holes, then any further misalignment can be corrected using beveled washers.

If the anchor rods are designed for fatigue or seismic loading and the vertical misalignment exceeds 1:40 but does not exceed 1:20, it may be straightened back to a maximum misalignment of 1:40 using the following procedures:

a) Striking with a hammer;
b) Applying pressure with a jack; or,
c) Bending it with a pipe.

Threads must be protected and examined for damage during the straightening operation.

For any of these methods, heat may also be applied to the anchor rod in accordance with Section 6.4 of ASTM F1554. If a galvanized anchor rod is heated, the galvanizing shall be repaired as specified in ASTM A780. Heating shall not be applied more than once.

If the anchor rods are designed for fatigue and the vertical misalignment exceeds 1:20, the anchor rods shall be replaced.

For double-nut moment joints where the anchor rod is not at least flush with the top of the nut, the leveling nuts and the baseplate may be lowered enough to achieve adequate thread projection. For other types of joints on grout pads, the thickness of the grout pad may be decreased. In either case, the effect of decreasing the elevation of the structural element attached to the baseplate shall be considered.

If the applied factored tension uplift force in the anchor rod is less than 90 percent of the design steel tensile strength calculated using Equation 4.1, consideration may be given to not correcting the insufficient thread engagement. The thread engagement as a proportion of the depth of the nut should exceed the ratio of the applied factored tensile force to the design steel tensile strength.

Another possible solution for insufficient thread engagement is to use a specially designed “shoulder” nut that will partly drop into the hole. The hole may be enlarged for this purpose if the minimum clear distances from the edge and from adjacent holes are maintained. The diameter of the enlarged hole shall not exceed the diameter of the part of the nut in the hole by more than $\frac{1}{8}$ inch.

When the anchor rod is damaged or the projecting end of an anchor rod is shorter than needed, concrete may be partially excavated, the anchor cut off if necessary, and a coupler (a threaded coupler or other coupling device approved by the Engineer of Record) used to join an extension onto the anchor rod. The coupler shall not interfere with the baseplate. The coupler shall have a proof load at least equal to that of the recommended nut in Table 2.1, and it shall be guaranteed that the threaded engagement length in both the anchor rod and the extension is at least equal to the thickness of their recommended nuts.

7 INSPECTION AND MAINTENANCE AFTER INSTALLATION

For all seismically loaded joints or joints that must be designed for the fatigue limit state, a regular maintenance plan shall be in place to verify their integrity at least once every four years or after a significant seismic event.

The plan shall include at least:

a) Verification that the joint is kept free of debris, water and vegetation;
b) Verification that there is not severe corrosion, gouges, or cracks;
c) Verification that the grout and concrete in the vicinity of the anchor rods is in good condition;
d) A hammer sound test of anchor rods;
e) Verification of the tightness of nuts (it shall be verified that the nuts still have a jam nut or other locking device or the tightness shall be verified by applying 110 percent of the verification torque computed using Equation 5.1);
f) Retightening of anchor rods, if needed, in accordance with Section 5;
g) If similar structures subject to similar loading have had anchor rod fatigue cracking problems, then an ultrasonic test of anchor rods shall be performed (the top of the rod or extension shall be ground flush and the ultrasonic test and its interpretation shall be in accordance with a procedure approved by a qualified Engineer).

PART 2

COMMENTARY ON RECOMMENDED SPECIFICATION FOR STEEL-TO-CONCRETE JOINTS USING ASTM F1554 GRADES 36, 55, AND 105 SMOOTH ANCHOR RODS, ASTM A615 AND A706 GRADE 60 DEFORMED BARS

C-1. GENERAL REQUIREMENTS

C-1.1. Scope

This Specification deals principally with cast-in-place ASTM F1554 smooth anchor rods (ref.1), ASTM A615 and A706 deformed bars (refs. 2 and 3), and with their design, installation, inspection, and repair in steel-to-concrete joints. ASTM F1554 is essentially the same as AASHTO M314-90, although there are some slight differences. Although the scope is limited, it is not intended to prohibit equivalent anchor devices such as post-installed anchorages and welded-headed studs. Post-installed anchor rods are installed after the concrete has hardened; therefore, a hole has to be drilled into the concrete. Welded-headed studs are specified in AWS D1.1 (ref. 4). These provisions may not be applicable to these alternative anchorages or cast-in-place anchors of other chemical composition, mechanical properties, or size. These provisions do not apply when material other than concrete or structural grout is used, nor are they applicable to structural bolts.

This Specification is intended to be used in combination with a structural design specification appropriate for the type of structure, such as sign, signal, and light supports (ref. 5), bridges (ref. 6), or buildings (ref. 7), which will be referred to as the invoking specification. The focus of the Specification has been on compatibility with American Association of State Highway and Transportation Officials (AASHTO) (refs. 5 and 6), American Institute of Steel Construction (AISC) (ref. 7), and American Concrete Institute (ACI) Specifications (refs. 8 and 9). It is expected that these Specifications could also be easily adapted to use with American Railway Engineers and Maintenance of Way Association (AREMA), American Petroleum Institute (API), or other structural design specifications.

Reference is made to American Society for Testing and Materials (ASTM) standards for material specifications. AASHTO specifications presently reference different material specifications, but these are essentially the same as the ASTM standards. AASHTO is expected to change to use ASTM standards in the future, therefore the particular equivalent AASHTO material specifications are not referenced.

Only those few aspects of the connected material (e.g. the steel baseplate and the concrete) that affect the performance of the fasteners are covered in this Specification. Many important aspects of design and construction of steel-to-concrete joints are not covered here but must not be overlooked. These aspects that are not covered in this Specification should be covered in the invoking specification. For more general information on design or issues relating to the connected material not covered herein, refer to standard steel and concrete design texts. For example, AISC has published a guide for the design of column baseplates (ref. 10).

For the design concrete strength of the assembly, this Specification refers to the design rules in the current American Concrete Institute (ref. 8). These provisions were new in the 2002 specification, and are based on recent research at the University of Stuttgart (refs. 11, 12, 13 and 14) and at the University of Texas at Austin (refs. 15 and 16). These new rules are a substantial improvement over previous ACI rules for pullout strength of concrete. Other codes and texts may still be using the outdated design rules and these are not recommended.

The ϕ factors specified in the Appendix of ACI-318 shall be used because these ϕ factors correspond with the load factors and load combinations given in this Specification in Section 1.2, which are consistent with ASCE-7. These are different than the load factors in the main body of ACI-318.

C-1.2. Loads, Load Factors, and Load Combinations

This Specification is written in the load and resistance factor design (LRFD) format, which provides a method of proportioning structural components such that no applicable limit state is exceeded when the structure is subject to all appropriate load combinations. When a structure or structural component ceases to fulfill the intended purpose in some way, it is said to have exceeded a limit state. Strength limit states concern maximum load-carrying capability, and are related to safety. Serviceability limit states are usually related to performance under normal service conditions, and usually are not related to strength or safety. Fatigue is considered a serviceability limit state and is checked with unfactored loads, even though in non-redundant structures fatigue can result in structural collapse. The term “resistance” includes both strength limit states and serviceability limit states.

The design strength is the nominal strength R_n multiplied by a resistance factor ϕ. The factored load is the sum of the nominal loads multiplied by load factors, with due recognition of load combinations that account for the probability of simultaneous occurrence of maximum load effects. The design strength ϕR_n of each structural component or assemblage must equal or exceed the effect of the factored loads. The design strength may be found from plastic analysis or other appropriate analysis methods that reflect the structural behavior just before the ultimate strength is reached.

C-1.3. Referenced Standards and Specifications

Familiarity with the referenced ACI, AISC, ASCE, ANSI/ASME, ASTM, and AWS specification requirements is necessary for the proper application of this Specification. The discussion of referenced specifications in this Commentary is limited to only a few frequently overlooked or misunderstood items.

C-1.4. Drawing Information

A summary of the information that the Engineer of Record is required to provide in the contract documents is provided in this section of the Specification. The parenthetical reference after each listed item indicates the location of the actual requirement in this Specification.

Supplementary requirements include weldability and galvanizing (see Section 2.3.2).

The Engineer of Record should consider whether anchor rods are specified in a case where they may not even be required. Often, in buildings, anchor rods are only required during erection, and could be removed after erection. In this case, the anchor rods may only need to be designed for the erection loads, even if they are left in place. Under service load, the column baseplate can get enough strength from friction since there is typically a high compressive axial force in the columns.

The Engineer of Record shall also approve some repair modifications as required in Section 6.

C-2. JOINT COMPONENTS

C-2.1. Manufacturer Certification of Components

Certification by the Manufacturer or Supplier of anchor rods, nuts, washers and other components of the fastener assembly is required to ensure that the components to be used are identifiable and meet the requirements of the applicable ASTM Specifications.

C-2.2. Shipping and Storage of Components

Fastener components shall be protected from dirt and corrosion. However, if fastener components become dry, dirty or rusty, they can be cleaned and relubricated by the fabricator or erector. Also, to avoid an unworkable assembly due to zinc coatings, galvanized anchor rods shall be shipped with nuts on. This shall be specified in the purchase order because it is not required in the ASTM specifications.

C-2.3. Anchor Rods

C-2.3.1. Specifications

There are three basic shapes of anchor rods:

a) Smooth Bent Rods
b) Smooth Headed Rods
c) Deformed Bars

These three basic shapes depend on the anchorage mechanism to concrete.

Smooth Bent Rods anchor by the hook's mechanical anchorage. Adherence between the smooth rod and the concrete is not reliable and therefore is not taken into account in the anchorage mechanism.

ASTM F1554 covers Smooth Bent Rods. ASTM F1554 currently provides for three grades (according to minimum yield strength) of smooth (both Bent and Headed) anchor rods. Grade 36 and grade 55 rods are supplied in diameters from ¼ in. to 4 in. inclusive. Grade 105 rods are supplied from ¼ in. to 3 in. inclusive. Grade 105 Smooth Bent Rods have been shown to straighten under axial tensile stress before reaching a more predictable mode of failure (ref. 17), so Smooth Bent Rods shall be limited up to Grade 55 inclusive. The basic dimensions are defined in Figure C-2.1.

Smooth Headed Rods are smooth straight rods with a head at the embedded end. The anchorage to the concrete is obtained through bearing at the head. The head can be forged (i.e. bolt), tapped (i.e. nut) or welded.

ASTM F1554 also covers Smooth Headed Rods.

The basic dimensions of ASTM F1554 headed rods, as defined in Figure C-2.2, are shown in Table C-2.1. Most common heads for ASTM F1554 headed rods are Hex or Heavy Hex nuts, as defined in Section 2.4. If the bearing area of the head is smaller than required by concrete's strength, anchor plates shall be added.

ASTM F1554 (both bent and headed) anchor rods are required by ASTM Specifications to be distinctively marked at the projected end. In addition to the mandatory markings,

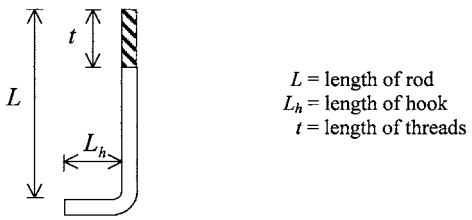

Figure C-2.1. Bent anchor rod (ASTM F1554 rod).

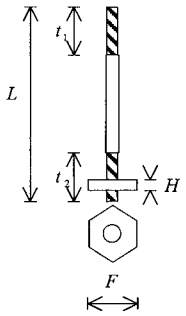

L = length of rod or stud
H = height of nut or head
F = width across flats or head diameter
t_1 = length of threads (exposed end)
t_2 = length of threads (embedded end)

Figure C-2.2. Headed anchor rods.

there are supplementary markings (they only apply if specified in the purchase order). Mandatory and supplementary markings are summarized in Table C-2.2.

ASTM Specifications permit the galvanizing of ASTM F1554 (both bent and headed) anchor rods. Most testing has shown that galvanizing does not affect the fatigue resistance of anchor rods (ref. 24), although some test data have shown a slight decrease in the fatigue resistance from galvanizing.

Galvanized smooth anchor rods and nuts must be considered as a manufactured matched assembly. Insofar as the hot-dip galvanized bolt and nut assembly is concerned, three principal factors must be considered so that the provisions of this Specification are understood and properly applied. These are:

(1) The effect of overtapping for hot-dip galvanized coatings on the nut stripping strength;
(2) The effect of galvanizing and lubrication on the torque required for pretensioning; and
(3) Shipping requirements.

Birkemoe and Herrschaft (ref. 18) showed that, in the as-galvanized condition, galvanizing increases the friction between the bolt and nut threads as well as the variability of the torque-induced pretension. A lower required torque and more consistent results are obtained if the nuts are lubricated. Thus, it is required that all nuts be lubricated prior to tightening.

Both the hot-dip galvanizing process (ASTM A153, ref. 19) and the mechanical galvanizing process (ASTM B695, ref. 20) are recognized in ASTM F1554. The effects of the two processes upon the performance characteristics and requirements for proper installation are distinctly different. Therefore, distinction between the two must be noted in the comments that follow. In accordance with ASTM F1554, all threaded components of the fastener assembly must be galvanized by the same process and the supplier's option is limited to one process per item with no mixed processes in a lot.

TABLE C-2.1 Nut head dimensions

Nominal Anchor Rod Diameter	Hex Nut Dimensions		Heavy Hex Nut Dimensions	
D, in.	Width across flats *F*, in.	Height *H*, in.	Width across flats *F*, in.	Height *H*, in.
1/4	7/16	7/32	1/2	15/64
3/8	9/16	21/64	11/16	23/64
1/2	3/4	7/16	7/8	31/64
5/8	15/16	35/64	1 1/16	39/64
3/4	1 1/8	41/64	1 1/4	47/64
7/8	1 5/16	3/4	1 7/16	55/64
1	1 1/2	55/64	1 5/8	63/64
1 1/8	1 11/16	31/32	1 13/16	1 7/64
1 1/4	1 7/8	1 1/16	2	1 7/32
1 1/2	2 1/4	1 9/32	2 3/8	1 15/32
1 3/4	-	-	2 3/4	1 23/32
2	-	-	3 1/8	1 31/32
2 1/4	-	-	3 1/2	2 13/64
2 1/2	-	-	3 7/8	2 29/64
2 3/4	-	-	4 1/4	2 45/64
3	-	-	4 5/8	2 61/64
3 1/4	-	-	5	3 3/16
3 1/2	-	-	5 3/8	3 7/16
3 3/4	-	-	5 3/4	3 11/16
4	-	-	6 1/8	3 15/16

TABLE C-2.2 ASTM F1554 anchor rod markings (at the exposed end)

Mandatory Markings	Supplementary Markings
• Grade Identification (paint mark): Grade — Color 36 — Blue 55 — Yellow 105 — Red	• Manufacture's Identification (steel die stamped) • Permanent Grade Identification (steel die stamped) • White paint mark for Grade 55 weldable rods (at the embedded end)

Mixing anchor rods that are galvanized by one process with nuts that are galvanized by the other may result in an unworkable assembly. The purchase of galvanized anchor rods and galvanized nuts from separate suppliers is not in accordance with the intent of the ASTM Specification.

Deformed Bars are common steel reinforcing bars. They rely on the deformations along the bar for the anchorage to the concrete.

ASTM A615 and A706 bars are the most widely available deformed bars allowed in ACI 318. ASTM A615 deformed bars shall not be used if there is seismic loading or if the anchor rods must be designed for the fatigue limit state, since these deformed bars may have low notch toughness. ASTM A615 provides for three grades (according to minimum yield strength) of deformed bars: grades 40, 60, and 75, although only grade 60 is widely available and explicitly covered by this specification. ASTM A706 provides for only grade 60. A706 deformed bars are more ductile than A615, but still they are not as ductile as F1554 smooth anchor rods. Both bars are supplied from $\frac{3}{8}$ in. to $2\frac{1}{4}$ in. inclusive.

Deformed bars shall be threaded and attached to the baseplate by nuts.

ASTM A767 covers galvanized deformed bars and permits hot-dip coating. Nuts shall be specified with the same zinc coating process.

C-2.3.2. Thread Dimensions and Tolerances

Whenever the anchor rod has threads, threads shall conform to ANSI/ASME B1.1 (ref. 22) and have class 1A or 2A tolerances. Class of threads is how tight internal and external threads will match. Class 1A threads will match looser than class 2A threads. The class does not affect strength of the anchor rod. Close to 90% of all commercial and industrial fasteners produced in North America are class 2A (ref. 23), so they may be less expensive and easier to find in the market. Class 1A threads are recommended when an easy and quick assembly—and disassembly—is needed. When the bolt class is not specified in the purchase order, class 2A shall be supplied.

Threads may be cut or rolled. There is no significant difference in the fatigue resistance (ref. 24).

Full thread engagement is defined as having the end of the rod at least flush with the face of the nut. Slightly greater strength can be obtained if two full threads protrude above the nut; therefore this is preferable but not required.

Manufacture and erection tolerances need to be taken into consideration when ordering anchor rods. Manufacture tolerances for ASTM F1554 anchor rods are ± 0.5 in. for lengths 24 in. or less and ± 1 in. for larger rods. Erection tolerances are specified in the invoking specification or in the AISC Code of Standard Practice for Steel Buildings and Bridges. A good way to account for the possibility of less length because of variation within these tolerances is to add 0.5 or 1.0 in., respectively, to the required length.

C-2.4. Nuts

Hex and heavy-hex nuts are required by ASTM Specifications (ref. 25) to be distinctively marked. Certain markings are mandatory. In addition to the mandatory markings, the manufacturer may apply additional distinguishing markings.

Hot-dip galvanizing affects the stripping strength of the bolt-nut assembly because, to accommodate the relatively thick zinc coatings of non-uniform thickness on bolt threads, it is usual practice to hot-dip galvanize the blank nut and then to tap the nut over-size. This results in a reduction of thread engagement with a consequent reduction of the stripping strength. Only the stronger hardened nuts have adequate strength to meet ASTM thread strength requirements after over-tapping. This requirement should not be overlooked if non-galvanized nuts are purchased and then sent to a local

galvanizer for hot-dip galvanizing. Because the mechanical galvanizing process results in a more uniformly distributed and smooth zinc coating, nuts may be tapped over-size before galvanizing by an amount that is less than that required for the hot-dip process before galvanizing.

ASTM A194 nuts (ref. 26) are not listed because of general lack of availability, but A194 Grade 2 nuts are acceptable equivalents for Grade C nuts.

ASTM A563 nuts are manufactured to dimensions as specified in ANSI/ASME B18.2.2 (ref. 27). The basic dimensions, as defined in Figure C-2.2, are shown in Table C-2.1.

C-2.5. Baseplates, Anchor Rod Holes, and Anchor Rod Assemblies

C-2.5.1. Baseplates

Structural grade steel is defined as the structural steel allowed in the current American Institute of Steel Construction LRFD Specification or American Association of State Highway and Transportation Officials (AASHTO) LRFD Bridge Specifications. Uncoated steel shall not remain in contact with moisture or vegetation because in such situations it continues corroding to unacceptable levels. The requirement that the thickness of the baseplate be equal to or greater than the nominal diameter of the anchor rod is intended to ensure even force distribution among anchor rods and to minimize prying (ref. 24). Although this is considered good practice, it may not be necessary for joints that will not experience fatigue or seismic loads.

C-2.5.2. Anchor Rod Holes

To obtain adequate transferring of shear forces from the baseplate to the concrete through anchor rods and to allow plastic redistribution of shear forces, anchor rod holes need to be not greater than the size for shear holes. Research (ref. 28) found that the maximum hole sizes in Table 2.2 are acceptable. If there are very large shear forces or if the shear is likely to be reversed, consideration should be given to using smaller holes or alternative details such as shear keys. One option is to use plate washers with holes that are only $\frac{1}{8}$-inch oversize and then field weld the plate washers to the baseplate after installation.

In many cases in buildings, the shear is effectively transferred directly to the concrete by friction. If anchor rods need not transfer shear forces, normal holes are recommended to facilitate installation of the baseplate (ref. 7).

C-2.5.3. Anchor Rod Group Assemblies

OSHA (ref. 33) gives the requirement for a minimum of four anchor rods. Provision shall be made to maintain the spacing and alignment of anchor rods within tolerances during placing and curing of the concrete. Experience has shown that the best way to do this is to use steel or wood annular rings at least $\frac{1}{4}$ inch thick with nuts on both sides that hold together the anchor rod group. The rings or plates are located at two positions along the length of the anchor rods to maintain the spacing and alignment of the anchor rods. It is important to maintain the alignment to 1:40 to limit local prying or bending forces from uneven contact between the nut and the baseplate. One of the plates or rings may be above the top of concrete so that it may be reused as a template.

The rings are typically about one or two inches wider than the anchor rod diameter. Plates may be used also, but large openings should be provided to allow the concrete to flow around and through the plate. If the ring or plate is also designed in accordance with the ACI-318 specifications, the ring or plate can act as an anchorage and the entire anchor rod group will work together. However, the beneficial effect of the ring on pullout can be ignored and the design does not have to be performed. In that case, the ring is nonstructural; it is only there for alignment.

C-3. JOINT TYPE

Because the best suited joint varies from application to application, the selection is best left to judgment and a decision on the part of the Engineer of Record.

Each joint type is characterized by the means that loads are transmitted to the foundation, the fatigue behavior, the installation, and the best suited anchor rods for that particular joint. In this Specification, the provisions for the design, installation and inspection of anchor rod joints are dependent upon the type of joint that is specified by the Engineer of Record. Consequently, it is required that the Engineer of Record identify the joint type in the contract documents.

C-3.1. Threaded-Shear-and-Uplift Joints

In threaded-shear-and-uplift joints, the baseplate is attached to anchor rods through single nuts (Figure C-3.1). This is the most common type of joint used for buildings.

For static loading, the threaded-shear-and-uplift joints can be pretensioned against the concrete, although there is no advantage to doing so since strength is not affected by pretension. Under dynamic loading, the pretension may be quickly lost due to wear of the concrete under the baseplate from movement, so no benefit can be accrued for fatigue either.

In threaded-shear-and-uplift joints, compression is transmitted directly by bearing of the baseplate on the concrete. Anchor rods transmit all the tension and might transmit shear, which can also be transmitted through friction depending on the level of axial load.

All types of anchor rods are adequate for this joint.

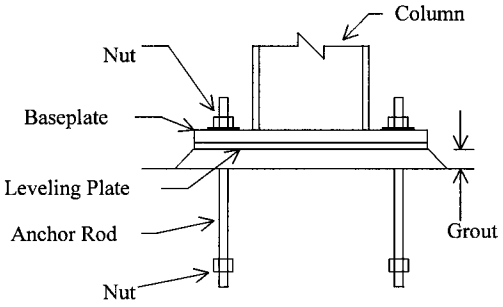

Figure C-3.1. Threaded-shear-and-uplift joint.

C-3.2. Double-Nut-Moment Joints

In this joint, the baseplate stands off from the concrete foundation and bears on leveling nuts. Thus, the baseplate is attached to anchor rods through double nuts (Figure C-3.2). Double-nut-moment joints are very reliable for transmitting moment to the foundation; therefore, they are satisfactory for non-redundant structures and fatigue or seismically loaded structures. Double-nut-moment joints are commonly used in sign, signal, and light support structures and other types of towers and poles. In double-nut-moment joints, anchor rods are subject to compression, tension, shear and moment. Anchor rods must be designed to resist shear in combination with axial loads. Smooth Headed Rods and Deformed Bars are best suited for double-nut-moment joints.

Double-nut joints are pretensioned between the nuts only, and the pretension has no effect on strength. Research has shown that the pretension gives slightly better fatigue resistance (ref. 24). More importantly, the pretension ensures that there is a good load distribution among the various anchor rods (ref. 24). Therefore, there are special tightening procedures for these joints.

The use of grout under the baseplate in double-nut-moment joints is not recommended because:

a) It may crack, retain moisture, and then promote corrosion.
b) It makes it impossible to inspect and retighten bottom nuts if necessary.
c) In order to place the grout after the baseplate is in place, the standoff distance between the top of concrete and the bottom of the leveling nut may exceed the recommended distance equal to the anchor rod diameter. Research has shown that the local bending of individual anchor rods from shear forces and torsion becomes very significant as this standoff distance increases much more than this one diameter limit (ref. 24).

C-3.3. Vibrating-Machinery Joints

Vibrating-machinery joints are sleeved (Figure C-3.3) so that a longer length may be pretensioned against the concrete. An alternative detail that is often used is a thick-walled tube above the baseplate within which the anchor rod is pretensioned. These vibrating-machinery joints are recommended for vibratory loads even though it's not so easy to level and plumb the attached structure. Only Smooth Headed Rods are recommended for vibrating-machinery joints.

In vibrating-machinery joints, the pretension force in the anchor rods reacts against the concrete or grout. Shear is transmitted by friction, and the normal force providing the friction is the pretension in the anchor rods, so it is independent of the applied axial load. Axial load and flexure are transmitted primarily through the concrete or grout. Applied uplift is reacted by partially unloading the concrete or grout, although some fraction of the applied uplift will be transmitted directly by the anchor rods in tension. However, it is very difficult to predict the fraction of the load transmitted to the anchor rods and the fraction transmitted through the concrete in these joints, so it is conservatively assumed that the entire uplift load is transmitted through the anchor rods. This is reasonable for strength design since at the limit state the pretension is likely to have been exceeded and the baseplate will be separated from the concrete or grout. However, at service loads relevant to fatigue, the load range applied to the anchor rods is undoubtedly much less than would be indicated by this assumption, and so vibrating-machinery joints are recommended for very-high-cycle applications like vibrating machinery.

The length of the rod to be pretensioned must be designed by the Engineer of Record. The method of pretensioning

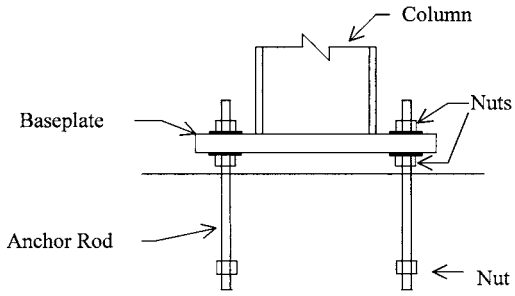

Figure C-3.2. Double-nut-moment joint.

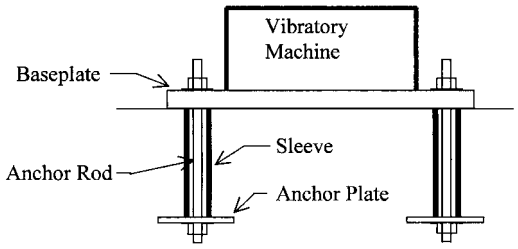

Figure C-3.3. Vibratory-machine joint.

often uses a special hydraulic cylinder and therefore the Engineer of Record must also specify this method. The pretension force must be greater than the unfactored uplift to prevent separation of the baseplate from the concrete or grout at service loads. As is the case with all these joints, there is no effect of the pretension on the strength.

When using epoxy grouts, the anchor rods must be isolated from the epoxy to prevent bonding to the rod.

C-4. LIMIT STATES IN ANCHOR ROD JOINTS

This section of the Specification provides the design requirements for anchor rods in anchor rod joints. However, this information is not intended to provide comprehensive coverage of the design of anchor rod connections. Other design considerations of importance to the satisfactory performance of the connected material, such as shear keys, block shear rupture, shear lag, prying action and baseplate stiffness and its effect on the performance of the structure, are beyond the scope of this Specification and Commentary and shall be designed in accordance with the invoking specification.

The general behavior and distribution of forces of a joint with anchor rods will be elastic until the concrete strength of the anchor group is reached. If this concrete strength is larger than the sum of the steel strength of contributing anchor rods, anchor rods will behave and the forces will redistribute plastically.

Ductility of the connection is highly desirable; consequently, it is desirable that the concrete tensile or shear strength of the anchor group should be greater than the sum of the steel tensile or shear strengths of the individual anchor rods respectively. However, it is recognized that it is not always possible to design a foundation that does not permit concrete failure.

In joint types other than double-nut-moment joints, the compression force over the concrete may develop shear friction. As stated in the Specification, the contribution of the shear friction for threaded-shear-and-uplift joints shall be based on the most unfavorable arrangement of loads that is also consistent with the lateral force that is being evaluated. The shear friction strength shall be calculated in accordance with current ACI criteria.

An important application of anchor rods is during erection of steel structures. Steel-to-concrete joints shall be checked for strength during erection and shall include a minimum lateral load equal to 5.0 percent of the gravity load. Furthermore, anchor rods may only be necessary during erection and not during the service life of the structure. Therefore, anchor rods might be designed only for erection loads.

The design tensile, compressive, and shear strengths of contributing anchor rods are provided in the following subsections. The interaction of combined shear and tension, the design bearing strength, and the fatigue strength of anchor rods are also provided in the following subsections.

Prying effects of the baseplate should be taken into consideration in the design strength of anchor rod joints. However, research (ref. 24) has shown that if the baseplate is equal to the anchor rod diameter, these prying effects may be neglected.

Threaded-shear-and-uplift and vibrating-machinery joints may resist the shear force through shear friction, and consequently anchor rods in those joints need not be designed to contribute to the shear strength. If the shear friction strength is smaller than the shear force in the joint, anchor rods shall be designed to transmit all the shear force (i.e. it is not permitted to combine the strength from the friction and from the anchor rods). This is because these two peak load resistances may occur at different slip or deformation levels and therefore may not be simultaneously active.

In double-nut-moment joints, the portion of an anchor rod between the concrete surface and the bottom of the leveling nut may be subject to local bending of the anchor rod itself. Therefore, it is highly desirable to maintain the clear distance between the concrete surface and the bottom of the leveling nut equal to or less than one anchor rod diameter, since research (ref. 24) has shown that for this clear distance the bending effects in the strength of an anchor rod may be neglected. If the clear distance is greater than one anchor rod diameter, the bending effects in the strength of an anchor rod shall be considered.

Pretension of the anchor rod in threaded-shear-and-uplift and vibrating-machinery joints will allow part of the uplift axial load to be transferred through partial unloading of the concrete or grout within the range of service loads. However, at ultimate uplift load, the baseplate may separate from the concrete or grout and therefore the anchor rods must be designed for the entire factored uplift load. At this point, the stress from the pretension has vanished since the concrete is no longer reacting against this pretension. Therefore, the effect of pretension is ignored in all design calculations that are related to strength limit-states and it is also neglected in the fatigue design, even though it is clearly beneficial in reducing the actual load range in the anchor rods at service load levels.

C-4.1. Design Tensile Strength

In steel-to-concrete joints loaded in tension due to axial tension or flexure, the load will be transferred from the baseplate to the anchor rods and then to the concrete. Consequently, the maximum tensile strength of the joint will be equal to the weakest of the concrete tensile strength of the anchor group (or just those anchor rods participating in tension in the case of tension due to moment) or the sum of the steel tensile strengths of the contributing anchor rods. For a ductile joint, the steel strength shall be smaller than the concrete strength.

There are two potential limit states in tension: yielding in the unthreaded section (if there is an unthreaded length) and fracture in the threaded section. With normal geometries and materials, the gross-section yielding limit-state will never govern and thus can be skipped in the design calculations.

The design strength equals the nominal strength multiplied by a resistance factor ϕ.

The nominal fracture tensile strength of a threaded anchor rod is the product of its ultimate tensile strength (per unit of area) and the tensile stress area.

The tensile stress area shown in Table 4.2 is calculated from the following equation:

$$A_{ts} = 0.7854\left[D - \frac{0.9743}{n}\right]^2$$

where

A_{ts} = tensile stress area, in.^{2}
D = nominal size, in.
n = threads per inch.

The concrete tensile strength of the anchor group shall be calculated accordingly with ACI-318 criteria. At least the following concrete strengths of fasteners in tension should be checked: concrete breakout strength, pullout strength, and concrete side-face blowout strength.

C-4.2. Design Compressive Strength

The compression force in threaded-shear-and-uplift and vibrating-machinery joints, due to axial compression or flexure, is assumed to be transferred directly by bearing of the baseplate over the concrete. Therefore, the bearing strength shall be calculated.

The compression force in double-nut-moment joints due to axial compression or flexure will be transmitted first to the anchor rods and then to the concrete. Consequently, the maximum compressive strength of the joint will be equal to the weakest of the concrete compressive strengths of the contributing anchor rods or the sum of the steel compressive strengths of the contributing anchors.

The nominal steel compression strength for anchor rods in double-nut-moment joints with clear distance equal to or less than four anchor rod diameters is the product of its yield stress (per unit of area) and the gross area. It is realized that yielding could initiate earlier on the reduced area of the threads, but it is presumed that the consequences of this yielding would be relatively minor.

Anchor rods with clear distance greater than four anchor rod diameters shall consider the flexural buckling effects of compression members.

Headed anchor rods will then transfer the compressive force to the concrete by bearing of the head, and deformed bars will transfer it through the deformations. Consequently, the correspondent compressive strength of the anchor rod due to concrete failure shall be calculated.

C-4.3. Design Shear Strength

When a threaded-shear-and-uplift joint or vibrating-machinery joint is loaded in shear, the load is first resisted by friction between the baseplate and the concrete. If this friction strength is less than the load, the baseplate will slip until an anchor rod bears against its hole in the baseplate. Then the anchor rod starts transferring the shear load through bearing. At this point, the friction load is diminishing and therefore cannot be counted together with the steel strength. If the concrete strength of this anchor rod is larger than its steel strength, the rod will undergo plasticity and there will be a plastic redistribution of forces between the rest of the anchor rods. There may be different failure modes for the concrete, and all possible failure modes must be checked. The first anchor rod bearing against its baseplate hole may be the closest one to an edge, as shown in Figures C-4.1-a and C-4.1-b. Consequently, both steel and concrete failure modes for this anchor rod must be checked. If the steel strength of this anchor rod is smaller than its concrete strength, there will be plastic redistribution of forces and the shear strength of the joint will be the sum of the steel shear strengths of individual anchor rods. If the steel strength of the anchor rod is greater than its concrete strength, the concrete will fail (see Figure C-4.1-c) and this anchor rod will not contribute to the strength of the joint. Consequently, steel and concrete strengths

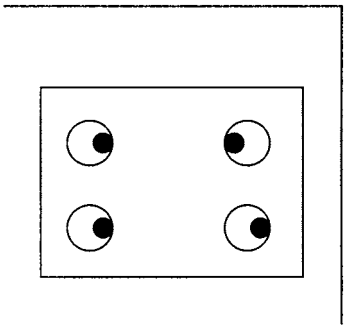

Figure C-4.1-a. Plan view of a baseplate close to concrete foundation edges and possible arrangement of anchor rods.

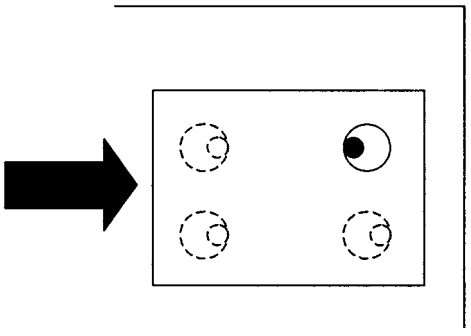

Figure C-4.1-b. Baseplate loaded in shear and possible first anchor rod bearing on its baseplate shear hole.

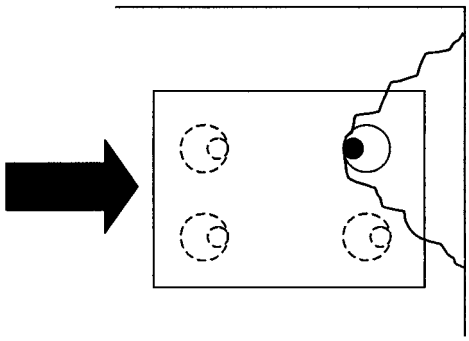

Figure C-4.1-c. Possible failure mode if the steel strength of the anchor rod is greater than the concrete strength.

and failure modes of the remaining contributing anchor rods must be checked (Figure C-4.1-d).

A double-nut-moment joint loaded in shear will behave in the same manner as a threaded-shear-and-uplift joint without the contribution of the friction strength.

In vibrating-machinery joints, shear forces will be transferred only by friction since sleeves surround anchor rods and good pretension can be obtained. Theoretically, the ultimate strength with a bearing condition should also be checked, but it is presumed that the slip load will always be less than the bearing load.

The design strength of an individual anchor rod equals the nominal strength multiplied by a resistance factor ϕ.

The nominal shear strength for anchor rods fastened with nuts to a baseplate with shear holes is based upon the observation that the shear strength of a single anchor rod is greater than 0.6 times its fracture strength (ref. 29).

The concrete shear strength of the anchor group shall be calculated according to ACI criteria. At a minimum, concrete breakout strength and concrete pryout strength must be checked.

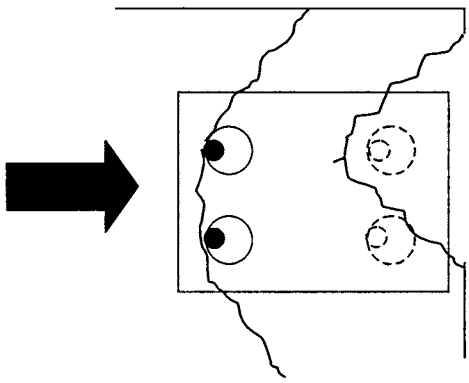

Figure C-4.1-d. Possible failure mode after possible first anchor rod bearing on its baseplate shear hole has failed.

C-4.4. Combined Shear and Tension

When both shear forces and tensile forces act on an anchor rod, the interaction can be conveniently expressed as an ellipse (ref. 32) that includes the elements of the anchors acting in shear alone and the anchors acting in tension alone. Equation 4.4 specifies that ϕR_t is the design tensile strength of anchors determined in accordance with Section 4.1, therefore ϕR_t is the smallest of the sum of the design steel tensile strengths of the contributing individual anchor rods, calculated with Equation 4.1, or the design concrete tensile strength of the anchor group, calculated accordingly with ACI criteria and the correspondent ϕ factors. In the same manner, ϕR_v is the smallest of the sum of the design steel shear strengths of the contributing individual anchor rods, determined with Equation 4.3, or the concrete design shear strength of the anchor group, determined accordingly with ACI criteria and the correspondent ϕ factors. R_v does not include the contribution of the friction strength since the friction is not transmitted by the anchor rods.

C-4.5. Design Bearing Strength at Anchor Rod Shear Holes

These provisions were adapted from those applied to high-strength bolts. It is assumed that the minimum edge distance will always be possible, so the equations are simplified.

C-4.6. Tensile Fatigue

Anchor rod joints subject to less than 20,000 repeated applications of axial tension and/or flexure need not be designed for fatigue. When the tensile fatigue stress range is less than the threshold fatigue stress range, 7 ksi, anchor rods need not be further checked for fatigue.

There is an unfortunate trend toward using fewer very large anchor rods. It is always better to use a greater number of smaller anchor rods than fewer bigger anchor rods. Although only four anchor rods are required, there should ideally be at least six and preferably eight anchor rods in any joint in a non-redundant structure subject to fatigue or seismic loading. When there are eight anchor rods in a joint and the first one fails from fatigue, the stress range on the neighboring rods increases only about 25 percent. These rods would then be expected to last an additional 35 to 50 percent of the time it took to fail the first rod, assuming the loading was more or less constant. This gives the joint some measure of redundancy, even if the structure is non-redundant Anchor rod joints with only four rods will fail completely only a short time after the first rod failure.

In steel-to-concrete joints subject to fatigue, the anchor rod will fail before the concrete fatigue strength is reached. Therefore, it is not necessary to consider the fatigue strength of the concrete.

Corrosion protection is particularly important for fatigue critical anchor rods, since corrosion pitting can degrade the fatigue resistance. Although there have been some tests that show a slight decrease in the fatigue strength of galvanized anchor rods, it is generally accepted that galvanizing does not decrease the fatigue strength significantly.

Stresses in anchor rods shall be based on elastic distribution of unfactored loads. The tensile stress area shall be used in the computation of stresses in threaded anchors. The stress range shall be calculated including the external load range due to repeated live loads and any prying action due to those loads.

The S-N curve for galvanized non-pretensioned anchor rods corresponds to detail Category E′. As previously mentioned, however, the fatigue threshold is much greater than for other Category E′ details—in the case of anchor rods the threshold, 7 ksi, is the threshold associated with Category D (ref. 24). If the anchor rod in double-nut-moment and vibrating-machinery joints is properly pretensioned, the S-N curve for finite life increases to Category E, however the fatigue threshold is not significantly increased. When tests were conducted with an eccentricity of 1:40, the appropriate category for both pretensioned and non-pretensioned anchor rods was Category E′. Therefore, for design, it is recommended that Category E′ (with a fatigue threshold of 7 ksi) is used regardless of the pretension. This design would then be tolerant of limited misalignment up to 1:40.

Since the fatigue resistance of various grades of anchor rod is the same, when the dimensions of the anchor rod are determined by fatigue rather than strength, it is not advantageous to use grades higher than Grade 55. The fracture toughness of the higher grades is also somewhat less, usually.

While fracture toughness is always a desirable material property, it is expensive to require supplemental Charpy specifications for anchor rods since they are not normally ordered this way.

Anchor rods typically have sufficient fracture toughness even without the supplemental specifications, with the exception of some A615 deformed bars. A615 deformed bars should not be used if the anchor rods are designed for fatigue or seismic loading, since these deformed bars may have low and inadequate fracture toughness. Michigan Department of Transportation has had some fatigue problems with its anchor rods for sign support structures and therefore has found it advantageous to specify the notch toughness of anchor rods—it requires 15 ft-lbs. at 40 F (ref. 34). Michigan also regularly inspects the anchor rods using ultrasonic testing (ref. 34).

Generally, additional fracture toughness does not make much difference in the time to failure for anchor rods that will fail by fatigue. This is because cracks grow at an exponential rate, and 95 percent of the life is consumed while the crack size is less than a few millimeters. Even though the fracture toughness may correspond with a greater crack length at the time of failure, it does not correspond with a significantly longer time to failure. This is also the reason why it is usually not cost-effective to perform ultrasonic testing or other non-destructive testing on anchor rods to look for existing fatigue cracks. There is only a small window in time when the cracks are both large enough to detect and small enough to not yet cause fracture. Generally, it would be more effective to spend the additional cost of the supplemental Charpy specifications on additional redundant anchor rods.

C-5. INSTALLATION AND CONSTRUCTION INSPECTION

Proper installation is the responsibility of the Contractor. However, the Engineer of Record or their representative may witness the inspection and testing.

It is recognized that in any anchor rod installation there will be some amount of misalignment. In this Specification it is assumed that the tolerances will be stated in the invoking specification and that these tolerances will correspond with the tolerances specified in the AISC Code of Standard Practice for Steel Buildings and Bridges (ref. 30). For anchor rods subjected to fatigue loading, it is also recommended that a tolerance be specified for vertical misalignment of anchor rods less than 1:40. Provisions shall be made to minimize the misalignments and meet the required tolerances. The best way to maintain alignment is the use of the template. Templates comprised of rings with nuts on both sides at two locations along the length of the anchor rods are recommended as shown in Figure C-5.1.

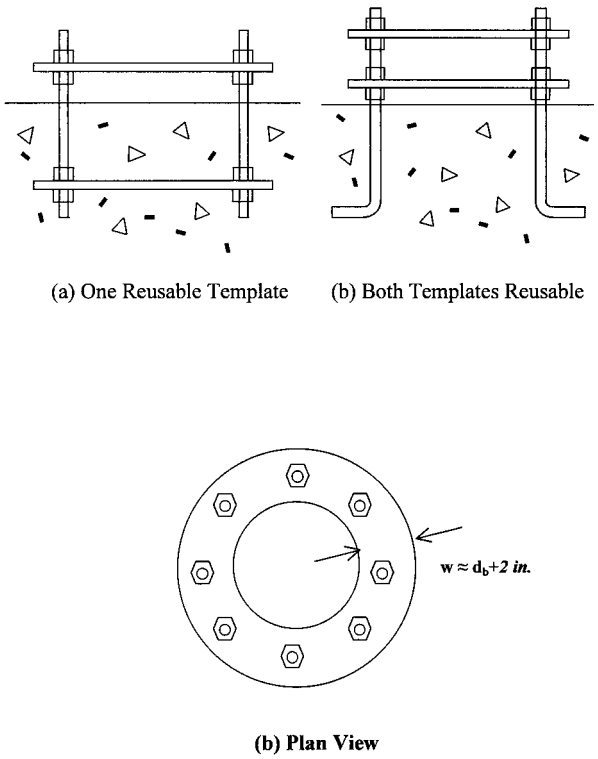

Figure C-5.1. Recommended installation template for anchor rods.

One of the plates or rings is usually above the top of concrete and is reused as a template. Usually the concrete strength is specified at 28 days after cast. Consequently it is expected that after 28 days the concrete has reached its design strength. However, it is also recognized that that the concrete may have sufficient strength at only 7 days after cast. In such a case, and if approved by the Engineer of Record, the baseplate may be placed. It is expected that the baseplate may have one element attached at this stage of installation. Besides this one attached element, it is not recommended that the baseplate be partially assembled with the structure during erection of the baseplate.

Joints other than the threaded-shear-and-uplift joints require controlled pretensioning. Failure to follow the nut-tightening procedure can lead to inadequately tensioned anchor rods and associated uneven distribution of loads among the contributing anchor rods. Inadequately tightened bolts can also lead to fatigue failures and further loosening of the nuts under cyclic loading. A less likely outcome of failure to follow the tightening procedure is overtightented rods and associated plastic deformation and stripping of the threads, which may require removal and replacement.

The starting point for tightening procedures is between 20 to 30 percent of the final tension. This is somewhat analogous to the "snug" condition for high-strength structural bolts (ref. 32). For the anchor rods, the snug condition is defined as a function of torque, which is defined by Equation 5.1. This equation is a well-known relationship of torque and pretension. Research (ref. 31) has shown that a value of 0.12 in this relationship is adequate for common sizes and coatings of anchor rods.

If an anchor rod has a nut-head or the head is fastened with nuts, this shall be prevented from rotation while the anchor rod is tightened. This can be achieved with a jam nut or another type of locking device. The jam nut will affect the ultimate or fatigue strength of the rod.

Very large torque may be required to properly tighten anchor rods greater than 1 inch in diameter. A cheater bar (i.e. a pipe or extension handle more than ten feet long) may be required for the torque wrench. For snugging the leveling nuts, an open-end wrench with a 10-foot long pipe or extension handle may be used. Tightening the top nuts for anchor rods greater than 1 inch in diameter may require either

a) A hydraulic torque wrench or
b) A box end "slug" or "knocker" wrench with a 10-foot long pipe or extension handle.

The box end wrench may be moved by impacts with a 16-pound sledgehammer or by the efforts of three or more workers. It is essential that the workers have good traction and are not slipping in mud.

C-5.1. Threaded-Shear-and-Uplift Joints

Before placing the concrete in threaded-shear-and-uplift joints, anchor rods shall be secured to a template or other device to avoid movement during placing and curing of the concrete that may lead to misalignments larger than what may be tolerated.

Unless the joint is to be designed for fatigue or seismic loading, it is not necessary to tighten the anchor rods in a controlled manner. Rather, it is only necessary to tighten to the full effort of the installer, using an ordinary wrench with a cheater bar. If nuts are required to be pretensioned, it shall be done also in a star pattern, as shown in Figure C-5.2, and in at least two full tightening cycles. Furthermore, nuts shall be prevented from loosening with a jam nut.

C-5.2. Double-Nut-Moment Joints

Prior to installation of anchor rods in a double-nut-moment joint, an Anchor Rod Rotation Capacity Test shall be run with at least one anchor rod from every lot. The test attempts to recreate the conditions to which the anchor rod will be subject during installation.

After the test and before placing the concrete in threaded-shear-and-uplift joints, anchor rods shall be secured to a template or other device to avoid movement during placing and curing of the concrete that may lead to misalignments larger than what may be tolerated.

As specified in Sections 2.6.3 and 5.3, beveled washers shall be used:

1. Under the leveling nut if the slope of the bottom face of the baseplate has a slope greater than 1:20;
2. Under the leveling nut if the leveling nut cannot be brought into firm contact with the baseplate;
3. Under the top nut if the slope of the top face of the baseplate has a slope greater than 1:20; and,
4. Under the top nut if the top nut cannot be brought into firm contact with the baseplate.

If any beveled washer is required, the contractor shall disassemble the joint, replace nuts adding the beveled washer(s)

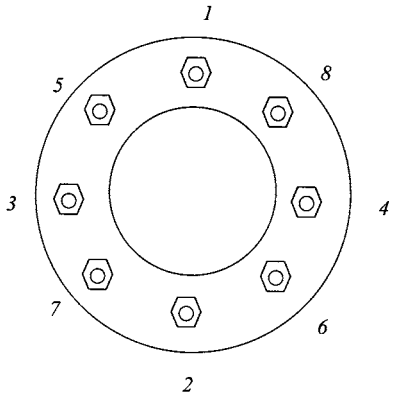

Figure C-5.2. Star pattern tightening sequence.

and retighten (in a star pattern) to the snug condition top and leveling nuts. Beveled washers can typically accommodate any slope up to 1:6.

After all this checking, top nuts shall be pretensioned. The procedure for pretensioning is a turn-of-nut procedure, although it is inspected using torque. Pretensioning the nuts shall be made in two full tightening cycles following a star pattern.

Experience indicates that even properly tightened galvanized anchor rods become loose, especially in the first few days after installation, presumably because of creep in the galvanizing. Therefore, a final installation check shall be done after at least 48 hours using a calibrated wrench and 110 percent of the torque calculated using Equation 5.1. It is expected that properly tightened joints will not move even if 110 percent of the minimum installation torque is applied. If a rod assembly cannot achieve the required torque, it is very likely that the threads have stripped.

The last step is to prevent nuts from loosening, if the joint may be subject to seismic loading or if the joint must be designed for fatigue. This can be attained with a jam nut or other suitable device. Any other method for preventing nut loosening shall be approved by the Engineer of Record. Tack welding the top side of the top nut has been used, although this is not consistent with the AWS Structural Welding Code–Steel. While tack welding to the unstressed top of the anchor rod is relatively harmless, under no circumstance shall any nut be tack welded to the washer or the baseplate.

C-5.3. Vibrating-Machinery Joints

The first steps of the installation procedure for vibrating-machinery joints are very similar to the first steps for double-nut-moment joints except for the inclusion of the sleeve. The sleeve must be cleaned and sealed off to prevent inclusion of debris.

These anchor rods are typically tensioned using a center-hole ram with access to the nut for retightening. The nut is tightened down while the tension is maintained on the anchor rod, and then the anchor rod tension is released. It is recognized that part of the tension will be lost to relaxation after the tension is released. Since there are many variations of vibrating-machinery joints, the Engineer of Record shall provide the specific procedures for tightening these joints.

C-6. REPAIR AND MODIFICATION

Anchor rods may require repair or modification during installation as well as later on during service. Repairs and modifications required during installation are discussed first. OSHA (ref. 33) requires that the Engineer of Record approve all modifications or repairs of anchor rods during construction. There is some successful experience with these repair methods discussed in the Specification, although many of them are still quite controversial. In any case, they may only be used at the discretion of the Engineer of Record. For structures in service, it is also essential that a qualified engineer approve any repairs.

Repairs and modifications required during installation—On a case-by-case basis, the Engineer of Record must evaluate the relative merits of rejecting the foundation because of the problem, forcing the foundation contractor to replace a large part of the top of the foundation, or allowing the foundation contractor or others to repair or modify the anchor rods. In many cases, it is most expedient and reasonably safe to repair or modify the anchor rods.

Records should be kept of the dates and results of these repairs or modifications, and these records shall be available for the Engineer of Record or their representative to review. The Engineer of Record may require that their representative witness the repairs and subsequent inspection. It is essential that any repairs of the anchor rods be documented for use in future inspections. These repaired locations should be especially scrutinized in future inspections, and if ultrasonic testing is ever performed in the future, it is essential to know if there are joints with threaded couplers, since they will appear the same as cracks.

This section covers most common repair methods used for anchor rod joints. Most of these common repairs are standard and simple and do not require design calculations. Less common or more complex repairs and any other repair modification not explicitly covered herein will require design.

The most common problems found in anchor rod joints are

a) A zinc coating too thick in anchor rods or nuts,
b) Vertical misalignment of projecting end of anchor rods out of tolerances,
c) Anchor rods bent or cracked during construction,
d) Projecting end of anchor rods that are too short, and
e) Baseplate holes not aligned with anchor rods.

The first source of problems may be avoided by requesting anchor rods shipped with nuts on in the purchase order. Nuts should be run onto the rod and back prior to installation. This is done in the Anchor Rod Rotation Capacity Test specified for double-nut-moment joints.

Running a die over the rods to remove excessive zinc should not be allowed. If for any reason the zinc coating is too thick, the full assembly should be discarded and a new one should be used; hence the importance of checking by running the nuts on and off before the anchor rod is embedded into the concrete.

While it is desirable to achieve the tolerances specified in the design drawings or in the Code of Standard Practice for Steel Buildings and Bridges (ref. 30), it may not necessarily be a good idea to modify the anchor rods in the event that these tolerances are not achieved. The modification or repair may create an even worse condition than the out-of-tolerance condition. Misalignment may increase the secondary stresses

slightly but does not necessarily need to be corrected unless the joint is subject to fatigue or seismic loading. For joints not subject to fatigue or seismic loading, if the anchor rods can still fit in the holes, the misalignment may be corrected using beveled washers. If the anchor rods cannot fit in the holes, the hole may be enlarged and plate washers used to cover the enlarged hole. The plate washer must be specially designed to span over the larger hole without dishing. Alternatively, the anchor rods may be bent back into alignment. Bending is allowed in the manufacture of the anchor rods (for hooks) according to ASTM F1554 so it is not necessarily harmful to bend them. However, A615 deformed bars should probably not be bent very much because of the potentially low fracture toughness. There is essentially no limit to the bending if the anchor rods are not to be exposed to fatigue or seismic loading. Of course, common sense must apply. However, if fatigue or seismic loads may occur, because of concerns about creating cracks during bending, the bending is limited to anchor rods that are less than 1:20 from vertical.

Heat may also be applied, since this is also allowed in Section 6.4 of ASTM F1554. This section provides for limits on the temperature and inspection for cracks after the bending. Heating shall not be applied more than once because of concerns about embrittlement.

Inadequate projection of threads beyond the top nut can often be solved for double-nut-moment joints by lowering the structure down the anchor rods. If the baseplate cannot be lowered further, the holes in the baseplate may be enlarged and a special "shoulder nut" machined to drop part of the way into the enlarged holes. In other cases, cutting off the anchor rod and using a threaded coupler to join an extension onto the anchor rod may also be considered. Typically, if more than two anchor rods must be spliced, it may be more cost-effective to replace a large part of the top of the foundation and install a new anchor rod group.

The Engineer of Record may consider welded repairs, although this is very controversial and risky for fatigue or seismically loaded anchor rods and therefore was not discussed in the main body of the Specifications. The anchor rod and the extension must meet the following requirements for welding:

a) An F1554 Grade 36 rod;
b) An F1554 Grade 55 rod that meets ASTM F1554 supplementary requirement S1;
c) An A706 deformed bar; or
d) A material with a chemical composition or carbon equivalent (CE) meeting the requirements of AWS D1.1 or AWS D1.4 (ref. 21).

The welding procedure of an anchor rod, or extension, should be as follows:

a) Bevel both the rod and the extension;
b) Weld together the rod and the extension using a full penetration weld;
c) Grind the weld;
d) Run an ultrasonic test (using the procedure described in ref. 34) to check the soundness of the weld;
e) If the anchor rod was galvanized, the galvanizing should be repaired per ASTM A780.

In-service corrections, repairs, and modifications—Typically, in-service inspection and repairs will only be necessary if the anchor rods are subject to fatigue or if there has been an earthquake. Therefore the following discussion applies only to these conditions. An incorrect baseplate thickness cannot be repaired; however, these anchor rods may be at greater risk than normal and should be inspected with ultrasonic testing at least once and then inspected visually at least every two years. An inadequate edge distance also cannot be repaired. If the edge distance is less than one anchor rod diameter, an engineer should check the baseplate for bearing under the strength limit state. Anchor rods that are identified in service to be significantly misaligned or bent to fit in the baseplate hole should be inspected carefully, possibly using ultrasonic testing. If the misalignment exceeds 1:40, beveled washers should be installed under each nut. Otherwise, this condition does not necessarily need to be repaired. If the anchor rod must be replaced, it is possible to repair one or two rods by cutting off the anchor rod and welding or using a threaded coupler to join an extension onto the anchor rod. If more than two rods must be re-welded, it is probably more cost-effective to replace the whole anchor rod group and a large part of the top of the foundation. The limitations on material to be welded and the procedures discussed in the previous section should be followed for any weld repairs.

Inadequate thread projection (it should be at least flush) does not necessarily need to be corrected when it is found in service if at least three-quarters of the nut is engaged. If lowering the structure down the anchor rods cannot solve inadequate projection, it may be necessary to replace the foundation. In some cases, the holes in the baseplate may be enlarged and a special "shoulder nut" machined to drop part of the way into the enlarged holes. In other cases, cutting off the anchor rod and welding or using a threaded coupler to join an extension onto the anchor rod may also be considered.

Missing nuts or washers should be replaced immediately. Loose nuts should be retightened using the procedures in Section 5. The nuts on the anchor rods should be prevented from loosening by using a jam nut or other locking device. Tack welding the nut to the anchor rod on the unstressed (top) side of the top nut has been used with success but this remains very controversial. Only ASTM F1554 grade 36 or grade 55 rod, or grade A706 reinforcing bar should be tack welded. Under no circumstance should any nut be tack welded to the washer or the baseplate. If there is no means to prevent the nuts from loosening, the top nuts and the leveling nuts should be checked with a calibrated torque wrench to be sure that it takes at least 110 percent of the verification torque

computed using Equation 5.1 to additionally tighten the leveling nuts and the top nuts.

Gouges or thread damage identified during service should be evaluated to see if they present a risk of cracking or will interfere with retightening the nuts. If the gouges or damage do not present any immediate problems, they do not need to be repaired. Anchor rods that are identified in service to be significantly misaligned or bent to fit in the baseplate hole should be inspected carefully, possibly using ultrasonic testing. If the misalignment exceeds 1:40, beveled washers should be installed under each nut. Otherwise, this condition does not necessarily need to be repaired. If the anchor rod must be replaced, it is possible to repair one or two rods by cutting off the anchor rod and welding or using a threaded coupler to join an extension onto the anchor rod.

Broken, cracked, or severely corroded anchor rods must be repaired. Either the foundation is replaced, or the anchor rods are cut off and an extension added by welding or using a threaded coupler.

Ultrasonic testing of anchor rods should be performed after a welded repair and at least once again after two years if the joint is designed for the fatigue limit state. If possible, ultrasonic testing should be performed on these weld repaired anchor rods at least every four years. Ultrasonic testing should also be used on a regular basis if similar structures subject to similar loading have had fatigue problems or if anchor rods were not adequately designed for fatigue in accordance with this Specification. Otherwise, ultrasonic tests are not encouraged in a regular maintenance plan. Michigan Department of Transportation (ref. 34) developed an ultrasonic testing procedure for anchor rods.

C-7. INSPECTION AND MAINTENANCE AFTER INSTALLATION

A regular inspection and maintenance plan shall be in place for the joints that are subject to fatigue or seismic loading.

1. **Anchor rod appearance**—Draw a diagram of the anchor rod pattern and number in a clockwise pattern. Check each anchor rod for corrosion, gouges, or cracks. Suspected cracks may be more closely examined using the dye-penetrant technique (ref. 4). If there is heavy corrosion near the interface with the concrete, there may be more severe corrosion hidden below the concrete where the pocket around the anchor rod stays wet. Verify that all the anchor rods have top nuts with washers. No lock washers should be used. Galvanized nuts or washers should not be used with unpainted weathering steel. Check for inadequately sized washers for oversize holes. If there is no grout pad, verify that all the anchor rods have leveling nuts with washers. Check for loose nuts, gouges, thread damage or corrosion. Note any anchor rods that are significantly misaligned or were bent to fit in the baseplate hole. Note any anchor rods that do not have at least one thread projecting past the nut. If the anchor rod is not projecting past the nut, measure the distance from the top of the nut to the top of the anchor rod.
2. **Sounding the anchor rods**—Anchor rods may be struck by a hammer (a large ball peen hammer is suggested) to detect broken bolts. Strike the side of the top nut and the top of the rod. Good tight anchor rods will have a similar ring, and broken or loose anchor rods will have a distinctly different and duller sound.
3. **Tightness of anchor rod nuts**—It shall be verified that the top nuts still have a sound tack weld (at the top of the top nut only) or a jam nut. (Tack welds to the washer or the baseplate are undesirable and should be reported.) If one of these is not used to prevent loosening of the nut, the tightness shall be verified by applying a torque equal to 110 percent of the torque computed using Equation 5.1, in accordance with step 20 of the above model installation procedure.

   If one nut in a joint is loose (the tack weld is fractured or the nut does not reach the required torque), it shall be unscrewed, cleaned, inspected for possible thread stripping, lubricated, placed and brought to the snug condition (as defined in this Specification) and retightened to the pretension specified in Section 5 using the turn-of-nut method or a new direct tension indicator (DTI). And it shall be prevented from becoming loose in accordance with Section 5.

   If more than one nut in a joint is loose, the entire joint shall be disassembled, all the anchor rods shall be visually inspected, and the joint shall be reassembled with new nuts following the procedures of Section 5. More than one loose nut may indicate a poorly installed joint or fatigue problems. A close following of the performance of the joint shall be made.
4. **Ultrasonic test of anchor rods**—An ultrasonic test of anchor rods need be performed only if
   - Welded repairs have been made;
   - Similar structures subject to similar loading have had fatigue problems; or
   - Anchor rods were not adequately designed for fatigue in accordance with this Specification.

REFERENCES

1. American Society for Testing Materials, “ASTM F1554 Standard Specification for Anchor Bolts, Steel, 36, 55, and 105-ksi Yield Strength,” West Conshohocken, PA, 1997.
2. American Society for Testing Materials, “ASTM A615 Standard Specification for Deformed and Plain Billet-Steel Bars for Concrete Reinforcement,” West Conshohocken, PA, 1996.
3. American Society for Testing Materials, “ASTM A706 Standard Specification for Low-Alloy Steel Deformed and Plain Bars for Concrete Reinforcement,” West Conshohocken, PA, 1996.

4. American Welding Society, AWS D1.1-2000, "Structural Welding Code—Steel," American Welding Society, Miami, 2000.
5. American Association of State Highway and Transportation Officials, "Standard Specifications for Structural Supports for Highway Signs, Luminaires and Traffic Signals," 4th Edition, American Association of State Highway and Transportation Officials, Washington, D.C., 2001.
6. American Association of State Highway and Transportation Officials. *LRFD Bridge Design Specifications.* Washington, DC. 1994.
7. American Institute of Steel Construction, "Manual of Steel Construction, Load and Resistance Factor Design," Second Edition, American Institute of Steel Construction, Inc., Chicago, IL, 1998.
8. American Concrete Institute, ACI 318-99, "Building Code Requirements for Structural Concrete and Commentary," American Concrete Institute, Farmington Hills, Michigan, 1999.
9. American Concrete Institute, "Draft of ACI 349 Code Requirements for Nuclear Safety Related Concrete Structures," American Concrete Institute, Farmington Hills, Michigan, 2000.
10. DeWolf, J. T. and Ricker D. T., "Column Baseplates," Steel Design Guide Series, American Institute of Steel Construction, Chicago, IL, 1990.
11. Fuchs, W., Eligehausen, R., and Breen, J. E., "Concrete Capacity Design (CCD) Approach for Fastening to Concrete," ACI Structural Journal, January-February 1995, pp. 73–94.
12. Eligehausen, R., Fuchs, W., and Mayer, B., "Loadbearing Behavior of Anchor Fastenings in Tension," *Betonwerk & Fertigteil-Technik* (Wiesbaden), No. 12, 1987, pp. 826–832, and No. 1, 1988, pp. 29–35.
13. Eligehausen, R. and Fuchs, W., "Loadbearing Behavior of Anchor Fastenings under Shear or Flexural Loading," *Betonwerk & Fertigteil-Technik* (Wiesbaden), No. 2, 1988, pp. 48–56.
14. Rehm, G., Eligehausen, R., and Mallee, R., "Befestigungstechnik (Fastening Technique)," *Betonkalender 1992,* V. II, Ernst & Sohn, Berlin, 1992, pp. 597–715. (in German)
15. Farrow, C. B. and Klingner, R. E., "Tensile Capacity of Anchors with Partial or Overlapping Failure Surfaces: Evaluation of Existing Formulas on an LRFD Basis," *ACI Structural Journal,* November-December 1995, pp. 698–710.
16. Farrow, C. B., Frigui, I., and Klingner, R. E., "Tensile Capacity of Single Anchors in Concrete: Evaluation of Existing Formulas on an LRFD Basis," *ACI Structural Journal,* January-February 1996, pp. 698–710.
17. Jirsa, J. O., Cichy, N. T., Calzadilla, M. R., Smart, W. H., Pavluvcik, M. P., and Breen, J. E., "Strength and Behavior of Bolt Installations in Concrete Piers," Research Report 305-1F, Center for Transportation Research, The University of Texas at Austin, Austin, Texas, November 1984.
18. Birkemoe, P. C. and Herrschaft, D. C., "Bolted Galvanized Bridges–Engineering Acceptance Near," *Civil Engineering,* ASCE, Reston, VA, April 1970.
19. American Society for Testing Materials, "ASTM A153 Standard Specification for Zinc Coating (Hot-Dip) on Iron and Steel Hardware," West Conshohocken, PA, 1995.
20. American Society for Testing Materials, "ASTM B695 Standard Specification for Coatings of Zinc Mechanically Deposited on Iron and Steel," West Conshohocken, PA, 1991.
21. American Welding Society, "AWS D1.4 Structural Welding Code–Reinforcing Steel."
22. American National Standards Institute, "ANSI/ASME B1.1 Unified Screw Threads," New York, NY, 1989.
23. Industrial Fastener Institute, "Fastener Standards," Sixth Edition, Cleveland, OH, 1998, page A-6.
24. Kaczinski, M. R., Dexter, R. J., and Van Dien, J. P., *NCHRP Report 412: Fatigue-Resistant Design of Cantilevered Signal, Sign, and Light Supports,* Transportation Research Board, National Research Council, Washington D.C., 1996.
25. American Society for Testing Materials, "ASTM A563 Standard Specification for Carbon and Alloy Steel Nuts," West Conshohocken, PA, 1996.
26. American Society for Testing Materials, "ASTM A194 Standard Specification for Carbon and Alloy Steel Nuts for Bolts for High-Pressure and High-Temperature Service," West Conshohocken, PA, 1995.
27. American National Standards Institute, "ANSI/ASME B18.2.2 Square and Hex Nuts," New York, NY, 1987.
28. Cook, R. A., "Behavior and Design of Ductile Multiple-Anchor Steel-to-Concrete Connections," Thesis Dissertation, The University of Texas at Austin, Austin, TX, 1989.
29. Kulak, G. L., Fisher, J. W., and Struik, J. H. A., "Guide to Design Criteria for Bolted and Riveted Joints," Second Edition, John Wiley and Sons, New York, 1987.
30. American Institute of Steel Construction, Inc., "Code of Standard Practice for Steel Buildings and Bridges," Chicago, IL, March 2000.
31. Till, R. D., and Lefke, N. A., "The Relationship Between Torque, Tension, and Nut Rotation of Large Diameter Anchor Bolts," Materials and Technology Division, Michigan Department of Transportation, October 1994.
32. Research Council on Structural Connections, "Specification for Structural Joints Using ASTM A325 or A490 Bolts," available from American Institute of Steel Construction (AISC), Chicago, Illinois, 2000.
33. 29 CFR Part 1926, *Safety Standards for Steel Erection,* Federal Register, Vol. 66, No. 12, Department of Labor, Occupational Safety and Health Administration (OSHA), 29 CFR Part 1926, Thursday, January 18, 2001.
34. McCrum, R., *Brief Summary of Michigan's Research Work with Anchor Bolts on Cantilevered Sign Structures,* Materials and Technology Division, Michigan Department of Transportation, Lansing, 1993.